CHAPTER 2

Transmitter and Receiver Systems

Table of Figures

Table of Tables

This page intentionally left blank.

Acronyms

µV	microvolt
AFTRCC	Aerospace and Flight Test Radio Coordinating Council
AM	amplitude modulation
AMT	aeronautical mobile telemetry
ARTM	Advanced Range Telemetry
ASM	attached synchronization marker
AWGN	additive white Gaussian noise
BPSK	binary phase shift keying
BEP	bit error probability
BER	bit error rate
Biφ	bi-phase
BSS	Broadcasting-Satellite Service
CPM	continuous phase modulation
CCSDS	Consultative Committee for Space Data Systems
dB	decibel
dBc	decibels relative to the carrier
dBi	decibels isotropic
dBm	decibels referenced to one milliwatt
dBW	decibels relative to one watt
DoD	Department of Defense
DQE	data quality encapsulation
DQM	data quality metric
EESS	Earth Exploration-Satellite Services
EIRP	effective isotropic radiated power
FCC	Federal Communications Commission
FEC	forward error correction
FM	frequency modulation
FQPSK	Feher's Quadrature Phase Shift Keying
Hz	hertz
IF	intermediate frequency
I/N	interference-to-noise ratio
I/Q	in-phase/quadrature-component
IPC	interference protection criteria
IRIG	Inter-Range Instrumentation Group
ITM	Irregular Terrain Model
kHz	kilohertz
LDPC	low-density parity-check
L-R	Longley-Rice
LTE	Long-Term Evolution
Mbps	megabits per second
MC4EB	Military Command, Control, Communications, and Computers Executive Board
MHz	megahertz
MIL-STD	Military Standard
MSK	minimum shift keying

NRZ-L	non-return-to-zero-level
NTIA	National Telecommunications and Information Administration
OOBE	out-of-band emission
OQPSK	offset quadrature phase shift keying
PAPR	peak-to-average-power-ratio
PCM	pulse code modulation
PFD	power flux density
PM	phase modulation
PSD	power spectral density
QPSK	quadrature phase shift keying
RCC	Range Commanders Council
RF	radio frequency
RLC	resistor-inductor-capacitor
RNRZ	randomized non-return-to-zero
SAW	surface acoustic wave
SDARS	Satellite Digital Audio Radio Service
SHF	super-high frequency
STC	space-time code
SOQPSK	shaped offset quadrature phase shift keying
UHF	ultra-high frequency
US&P	United States and Possessions
VCO	voltage-controlled oscillator
VHF	very-high frequency
WCS	Wireless Communication Service

CHAPTER 2

Transmitter and Receiver Systems

2.1   Radio Frequency Standards for Telemetry

These standards provide the criteria to determine equipment and frequency use requirements and are intended to ensure efficient and interference-free use of the radio frequency (RF) spectrum. These standards also provide a common framework for sharing data and providing support for test operations between ranges. The RF spectrum is a limited natural resource; therefore, efficient use of available spectrum is mandatory. In addition, susceptibility to interference must be minimized. Systems not conforming to these standards require justification upon application for frequency assignment, and the use of such systems is highly discouraged. The standards contained herein are derived from the National Telecommunications and Information Administration's (NTIA) Manual of Regulations and Procedures for Federal Radio Frequency Management.[1]

2.2   Bands

The bands used for telemetry are described in Table 2-1.

Table 2-1. Telemetry Frequency Allocations			
Frequency Range (MHz)	**Unofficial Designation**	**Comments**	**Refer to:**
1435-1525	Lower L-band	Telemetry primary service (part of mobile service) in USA	2.2.1
2200-2290	Lower S-band	Telemetry co-primary service in USA	2.2.2
2310-2360	Upper S-band	Wireless Communications Service (WCS) and Broadcasting-Satellite Service (BSS) are primary services. Telemetry is a secondary service in the USA for federal users only in 2310-2320 MHz and 2345-2360 MHz.	2.2.3
2360-2395	Upper S-band	Telemetry primary service in USA	2.2.3
4400-4940	Lower C-band	See Paragraph 2.2.4	2.2.4
5091-5150	Middle C-band	See Paragraph 2.2.5	2.2.5
5925-6700	Upper C-band	See Paragraph 2.2.6	2.2.6

The 1780-1850 MHz band (unofficially called "upper L-band") can also be used for telemetry at many test ranges, although it is not explicitly listed as a telemetry band in the NTIA Table of Frequency Allocations.[2] The mobile service is a primary service in the 1780-1850 MHz band and telemetry is a part of the mobile service. Since the 1780-1850 MHz band is not considered a standard telemetry band per this document, potential users must coordinate, in advance, with the individual range(s) and ensure use of this band can be supported at the subject

---

[1] National Telecommunications and Information Administration. "Manual of Regulations and Procedures for Federal Radio Frequency Management." September 2015. May be superseded by update. Retrieved 17 May 2021. Available at https://www.ntia.doc.gov/files/ntia/publications/manual_sep_2015.pdf.
[2] Code of Federal Regulations, Table of Frequency Allocations, title 47, sec. 2.106.

range and that it will meet their technical requirements. While these band designations are common in telemetry parlance, they may have no specific meaning to anyone else. Telemetry assignments are made for testing[3] manned and unmanned aircraft, for missiles, space, land, and sea test vehicles, and for rocket sleds and systems carried on such sleds. Telemetry assignments are also made for testing major components of the aforementioned systems.

2.2.1   Allocation of the Lower L-Band (1435 to 1535 MHz)

This band is allocated in the United States and Possessions (US&P) for government and nongovernmental aeronautical telemetry use on a shared basis. The Aerospace and Flight Test Radio Coordinating Council (AFTRCC) works with the government Area Frequency Coordinators on the non-governmental use of this band. The frequencies in this range will be assigned for aeronautical telemetry and associated remote-control operations[4] for testing of manned or unmanned aircraft, missiles, rocket sleds, and other vehicles or their major components. Authorized usage includes telemetry associated with launching and reentry into the earth's atmosphere as well as any incidental orbiting prior to reentry of manned or unmanned vehicles undergoing flight tests. The following frequencies are shared with flight telemetering mobile stations: 1444.5, 1453.5, 1501.5, 1515.5, and 1524.5 MHz. The frequency range 1435 to 1525 MHz is allocated for the exclusive use of aeronautical telemetry in the United States of America.

2.2.2   Allocation of the Lower S-Band (2200 to 2300 MHz)

No provision is made in this band for the flight testing of manned aircraft.

2.2.2.1   2200 to 2290 MHz

These frequencies are shared equally by the United States Government's fixed, mobile, space research, space operation, and the Earth Exploration-Satellite Services (EESS), and include telemetry associated with launch vehicles, missiles, upper atmosphere research rockets, and space vehicles regardless of their trajectories.

2.2.2.2   2290 to 2300 MHz

Allocations in this range are for the space research service (deep space only) on a shared basis with the fixed and mobile (except aeronautical mobile) services.

2.2.3   Allocation of the Upper S-Band (2310 to 2395 MHz)

This band is allocated to the fixed, mobile, radiolocation, and BSS in the United States of America. Government and nongovernmental telemetry users share portions of this band, chiefly 2360-2390 MHz, in a manner similar to that of the L-band. Telemetry assignments are made for flight-testing of manned or unmanned aircraft, missiles, space vehicles, or their major components.

2.2.3.1   2310 to 2360 MHz

These frequencies have been reallocated and were auctioned by the Federal Communications Commission (FCC) in April 1997. The WCS is the primary service in the frequencies 2305-2320 MHz and 2345-2360 MHz.

---

[3] A telemetry system as defined here is not critical to the operational (tactical) function of the system.
[4] The word used for remote-control operations in this band is *telecommand*.

2.2.3.2   2360 to 2395 MHz
    The mobile service (including aeronautical telemetry) is a primary service in this band.

2.2.4   Allocation of the Lower C-Band (4400 to 4940 MHz)
    Telemetry is an operation that is currently allowed under the mobile service allocation. Bi-directional telemetry network systems should be operated in the upper part of this band from 4880-4940 MHz. See Chapter 27 Subsection 27.3.1.2 for more information.

2.2.5   Allocation of the Middle C-Band (5091 to 5150 MHz)
    Telemetry is an operation that is currently allowed under the mobile service allocation.

2.2.6   Allocation of the Upper C-Band (5925 to 6700 MHz)
    This band is not currently allocated as a government band. The process of incorporating federal government use of aeronautical telemetry operations into the NTIA Table of Frequency Allocations for this band has been initiated but not yet completed.

2.3   Telemetry Transmitter Systems

    Telemetry requirements for air, space, and ground systems are accommodated in the appropriate bands as described in Section 2.2.

2.3.1   Center Frequency Tolerance
    Unless otherwise dictated by a particular application, the frequency tolerance for a telemetry transmitter shall be ±0.002% of the transmitter's assigned center frequency. Transmitter designs shall control transient frequency errors associated with startup and power interruptions. During the first second after turn-on, the transmitter output frequency shall be within the occupied bandwidth of the modulated signal at any time when the transmitter output power exceeds −25 decibels (dB) referenced to one milliwatt (dBm). Between 1 and 5 seconds after initial turn-on, the transmitter frequency shall remain within twice the specified limits for the assigned radio frequency. After 5 seconds, the standard frequency tolerance is applicable for any and all operations where the transmitter power output is −25 dBm or greater (or produces a field strength greater than 320 microvolts [µV]/meter at a distance of 30 meters from the transmitting antenna in any direction). Specific uses may dictate tolerances more stringent than those stated.

2.3.2   Output Power
    Emitted power levels shall always be limited to the minimum required for the application. The output power shall not exceed 25 watts[5]. The effective isotropic radiated power (EIRP) shall not exceed 25 watts.

2.3.3   Modulation
    The modulations used for aeronautical telemetry, whether analog or digital, have been constant amplitude modulations. Such modulations carry all their information in the phase or instantaneous frequency. Because no information is carried in the amplitude, RF power

---

[5] An exemption from this EIRP limit will be considered; however, systems with EIRP levels greater than 25 watts will be considered nonstandard systems and will require additional coordination with affected test ranges.

amplifiers may operate in full saturation (the most power-efficient mode of operation) and the information is not corrupted by amplitude variations due to transmission.

The standard method for the transmission of digital information is continuous phase modulation (CPM). The three standard modulations are variations of CPM. These three modulations are called pulse code modulation/frequency modulation (PCM/FM), Shaped Offset Quadrature Phase Shift Keying version TG (SOQPSK-TG), and Advanced Range Telemetry CPM (ARTM CPM). Because the characteristics of each are described in CPM terms, this section begins with a technical description of CPM.

2.3.3.1   Continuous Phase Modulation

The combination of Equations 2-1, 2-2, and 2-3 define CPM. A carrier signal can be defined as

$$s(t) = A_c \cos\big(2\pi f_c t + \phi(t)\big) \qquad\qquad \text{2-1}$$

$$\phi(t) = 2\pi \sum_i h_i \alpha_i q(t - iT_s) \qquad\qquad \text{2-2}$$

$$q(t) = \int_{-\infty}^{t} g(u)du \qquad\qquad \text{2-3}$$

where A_C is the constant carrier amplitude, f_c is the carrier frequency (in Hertz), and $\phi(t)$ is the time-varying phase that carries the information. The phase is given by Equation 2-2, where i indexes the data symbols, h_i is the modulation index applied to the i-th data symbol, α_i is the i-th data symbol, T_S is the symbol time (the reciprocal of the symbol rate), and $q(t)$ is the phase response. The time-integral of a frequency pulse $g(t)$ defines the phase response, as shown in Equation 2-3.

The length of the frequency pulse $g(t)$ is an integer multiple of the symbol time T_S, that is, the frequency pulse spans an integer number of symbols. The number of symbols spanned by the frequency pulse is denoted by L. If $L=1$, then the modulated carrier is called *full response* CPM. If $L>1$, then the modulated carrier is called *partial response* CPM. Partial response frequency pulses produce smoother, more gradual phase transitions that reduce the bandwidth of the modulated carrier.

The convention in CPM is to scale the amplitude of the frequency pulse so that it has an area 1/2. As a consequence of this phase response $q(t)$ may be expressed as

$$q(t) = \begin{cases} 0 & t < 0 \\ \int_0^t g(u)du & 0 \le t < LT_s \\ 1/2 & t \ge LT_s \end{cases} \qquad\qquad \text{2-4}$$

Equation 2-4 shows that the phase response $q(t)$ lasts forever.

A CPM signal may be created using an FM modulator in the arrangement shown in Figure 2-1.
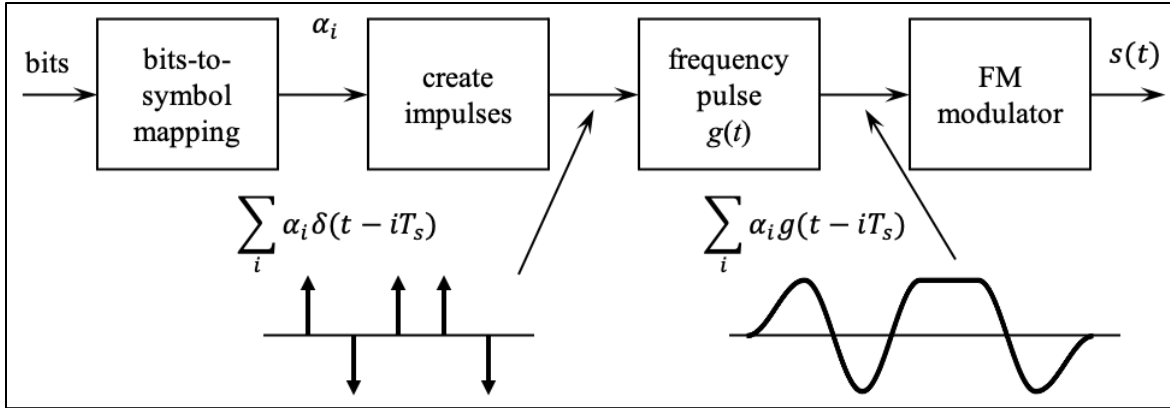
Figure 2-1.   A Conceptual CPM Modulator

The diagram illustrates a conceptual method for generating the frequency pulse train that uses a filter whose impulse response is the frequency pulse $g(t)$ and whose input is a train of weighted impulse functions. The peak frequency deviation of the FM modulator Δf_i applied to the i-th data symbol α_i is given by

$$h_i = 2\Delta f_i T_s \qquad\qquad 2\text{-}5$$

In words, the digital modulation index is two times the peak frequency deviation divided by the symbol rate.

In summary CPM is defined by the set of parameters listed in Table 2-2.

Table 2-2. CPM Parameters		
Name	**Symbol**	**Description**
alphabet	α	the symbols used to carry digital information
frequency pulse	$g(t)$	frequency pulse with span L symbol times
modulation index(es)	h	the ratio of the peak-to-peak frequency deviation to the symbol rate

All three waveforms, PCM/FM, SOQPSK-TG, and ARTM CPM, may all be described using these parameters.

Because the phase response $q(t)$ lasts forever, CPM is a modulation with memory. Consequently, the optimum detector finds the symbol *sequence* that best matches the received signal. In CPM, the i-th symbol α_i advances the phase of the modulated carrier by $\pi h_i \alpha_i$ radians after L symbol times. The cumulative contribution of the phase changes is called the phase state and, due to the modulo-2π nature of phase and the finite size of the alphabet, there is only a finite number of phase states. During any symbol interval, the CPM waveform is completely defined by the phase state and the $L-1$ previous symbols. During any symbol interval, the CPM waveform is completely defined by the phase state and the $L-1$ previous symbols, as the phase state and the $L-1$ previous symbols comprise the CPM state. The set of possible CPM states forms a finite state machine. Adding the time dimension to the state transitions produces a trellis. The optimum detector, in the maximum likelihood sense, searches the trellis for the CPM state

sequence that most closely matches the received signal. The most commonly used search algorithm is called the Viterbi algorithm.

2.3.3.2 PCM/FM

This modulation has been in use since the 1970s and thus is used in a large number of legacy systems. The CPM parameters for *unfiltered* PCM/FM are

$$\alpha_i = \begin{cases} -1 & i\text{-th bit} = 0 \\ +1 & i\text{-th bit} = 1 \end{cases} \tag{2-6}$$

$$h_i = 0.7, \text{ all } i \tag{2-7}$$

$$g_1(t) = \begin{cases} \dfrac{1}{2T_b} & 0 \le t \le T_b \\ 0 & \text{otherwise} \end{cases} \tag{2-8}$$

When it was adopted, PCM/FM was generated using the technology available. In place of the "create-impulses" block in Figure 2-1, a circuit that created a non-return-to-zero level (NRZ-L) waveform from the bits was used. The FM modulator was usually a voltage-controlled oscillator (VCO).

To reduce the bandwidth of the modulated carrier, a smoother frequency pulse is required. This pulse was created by applying a low-pass filter, called a premodulation filter, to the NRZ-L pulse train. The filter was usually a multi-pole linear phase filter whose −3 dB corner frequency was 0.7 times the bit rate. The concept is illustrated in Figure 2-2.
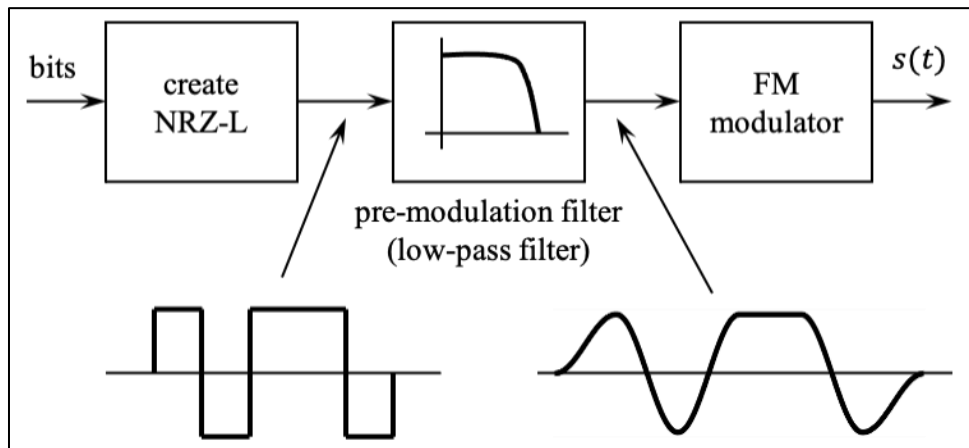
Figure 2-2.   PCM/FM Modulator Using a Pre-modulation Filter

The end result is a frequency pulse that is defined as the output of premodulation filter in response to the frequency pulse $g_1(t)$ in Equation 2-8. The most common continuous-time filter with linear phase is the Bessel filter. The parameters for *filtered* PCM/FM are

$$\alpha_i = \begin{cases} -1 & i\text{-th bit} = 0 \\ +1 & i\text{-th bit} = 1 \end{cases} \tag{2-9}$$

$$h_i = 0.7, \text{ all } i \qquad\qquad 2\text{-}10$$

$$g_2(t) = \begin{cases} A \sum_{n=1}^{N} \left[B_n \left(\frac{t}{T_b} \right) - B_n(0) \right] & 0 \leq \frac{t}{T_b} < 1 \\[4mm] A \sum_{n=1}^{N} \left[B_n \left(\frac{t}{T_b} \right) - B_n \left(\frac{t - T_b}{T_b} \right) \right] & 1 \leq \frac{t}{T_b} \end{cases} \qquad 2\text{-}11$$

for an even-ordered Bessel filter and

$$g_2(t) = \begin{cases} A \dfrac{C_0}{a_0} \left[1 - e^{a_0(t/T_b)} \right] + A \sum_{n=1}^{N} \left[B_n \left(\frac{t}{T_b} \right) - B_n(0) \right] & 0 \leq \frac{t}{T_b} < 1 \\[4mm] A \dfrac{C_0}{a_0} \left[e^{a_0(t-T_b)/T_b} - e^{a_0(t/T_b)} \right] + A \sum_{n=1}^{N} \left[B_n \left(\frac{t}{T_b} \right) - B_n \left(\frac{t - T_b}{T_b} \right) \right] & 1 \leq \frac{t}{T_b} \end{cases} \qquad 2\text{-}12$$

for an odd-ordered Bessel filter, where

$$B_n(x) = \frac{2 C_n e^{a_n b x}}{a_n^2 + \omega_n^2} \left[(\omega_n \sin(\theta_n) - a_n \cos(\theta_n)) \cos(\omega_n b x) \right.$$
$$\left. + (a_n \sin(\theta_n) + \omega_n \cos(\theta_n)) \sin(\omega_n b x) \right] \qquad 2\text{-}13$$

b is the -3dB corner frequency relative to the bit rate given by

$$b = 2\pi \times 0.7 \qquad\qquad 2\text{-}14$$

and where A is a constant chosen to normalize the area of $g(t)$ to the standard value of 1/2. The parameters $C_n, a_n, \omega_n,$ and θ_n for orders $4 - 8$ are listed in <u>Table 2-3</u>.

Table 2-3.	Parameters for the Bessel Filtered NRZ Frequency Pulse			
Fourth-order Bessel filter (*N*=2)				
n	C_n	a_n	ω_n	θ_n (deg)
1	1.321405	−0.995209	1.257106	126.547182
2	4.049108	−1.370068	0.410250	−78.794227
Fifth-order Bessel filter (*N*=2)				
n	C_n	a_n	ω_n	θ_n (deg)
0	8.594891	−1.502316	0.717910	−152.010950
1	1.261186	−0.957677	1.471124	60.587298
2	5.568066	−1.380877	0.717910	−152.010950
Sixth-order Bessel filter (*N*=3)				
n	C_n	a_n	ω_n	θ_n (deg)
1	1.174080	−0.930657	1.661863	−3.657188

2	7.027081	−1.381858	0.971472	138.041767
3	15.136528	−1.571490	0.320896	−74.465371
Seventh-order Bessel filter (_N_=3)				
_n_	C_n	a_n	ω_n	θ_n (deg)
0	32.675401	−1.684368	0.589245	−146.065944
1	1.070723	−0.909868	1.836451	−66.775408
2	8.331228	−1.378903	1.191567	70.220403
3	23.598522	−1.612039	0.589245	−146.065944
Eighth-order Bessel filter (_N_=4)				
_n_	C_n	a_n	ω_n	θ_n (rads)
1	0.959732	−0.892870	1.998326	−129.100317
2	9.414294	−1.373841	1.388357	3.883967
3	33.701870	−1.636939	0.822796	144.350081
4	60.742083	−1.757408	0.272868	−72.170321

A plot of the frequency pulses is shown in Figure 2-3. The frequency pulses span _L_=3 symbol times. Consequently, filtered PCM/FM is a partial response CPM. The frequency pulses are more similar than they are different. The different delays shown in the figure are due to the increasing (and more linear) group delay as the order of the Bessel filter increases.
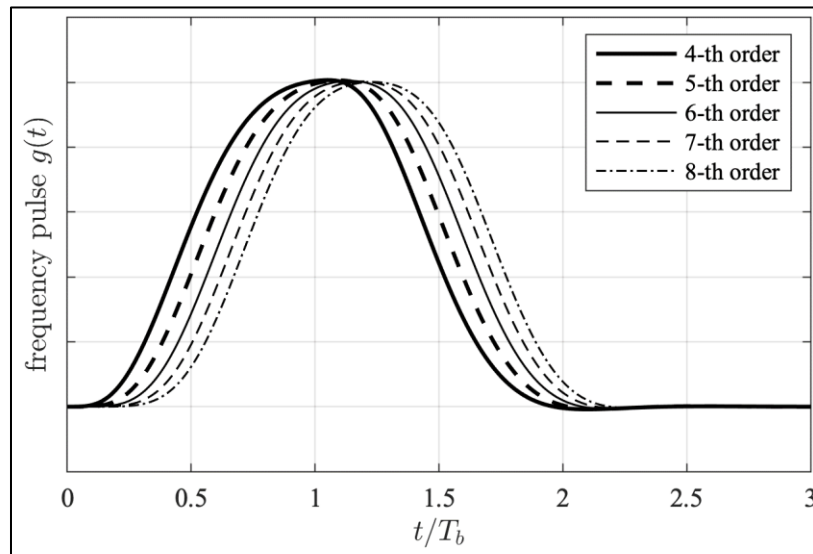
Figure 2-3.   Frequency Pulse Shapes Generated by Filtering an NRZ Pulse Shape

In legacy transmitters based only on continuous-time processing, the peak frequency deviation needed to be carefully measured and was set by hand. Modern modulators often use discrete-time processing to create sampled versions of the waveforms and do not suffer from this problem.

The optimum detector is the trellis-based detector described in Subsection 2.3.3.1. However, the technology of the day could not perform the computations required to implement optimum detection. Consequently, the most common detectors in use from the early 1970s to the early 2000s were based on limiter-discriminators to produce a noisy version of the waveform

$$\frac{d}{dt}\phi(t) = 2\pi h \sum_i \alpha_i g(t - iT_b)$$

2-15

The limiter-discriminator output was connected to a timing phase-lock-loop circuit (commonly called a bit synchronizer) to recover the clock and underlying bit sequence. As technology advanced, optimum detection based on a trellis search became feasible. However, optimum detection requires the modulation index to be precisely $h=0.7$, which can be difficult to achieve using legacy modulators as described above. The trellis-based detectors currently available accommodate small variations in the modulation index at the cost of modest reductions in detection efficiency.

2.3.3.3   SOQPSK-TG

This modulation was introduced to this standard in 2004 as a more bandwidth-efficient alternative to PCM/FM. It is a partial response CPM with a constrained ternary alphabet. The frequency pulse is a spectral raised-cosine pulse windowed by a modified temporal raised-cosine function. The CPM parameters of SOQPSK-TG are

$$a_i = \begin{cases} -1, & i\text{-th bit} = 0 \\ +1, & i\text{-th bit} = 1 \end{cases}$$

2-16

$$\alpha_i = (-1)^{i+1} \frac{a_{i-1}(a_i - a_{i-2})}{2}$$

2-17

$$h_i = 0.5, \text{ all } i$$

2-18

$$g(t) = \left[\frac{A\cos\left(\frac{\pi\rho Bt}{2T_b}\right)}{1 - 4\left(\frac{\rho Bt}{2T_b}\right)^2} \right] \left[\frac{\sin\left(\frac{\pi Bt}{2T_b}\right)}{\frac{\pi Bt}{2T_b}} \right] w(t)$$

2-19

where the window $w(t)$ is

$$w(t) = \begin{cases} 1 & |t/2T_b| \leq T_1 \\ \frac{1}{2} + \frac{1}{2}\cos\left(\frac{\pi\left(\left|\frac{t}{2T_b}\right| - T_1\right)}{T_2}\right) & T_1 < |t/2T_b| \leq T_1 + T_2 \\ 0 & |t/2T_b| > T_1 + T_2 \end{cases}$$

2-20

Equation 2-17 is a precoder that converts binary symbols in the set $\{-1,+1\}$, to ternary symbols in the set $\{-1,0,+1\}$. The ternary symbol sequence is constrained. The purpose of this precoder is discussed below in the context of detection. A new bit occurs every T_b seconds. The precoder produces a new ternary symbol every T_b seconds.

The SOQPSK-TG frequency pulse is illustrated in Figure 2-4.
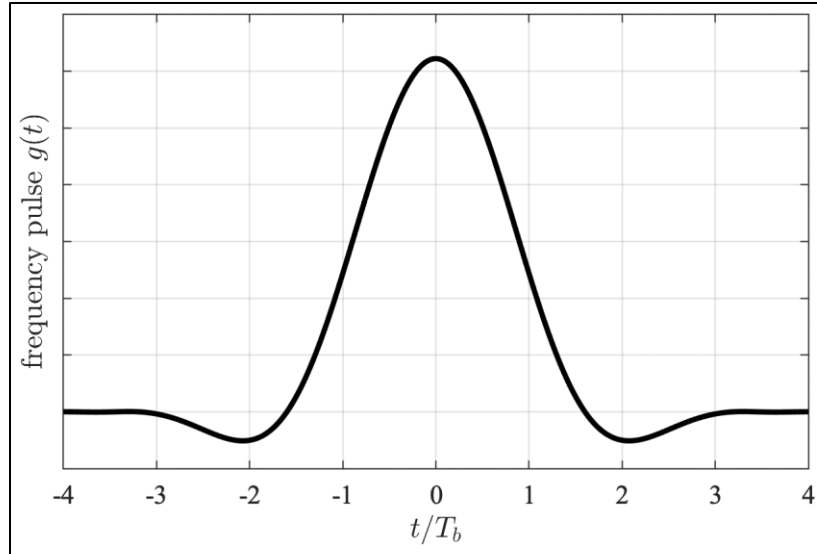
Figure 2-4.   The Frequency Pulse for SOQPSK-TG

Observe that the independent time variable in the plot is $-4T_b \le t \le 4T_b$ and follows from the way the frequency pulse is defined in Equations 2-19 and 2-20. The frequency pulse is not really non-causal; the mathematical expressions are more convenient when the time variable is centered at zero. The frequency pulse spans L=8 bit times. The constant A in Equation 2-19 is chosen to normalize the area of $g(t)$ to the standard value of 1/2:

$$\int_{-(T_1+T_2)2T_b}^{(T_1+T_2)2T_b} g(t)dt = \frac{1}{2} \qquad\qquad 2\text{-}21$$

There are four other parameters in Equations 2-19 and 2-20 that define the frequency pulse: ρ, B, T_1, T_2. Adjusting these parameters produces a trade-off between spectral efficiency and detection efficiency. The -TG version of SOQPSK is defined by the parameters listed in Table 2-4.

Table 2-4. SOQPSK-TG Parameters				
Parameter	ρ	B	T_1	T_2
Value	0.70	1.25	1.5	0.5

The frequency pulse is a complicated pulse shape that is not easily approximated by applying a continuous-time low-pass filter to an NRZ-L pulse train. Consequently, most transmitters use sophisticated digital signal processing techniques to generate a discrete-time version of the input to the FM modulator.

The optimum detector is the trellis-based detector described in Subsection 2.3.3.1 and a number of reduced-complexity versions with very good performance have been developed.[6,7] When SOQPSK-TG was adopted, its interoperability with offset QPSK (OQPSK) was an important consideration. It is well known that CPM with a binary alphabet and with $h=5$ is closely related to OQPSK[8]. This relationship is illustrated by the eye diagrams formed by the inphase and quadrature components of SOQPSK-TG illustrated in Figure 2-5. In this plot, the equivalent OQPSK symbol time $T_S = 2T_b$ is used for the time axis. The figure shows that sampling the inphase and quadrature components of SOQPSK-TG at the instants corresponding to the maximum eye openings can be used to recover the data. Note that the time instants for the inphase and quadrature components are offset by $T_S/2$ relative to each other.
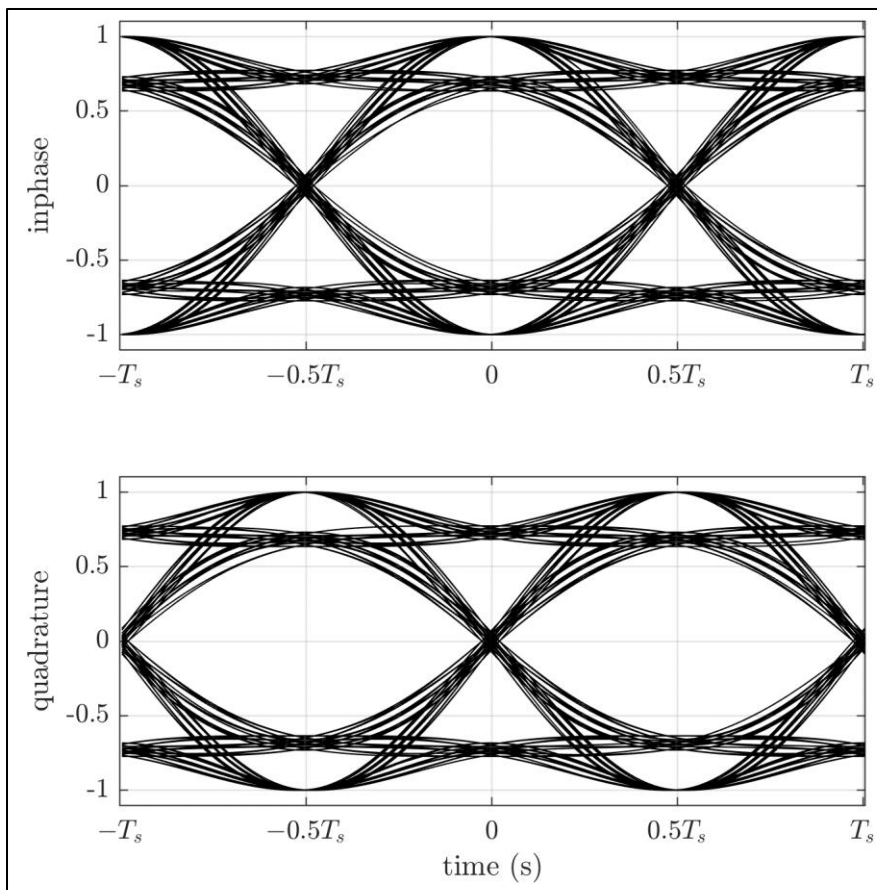
Figure 2-5.　　Eye Diagrams for the Inphase (Top) and Quadrature (Bottom) Components of SOQPSK-TG

For a generic CPM with a binary alphabet and $h=5$, the relationship to OQPSK follows from the fact that each binary symbol changes the CPM phase by $\pi/2$ rads. Because of the cumulative phase memory in CPM, the phase state must be tracked to recover the data. The

---

[6] Mark Geoghegan. "Implementation and Performance Results for Trellis Detection of SOQPSK." In *Proceedings of the International Telemetering Conference*, Las Vegas, NV, October 2001.

[7] Perrins, E. and M. Rice. "Reduced-Complexity Approach to Iterative Detection of Coded SOQPSK." *IEEE Transactions on Communications*, vol 55, no. 7, pp 1354-1362, July 2007.

[8] P. Laurent. "Exact and Approximate Construction of Digital Phase Modulations by Superposition of Amplitude Modulated Pulses (AMP)." *IEEE Transactions on Communications*, vol. 34, no. 2, pp. 150-160, February 1986.

precoder in Equation [2-17](#) removes the cumulative phase memory from SOQPSK-TG and permits symbol-by-symbol detection using an OQPSK detector with a detection filter in place of a matched filter.[9,10] The precoder converts the phase *shift* normally associated with a CPM symbol to an *absolute* phase as in OQPSK.

The benefits of the precoder (symbol-by-symbol detection) are achieved at the cost of a 90° phase ambiguity exists in the recovered carrier phase reference when using decision directed techniques. To allow correct detection in the presence of the 90° phase ambiguity, differential encoding is applied to the bits prior to the precoder given by Equation [2-17](#). The differential encoder[11] operates on user bit pairs (b_{2i}, b_{2i+1}) to produce a pair of differentially encoded bits $(\delta_{2i}, \delta_{2i+1})$. The differential encoding operation is defined by

$$\delta_{2i} = b_{2i} \oplus \bar{\delta}_{2i-1}$$
$$\delta_{(2i+1)} = b_{(2i+1)} \oplus \delta_{2i}$$

2-22

where the bits are their "logical values" $b_{2i}, b_{2i+1} \in \{0,1\}$, $\oplus$ is the Boolean exclusive or operation, and $\bar{\delta}_{2i-1}$ is the logical complement of δ_{2i-1}. The corresponding differential decoder must be applied to the bit decisions at the detector output. The differential decoder operates on pairs of differential encoded bits $(\delta_{2i}, \delta_{2i+1})$ to produce a pair of user bits (b_{2i}, b_{2i+1}). The differential decoder is defined by

$$b_{2i} = \delta_{2i} \oplus \bar{\delta}_{2i-1}$$
$$b_{2i+1} = \delta_{2i+1} \oplus \delta_{2i}$$

2-23

A block diagram illustrating the inclusion of the differential encoder in an SOQPSK-TG modulator is shown in [Figure 2-6](#).
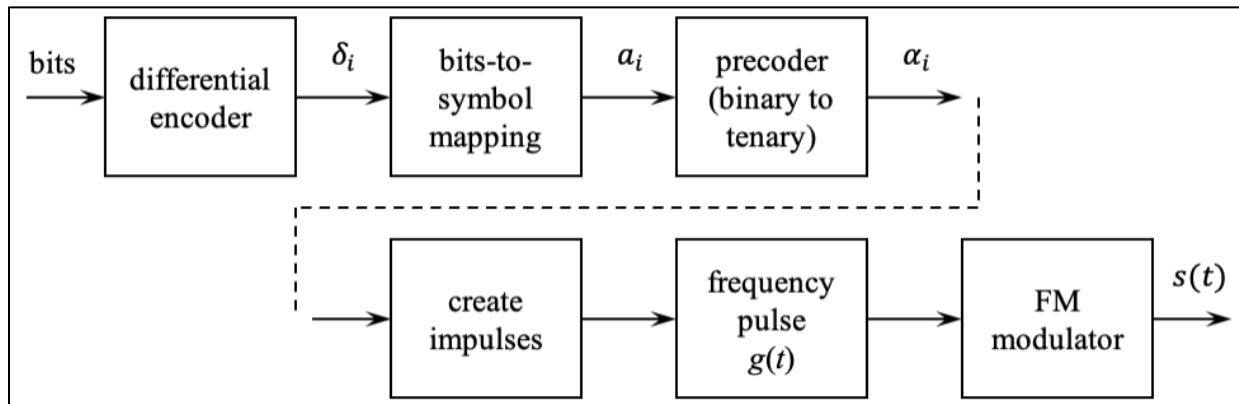
Figure 2-6.   Block Diagram of an SOQPSK-TG Modulator Showing the Placement of the Differential Encoder

[9] Mark Geoghegan. "Optimal Linear Detection of SOQPSK." In *Proceedings of the International Telemetering Conference*, San Diego, CA, October 2002.

[10] E. Perrins, "FEC Systems for Aeronautical Telemetry." *IEEE Transactions on Aerospace and Electronic Systems*, vol 49, no. 4, pp 2340-2352, October 2013.

[11] A more detailed description of the differential encoder and decoding, including some encoding and decoding examples, is found in [Appendix 2-B](#).

There is an alternative description[12] of SOQPSK-TG based on a longer frequency pulse but eliminates the need for the precoder (Equation 2-18) (and the resulting constrained ternary alphabet) and the differential encoder (Equation 2-22).

2.3.3.4 ARTM CPM

This modulation was introduced to this standard in 2007 as a more bandwidth-efficient alternative to SOQPSK-TG. It is a partial response CPM with a quaternary alphabet, two alternating modulation indexes, and a temporal raised-cosine frequency pulse. The CPM parameters of ARTM CPM are

$$\alpha_i \in \{-3, -1, +1, +3\} \text{ according to Table 2-5} \qquad \text{2-24}$$

$$h_i = \begin{cases} 4/16 & i \text{ even} \\ 5/16 & i \text{ odd} \end{cases} \qquad \text{2-25}$$

$$g(t) = \begin{cases} \dfrac{1}{6T_s}\left[1 - \cos\left(\dfrac{2\pi t}{3T_s}\right)\right] & 0 \le t \le 3T_s \\ 0 & \text{otherwise.} \end{cases} \qquad \text{2-26}$$

Table 2-5. ARTM CPM Dibit to Symbol Mapping	
Input Dibit $[b_{2i}, b_{2i+1}]$	Symbol value α_i
0 0	−3
0 1	−1
1 0	+1
1 1	+3

Because the symbols are quaternary, two bits (called a *dibit*) define a symbol. A new bit is input every T_b seconds. A quaternary symbol is output every $T_S = 2T_b$ seconds. A plot of the frequency pulse is shown in Figure 2-7. The frequency pulse spans $L=3$ symbol times and has area 1/2.

---

[12] Perrins, E. and M. Rice. "Unification of Signal Models for SOQPSK." In *Proceedings of the International Telemetering Conference*, Glendale, AZ, 5-8 November 2018.
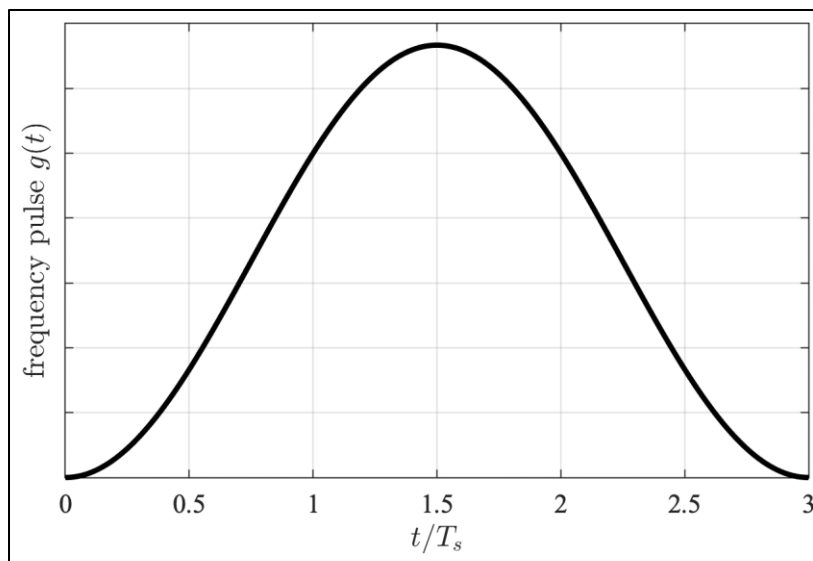
Figure 2-7.   The Frequency Pulse for ARTM CPM

The frequency pulse could be approximated by applying a continuous-time low-pass filter to an NRZ-L pulse train. Unfortunately, the alternating modulation indexes and strict spectral containment requirements render the approximate approach unusable. Consequently, transmitters use sophisticated digital signal processing techniques to generate a discrete-time version of the input to the FM modulator.

The optimum detector is the trellis-based detector described in Subsection 2.3.3.1. The trellis associated with the optimum detector possesses a large number of states. Reduced-complexity detectors for ARTM CPM have been described and analyzed.[13]

2.3.3.5   Data Randomization

The data input to the transmitter shall be randomized using either an encryptor that provides randomization or an Inter-Range Instrumentation Group (IRIG) 15-bit randomizer as described in Chapter 6 and Annex A.2. The purpose of the randomizer is to prevent degenerative data patterns from degrading data quality.

2.3.3.6   Bit Rate

Bit rate is defined as the over-the-air bit rate which includes any and all added overhead associated with coding. Without coding the input bit rate to the transmitter equals the output bit rate.

2.3.3.7   Transmitter Phase Noise

The sum of all discrete spurious spectral components (single-sideband) shall be less than −36 dBc. The continuous single-sideband phase noise power spectral density (PSD) shall be below the curve shown in Figure 2-8. The maximum frequency for the curve is one-fourth of the bit rate. For bit rates greater than 4 megabits per second (Mbps), the phase noise PSD shall be less than −100 dBc/hertz (Hz) between 1 MHz and one-fourth of the bit rate.

---

[13] Perrins, E. and M. Rice. "Reduced-complexity Detectors for Multi-h CPM in Aeronautical Telemetry." In *IEEE Transactions on Aerospace and Electronic Systems*, vol. 40, no. 1, pp. 286-300, January 2007.
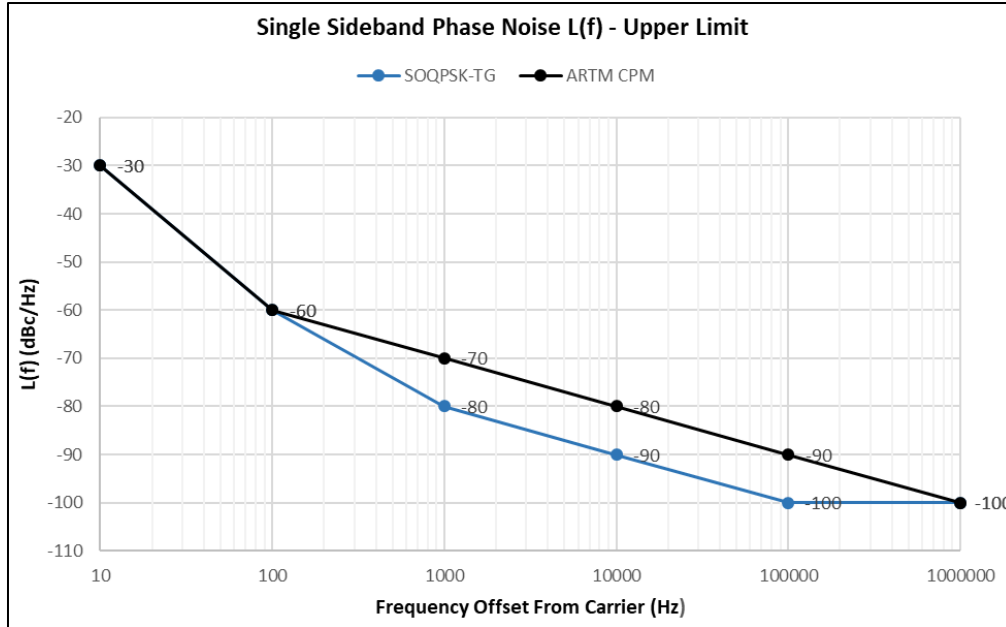
Figure 2-8.   Continuous Single-Sideband Phase Noise Power Spectral Density

2.3.3.8   Modulation Polarity

An increasing voltage at the input of an FM transmitter shall cause an increase in output carrier frequency. An increase in voltage at the input of a phase modulation (PM) transmitter shall cause an advancement in the phase of the output carrier. An increase in voltage at the input of an amplitude modulation (AM) transmitter shall cause an increase in the output voltage of the output carrier.

2.3.4   Spurious Emission and Interference Limits

Spurious[14] emissions from the transmitter case, through input and power leads, and at the transmitter RF output and antenna-radiated spurious emissions are to be within required limits shown in Military Standard (MIL-STD)-461,[15] CE106 with the following clarifications.

a. Harmonics (except the second and third) and all other spurious emissions shall be at least 80 dB down from the level of the fundamental, which is equal to −80 dBc.

b. The second and third harmonics shall be suppressed to a limit of −25 dBm.

c. Spurious emission limits are not applicable within the bandwidth of the transmitted signal defined in Subsection 2.3.6.

d. Testing shall occur with a modulated carrier.

2.3.4.1   Transmitter-Antenna System Emissions

Emissions from the antenna are of primary importance. For example, a tuned antenna may or may not attenuate spurious frequency products produced by the transmitter, and an

---

[14] Any unwanted signal or emission is spurious whether or not it is related to the transmitter frequency (harmonic).
[15] Department of Defense. "Requirements for the Control of Electromagnetic Interference Characteristics of Subsystems and Equipment." MIL-STD-461-G. 11 December 2015. May be superseded by update. Retrieved 17 May 2021. Available at https://quicksearch.dla.mil/qsDocDetails.aspx?ident_number=35789.

antenna or multi-transmitter system may generate spurious outputs when a pure signal is fed to its input. The transmitting pattern of such spurious frequencies is generally different from the pattern at the desired frequency. Antenna-radiated spurious outputs shall be no greater than 320 µV/meter at 30 meters in any direction, which is equal to −25 dBm when cable losses plus antenna gain are assumed to be unity.

WARNING	Spurious levels of −25 dBm may severely degrade performance of sensitive receivers whose antennas are located in close proximity to the telemetry transmitting antenna. Therefore, lower spurious levels may be required in certain frequency ranges, such as near Global Positioning System frequencies.

2.3.4.2 Conducted and Radiated Interference

Interference (and the RF output itself) radiated from the transmitter or fed back into the transmitter power, signal, or control leads could interfere with the normal operation of the transmitter or the antenna system to which the transmitter is connected. All signals conducted by the transmitter's leads (other than the RF output cable) in the range of 150 kilohertz (kHz) to 50 MHz and all radiated fields in the range of 150 kHz to 10 gigahertz (GHz) (or other frequency ranges as specified) must be within the limits of the applicable standards or specifications.

2.3.5 Operational Flexibility

Each transmitter shall be capable of operating at all frequencies within its allocated band without design modification.[16]

2.3.6 Modulated Transmitter Bandwidth[17]

Telemetry applications covered by this standard shall use 99-percent power bandwidth to define occupied bandwidth and −25 dBm bandwidth as the primary measure of spectral efficiency. The −25 dBm bandwidth is the minimum bandwidth that contains all spectral components that are −25 dBm or larger. A power level of −25 dBm is exactly equivalent to an attenuation of the transmitter power by $55 + 10 \times \log(P)$ dBc where P is the transmitter power expressed in watts. The spectra are assumed symmetrical about the transmitter's center frequency unless specified otherwise. All spectral components larger than $-(55 + 10 \times \log(P))$ dBc at the transmitter output must be within the spectral mask calculated using the following equation:

$$M(f) = K + 90 \log R - 100 \log|f - f_c|; |f - f_c| \geq \frac{R}{m} \qquad \text{2-27}$$

where $M(f)$ = power relative to P (i.e., units of dBc) at frequency f (MHz)

  K = −20 for analog signals
   = −28 for binary signals
   = −61 for SOQPSK-TG
   = −73 for ARTM CPM

  f_c = transmitter center frequency (MHz)

---

[16] The intent is that fixed-frequency transmitters can be used at different frequencies by changing crystals or other components. All applicable performance requirements will be met after component change.

[17] These bandwidths are measured using a spectrum analyzer with the following settings: 30-kHz resolution bandwidth, 300-Hz video bandwidth, and no max hold detector or averaging.

R = bit rate (Mbps) for digital signals or ($\Delta f + f_{max}$) (MHz) for analog FM signals

m = number of states in modulating signal

    m = 2 for binary signals

    m = 4 for quaternary signals and analog signals

Δf = peak deviation

f_{max} = maximum modulation frequency

Note that the mask in this standard is different than the masks contained in earlier versions of the Telemetry Standards. Equation 2-27 does not apply to spectral components separated from the center frequency by less than *R/m*. The −25 dBm bandwidth is not required to be narrower than 1 MHz. Binary signals include all modulation signals with two states while quaternary signals include all modulation signals with four states (quadrature phase shift keying [QPSK] is one example of four-state signals). Section A.6 contains additional discussion and examples of this spectral mask.

2.3.7 Valid Center Frequencies Near Telemetry Band Edges

The telemetry bands, as specified, start and stop at discrete frequencies. Telemetry transmitters transmitting PCM/FM, SOQPSK-TG, or ARTM CPM, even with optimal filtering, do not have discrete start and stop frequencies. In order to determine a valid carrier frequency, the transmitter power, modulation scheme, and data rate must be known. The distance, in frequency, from the point in which the spectral masks, as described in Subsection 2.3.6, intersect the absolute value of −25 dBm equals the amount in which the transmitter carrier frequency must be from the band edge frequency. Subsection A.11 contains additional discussion and examples of center frequency determination when operating near telemetry band edges.

2.4 Telemetry Receiver Systems

As a minimum, receiver systems shall have the following characteristics.

2.4.1 Spurious Emissions

The RF energy radiated from the receiver itself or fed back into the power supply, and/or the RF input, output, and control leads in the range from 150 kHz to 10 GHz shall be within the limits specified in MIL-STD-461. The receiver shall be tested in accordance with MIL-STD-461 or RCC Document 118, Volume II.[18] Other applicable standards and specifications may be used in place of MIL-STD-461, if necessary.

2.4.2 Frequency Tolerance

The accuracy of all local oscillators within the receiver shall be such that the conversion accuracy at each stage and overall is within ±0.001 percent of the indicated tuned frequency under all operating conditions for which the receiver is specified.

2.4.3 Receiver Phase Noise

The sum of all discrete spurious spectral components (single-sideband) shall be less than −39 dBc. The continuous single-sideband phase noise PSD shall be 3 dB below the curve shown in Figure 2-8. The maximum frequency for the curve in Figure 2-8 is one-fourth of the bit rate.

---

[18] Range Commanders Council. *Test Methods for Telemetry Systems and Subsystems Volume 2*. RCC 118-20. June 2020. May be superseded by update. Retrieved 17 May 2021. Available at https://www.trmc.osd.mil/wiki/x/fIu8Bg.

For bit rates greater than 4 Mbps, the phase noise PSD shall be less than −103 dBc/Hz between 1 MHz and one-fourth of the bit rate.

2.4.4   Spurious Responses
        Rejection of any frequency other than the one to which the receiver is tuned shall be a minimum of 60 dB referenced to the desired signal over the range 150 kHz to 10 GHz.
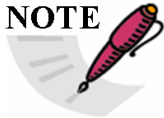
2.4.5   Operational Flexibility
        All ground-based receivers shall be capable of operating over the entire band for which they are designed. External down-converters may be either intended for the entire band or a small portion but capable of retuning anywhere in the band without modification.

2.4.6   Intermediate Frequency Bandwidths
        The standard receiver intermediate frequency (IF) bandwidths are shown in Table 2-6. These bandwidths are separate from and should not be confused with post-detection low-pass filtering that receivers provide.[19] The ratio of the receiver's −60 dB bandwidth to the −3 dB bandwidth shall be less than 3 for new receiver designs.

Table 2-6. Standard Receiver Intermediate Frequency Bandwidths		
300 kHz	1.5 MHz	6 MHz
500 kHz	2.4 MHz	10 MHz
750 kHz	3.3 MHz	15 MHz
1000 kHz	4.0 MHz	20 MHz

NOTE	1. For data receivers, the IF bandwidth should typically be selected so that 90 to 99 percent of the transmitted spectrum is within the receiver 3 dB bandwidth. In most cases, the optimum IF bandwidth will be narrower than the 99 percent power bandwidth.
	2. Bandwidths are expressed at the points where response is 3 dB below the response at the design center frequency, assuming that passband ripple is minimal, which may not be the case. The 3-dB bandwidth is chosen because it closely matches the noise bandwidth of a "brick-wall" filter of the same bandwidth. The "optimum" bandwidth for a specific application may be other than that stated here. Ideal IF filter response is symmetrical about its center frequency; in practice, this may not be the case.
	3. Not all bandwidths are available on all receivers or at all test ranges. Additional receiver bandwidths may be available at some test ranges, especially if the range has receivers with digital IF filtering

2.4.7   C-band Downconversion
        For telemetry receive systems employing C-band downconversion, the following mapping of C-band RF to C-band IF frequencies is recommended for the lower C and middle C bands. This downconversion scheme utilizes a high-side local oscillator frequency of 5550 MHz

---

[19] In most instances, the output low-pass filter should *not* be used to "clean up" the receiver output prior to use with demultiplexing equipment.

to minimize the potential of mixing products interfering with received telemetry signals. Additionally, using a standardized approach fosters interoperability between manufacturers of telemetry antenna systems employing downconversion and manufacturers of telemetry receivers with C-IF tuners.

No recommendation will be made at this point for the downconversion of the upper C band (5925-6700 MHz).

Examples:

C-IF Frequency = (5550 MHz − C-RF Frequency)
1150 MHz = (5550 MHz − 4400 MHz)
610 MHz = (5550 MHz − 4940 MHz)
459 MHz = (5550 MHz − 5091 MHz)
400 MHz = (5550 MHz − 5150 MHz)

2.5 Codes for Telemetry Systems

2.5.1 Low-Density Parity-Check Code
Forward error correction (FEC) is a way of adding additional information to a transmitted bit stream in order to decrease the required signal-to-noise ratio to the receiver for a given bit error rate (BER). Low-density parity-check (LDPC) code is a block code, meaning that a block of information bits has parity added to them in order to correct for errors in the information bits. The term "low-density" stems from the parity check matrix containing mostly 0's and relatively few 1's. This specific LDPC variant comes from the satellite link community and is identical to the Accumulate-Repeat-4-Jagged-Accumulate code described by the Consultative Committee for Space Data Systems (CCSDS) standard 131.1-O-2-S.1,[20] which describes nine different LDPC codes with different coding rates (rate 1/2, 2/3, 4/5) and information block sizes (1024, 4096, 16384). In the trade between the transmission channel characteristics, bandwidth efficiency, coding gain, and block size all three rates and block sizes 1024 and 4096 are considered in this standard. Additional information on this LDPC code is contained in Appendix 2-D.

2.5.2 Space-Time Code
As the name suggests, this code uses space diversity and time diversity to overcome the two-antenna problem, which is characterized by large variances in the antenna gain pattern from a test article caused by transmitting the same telemetry signal time through two transmit antennas. These signals are typically delayed in time and have differing amplitudes. The space-time code (STC) in this standard applies to only SOQPSK-TG modulation. The input bit stream is space-time coded, resulting in two parallel bit streams that then have a pilot sequence added to each at fixed bit intervals (or blocks). These encoded/pilot-added streams are then individually modulated through phase-locked transmitters to a carrier using SOQPSK-TG modulation, power amplified, then connected to a top and bottom antenna. The job of estimating frequency offset, delays, gains, and phase shifts due to the transmission channel then space-time decode the signal is done with the STC receiver. Additional information on the STC is contained in Appendix 2-E.

---

[20] Consultative Committee for Space Data Systems. *Low Density Parity Check Codes for Use in Near-Earth and Deep Space Applications*. Standard CCSDS 131.1-O-2-S. September 2007. Rescinded. Retrieved 17 May 2021. Available at https://public.ccsds.org/Pubs/131x1o2e2s.pdf.

2.6   Randomization Methods for Telemetry Systems

2.6.1   Introduction
        The following randomization and de-randomization methods are recommended for wireless serial streaming telemetry data links. The choice of randomization method used should be based on whether or not a self-synchronizing randomizer is required for the application.

2.6.2   Randomizer Types

2.6.2.1   Self-Synchronizing Randomizers
        Self-synchronizing randomizers, such as the traditional IRIG randomizer described in Annex A.2, work best when there are no known identifiers in the bit stream to aid in synchronizing the de-randomizer. This type of de-randomizer has the characteristic of creating additional bit errors when a bit error is received at the de-randomizer input. For this randomizer a single bit error at the input will create an additional two bit errors in the output stream. This BER extension will cause a degradation in detection efficiency of the link of approximately 0.5 dB.

2.6.2.2   Non-Self-Synchronizing Randomizers
        Non-self-synchronizing randomizers, such as the CCSDS randomizer described in Appendix 2-D, do not create additional bit errors when a bit error is received at the de-randomizer input. Therefore there is no extension of BER; however, these types of randomizers need to be synchronized with the incoming bit stream. This is usually accomplished through the use of pilot bits or synchronization markers in the data stream to aid in synchronization. Performance of this type of randomizer will exceed that of a self-synchronizing randomizer lending itself as a better choice for coded links or links requiring data-aided synchronization.

2.6.3   Randomizer Application
        As defined in Appendix 2-D, CCSDS randomization should be used for coded links such as LDPC links or links exhibiting a block structure with synchronization markers.

        Traditional IRIG randomization as defined in Annex A.2 should be used for non-encrypted links that are absent of synchronization markers or do not contain markers of any type. Encrypted telemetry links do not require randomization.

2.7   Data Quality Metrics and Data Quality Encapsulation

        A reliable metric for estimating data quality can be very useful when controlling telemetry data processing equipment, such as Best Source Selectors, that require an understanding of received data quality in order to operate effectively. To accomplish this, a standardized method for estimating bit error probability (BEP) is needed. In addition to the metric, a standardized method for transporting the metric with the associated data is required. Appendix 2-G provides a standard for a data quality metric (DQM), determined in the telemetry receiver demodulator, and a standard for data quality encapsulation (DQE) allowing for transport of the received telemetry data and associated DQM.

2.8   Interference Protection Criteria for Aeronautical Mobile Telemetry Systems

        Aeronautical mobile telemetry (AMT) ground stations use very high gain directional antenna systems that are sensitive to interference from other RF communication systems.

Without appropriate interference protection, these systems could be severely impacted or even rendered useless for mission support. To prevent this from happening, appropriate interference protection criteria (IPC) are needed.

Table 2-7 lists the acceptable power flux density (PFD) levels for interference in each telemetry band. These levels are based on the well-established and accepted IPC contained in International Telecommunications Union Radio Service (ITU-R) Recommendation M.1459[21] (Rec M.1459). These IPCs provide AMT protection for aggregate interference from satellites and terrestrial emitters as a function of the angle of arrival α of the interfering signal(s) at or above the horizon derived using the methodology given in Annex A of Rec M.1459.

Table 2-7.	Interference Protection Criteria by Band and Angle of Arrival	
L band, from 1435 – 1535 MHz		
−181.0	dB(W/m^2) in 4 kHz	for $0 \leq \alpha \leq 4°$
−193.0 + 20 log α	dB(W/m^2) in 4 kHz	for $4 < \alpha \leq 20°$
−213.3 + 35.6 log α	dB(W/m^2) in 4 kHz	for $20 < \alpha \leq 60°$
−150.0	dB(W/m^2) in 4 kHz	for $60 < \alpha \leq 90°$
Upper L band, from 1755 – 1855 MHz		
−181.0	dB(W/m^2) in 4 kHz	for $0° \leq \alpha \leq 3°$
−190.878 + 21.948 log α	dB(W/m^2) in 4 kHz	for $3° < \alpha \leq 15°$
−185.722 + 18.286 log α	dB(W/m^2) in 4 kHz	for $15° < \alpha \leq 60°$
−153.7	dB(W/m^2) in 4 kHz	for $60° < \alpha \leq 90°$
Lower S band, from 2200 – 2290 MHz		
−180.0	dB(W/m^2) in 4 kHz	for $0° \leq \alpha \leq 2°$
−186.613 + 21.206 log α	dB(W/m^2) in 4 kHz	for $2° < \alpha \leq 15°$
−161	dB(W/m^2) in 4 kHz	for $15° < \alpha \leq 90°$
Upper S band, from 2310 – 2390 MHz		
−180.0	dB(W/m^2) in 4 kHz	for $0° \leq \alpha \leq 2°$
−187.5 + 23.66 log α	dB(W/m^2) in 4 kHz	for $2° < \alpha \leq 11.5°$
−162	dB(W/m^2) in 4 kHz	for $11.5° < \alpha \leq 90°$
Lower C band, from 4400 – 4940 MHz		
−178.0	dB(W/m^2) in 4 kHz	for $0° \leq \alpha \leq 1°$
−180.333 + 2.333 α	dB(W/m^2) in 4 kHz	for $1° < \alpha \leq 4°$
−171.0	dB(W/m^2) in 4 kHz	for $4° < \alpha \leq 90°$
Middle C band, from 5091 – 5150 MHz		
−178.0	dB(W/m^2) in 4 kHz	for $0° \leq \alpha \leq 1°$
−180.0 + 2.0 α	dB(W/m^2) in 4 kHz	for $1° < \alpha \leq 3°$
−174.0	dB(W/m^2) in 4 kHz	for $3° < \alpha \leq 90°$
Upper C band, from 5925 – 6700 MHz		
−178.0	dB(W/m^2) in 4 kHz	for $0° \leq \alpha \leq 1°$

---

[21] International Telecommunication Union. "Protection criteria for telemetry systems in the aeronautical mobile service…" ITU-R Recommendation M.1459. May 2000. May be superseded by update. Retrieved 17 May 2021. Available at https://www.itu.int/rec/R-REC-M.1459-0-200005-I/en.

Table 2-7.	Interference Protection Criteria by Band and Angle of Arrival	
$-181.6 + 3.6\,\alpha$	dB(W/m^2) in 4 kHz	for $1° < \alpha \le 2°$
-174.4	dB(W/m^2) in 4 kHz	for $2° < \alpha \le 90°$

Appendix 2-F provides additional explanation and example calculations to aid in understand the application of these IPCs for different interference scenarios.

APPENDIX 2-A

Frequency Considerations for Telemetry

A.1.   Purpose

This appendix was prepared with the cooperation and assistance of the Range Commanders Council (RCC) Frequency Management Group. This appendix provides guidance to telemetry users for the most effective use of the telemetry bands. Coordination with the frequency managers of the applicable test ranges and operating areas is recommended before a specific frequency band is selected for a given application. Government users should coordinate with the appropriate Area Frequency Coordinator and commercial users should coordinate with the AFTRCC. A list of the points of contact can be found in the NTIA manual (NTIA 2015).

A.2.   Scope

This appendix is to be used as a guide by users of telemetry frequencies at Department of Defense (DoD)-related test ranges and contractor facilities. The goal of frequency management is to encourage maximal use and minimal interference among telemetry users and between telemetry users and other users of the electromagnetic spectrum.

A.2.a.   Definitions

The following terminology is used in this appendix.

Allocation (of a Frequency Band). Entry of a frequency band into the Table of Frequency Allocations[22] for use by one or more radio communication services or the radio astronomy service under specified conditions.

Assignment (of a Radio Frequency or Radio Frequency Channel). Authorization given by an administration for a radio station to use an RF or RF channel under specified conditions.

Authorization. Permission to use an RF or RF channel under specified conditions.

Certification. The Military Command, Control, Communications, and Computers Executive Board's (MC4EB) process of verifying that a proposed system complies with the appropriate rules, regulations, and technical standards.

J/F 12 Number. The identification number assigned to a system by the MC4EB after the Application for Equipment Frequency Allocation (DD Form 1494) is approved; for example, J/F 12/6309 (sometimes called the J-12 number).

Resolution Bandwidth. The −3 dB bandwidth of the measurement device.

A.2.b.   Modulation methods

A.2.b(1)   Traditional Modulation Methods

The traditional modulation methods for aeronautical telemetry are FM and PM. The PCM/FM method has been the most popular telemetry modulation since around 1970. The RF

---

[22] The definitions of the radio services that can be operated within certain frequency bands contained in the radio regulations as agreed to by the member nations of the International Telecommunications Union. This table is maintained in the United States by the Federal Communications Commission and the NTIA.

signal is typically generated by filtering the baseband NRZ-L signal and then frequency modulating a VCO. The optimum peak deviation is 0.35 times the bit rate and a good choice for a premodulation filter is a multi-pole linear phase filter with bandwidth equal to 0.7 times the bit rate. Both FM and PM have a variety of desirable features but may not provide the required bandwidth efficiency, especially for higher bit rates.

A.2.b(2)   Improved Bandwidth Efficiency

When better bandwidth efficiency is required, the standard modulation methods for digital signal transmission are SOQPSK-TG and ARTM CPM. These methods offer constant characteristics and is compatible with nonlinear amplifiers with minimal spectral regrowth and minimal degradation of detection efficiency. Modulation method SOQPSK-TG requires the use of the differential encoder described in Appendix 2-B. All of these bandwidth-efficient modulation methods require the data to be randomized either with the IRIG randomizer or through encryption.

A.2.c. Other Notations

The following notations are used in this appendix. Other references may define these terms slightly differently.

a. **B99% -** Bandwidth containing 99% of the total power.

b. **B$_{-25dBm}$ -** Bandwidth containing all components larger than −25 dBm.

c. **B$_{-60dBc}$ -** Bandwidth containing all components larger than the power level that is 60 dB below the unmodulated carrier power.

d. **dBc** - Decibels relative to the power level of the unmodulated carrier.

e. **f$_c$** - Assigned center frequency.

A.3.   Authorization to Use a Telemetry System

All RF emitting devices must have approval to operate in the US&P via a frequency assignment unless granted an exemption by the national authority. The NTIA is the President's designated national authority and spectrum manager. The NTIA manages and controls the use of RF spectrum by federal agencies in US&P territory. Obtaining a frequency assignment involves the two-step process of obtaining an RF spectrum support certification of major RF systems design, followed by an operational frequency assignment to the RF system user. These steps are discussed below and further explained in RCC 120 Appendix A.[23]

A.3.a. RF Spectrum Support Certification

All major DoD RF systems used by federal agencies must be submitted to the NTIA, via the Interdepartment Radio Advisory Committee, for system review and spectrum support certification prior to committing funds for acquisition and procurement. During the system review process, compliance with applicable standards, allocation tables, rules, and regulations is checked. For DoD agencies and for support of DoD contracts, this is accomplished via the

---

[23] Range Commanders Council. "Application for Equipment Frequency Allocation for Aeronautical Mobile Telemetry Systems." In *Telemetry Systems Radio Frequency Handbook*, Appendix A. RCC 120-21. July 2021. May be superseded by update. Retrieved July 10 2021. Available at https://www.trmc.osd.mil/wiki/x/iYu8Bg.

submission of technical data describing the system that will operate in the RF spectrum to the MC4EB. Noncompliance with standards, tables, rules, or regulations can result in denial of support, limited support, or support on an unprotected non- priority basis. All DoD RF users must obtain frequency assignments for any RF system (even if not considered major). This assignment is accomplished by submission of frequency use proposals through the appropriate frequency management offices. Frequency assignments may not be granted for major systems that have not obtained spectrum support certification.

A.3.a(1)   Frequency Allocation

Telemetry systems must normally operate within the frequency bands designated for their use in the Table of Frequency Allocations. With sufficient justification, use of other bands may at times be permitted, but the certification process is much more difficult. If certification is granted on a noninterference basis to incumbent users, the local frequency manager is often unable to grant assignments because of interference to incumbent users.

a.   Telemetry Bands

Air and space-to-ground telemetering is allocated in the ultra-high frequency (UHF) bands 1435 to 1535, 2200 to 2290, and 2310 to 2390 MHz (commonly known as the lower L-band, the lower S-band, and the upper S-band) and in the super-high frequency (SHF) bands 4400 to 4940 and 5091 to 5150 MHz (commonly known as lower C-band and middle C-band). Other mobile bands, such as 1780-1850 MHz, can also be used at many test ranges. Since these other bands are not considered a standard telemetry band per this document, potential users must coordinate, in advance, with the individual range(s) and ensure use of this band can be supported at the subject range(s) and that their technical requirements will be met.

b.   Very High Frequency Telemetry

The very-high frequency (VHF) band, 216-265 MHz, was used for telemetry operations in the past. Telemetry bands were moved to the UHF bands as of 1 January 1970 to prevent interference to critical government land mobile and military tactical communications. Telemetry operation in this band is strongly discouraged and is considered only on an exceptional case-by-case basis. Refer to the Table of Frequency Allocations within the NTIA Red Book.

A.3.a(2)   Technical Standards

The MC4EB and the NTIA review proposed telemetry systems for compliance with applicable technical standards. For the UHF and SHF telemetry bands, the current revisions of the following standards are considered applicable:

   a.   RCC Document IRIG 106, Telemetry Standards;

   b.   MIL-STD-461;

   c.   NTIA Manual of Regulations and Procedures for Federal Radio Frequency Management (also referred to as the NTIA Red Book).

Applications for certification are also thoroughly checked in many other ways, including necessary and occupied bandwidths, modulation characteristics, reasonableness of output power, correlation between output power and amplifier type, and antenna type and characteristics. The associated receiver normally must be specified or referenced. The characteristics of the receiver and transmit and receive antennas are also verified.

A.3.b. Frequency Authorization

Spectrum certification of a telemetry system verifies that the system meets the technical requirements for successful operation in the electromagnetic environment; however, a user is not permitted to radiate with the telemetry system before requesting and receiving a specific frequency assignment. The assignment process considers when, where, and how the user plans to radiate. Use of the assignments is tightly scheduled by and among the individual ranges to make the most efficient use of the limited telemetry RF spectrum and to ensure that one user does not interfere with other users.

A.4.   Frequency Usage Guidance

Frequency usage is controlled by scheduling in the areas where the tests will be conducted. Figure A-1 displays the modulated spectrum for the uncoded modulation methods of PCM/FM, SOQPSK-TG, and ARTM CPM. Also considered are the coded waveforms of SOQPSK-STC, SOQPSK-LDPC, and SOQPSK-STC/LDPC. The spectra for these coded waveforms are identical to uncoded SOQPSK except for the occupied bandwidth.
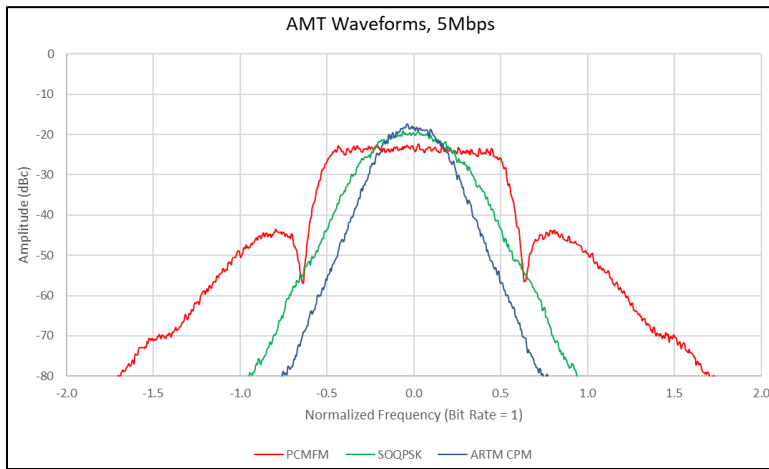
Figure A-1.   Spectra of 5-Mbps PCM/FM, SOQPSK-TG, and ARTM CPM Signals

Coded waveforms increase the over-the-air bit rate and thus the transmitted bandwidth. This increase is due to the coding overhead added by each coding scheme. The following recommendations are based on extensive testing coupled with good engineering practice for scheduling spectrum usage. It is assumed that the occupied bandwidth of the waveforms fits within the telemetry band of interest in all cases.

A.4.a. Minimum Frequency Separation

The minimum required frequency separation can be calculated using Equation A-1.

$$\Delta F_0 = a_s n_s R_s + a_i n_i R_i \qquad\qquad \text{A-1}$$

where ΔF_0 = the minimum required center frequency separation in MHz;
R_s = bit rate of desired **s**ignal in Mbps;
R_i = bit rate of **i**nterfering signal in Mbps;
a_s = spacing coefficient determined by the desired **s**ignal type;

a_i = spacing coefficient determined by the **i**nterfering signal type and waveform characteristics;

n_s = over-the-air bit rate multiplier for the desired **s**ignal;

n_i = over-the-air bit rate multiplier for the **i**nterfering signal.

When neither signal is coded, use the spacing coefficients in Table A-1. The over-the-air bit rate multiplier for the desired and interfering signals is 1 for uncoded waveforms.

Table A-1.   Coefficients for Minimum Frequency Separation Calculation for Uncoded Waveforms

Modulation Type	a_s	a_i
PCM/FM	0.80	0.95
SOQPSK-TG	0.60	0.45
ARTM CPM	0.55	0.30

When coded waveforms are the desired signal, the same equation (Equation A-1) for calculating the minimum frequency separation is used but with a different value of a_i depending upon the interfering signal per Table A-2. This places the interfering signal closer to the coded desired signal. In addition, the appropriate over-the-air bit rate multiplier n_s and n_i for each signal should also be used per Table A-3.

Table A-2.   Coefficients for Minimum Frequency Separation Calculation for Coded Waveforms

Modulation-Coding Type	a_s	a_i
PCM/FM		0.75
SOQPSK-TG		0.35
ARTM CPM		0.25
SOQPSK-STC	0.60	
SOQPSK-LDPC	0.60	
SOQPSK-STC/LDPC	0.60	

Table A-3.   Multipliers for Over-The-Air Bit Rate Calculation

Modulation-Coding Type	Multiplier n_s, n_i
PCM/FM, SOQPSK-TG, ARTM CPM	1
SOQPSK-STC	26/25
SOQPSK-LDPC Code Rate $r = 4/5$	21/16
SOQPSK-LDPC Code Rate $r = 2/3$	25/16
SOQPSK-LDPC Code Rate $r = 1/2$	33/16
SOQPSK-STC/LDPC $r = 4/5$	273/200
SOQPSK-STC/LDPC $r = 2/3$	13/8
SOQPSK-STC/LDPC $r = 1/2$	429/200

The minimum spacing needs to be calculated for the desired signal and the interferer and vice versa. The spacing factors have subscripts of s for signal and i for interferer. The required frequency spacing from the interferer, a_i, is directly related to the power spectrum of the interfering signal. The values for a_s are a function of the effective detection filter bandwidths, the adjacent channel interference resistance of the desired signal modulation and coding method, and the type of detector employed within the receiver. The values for a_s and a_i are slightly conservative for most cases and assume the receiver being used does not have spurious responses that cause additional interference. The main assumptions are as follows:

a. The NRZ PCM/FM signals are assumed to be premodulation filtered with a multi-pole Bessel filter with −3 dB point of exactly 0.7 times the bit rate and the peak deviation of exactly 0.35 times the bit rate. The modulation index $h = 0.7$.

b. With the stipulation given in a., a multi-symbol detector is assumed for NRZ PCM/FM.

c. The receiver IF filter is assumed to be no narrower than 1.5 times the bit rate and no wider than 2 times the bit rate and provides at least 6 dB of attenuation of the interfering signal.

d. The interfering signal is assumed to be no more than 20 dB stronger than the desired signal. resulting in a carrier-to-interferer ratio **C/I ≤ −20 dB**.

e. The receiver is assumed to be operating in linear mode and not in saturation; no significant intermodulation products or spurious responses are present.

The following examples are grouped into two categories that correspond to Table A-1, Table A-2, and Table A-3. The first category is for calculating the required spacing when only uncoded waveforms are being scheduled. For these waveforms the bit rate multiplier is 1; therefore, the bit rate equals the over-the-air bit rate. The second category is for calculating the required spacing when there are both uncoded and coded waveforms being scheduled. In each example the desired and interfering signals are swapped for the spacing calculation with the larger resulting spacing being chosen. The reason for this is that both signals are desired, just by different users.

Uncoded Waveform Examples

1. Desired Signal: 5 Mbps PCM/FM; Interfering Signal: 3 Mbps SOQPSK-TG

   Desired Signal: 3 Mbps SOQPSK-TG; Interfering Signal: 5 Mbps PCM/FM

   $0.85*1*5 + 0.45*1*3 = 5.6$ MHz $0.60*1*3 + 0.95*1*5 = 6.6$ MHz

The larger value is 6.6 MHz; center frequencies are assigned in 1 MHz steps so the minimum spacing is 7 MHz. An example of this minimum frequency spacing is shown in Figure A-2.
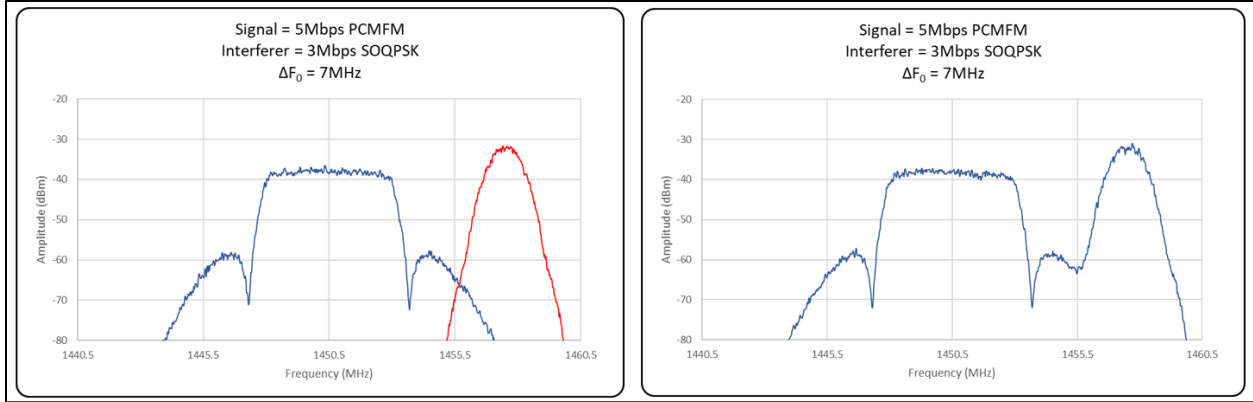
Figure A-2.   Center Frequency Spacing 5 Mbps PCM/FM and 3 Mbps SOQPSK-TG

2.   Desired Signal: 12.5 Mbps SOQPSK-TG; Interfering Signal: 6 Mbps ARTM CPM

Desired Signal: 6 Mbps ARTM CPM; Interfering Signal: 12.5 Mbps SOQPSK-TG

$0.60*1*12.5 + 0.30*1*6 = 9.3$ MHz $0.55*1*6 + 0.45*1*12.5 = 8.9$ MHz

The larger value is 9.3 MHz; center frequencies are assigned in 1 MHz steps so the minimum spacing is 10 MHz. An example of this minimum frequency spacing is shown in Figure A-3.
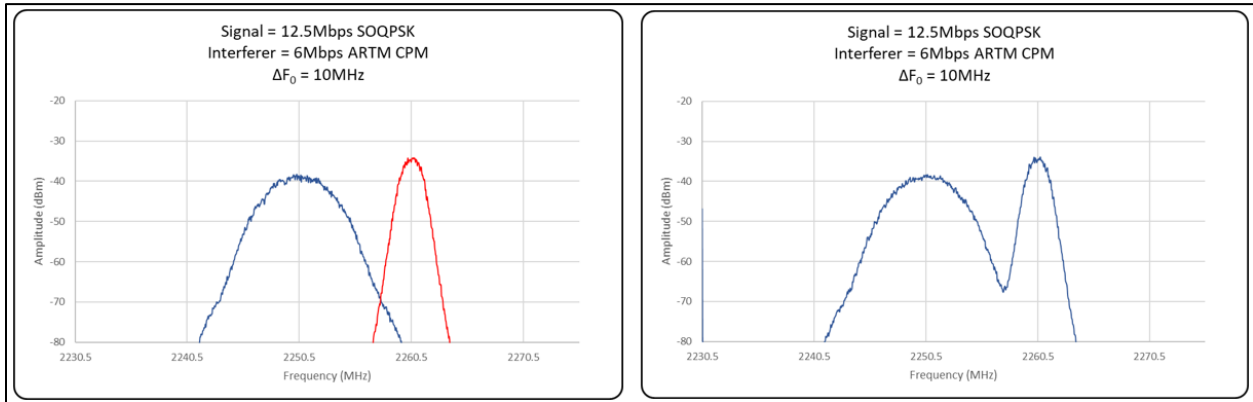
Figure A-3.   Center Frequency Spacing 12.5 Mbps PCM/FM and 6 Mbps ARTM CPM

3.   Desired Signal: 4.3 Mbps SOQPSK-TG; Interfering Signal: 7.25 Mbps SOQPSK-TG

Desired Signal: 7.25 Mbps SOQPSK-TG; Interfering Signal: 4.3 Mbps SOQPSK-TG

$0.60*1*4.3 + 0.45*1*7.25 = 5.8$ MHz $0.60*1*7.25 + 0.45*1*4.3 = 6.3$ MHz

The larger value is 6.3 MHz; center frequencies are assigned in 1 MHz steps, so the minimum spacing is 7 MHz. An example of this minimum frequency spacing is shown in Figure A-4.
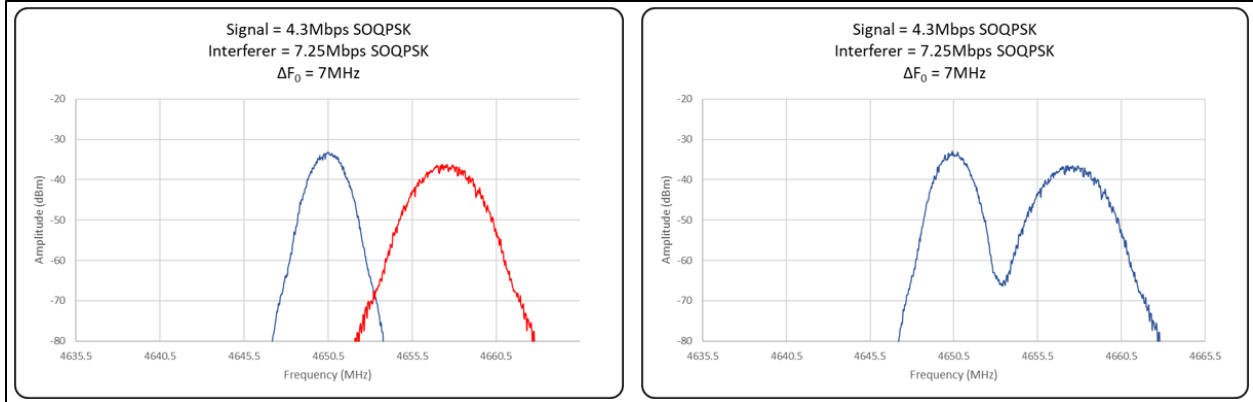
Figure A-4.   Center Frequency Spacing 4.3 Mbps SOQPSK-TG and 7.25 Mbps SOQPSK-TG

Coded Waveform Examples

When calculating the minimum frequency separation using the spacing coefficients in Table A-2, note that the interfering signal can be placed closer in frequency when the desired signal is coded. This is reflected in the spacing factor a_i for the interfering signal decreasing in value when compared to the uncoded case (Table A-1). The bit rate r used in these calculations is the over-the-air bit rate after coding is applied. Table A-3 gives the multipliers used in determining the over-the-air bit rate for each possible combination of modulation and coding scheme.

1.   Desired Signal: 8 Mbps SOQPSK-LDPC (r=4/5, k=1024); Interfering Signal: 4.2 Mbps PCM/FM

     Desired Signal: 4.2 Mbps PCM/FM; Interfering Signal: 8 Mbps SOQPSK-LDPC (r=4/5, k=1024)

     $0.60*(21/16)*8 + 0.75*1*4.2 = 9.45$ MHz $0.80*1*4.2 + 0.45*(21/16)*8 = 8.09$ MHz[1]

The largest value is 9.45 MHz; frequencies are assigned in 1 MHz steps so the minimum spacing is 10 MHz. [1] In this calculation, the spacing coefficient of 0.45 for SOQPSK-TG in Table A-1 should be used for the coded interfering signal as the desired signal is uncoded. An example of this minimum frequency spacing is shown in Figure A-5.
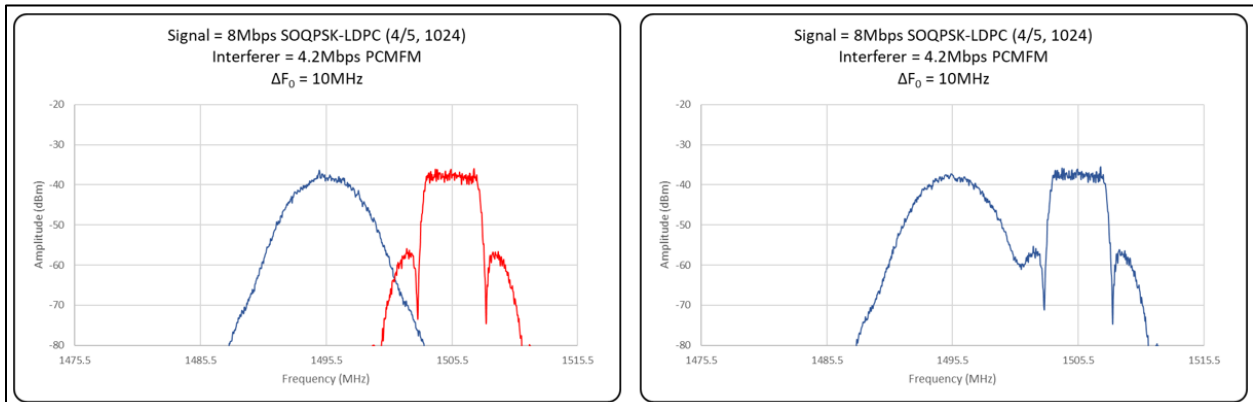
Figure A-5.   Center Frequency Spacing 8 Mbps SOQPSK-LDPC and 4.2 Mbps PCM/FM

2. Desired Signal: 3.6 Mbps SOQPSK-LDPC (r=1/2, k=4096); Interfering Signal: 12 Mbps SOQPSK-TG
    Desired Signal: 12 Mbps SOQPSK-TG; Interfering Signal: 3.6 Mbps SOQPSK-LDPC (r=1/2, k=4096)

$0.60*(33/16)*3.6 + 0.35*1*12 = 8.655$ MHz $0.60*1*12 + 0.45*(33/16)*3.6 = 10.54$ MHz[1]

The largest value is 10.54 MHz; frequencies are assigned in 1 MHz steps so the minimum spacing is 11 MHz. [1] In this calculation, the spacing coefficient of 0.45 for SOQPSK-TG in Table A-1 should be used for the coded interfering signal as the desired signal is uncoded. An example of this minimum frequency spacing is shown in Figure A-6.
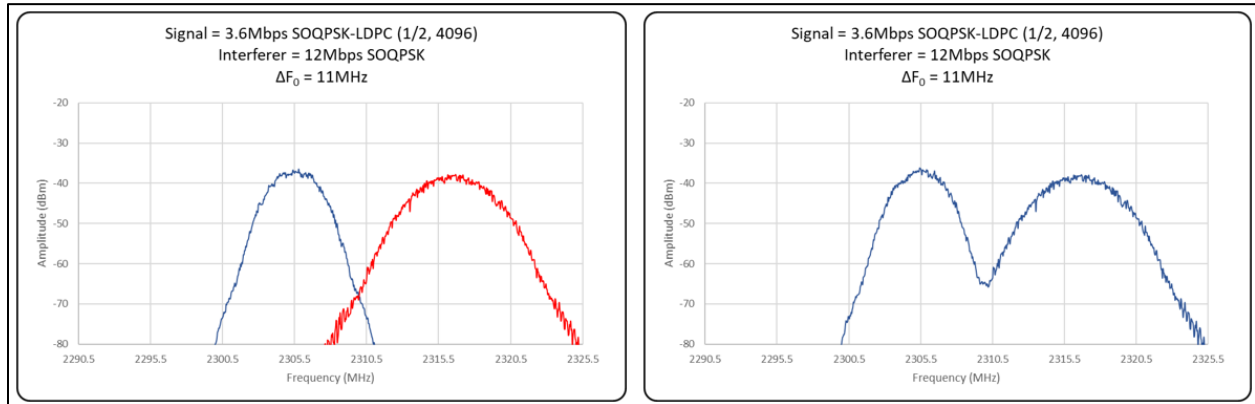
Figure A-6.   Center Frequency Spacing 3.6 Mbps SOQPSK-LDPC and 12 Mbps SOQPSK-TG

3. Desired Signal: 8 Mbps SOQPSK-STC; Interfering Signal: 2 Mbps PCM/FM
    Desired Signal: 2 Mbps PCM/FM; Interfering Signal: 8 Mbps SOQPSK-STC

$0.60*(26/25)*8 + 0.75*1*2 = 6.49$ MHz $0.80*1*2 + 0.45*(26/25)*8 = 5.34$ MHz[1]

The largest value is 6.49 MHz; frequencies are assigned in 1 MHz steps so the minimum spacing is 7 MHz. [1] In this calculation, the spacing coefficient of 0.45 for SOQPSK-TG in Table A-1 should be used for the coded interfering signal as the desired signal is uncoded. An example of this minimum frequency spacing is shown in Figure A-7.
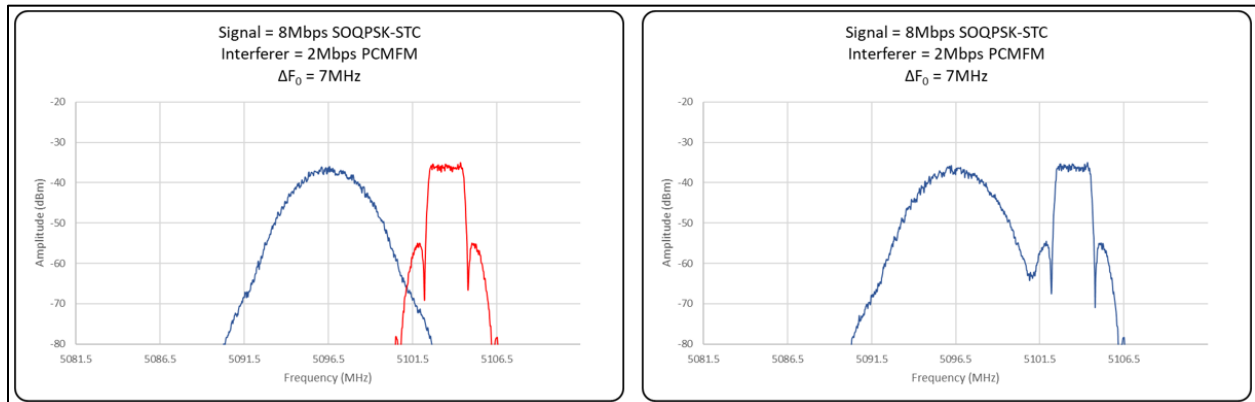
Figure A-7.   Center Frequency Spacing 8 Mbps SOQPSK-STC and 2 Mbps PCM/FM

4. Desired Signal: 5.8 Mbps SOQPSK-STC/LDPC (*r*=2/3, *k*=1024); Interfering Signal: 6.95 Mbps SOQPSK-LDPC (*r*=4/5, *k*=4096)

   Desired Signal: 6.95 Mbps SOQPSK-LDPC (*r*=4/5, *k*=4096); Interfering Signal: 5.8 Mbps SOQPSK-STC/LDPC (*r*=2/3, *k*=1024)

$$0.60*(13/8)*5.8 + 0.35*(21/16)*6.95 = 8.85 \text{ MHz}[1]$$

$$0.60*(21/16)*6.95 + 0.35*(13/8)*5.8 = 8.77 \text{ MHz}[1]$$

The largest value is 8.85 MHz; frequencies are assigned in 1 MHz steps so the minimum spacing is 9 MHz. [1] In both of these calculations the spacing coefficient of 0.35 for SOQPSK-TG in Table A-2 should be used for the coded interfering signal as the desired signal is also coded. An example of this minimum frequency spacing is shown in Figure A-8.
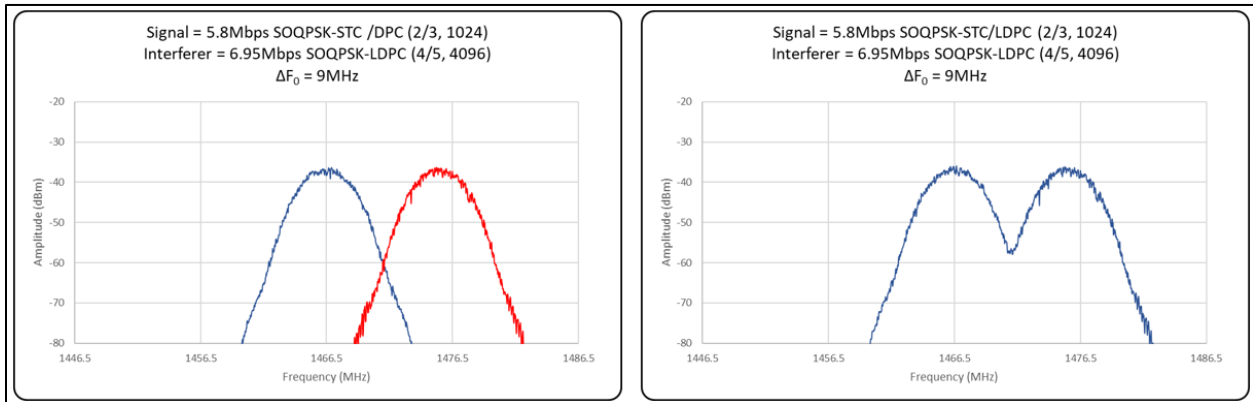
Figure A-8.   Center Frequency Spacing 5.8 Mbps SOQPSK-STC/LDPC and 6.95 Mbps SOQPSK-LDPC

5. Desired Signal: 11 Mbps SOQPSK; Interfering Signal: 2.7 Mbps SOQPSK-LDPC (*r*=4/5, *k*=1024)

   Desired Signal: 2.7 Mbps SOQPSK-LDPC (*r*=4/5, *k*=1024); Interfering Signal: 11 Mbps SOQPSK

$$0.60*(1)*11 + 0.45*(21/16)*2.7 = 8.19 \text{ MHz} \qquad 0.60*(21/16)*2.7 + 0.35*(1)*11 = 5.98 \text{ MHz}[1]$$

The largest value is 8.19 MHz; frequencies are assigned in 1 MHz steps so the minimum spacing is 9 MHz. [1] In this calculation the spacing coefficient of 0.35 for SOQPSK-TG in Table A-2 should be used for the uncoded interfering signal as the desired signal is coded. An example of this minimum frequency spacing is shown in Figure A-9.
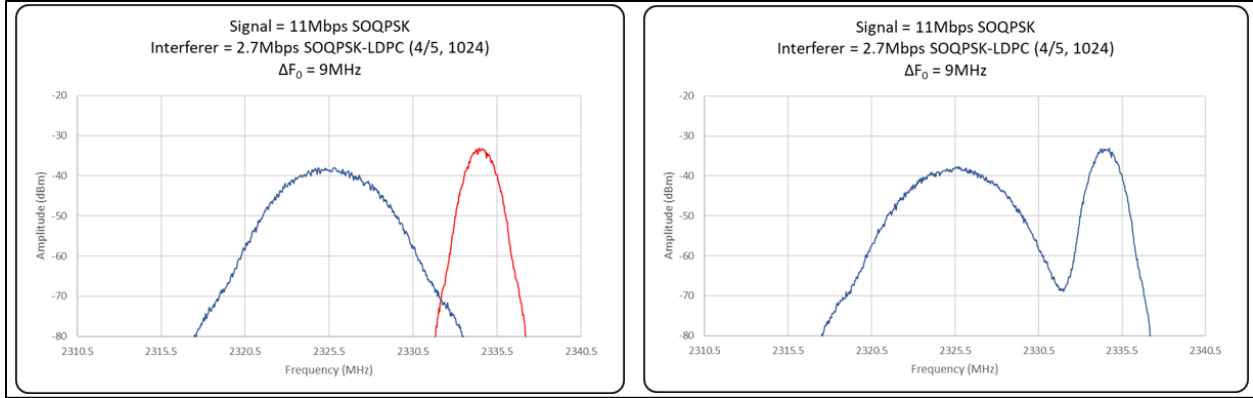
Figure A-9.   Center Frequency Spacing 11 Mbps SOQPSK and 2.7 Mbps SOQPSK-LDPC

6.   Desired Signal: 5 Mbps SOQPSK-STC; Interfering Signal: 5 Mbps SOQPSK-STC

$$0.60*(26/25)*5 + 0.35*(26/25)*5 = 4.94 \text{ MHz}[1]$$

Only one calculation was done as both signals are identical, resulting a value of 4.94 MHz; frequencies are assigned in 1 MHz steps so the minimum spacing is 5 MHz. [1] In this calculation, the spacing coefficient of 0.35 for SOQPSK-TG in Table A-2 should be used for the coded interfering signal as the desired signal is also coded. An example of this minimum frequency spacing is shown in Figure A-10.
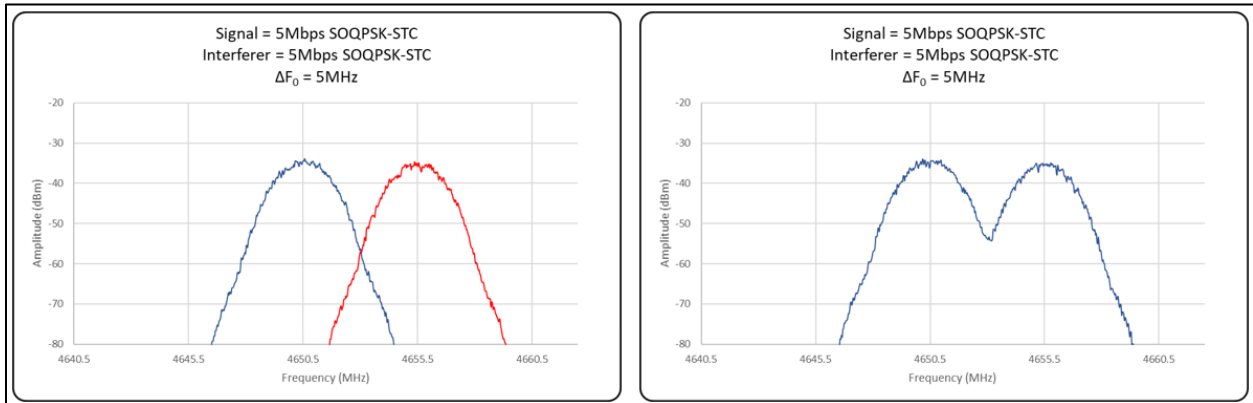
Figure A-10.   Center Frequency Spacing 5 Mbps SOQPSK-STC and 5 Mbps SOQPSK-STC

In some cases it may be desirable to set aside a bandwidth for each signal independent of other signals based solely on modulation scheme and over-the-air bit rate. Typical values for spacing factors for this type of frequency spacing are 2.5 for PCM/FM, 1.5 for SOQPSK, and 1.3 for ARTM CPM. One problem with this approach is that it does not include receiver or detector characteristics or coding and therefore the calculated frequency separations are often much wider than those calculated using Equation A-1.

Several examples of this type of frequency separation calculation are shown below.

1.   Desired Signal: 5 Mbps PCM/FM; Interfering Signal: 3 Mbps SOQPSK
[2.5*(1)*5 + 1.5*(1)*3]/2 = 8.5 MHz

In order to arrive at the center-to-center spacing, the total calculated bandwidth must be divided by a factor of 2. The frequencies are assigned in 1 MHz steps, so the minimum spacing is 9 MHz. Compare this value to 7 MHz using Equation A-1 and it becomes evident this type of calculation is pessimistic.

2. Desired Signal: 5.8 Mbps SOQPSK-STC/LDPC (r=2/3, k=1024); Interfering Signal: 6.95 Mbps SOQPSK-LDPC (r=4/5, k=4096)

$[1.5*(13/8)*5.8 + 1.5*(21/16)*6.95]/2 = 13.9$ MHz

The frequencies are assigned in 1 MHz steps, so the minimum spacing is 14 MHz. Compare this to 9 MHz when using Equation A-1.

3. Desired Signal: 5 Mbps SOQPSK-STC; Interfering Signal: 5 Mbps SOQPSK-STC

$[1.5*(26/25)*5 + 1.5*(26/25)*5]/2 = 7.8$ MHz

The frequencies are assigned in 1 MHz steps, so the minimum spacing is 8 MHz. Compare this to 5 MHz when using Equation A-1.

A.4.b. Geographical Separation

Geographical separation can be used to further reduce the probability of interference from adjacent signals.

A.4.c. Multicarrier Operation

If two transmitters are operated simultaneously and sent or received through the same antenna system, interference due to intermodulation is likely at frequencies of ($2f_1 - f_2$) and ($2f_2 - f_1$). Between three transmitters, the two-frequency possibilities still exist, but intermodulation products may exist as well at ($f_1 + f_2 - f_3$), ($f_1 + f_3 - f_2$), and ($f_2 + f_3 - f_1$), where f_1, f_2, and f_3 represent the output frequencies of the transmitters. Intermodulation products can arise from nonlinearities in the transmitter output circuitry that cause mixing products between a transmitter output signal and the fundamental signal coming from nearby transmitters. Intermodulation products also can arise from nonlinearities in the antenna systems. The generation of intermodulation products is inevitable, but the effects are generally of concern only when such products exceed −25 dBm. The general rule for avoiding third-order intermodulation interference is that in any group of transmitter frequencies, the separation between any pair of frequencies should not be equal to the separation between any other pair of frequencies. Because individual signals have sidebands, it should be noted that intermodulation products have sidebands spectrally wider than the sidebands of the individual signals that caused them.

A.4.d. Transmitter Antenna System Emission Testing

Radiated tests will be made in lieu of transmitter output tests only when the transmitter is inaccessible. Radiated tests may still be required if the antenna is intended to be part of the filtering of spurious products from the transmitter or is suspected of generating spurious products by itself or in interaction with the transmitter and feed lines. These tests should be made with modulation enabled.

A.5. Bandwidth

The definitions of bandwidth in this section are universally applicable. The limits shown here are applicable for telemetry operations in the telemetry bands specified in Chapter 2. For the

purposes of telemetry signal spectral occupancy, the bandwidths used are B99% and B$_{-25\text{dBm}}$. A power level of −25 dBm is exactly equivalent to an attenuation of the transmitter power by 55 + 10×log(P) dB where P is the transmitter power expressed in watts. How bandwidth is actually measured and what the limits are, expressed in terms of that measuring system, are detailed in the following paragraphs.

A.5.a. Concept

The term "bandwidth" has an exact meaning in situations where an AM, double-sideband, or single-sideband signal is produced with a band-limited modulating signal. In systems employing FM or PM, or any modulation system where the modulating signal is not band limited, bandwidth is infinite with energy extending toward zero and infinite frequency falling off from the peak value in some exponential fashion. In this more general case, bandwidth is defined as the band of frequencies in which most of the signal's energy is contained. The definition of "most" is imprecise. The following terms are applied to bandwidth.

A.5.a(1) Authorized Bandwidth

For purposes of this document, the authorized bandwidth is the necessary bandwidth required for transmission and reception of intelligence and does not include allowance for transmitter drift or Doppler shift.

A.5.a(2) Occupied Bandwidth

The width of a frequency band such that below the lower and above the upper frequency limits, the mean powers emitted are each equal to a specified percentage of the total mean power of a given emission. Unless otherwise specified by the ITU for the appropriate class of emission, the specified percentage shall be 0.5%. In this document occupied bandwidth and B99% are interchangeable.

A.5.a(3) Necessary Bandwidth for a Given Class of Emission

For a given class of emission, the width of the frequency band that is just sufficient to ensure the transmission of information at the rate and with the quality required under specified conditions. Note: the term "under specified conditions" does not include signal bandwidth required when operating with adjacent channel signals (i.e., potential interferers).

a.   The NTIA Manual

This manual states that "All reasonable effort shall be made in equipment design and operation by Government agencies to maintain the occupied bandwidth of the emission of any authorized transmission as closely to the necessary bandwidth as is reasonably practicable."

b.   Necessary Bandwidth (DD Form 1494)

The necessary bandwidth is part of the emission designator on the DD Form 1494. For telemetry purposes, the necessary bandwidth can be calculated using the equations shown in Table A-4. Equations for these and other modulation methods are contained in Annex J of the NTIA Manual.

Table A-4. B99% for Various Digital Modulation Methods	
Description	**B99%**
NRZ PCM/FM, premod filter BW=0.7R, Δf=0.35R	1.16 R
NRZ PCM/FM, no premod filter, Δf=0.25R	1.18 R

NRZ PCM/FM, no premod filter, Δf=0.35R	1.78 R
NRZ PCM/FM, no premod filter, Δf=0.40R	1.93 R
NRZ PCM/FM, premod filter BW=0.7R, Δf=0.40R	1.57 R
Minimum shift keying (MSK), no filter	1.18 R
SOQPSK-TG	0.78 R
ARTM CPM	0.56 R

Filtered NRZ PCM/FM. B_n = 1.16*bit rate with h=0.7 and premodulation filter bandwidth = 0.7 times bit rate. Example: PCM/FM modulation used to send 5 Mbps using PCM/FM with 2 signaling states and 1.75 MHz peak deviation; bit rate=$5*10^6$; necessary bandwidth (B_n) = 5.8 MHz.

SOQPSK-TG. B_n = 0.78*bit rate. Example: SOPQSK-TG modulation used to send 5 Mbps using 4 signaling states; bit rate=$5*10^6$; B_n = 3.9 MHz.

ARTM CPM. B_n = 0.56*bit rate with h=4/16 and 5/16 on alternating symbols; digital modulation used to send 5 Mbps using FM with 4 signaling states and with alternating modulation index each symbol; bit rate=$5*10^6$; B_n = 2.8 MHz.

A.5.a(4)   Received (or Receiver) Bandwidth
        The received bandwidth is usually the −3 dB bandwidth of the receiver IF section.

A.5.b. Bandwidth Estimation and Measurement

        Various methods are used to estimate or measure the bandwidth of a signal that is not band limited. The bandwidth measurements are performed using a spectrum analyzer (or equivalent device) with the following settings: 30-kHz resolution bandwidth, 300-Hz video bandwidth, and no max hold detector or averaging. These settings are different than those in earlier versions of the Telemetry Standards. The settings were changed to get more consistent results across a variety of bit rates, modulation methods, and spectrum analyzers. The most common measurement and estimation methods are described in the following paragraphs.

A.5.b(1)   B99%
        This bandwidth contains 99% of the total power. Typically, B99% is measured using a spectrum analyzer or estimated using equations for the modulation type and bit rate used. If the two points that define the edges of the band are not symmetrical about the assigned center frequency, their actual frequencies and difference should be noted. The B99% edges of randomized NRZ (RNRZ) PCM/FM signals are shown in Figure A-11. Table A-4 presents B99% for several digital modulation methods as a function of the bit rate (R).
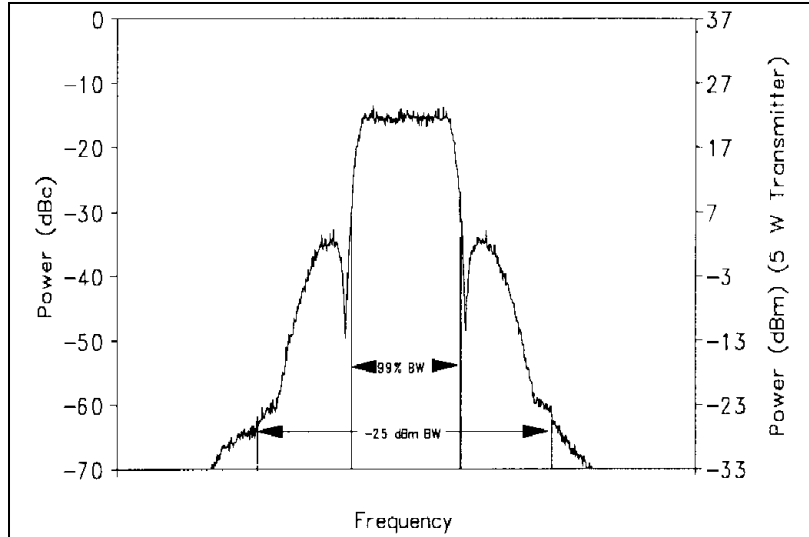
Figure A-11.   RNRZ PCM/FM Signal

A.5.b(2) B_{-25dBm}

B_{-25dBm} is the bandwidth containing all components larger than −25 dBm. A power level of −25 dBm is exactly equivalent to an attenuation of the transmitter power by 55 + 10×log(P) dB where P is the transmitter power expressed in watts. B_{-25dBm} limits are shown in Figure A-11. B_{-25dBm} is primarily a function of the modulation method, transmitter power, and bit rate. The transmitter design and construction techniques also strongly influence B_{-25dBm}. With a bit rate of 5 Mbps and a transmitter power of 5 watts, the B_{-25dBm} of an NRZ PCM/FM system with near optimum parameter settings is about 13.3 MHz, while B_{-25dBm} of an equivalent SOQPSK-TG system is about 7.5 MHz, and B_{-25dBm} of an equivalent ARTM CPM system is about 5.8 MHz.

A.5.b(3)   Scheduled Bandwidth

This bandwidth should be used by organizations responsible for either requesting or scheduling bandwidth required for telemetry signals. These signals are either packed tightly within existing telemetry bands, operating without adjacent signals, or are scheduled near telemetry band edges. Scheduled bandwidth should be calculated for these three cases in the following manner.

   a. If the telemetry signal will be operating in the absence of adjacent signals, use the B99% (occupied bandwidth) calculations in Table A-4 to determine scheduled bandwidth.

   b. If the telemetry signal will be operating in the in the presence of adjacent telemetry signals, use the minimum frequency separation calculations in Table A-1 to determine scheduled bandwidth.

   c. If the telemetry signal will be operating near a telemetry band edge, use the calculations in Section A.11 to determine proper spacing from the band edge.

A.5.c. Other Bandwidth Measurement Methods

The methods discussed above are the standard methods for measuring the bandwidth of telemetry signals. The following methods are also sometimes used to measure or to estimate the bandwidth of telemetry signals.

A.5.c(1) Below Unmodulated Carrier

This method measures the power spectrum with respect to the unmodulated carrier power. To calibrate the measured spectrum on a spectrum analyzer, the unmodulated carrier power must be known. This power level is the 0-dB reference (commonly set to the top of the display). In AM systems, the carrier power never changes; in FM and PM systems, the carrier power is a function of the modulating signal. Therefore, a method to estimate the unmodulated carrier power is required if the modulation cannot be turned off. For most practical angle modulated systems, the total carrier power at the spectrum analyzer input can be found by setting the spectrum analyzer's resolution and video bandwidths to their widest settings, setting the analyzer output to max hold, and allowing the analyzer to make several sweeps. The maximum value of this trace will be a good approximation of the unmodulated carrier level. Figure A-12 shows the spectrum of a 5-Mbps RNRZ PCM/FM signal measured using the standard spectrum analyzer settings discussed previously and the spectrum measured using 3-MHz resolution, video bandwidths, and max hold.
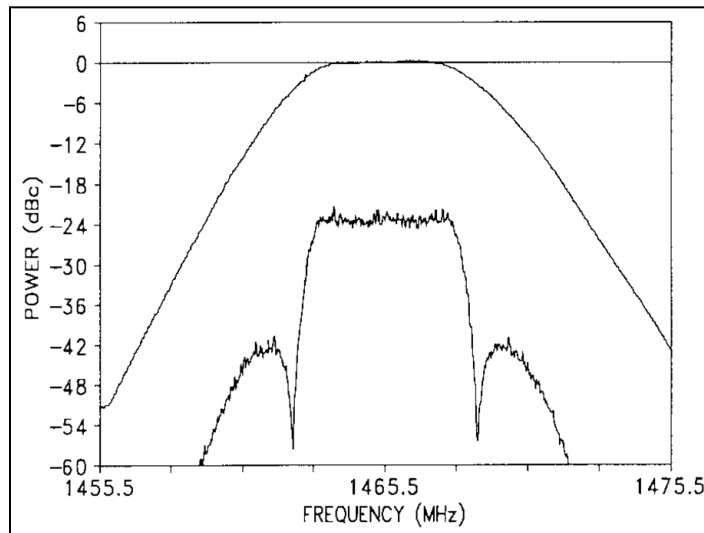
Figure A-12.   Spectrum Analyzer Calibration of 0-dBc Level

The peak of the spectrum measured with the latter conditions is very close to 0-dBc and can be used to estimate the unmodulated carrier power (0-dBc) in the presence of FM or PM. In practice, the 0-dBc calibration would be performed first, and the display settings would then be adjusted to use the peak of the curve as the reference level (0-dBc level) to calibrate the spectrum measured using the standard spectrum analyzer settings. With the spectrum analyzer set for a specific resolution bandwidth, video bandwidth, and detector type, the bandwidth is taken as the distance between the two points outside of which the spectrum is thereafter some number (say, 60 dB) below the unmodulated carrier power determined above. B_{-60dBc} for the 5-Mbps signal shown in Figure A-12 is approximately 13 MHz.

B_{-60dBc} of an RNRZ PCM/FM signal with a peak deviation of 0.35R, a four-pole premodulation filter with −3 dB corner at 0.7R, and a bit rate greater than or equal to 1 Mbps can be approximated by the following equation:

$$B_{-60dBc} = [2.78 - 0.3 * \log_{10}(R)] * R \qquad\qquad\text{A-2}$$

where   B is in MHz;
         R is in Mbps.

Thus B_{-60dBc} of a 5-Mbps RNRZ signal under these conditions would be approximately 12.85 MHz. B_{-60dBc} will be greater if peak deviation is increased or the number of filter poles is decreased.

A.5.c(2)   Below Peak

This method is not recommended for measuring the bandwidth of telemetry signals. The modulated peak method, the least accurate measurement method, measures between points where the spectrum is thereafter XX dB below the level of the highest point on the modulated spectrum. Figure A-13 shows the RF spectrum of a 400-kbps bi-phase (Biϕ)-level PCM/PM signal with a peak deviation of 75° and a pre-modulation filter bandwidth of 800 kHz.
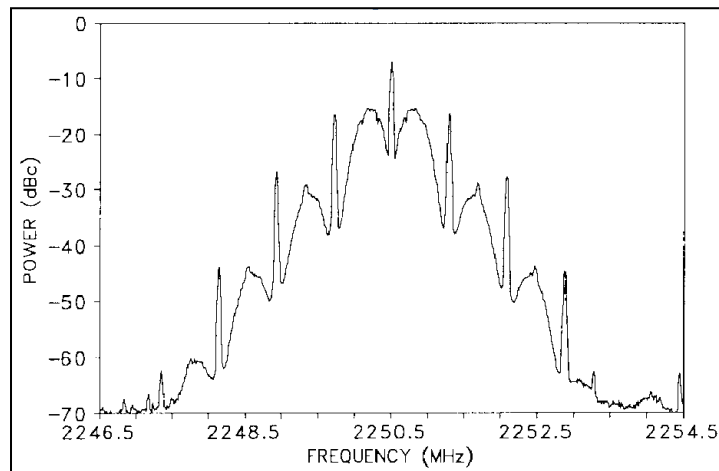
Figure A-13.   Biϕ PCM/PM Signal

The largest peak has a power level of −7 dBc. In comparison, the largest peak in Figure A-13 had a power level of −22 dBc. This 15-dB difference would skew a bandwidth comparison that used the peak level in the measured spectrum as a common reference point. In the absence of an unmodulated carrier to use for calibration, the below-peak measurement is often (erroneously) used and described as a below-unmodulated-carrier measurement. Using max hold exacerbates this effect still further. In all instances the bandwidth is overstated, but the amount varies.

A.5.c(3)   Carson's Rule

Carson's Rule is a method to estimate the bandwidth of an FM subcarrier system. Carson's Rule states the following:

$$B = 2(\Delta f + f_{max}) \qquad\qquad\text{A-3}$$

where   B is the bandwidth;
         Δf is the peak deviation of the carrier frequency;

f_{max} is the highest frequency in the modulating signal.

Figure A-14 shows the spectrum that results when a 12-channel constant bandwidth multiplex with 6-dB/octave pre-emphasis frequency modulates an FM transmitter. B99% and the bandwidth calculated using Carson's Rule are also shown. Carson's Rule will estimate a value greater than B99% if little of the carrier deviation is due to high-frequency energy in the modulating signal.
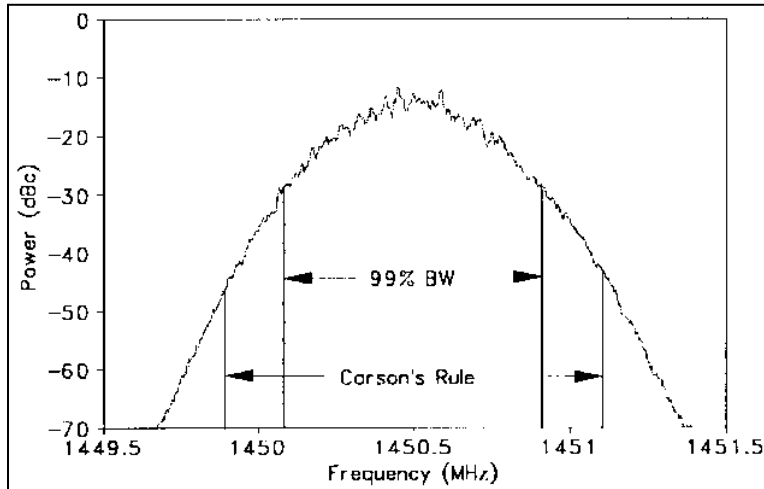
Figure A-14.   FM/AM Signal and Carson's Rule

A.5.d. Spectral Equations

The following equations can be used to calculate the RF spectra for several digital modulation methods with unfiltered waveforms.[24, 25, 26] These equations can be modified to include the effects of filtering.[27, 28]

RNRZ PCM/FM (valid when D≠integer, D = 0.5 gives MSK spectrum)

$$S(f) = \frac{4\,B_{SA}}{R}\left(\frac{D}{\pi(D^2 - X^2)}\right)^2 \frac{(\cos \pi D - \cos \pi X)^2}{1 - 2\cos \pi D \cos \pi X + \cos^2 \pi D}, \quad \cos \pi D < Q \qquad \text{A-4}$$

---

[24] I. Korn. *Digital Communications*, New York, Van Nostrand, 1985.

[25] M. G. Pelchat. "The Autocorrelation Function and Power Spectrum of PCM/FM with Random Binary Modulating Waveforms," IEEE Transactions, Vol. SET-10, No. 1, pp. 39-44, March 1964.

[26] Tey, W. M. and T. Tjhung. "Characteristics of Manchester-Coded FSK," *IEEE Transactions on Communications*, Vol. COM-27, pp. 209-216, January 1979.

[27] Watt, A. D., V. J. Zurick, and R. M. Coon. "Reduction of Adjacent-Channel Interference Components from Frequency-Shift-Keyed Carriers," *IRE Transactions on Communication Systems*, Vol. CS-6, pp. 39-47, December 1958.

[28] E. L. Law. "RF Spectral Characteristics of Random PCM/FM and PSK Signals," *International Telemetering Conference Proceedings*, pp. 71-80, 1991.

RNRZ PSK

$$S(f) = \frac{B_{SA}}{R} \frac{\sin^2\left(\frac{\pi X}{2}\right)}{\left(\frac{\pi X}{2}\right)^2}$$

A-5

RNRZ QPSK and OQPSK

$$S(f) = \frac{2B_{SA}}{R} \frac{\sin^2(\pi X)}{(\pi X)^2}$$

A-6

Random Biϕ PCM/FM

$$S(f) = \frac{B_{SA}}{4R}\left(\frac{\pi D}{2} \frac{\sin\left(\frac{\pi(X-D)}{4}\right)}{\frac{\pi(X-D)}{4}} \frac{\sin\left(\frac{\pi(X+D)}{4}\right)}{\frac{\pi(X+D)}{4}}\right)^2 + \left(\frac{D\sin(\frac{\pi D}{2})}{\frac{\pi(X^2-D^2)}{2}}\right)^2 \delta\{(f-f_c)-nR\}$$

A-7

Random Biϕ PCM/PM

$$S(f) = \frac{B_{SA}\sin^2(\beta)}{R} \frac{\sin^4\left(\frac{\pi X}{4}\right)}{\left(\frac{\pi X}{4}\right)^2} + \cos^2(\beta)\delta(f-f_c), \quad \beta \le \frac{\pi}{2}$$

A-8

where $S(f)$ = power spectrum (dBc) at frequency f
B_{SA} = spectrum analyzer resolution bandwidth*
R = bit rate
$D = 2\Delta f/R$
$X = 2(f-f_c)/R$
Δf = peak deviation
β = peak phase deviation in radians
f_c = carrier frequency
δ = Dirac delta function
$N = 0, \pm1, \pm2, \ldots$
Q = quantity related to narrow band spectral peaking when D≈1, 2, 3, ...
$Q \approx 0.99$ for $B_{SA} = 0.003$ R, $Q \approx 0.9$ for $B_{SA} = 0.03$ R
*The spectrum analyzer resolution bandwidth term was added to the original equations.

A.5.e. Receiver Bandwidth

Receiver predetection bandwidth is typically defined as the points where the response to the carrier before demodulation is −3 dB from the center frequency response. The carrier bandwidth response of the receiver is, or is intended to be, symmetrical about the carrier in most instances. Figure A-15 shows the response of a typical older-generation telemetry receiver with RLC IF filters and a 1-MHz IF bandwidth selected. Outside the stated bandwidth, the response usually falls fairly rapidly, often 20 dB or more below the passband response at 1.5 to 2 times the passband response.
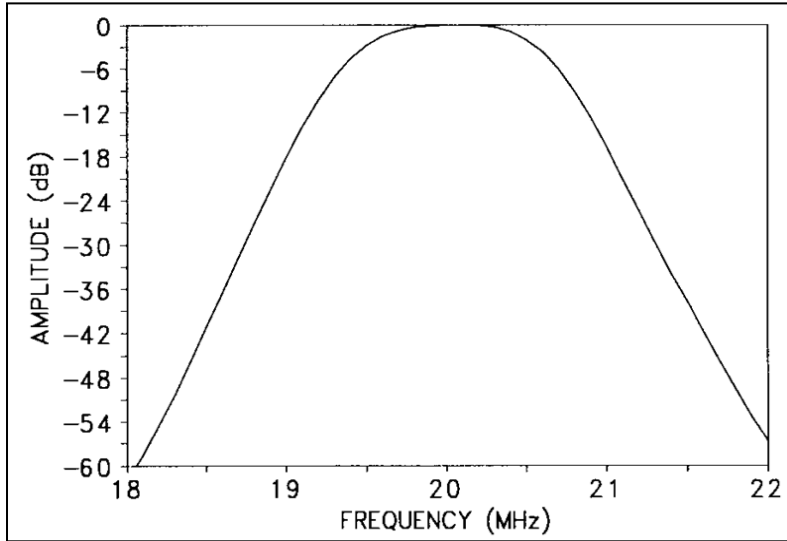
Figure A-15.   Typical Receiver RLC IF Filter Response (−3 dB Bandwidth = 1 MHz)

Figure A-16 shows an overlay of an RLC IF filter and a SAW filter. Note that the SAW filter rolls off much more rapidly than the RLC filter. The rapid falloff outside the passband helps reduce interference from nearby channels and has minimal effect on data.
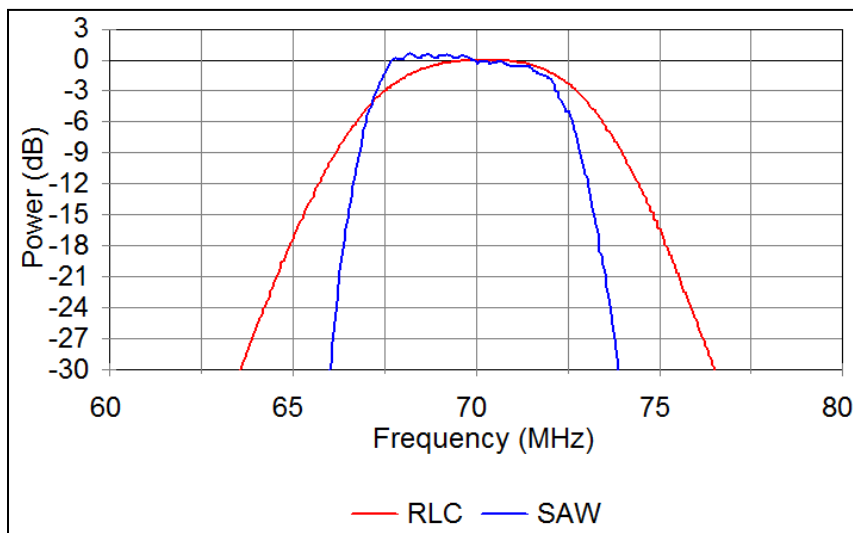
Figure A-16.   RLC and SAW IF Filters

A.5.f. Receiver Noise Bandwidth

For the purpose of calculating noise in the receiver, the bandwidth must be integrated over the actual shape of the IF, which, in general, is not a square-sided function. Typically, the value used for noise power calculations is the −3 dB bandwidth of the receiver.

A.5.g. Symmetry

Many modulation methods produce a spectrum that is asymmetrical with respect to the carrier frequency. Exceptions include FM/FM systems, RNRZ PCM/FM systems, and randomized SOQPSK-TG, and ARTM CPM systems. The most extreme case of asymmetry is due to single-sideband transmission, which places the carrier frequency at one edge of the occupied spectrum. If the spectrum is not symmetrical about the band center, the bandwidth and the extent of asymmetry must be noted for frequency management purposes.

A.5.h. FM Transmitters (alternating current-coupled)

Alternating current-coupled FM transmitters should not be used to transmit NRZ signals unless the signals to be transmitted are randomized. This is because changes in the ratio of 1s to 0s will increase the occupied bandwidth and may degrade the BER. When alternating current-coupled transmitters are used with RNRZ signals, it is recommended that the lower −3 dB frequency response of the transmitter be no greater than the bit rate divided by 4000. For example, if a randomized 1-Mbps NRZ signal is being transmitted, the lower −3 dB frequency response of the transmitter should be no larger than 250 Hz.

A.6. Spectral Occupancy Limits

Telemetry applications covered by this standard shall use B99% to define occupied bandwidth and B$_{-25\text{dBm}}$ as the primary measure of spectral efficiency. The spectra are assumed symmetrical about the center frequency unless otherwise specified. The primary reason for controlling the spectral occupancy is to control adjacent channel interference, thereby allowing more users to be packed into a given amount of frequency spectrum. The adjacent channel interference is determined by the spectra of the signals and the filter characteristics of the receiver.

A.6.a. Spectral Mask

One common method of describing the spectral occupancy limits is a spectral mask. The aeronautical telemetry spectral mask is described below. Note that the mask in this standard is different than the masks contained in the earlier versions of the Telemetry Standards. All spectral components larger than −[55 + 10×log(P)] dBc (i.e., larger than −25 dBm) at the transmitter output must be within the spectral mask calculated using the following equation:

$$M(f) = K + 90\log R - 100\log|f - f_c|; \qquad |f - f_c| \geq \frac{R}{m} \qquad \text{A-9}$$

where $M(f)$ = power (dBc) at frequency f (MHz)
$K = -20$ for analog signals
$K = -28$ for binary signals
$K = -61$ for SOQPSK-TG

K = −73 for ARTM CPM
f_c = transmitter center frequency (MHz)
R = bit rate (Mbps) for digital signals or $(\Delta f + f_{max})(MHz)$ for analog FM signals
m = number of states in modulating signal (m = 2 for binary signals, m = 4 for quaternary signals and analog signals)
Δf = peak deviation
f_{max} = maximum modulation frequency

These bandwidths are measured using a spectrum analyzer with settings of 30-kHz resolution bandwidth, 300-Hz video bandwidth, and no max hold detector or averaging. Note that these settings are different than those listed in previous editions of the Telemetry Standards. The changes were made to get more consistent results with various bit rates and spectrum analyzers. The spectra measured with these settings give slightly larger power levels than with the previous settings; this is why the value of K was changed from −63 to −61 for SOQPSK signals. The power levels near center frequency should be approximately J−10log(R) dBc where J= −10 for ARTM CPM, −12 for SOQPSK-TG, and −15.5 for PCM/FM signals. For a bit rate of 5 Mbps, the level is approximately −17 dBc for ARTM CPM, −19 dBc for SOQPSK-TG, and −22.5 dBc for PCM/FM. If the power levels near center frequency are not within 3 dB of these values, then a measurement problem exists and the carrier power level (0 dBc) and spectrum analyzer settings should be verified.

$B_{−25dBm}$ is not required to be narrower than 1 MHz. The first term K in Equation A-9 accounts for bandwidth differences between modulation methods. Equation A-9 can be rewritten as M(f) = K − 10logR − 100log|(f−f_c)/R|. When Equation A-9 is written this way, the 10logR term accounts for the increased spectral spreading and decreased power per unit bandwidth as the modulation rate increases. The last term forces the spectral mask to roll off at 30 dB/octave (100 dB/decade). Any error detection or error correction bits, which are added to the data stream, are counted as bits for the purposes of this spectral mask. The spectral masks are based on the power spectra of random real-world transmitter signals. For instance, the binary signal spectral mask is based on the power spectrum of a binary NRZ PCM/FM signal with peak deviation equal to 0.35 times the bit rate and a multipole premodulation filter with a −3 dB frequency equal to 0.7 times the bit rate (see Figure A-11). This peak deviation minimizes the BER with an optimum receiver bandwidth while also providing a compact RF spectrum. The premodulation filter attenuates the RF sidebands while only degrading the BER by the equivalent of a few tenths of a dB of RF power. Further decreasing of the premodulation filter bandwidth will only result in a slightly narrower RF spectrum, but the BER will increase dramatically. Increasing the premodulation filter bandwidth will result in a wider RF spectrum, and the BER will only be decreased slightly. The recommended premodulation filter for NRZ PCM/FM signals is a multipole linear phase filter with a −3 dB frequency equal to 0.7 times the bit rate. The unfiltered NRZ PCM/FM signal rolls off at 12 dB/octave so at least a three-pole filter (filters with four or more poles are recommended) is required to achieve the 30 dB/octave slope of the spectral mask. The spectral mask includes the effects of reasonable component variations (unit-to-unit and temperature).

A.6.b. Spectral Mask Examples

Figure A-17 and Figure A-18 show the binary spectral mask of Equation A-9 and the RF spectra of 5-Mbps RNRZ PCM/FM signals. The RF spectra were measured using a spectrum analyzer with 30-kHz resolution bandwidth, 300-Hz video bandwidth, and no max hold detector. The span of the frequency axis is 20 MHz. The transmitter power was 5 watts, and the peak deviation was 1750 kHz. The modulation signal for Figure A-17 was filtered with a 4-pole linear-phase filter with −3 dB frequency of 3500 kHz. All spectral components in Figure A-17 were contained within the spectral mask. The minimum value of the spectral mask was −62 dBc (equivalent to −25 dBm). The peak modulated signal power levels were about 22.5 dB below the unmodulated carrier level (−22.5 dBc). Figure A-18 shows the same signal with no premodulation filtering. The signal was not contained within the spectral mask when a premodulation filter was not used.
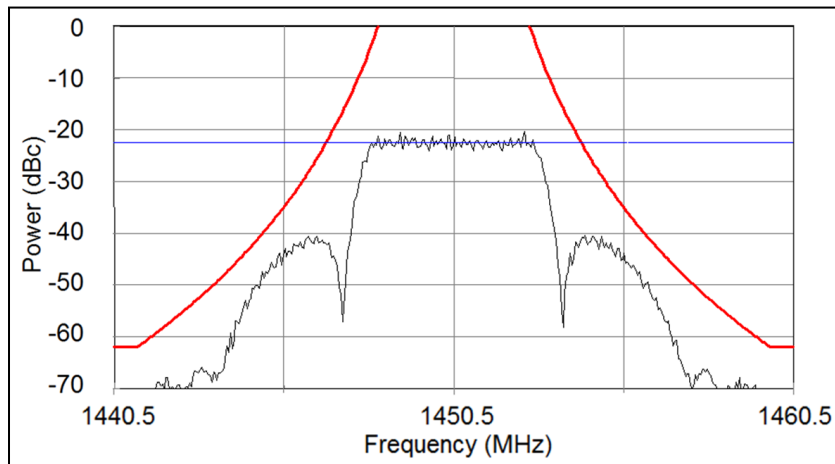
Figure A-17.   Filtered 5-Mbps RNRZ PCM/FM Signal and Spectral Mask
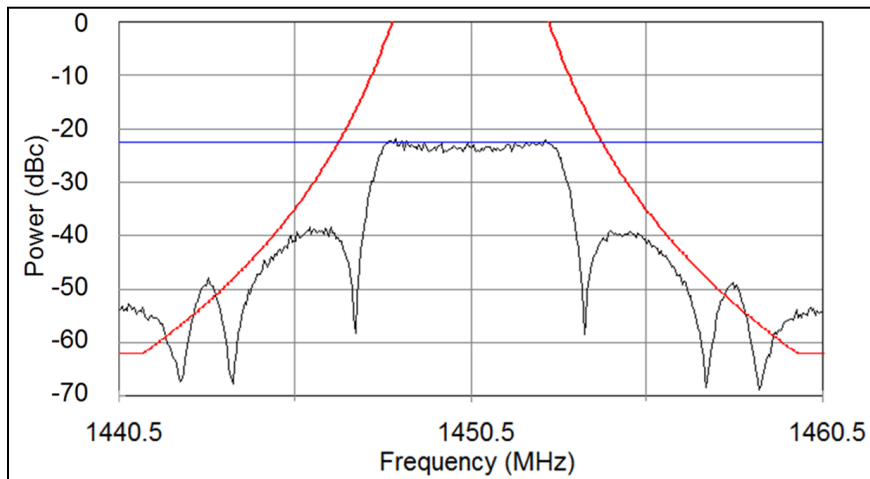
Figure A-18.   Unfiltered 5-Mbps RNRZ PCM/FM Signal and Spectral Mask

Figure A-19 shows the SOQPSK mask of Equation A-9 and the RF spectrum of a 5-Mbps SOQPSK-TG signal. The transmitter power was assumed to be 5 watts in this example. The peak value of the SOQPSK-TG signal was about −19 dBc. Figure A-20 shows a typical 5-

Mbps ARTM CPM signal and its spectral mask. The peak value of the ARTM CPM signal was about −17 dBc.
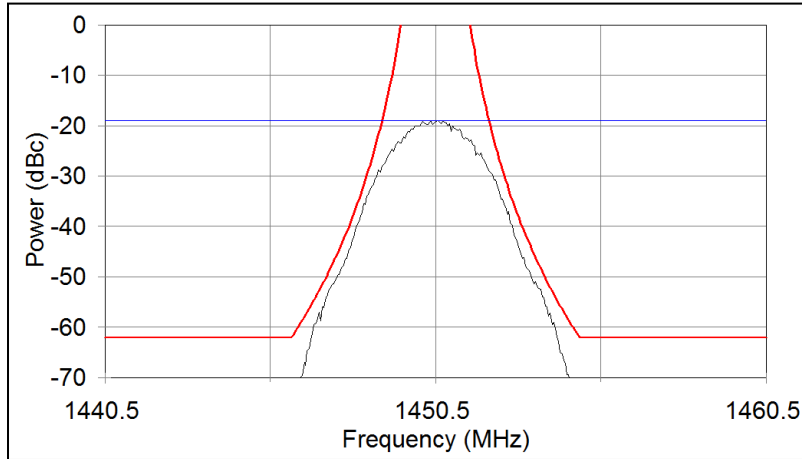
Figure A-19.   Typical 5-Mbps SOQPSK TG Signal and Spectral Mask
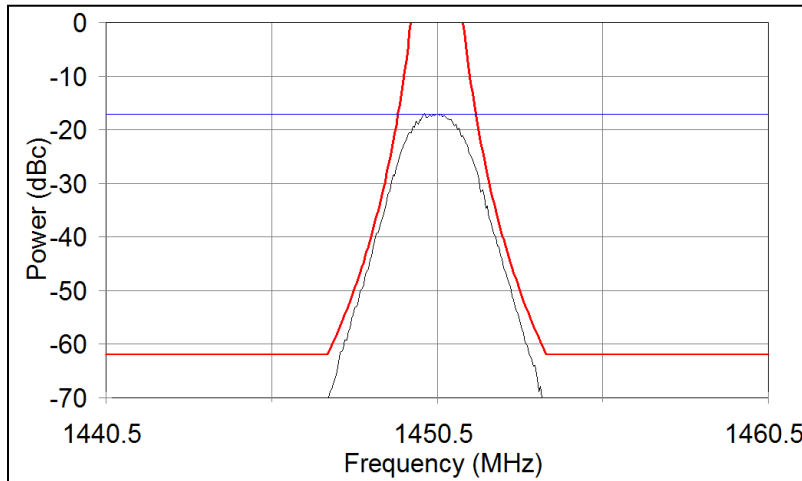
Figure A-20.   Typical 5-Mbps ARTM CPM Signal and Spectral Mask

A.7.   Technical Characteristics of Digital Modulation Methods

Table A-5 provides a summary of some of the technical characteristics of the modulation methods discussed in this summary.

Table A-5. Characteristics of Various Modulation Methods				
Characteristic	PCM/FM with single symbol detection	PCM/FM with multi-symbol detection	SOQPSK-TG	ARTM CPM
Occupied Bandwidth	1.16 bit rate	1.16 bit rate	0.78 bit rate	0.56 bit rate
Detection Efficiency (E_b/N_0 for BEP=1e−5)	11.8-15+ dB	9.5 dB	11.5-12 dB	12.5-13 dB
Synchronization time	100 to 10,000 bits	250 bits	200 to 5,000 bits	10,000 to 40,000 bits

E_b/N_0 for BEP=1e−3	9-12+ dB	6.5 dB	8.5 dB	10.5 dB
Phase noise susceptibility*	2	1	3	4
Co-channel interference susceptibility*	2	1	3	4
* Scale 1-4, 1 Being Best				

A.8.   SOQPSK-TG Characteristics

The SOQPSK is a family of constant envelope CPM waveforms defined by Hill.[29] The details of SOQPSK-TG are described in Subsection 2.3.3.3. The SOQPSK-TG signal amplitude is constant and the phase trajectory is determined by the coefficients in Table 2-4. Therefore, SOQPSK-TG can be implemented using a precision phase or frequency modulator with proper control of the phase trajectory. Figure A-21 illustrates the measured phase trajectory of an SOQPSK-TG signal. The vertical lines correspond approximately to the "bit" decision times.
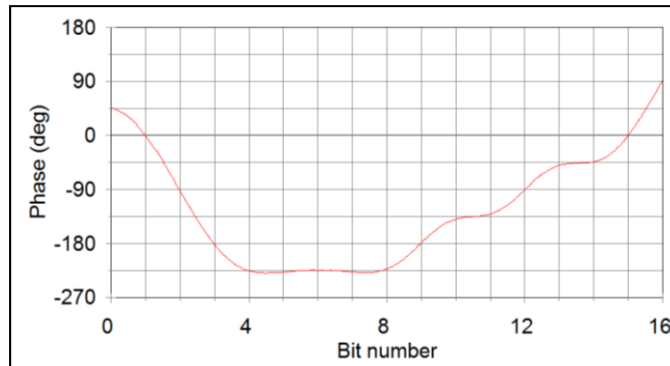
Figure A-21.   Measured SOQPSK-TG Phase Trajectory

The power spectrum of a random 5-Mbps SOQPSK-TG signal is shown in Figure A-22. B_{-60dBc} of this 5-Mbps signal was about 7.34 MHz. Note that the maximum power level is about −19 dBc.

---

[29] T.J. Hill. "An Enhanced, Constant Envelope, Interoperable Shaped Offset QPSK (SOQPSK) Waveform for Improved Spectral Efficiency." Paper presented during 36th Annual International Telemetering Conference, San Diego, CA. October 23-26, 2000.
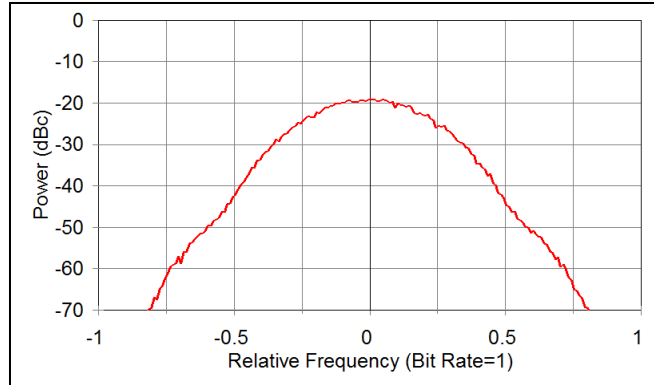
Figure A-22. SOQPSK-TG Power Spectrum (5 Mbps)

Figure A-23 shows the measured BEP versus signal energy per bit/noise power per Hz (E_b/N_0) of two SOQPSK-TG modulator/demodulator combinations including nonlinear amplification and differential encoding/decoding in an AWGN environment with no fading. Other combinations of equipment may have different performance. Phase noise levels higher than those recommended in Chapter 2 can significantly degrade the BEP performance.
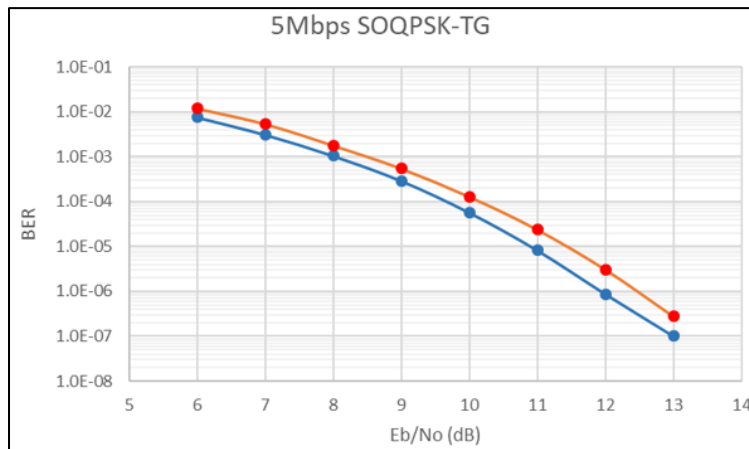
Figure A-23. BEP vs. E_b/N_0 Performance of 5 Mbps SOQPSK-TG

A.9.   Advanced Range Telemetry Continuous Phase Modulation Characteristics

The ARTM CPM is a quaternary signaling scheme in which the instantaneous frequency of the modulated signal is a function of the source data stream. The frequency pulses are shaped for spectral containment purposes. As defined for this standard, the modulation index alternates at the symbol rate between h=4/16 and h=5/16. The purpose of alternating between two modulation indices is to maximize the minimum distance between data symbols, which results in minimizing the BEP. These particular modulation indices were selected as a good tradeoff between spectral efficiency and data-detection ability. Figure A-24 shows the power spectrum of a 5-Mbps ARTM CPM signal and Figure A-25 shows the measured BEP versus E_b/N_0. The maximum power level was about −19 dBc. B_{-60dBc} of this 5-Mbps signal was about 5.54 MHz. Note that the power spectrum of ARTM CPM is about 25% narrower than that of SOQPSK-TG but the BEP performance is worse. The ARTM CPM modulation is also more susceptible to phase noise than SOQPSK-TG.
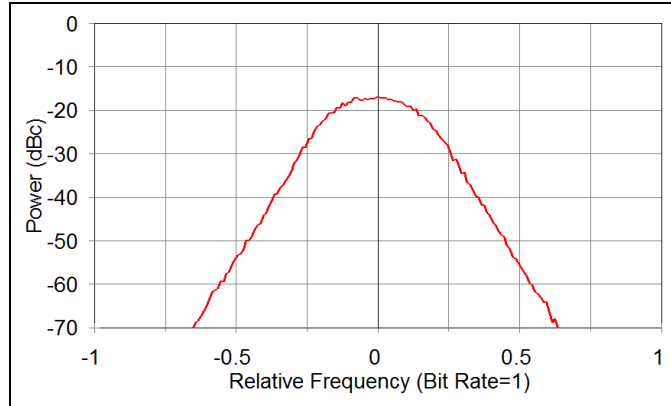
Figure A-24.   Power Spectrum of 5 Mbps ARTM CPM
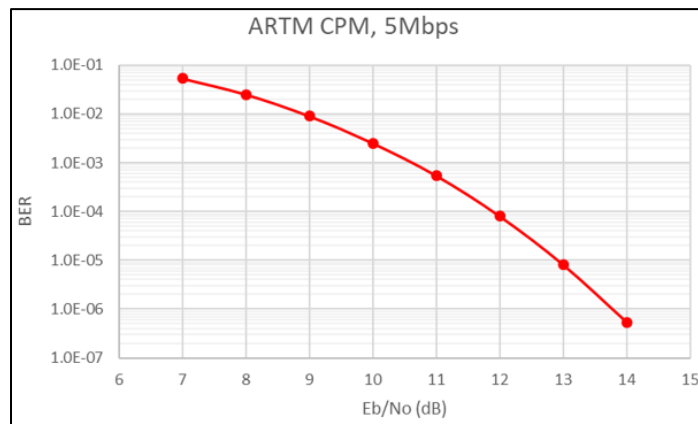
Figure A-25.   BEP vs. E_b/N_0 Performance of 5 Mbps ARTM CPM

A.10. PCM/FM

The most popular telemetry modulation since 1970 is PCM/FM. The RF signal is typically generated by filtering the baseband NRZ-L signal and then frequency modulating a VCO. The optimum peak deviation is 0.35 times the bit rate (h=0.7) and a good choice for a premodulation filter is a multi-pole linear phase filter with bandwidth equal to 0.7 times the bit rate. Figure A-26 shows the power spectrum of a pseudo-random 5-Mbps PCM/FM signal with peak deviation of 1.75 MHz and a 3.5-MHz linear phase low-pass filter. Note that the spectrum is nearly flat from a frequency equal to −0.5 times the bit rate to a frequency equal to +0.5 times the bit rate. The power level near the center frequency is about −22.5 dBc for a bit rate of 5 Mbps and the standard spectrum analyzer settings.
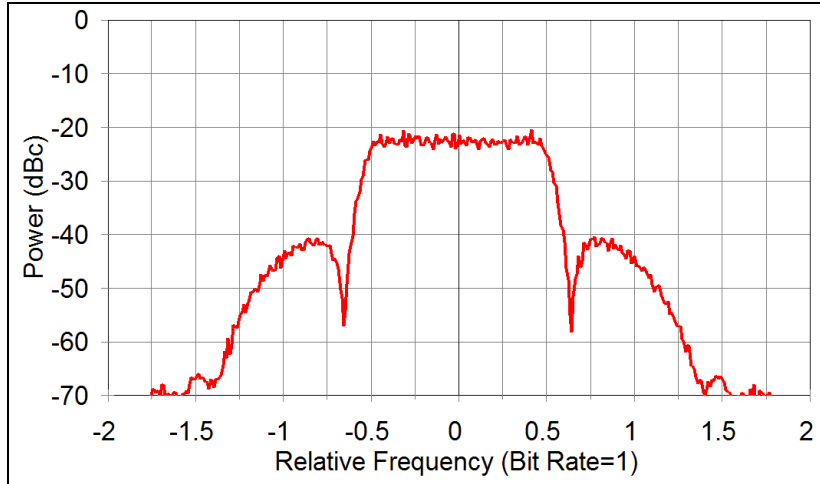
Figure A-26.   Power Spectrum of 5 Mbps PCM/FM Signal

Figure A-27 shows the BEP versus E_b/N_0 performance of 5-Mbps PCM/FM with a multi-symbol bit detector and with three different receivers/detectors. Note that an E_b/N_0 of about 9 dB is required to achieve a BEP of about 10^{-5} with the multi-symbol detector[30,31] while an E_b/N_0 of about 12 to 14 dB is typically required to achieve a BEP of about 10^{-5} with typical FM demodulators and single-symbol detectors. These are typical detection performance numbers and will vary depending upon receiver/demodulator implementations and whether or not trellis demodulation is used. The PCM/FM modulation method is fairly insensitive to phase noise.
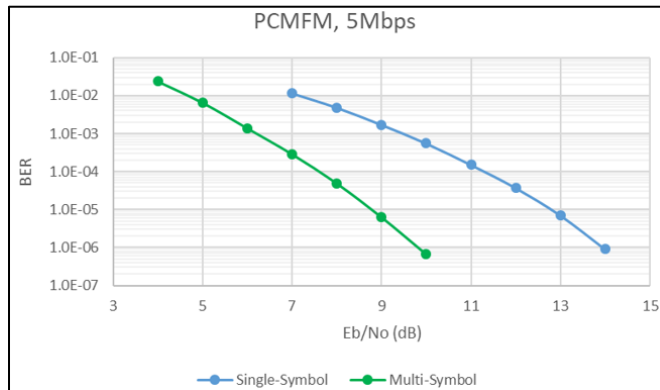
Figure A-27.   BEP vs. E_b/N_0 Performance of 5-Mbps PCM/FM

A.11.   Valid Center Frequencies Near Telemetry Band Edges

The telemetry bands and associated frequency ranges identified in Table 2-1 identify the frequency limits for each band. Telemetry transmitters cannot be centered at the band edges due to obvious out-of-band emissions (OOBE). Bit rate to the transmitter and modulation scheme drive the amount of separation required between the center frequency and the band edge. To

---

[30] Osborne, W. P. and M. B. Luntz. "Coherent and Noncoherent Detection of CPFSK," IEEE Transactions on Communications, August 1974.

[31] Mark Geoghegan. "Improving the Detection Efficiency of Conventional PCM/FM Telemetry by using a Multi-Symbol Demodulator." *Proceedings of the 2000 International Telemetry Conference*, Volume XXXVI, 675-682, San Diego CA, October 2000.

determine the amount of back-off required, the distance from the center of the spectral masks for each modulation scheme (see Subsection 2.3.6) to the intersection of the mask and the absolute limit of −25 dBm must be calculated. To illustrate this, see Figure A-28. Using these calculations will assure that outside the specified telemetry bands no part of the modulated spectrum is over the absolute limit of −25 dBm.
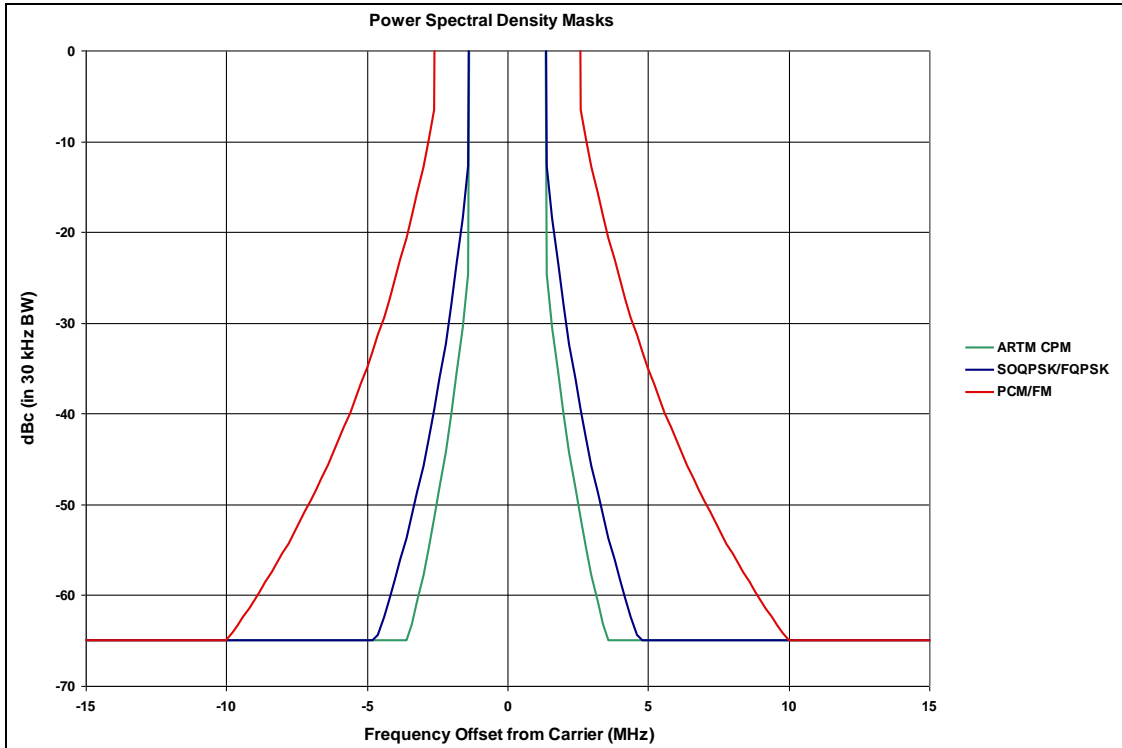
Figure A-28.   Spectral Masks at −25 dBm

The mask is calculated for all the modulation schemes at a bit rate of 5 Mbps with transmitter output power assumed to be 10 W. This transmitter operating with PCM/FM as its modulation scheme requires a back-off from band edge of 9.98 MHz; since channelization in these bands is limited to 0.5-MHz steps, this value is rounded up to 10 MHz. This same transmitter operating with SOQPSK will require 4.67 MHz, rounded up to 5 MHz, of back-off from band edge. Likewise, for ARTM-CPM the back-off is 3.54 MHz or 4 Mbps when rounded up. To further this example, if this was an L-band transmitter, viable carrier frequencies would be as specified in Table A-6.

Table A-6. L-Band Frequency Range (10 W, 5 Mbps)	
Modulation Type	Viable L-Band Frequency Range
PCM/FM	1445-1515 MHz
SOQPSK-TG	1440-1520 MHz
ARTM CPM	1439-1521 MHz

For a given modulation scheme and transmitter output power, as the bit rate increases, the amount of back-off from the band edge also increases. Figure A-29 illustrates this point.
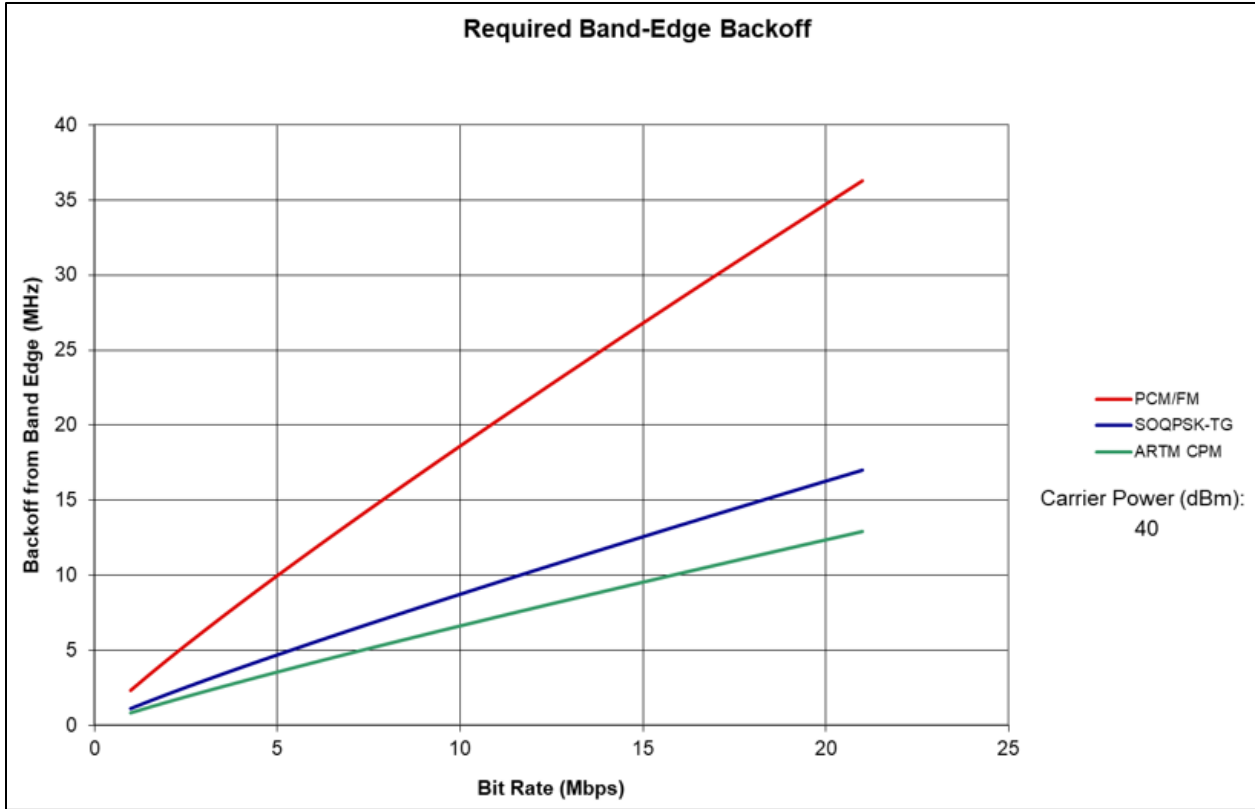
Figure A-29.   Bit Rate vs. Band Edge Back-off

NOTE	For ease in making calculations, an Excel spreadsheet application can be used. Table A-7 provides an example of a 10-watt transmitter (+40 dBm) operating at 1 Mbps in L-band and S-band using the formulas in the spreadsheet. The Excel file that created Table A-7 can be downloaded here and used for interactive calculations. The input values for transmitter output power and bit rate are in the cells highlighted in yellow. The amount of back-off will be displayed in the cells highlighted in light blue. Additionally, each telemetry band is displayed with the useable carrier frequency range for each modulation scheme given in blue.

Table A-7. Valid Center Frequency, Band Edge Back-Off

		PCM/FM	SOQPSK	ARTM CPM	
Carrier Power or EIRP (dBm):		40			Input Number
Mask floor (at this nominal TX power):		−65	dBc		
Bit Rate (Mbps):		1.00	1.00	1.00	Input Number
K =		−28	−61	−73	
m =		2	4	4	
Bit Rate (bps)		1.00E+06	1.00E+06	1.00E+06	
Mask hits floor at offset of (MHz)		2.34	1.10	0.83	
Band-edge backoff (MHz, rounded to nearest 0.5 MHz)		2.5	1.5	1	Result

		PCM/FM	SOQPSK	ARTM CPM
L-Band	Band Edge, Lower (MHz)	1435		
	Band Edge, Upper (MHz)	1525		
	Lower center freq. at this bit rate (MHz)	1437.5	1436.5	1436.0
	Upper center freq. at this bit rate (MHz)	1522.5	1523.5	1524.0
L-Band	Band Edge, Lower (MHz)	1780		
	Band Edge, Upper (MHz)	1850		
	Lower center freq. at this bit rate (MHz)	1782.5	1781.5	1781.0
	Upper center freq. at this bit rate (MHz)	1847.5	1848.5	1849.0
S-Band	Band Edge, Lower (MHz)	2200		
	Band Edge, Upper (MHz)	2290		
	Lower center freq. at this bit rate (MHz)	2202.5	2201.5	2201.0
	Upper center freq. at this bit rate (MHz)	2287.5	2288.5	2289.0
S-Band	Band Edge, Lower (MHz)	2360		
	Band Edge, Upper (MHz)	2395		
	Lower center freq. at this bit rate (MHz)	2362.5	2361.5	2361.0
	Upper center freq. at this bit rate (MHz)	2392.5	2393.5	2394.0
C-Band	Band Edge, Lower (MHz)	4400		
	Band Edge, Upper (MHz)	4940		
	Lower center freq. at this bit rate (MHz)	4402.5	4401.5	4401.0
	Upper center freq. at this bit rate (MHz)	4937.5	4938.5	4939.0
C-Band	Band Edge, Lower (MHz)	5091		
	Band Edge, Upper (MHz)	5150		
	Lower center freq. at this bit rate (MHz)	5093.5	5092.5	5092.0
	Upper center freq. at this bit rate (MHz)	5147.5	5148.5	5149.0

This page intentionally left blank.

APPENDIX 2-B

Properties of the Differential Encoder Specified in IRIG Standard 106 for OQPSK Modulations

B.1. Introduction

This appendix summarizes a study of the differential encoder originally adopted by the US DoD ARTM project and the RCC and incorporated into the IRIG 106 for Feher's Quadrature Phase Shift Keying (FQPSK)-B modulation. The study, performed by Mr. Robert Jefferis of the TYBRIN Corporation, was prompted by inquiries from industry representatives who were concerned that this particular differential code was not associated with commercial telecommunication standards and the fact that manufacturers had experienced confusion over correct implementation. The study results shown in this appendix prove the code to be robust, reliable, and applicable to SOQPSK-TG as well as FQPSK-B and FQPSK-JR.[32]

This appendix is organized along the following structure. Section B.2 describes the need for differential encoding. Section B.3 explains the IRIG-106 differential code for OQPSK. Section B.4 demonstrates differential code's invariance with respect to constellation rotation. Section B.5 shows the differential decoder to be self-synchronizing. Section B.6 reviews the differential decoder's error propagation characteristics. Section B.7 analyzes a recursive implementation of the differential code. Section B.8 describes use of this code with frequency modulator-based SOQPSK transmitters. Section B.9 provides a summary of the findings. A description of the implementation of the entire coding and decoding process can be seen at B.10 to this appendix.

B.2. The Need For Differential Encoding

Practical carrier recovery techniques like Costas loops and squaring loops exhibit a troublesome M-fold carrier phase ambiguity. The following paragraphs provide a description of ambiguity problems and how to overcome them.

Figure B-1 shows a simplified quadriphase transmission system that is one of the methods recommended for transparent point-to-point transport of a serial binary data stream. Transparent means that only revenue-bearing data is transmitted. There is no in-line channel coding nor is special bit pattern insertion allowed. The assumption is made for an NRZ-L data stream containing the bit sequence $b(nTb)$ transmitted at rate $r_b = 1/T_b$ bits per second. For QPSK and OQPSK modulations, the bit stream is divided into subsets e containing even-numbered bits and o containing odd numbered bits. The transmission rate associated with the split symbol streams is $r_s = r_b/2$ symbols per second. Symbol values are converted to code symbols by the differential encoder described in Section B.3. A baseband waveform generator converts the digital symbol time series into continuous time signals suitable for driving the vector modulator as prescribed for the particular modulation in use. Thus, each subset modulates one of two orthogonal subcarriers, the in-phase *(I)* channel, and the quadrature *(Q)* channel. The modulator combines these subcarriers, creating a phase-modulated RF signal *S(t)*. On the receive side, demodulation separates the subcarriers, translates them back to baseband, and constructs

---

[32] FQPSK-JR is an FQPSK variant developed by Mr. Robert Jefferis, TYBRIN Corporation, and Mr. Rich Formeister, RF Networks, Inc.

replicas of the code symbol series $E'(nT_s)$ and $O'(nT_s)$. Decoding reverses the encoding process and a multiplexer recreates a replica of the bit stream $b'(nT_b)$.
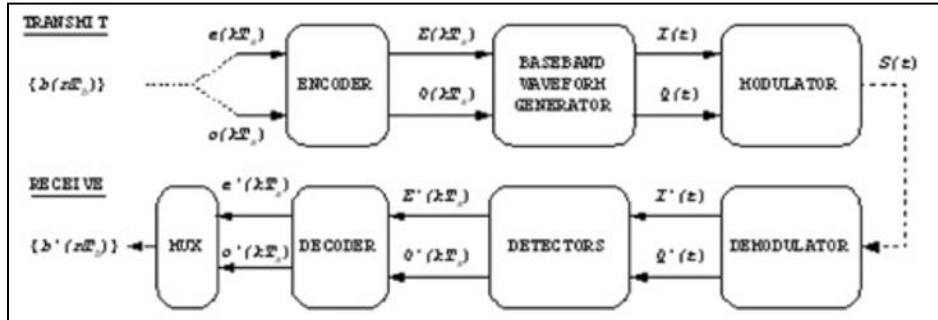
Figure B-1.   Transmission System

Most QPSK and OQPSK systems employ coherent demodulation. Figure B-2 is a simplified diagram of commonly used modulation and demodulation structures. Note the optional single-bit delay shown in the odd symbol path. This creates the significant difference between QPSK and OQPSK, the delay being inserted to create OQPSK.[33] Practical carrier recovery techniques like Costas loops and squaring loops exhibit a troublesome M-fold phase ambiguity (M=4 for QPSK and OQPSK).[34] Each time the demodulator carrier synchronizer phase locks to the modulator local oscillator its absolute phase relationship to the local oscillator contains the offset term β, which can take on values of 0, $\pm \pi/2$, or π radians.[35]
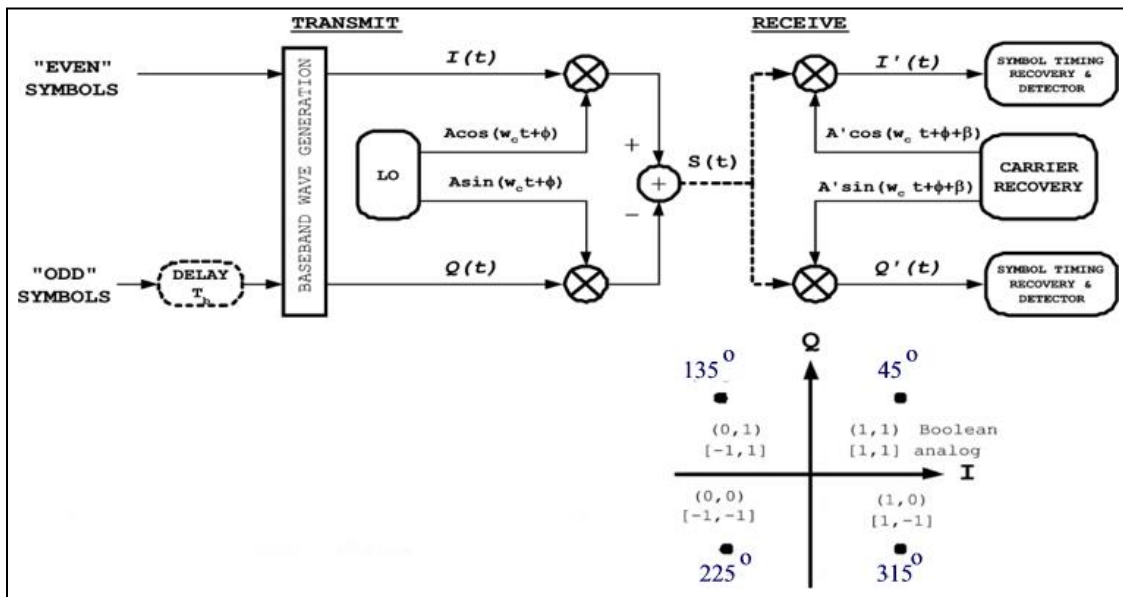
Figure B-2.   OQPSK 106 Symbol-to-Phase Mapping Convention

---

[33] The delay can be inserted into either channel. The IRIG-106 convention and most published literature regarding FQPSK and SOQPSK indicate the delay in the odd (or Q) channel.

[34] Proakis, J. G. and M. Salehi. *Digital Communications*. 5th Edition. Boston: McGraw-Hill, 2008.

[35] The initial offset angle ϕ is generally unknown and uncontrolled; it is tracked by the carrier recovery circuitry and the symbol timing circuits automatically ignore.

The symbol detectors have insufficient information to determine which phase offset exists. They always interpret demodulator output with the assumption that β=0. The resulting constellation axis rotations and their impact on demodulator output are shown at Figure B-3 and Table B-1. The 180° rotation is symmetric. The Axis (subcarrier) assignment is unchanged but the sense (polarity) of both axes gets reversed. The 90° and 270° rotations are asymmetric. Axis assignment is swapped and one axis polarity is reversed in each case.
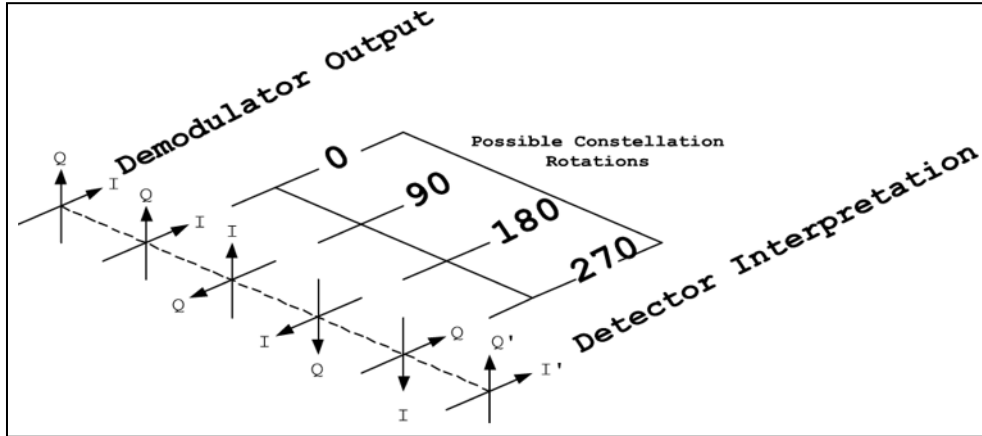
Figure B-3.   Detection Ambiguity

Table B-1. Constellation Axis Rotations		
Rotation	**$+I'$**	**$+Q'$**
0	I	Q
$\pi/2$	$-Q$	I
π	$-I$	$-Q$
$3\pi/2$	Q	$-I$

B.3.   A Simple Solution To The Carrier Phase Ambiguity Problem

Differential encoding has been used to work around the carrier ambiguity for many years. For phase modulations, source data is coded such that phase differences rather than absolute phase coordinates become the information-bearing attribute of the signal. The QPSK and OQPSK modulations use *I* and *Q* independently, with each channel transporting one symbol stream. Starting with the first binary digit, bit 0, even-numbered bits form the sequence $\{e_k\}$ and odd-numbered bits form the sequence $\{o_{k+1}\}$ where the counting index is changed from the bit index *n* to the symbol pair index

$$k = 2n \quad k \in \{0,2,4,6,...\} \quad\quad\quad\quad \text{B-1}$$

Figure B-4 illustrates how QPSK modulators process bits in pairs (dibits), mapping and asserting time coincident symbol phase coordinates (I_k, Q_k).[36] Phase state changes commence and end on symbol interval timing boundaries, each state taking on one of four possible values at detector decision instants; however, the case of interest is shown in Figure B-5.

---

[36] Rectangular I and Q baseband waveforms are used only for illustration.
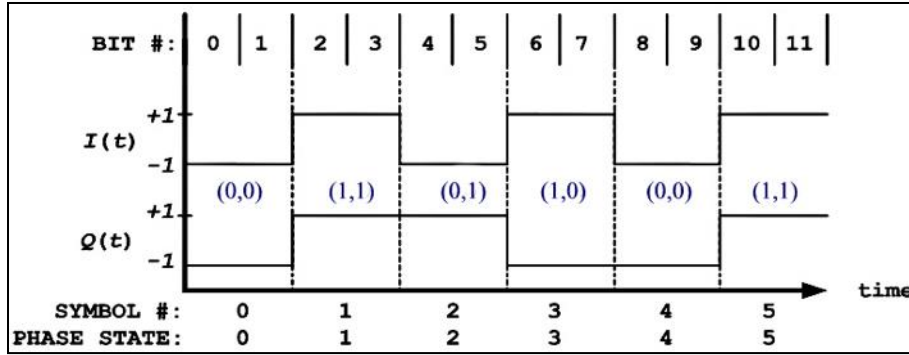
Figure B-4.   QPSK State Timing
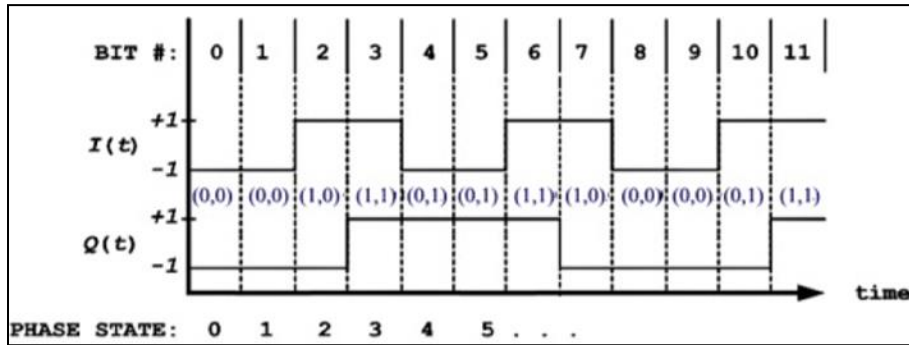
Figure B-5.   OQPSK State Timing

The Q channel half-symbol delay causes OQPSK phase trajectories to evolve on a half-symbol (bit) rate basis. For the particular cases of FQPSK and SOQPSK-TG, carrier phase either remains unchanged or changes by $\pm\pi/4$ or $\pm\pi/2$ radians over the pending bit interval.

The OQPSK inter-channel delay might at first seem a difficult complication because it creates additional ambiguity; in other words, the receiver must resolve relative inter-channel delay; however, as shown below, this is not a problem.

The differential encoding rule adopted in IRIG-106 for OQPSK appears in Feher[37] and is therein attributed to Clewer[38] and Weber.[39] Bit by bit, the code symbol sets $\{E_k\}$ and $\{O_{k+1})$ are formed with the Boolean expressions:

$$E_k \equiv e_k \oplus \overline{O}_{k-1} \qquad \text{(B-2a)}$$

B-2

$$O_{(k+1)} \equiv o_{k+1} \oplus E_k \qquad \text{(B-2b)}$$

---

[37] Kamilo Feher. *Digital Communications: Satellite/Earth Station Engineering*. Englewood Cliffs: Prentice-Hall, 1983, pp. 168-170.

[38] R. Clewer. "Report on the Status of Development of the High Speed Digital Satellite modem", RML-009-79-24, Spar Aerospace Limited, St. Anne de Bellevue, P.Q., Canada, November 1979. Quoted in Kamilo Feher. *Digital Communications: Satellite/Earth Station Engineering*. Englewood Cliffs: Prentice-Hall, 1983.

[39] W. J. Weber III. "Differential Encoding for Multiple Amplitude and Phase Shift Keying Systems." In IEEE Transactions on Communications, Vol. COM-26, No. 3, March 1978.

Two bits are coded for each value of k in a two-step process. First, the even symbol E_k is coded with current bit e_k. Then the next bit, o_{k+1} becomes current and the odd symbol O_{k+1} is computed. In each code set the exclusive-or operator is applied to the state defining variables just like binary phase shift keying (BPSK) differential encoding. Unlike BPSK however, the current source bit and the most recent code symbol from the other channel determine adjacent phase transitions. The inverted code symbol in Equation B-2a introduces asymmetry in the equations. Its significance will become evident in the next section.

The code symbol sets $\{E\}$ and $\{O\}$ are applied to the I and Q channels of the OQPSK modulator. The initial assignment of $\{E\}$ to either I or Q can be made arbitrarily; however, with this code definition, once the choice is made at the modulator, decoding will fail if channel assignment conventions change anywhere during the transmission or decoding processes. Thus, the assignment convention must extend to the physical modulator and demodulator. The IRIG-106 assigns I to the physical I subcarrier (also known as the "real" or "cosine" subcarrier) and Q is applied to the physical Q subcarrier (also known as the "imaginary" or "sine" subcarrier). In order to stress this assignment convention, IRIG-106 expresses Equation B-2 explicitly in terms of the I and Q channel variables:

$$I_k \equiv e_k \oplus \overline{Q}_{(k-1)} \qquad \text{(B-3a)}$$

$$Q_{(k+1)} \equiv o_{(k+1)} \oplus I_k \qquad \text{(B-3b)}$$

B-3

Decoding is straightforward. When $\beta=0$, $I'=I$, and $Q'=Q$, inspection of the following truth tables reveals simple decoding instructions:

Equation B-3a | Equation B-3b

I_k	$\overline{Q}_{(k-1)}$	e_k		$Q_{(k+1)}$	I_k	$o_{(k+1)}$	
0	0	0		0	0	0	
0	1	1		1	0	1	$\Rightarrow$ decoding equation
1	0	1		0	1	1	
1	1	0		1	1	0	

Equation B-3

$$e'_k = I'_k \oplus \overline{Q}'_{k-1} \qquad \text{(B-4a)}$$

$$o'_{k+1} = Q'_{k+1} \oplus I'_k \qquad \text{(B-4b)}$$

B-4

The equations at B-3 may not convey an intuitive sense of the shift from absolute phase states to phase differences. Extending B-3a backwards in time by substituting B-3b into B-3a results in:

$$I_k = e_k \oplus (\overline{o_{k-1} \oplus I_{k-2}}) = I_{k-2} \oplus (\overline{e_k \oplus o_{k-1}}) \qquad \text{B-5}$$

Similarly, for the next bit interval the results are:

$$Q_{k+1} = o_{k+1} \oplus (e_k \oplus \overline{Q}_{k-1}) = Q_{k-1} \oplus (\overline{o_{k+1} \oplus e_k}) \qquad \text{B-6}$$

This recursive form clearly shows that on a bit-by-bit basis, the current and most recent bits control phase trajectory motion, not absolute phase. Note that B-5 and B-6 do not define the sign of a phase change. Predictable decoder output requires that two additional conventions be established and maintained. Boolean logic polarity conventions used throughout the system must be consistent. The IRIG-106 assumes positive true logic. Finally, sign conventions and channel assignment used within the transmitter (baseband signal generator and modulator) and the receiver (demodulator) must be constrained to produce a consistent code symbol-to-phase mapping convention. The IRIG-106 convention is shown in Figure B-2. For example, if {b} were to consist entirely of logic one values, i.e., a run of 1s, the differential encoding process and mapping convention will produce the phase trajectory shown in Table B-2.

Table B-2. Response to Run of 1s							
n	**b(n)**	**k**	**I_k**	**Q_{k-1}**	**Q_{k+1}**	**Phase (deg)**	**Phase Δ**
0	1	0	0	0*		225*	
1	1				1	135	$-\pi/2$
2	1	1	1	1		45	$-\pi/2$
3	1				0	315	$-\pi/2$
4	1	2	0	0		225	$-\pi/2$
5	1				1	135	$-\pi/2$
* denotes assumed initial conditions							

The trajectory spins clockwise, and the phase is retarded by 90° during each bit interval.[40] Obviously, any single (unbalanced) sign change and any change to the mapping convention will alter the trajectory.

B.4. Immunity to Carrier Phase Rotation

The equations at B-3 and B-4 are invariant with respect to cardinal constellation rotation as shown in the following.

Proof:

The β=0 case is decoded correctly by definition according to equations B-5 and B-6. At Table B-1, when β = π there is no axis swap but the decoder is presented with

$$I'_k = \bar{I}_k$$
$$Q'_{k+1} = \overline{Q}_{k+1}$$

Decoding will progress as follows:

Step 1. Even channel; apply Equation B-4a;

$$e'_k = I'_k \oplus \overline{Q}'_{k-1} = \bar{I}_k \oplus Q_{k-1} = I_k \oplus \overline{Q}_{k-1} = e_k$$

---

[40] FQPSK-B, FQPSK-JR, and SOQPSK-TG modulations respond to a run of 1s with an S(t) that is ideally, a pure tone at frequency f_c-r_b/4 Hz. This is referred as "lower sideband" mode. Similarly, a run of zeroes will produce a constant anti-clockwise trajectory spin and a tone at f_c+r_b/4 Hz ("upper sideband" mode).

Step 2. Odd channel; apply equation B-4b;

$$o'_{k+1} = Q'_{k+1} \oplus I'_k = \overline{Q}_{k+1} \oplus \bar{I}_k = Q_{k+1} \oplus I_k = o_{k+1}$$

Thus, symmetric rotation is transparent to the code. When $\beta = \pi/2$ the decoder sees the following.

$$I'_k = \overline{Q}_{k-1}$$
$$Q'_{k+1} = I_k$$

Decoding takes place in the same sequence:

Step 1. Even channel, apply equation B-4a;

$$e'_k = I'_k \oplus \overline{Q}'_{k-1} = \overline{Q}_{k-1} \oplus \bar{I}_k = I_k \oplus Q_{k-1} = o_{k-1}$$

Step 2. Odd channel, apply equation B-4b;

$$o'_{k+1} = Q'_{k+1} \oplus I'_k = I_k \oplus \overline{Q}_{k-1} = e_k$$

In this case the bit sequence is recovered correctly and the code definition coupled with consistent sign conventions automatically compensates for the asymmetric rotation by reversing the application order of B-4a and B-4b. As a result, the output indices are shifted back in time one bit period. Asymmetric rotation causes a one-bit delay in the decoding process. Finally, the same result is seen when $\beta = 3\pi/2$:

$$I'_k = Q_{k-1}$$
$$Q'_{k+1} = \bar{I}_k$$

Step 1. Even channel; apply equation B-4a;

$$e'_k = I'_k \oplus \overline{Q}'_{k-1} = Q_{k-1} \oplus I_k = I_k \oplus Q_{k-1} = o_{k-1}$$

Step 2. Odd channel; apply equation B-4b;

$$o'_{k+1} = Q'_{k+1} \oplus I'_k = \bar{I}_k \oplus Q_{k-1} = I_k \oplus \overline{Q}_{k-1} = e_k$$

In all cases the decoder correctly reproduces the original bit sequence. Decoding is instantaneous for symmetric rotations but it is delayed by one bit in 2 out of 4 possible asymmetric rotation startup scenarios.

The need for consistent function assignment now becomes clear. Application of B-4b to a code symbol formed with B-3a produces the complement of the original bit. Likewise, application of B-4a to a symbol coded with B-3b inverts the result.

At this point, the OQPSK inter-channel delay ambiguity mentioned in Section B.2 has not been resolved. The roles of I' and Q' reverse with asymmetric rotations and there is no way to determine when this occurs; however, as long as the code symbol time sequence is preserved at the decoder and the roles of I' and Q' do not get reversed in terms of the application of B-4a

and [B-4]b, inter-channel delay is transparent to the code with respect to reconstruction of the original data sequence.[41]

B.5.   Initial Values

Equations [B-3] and [B-4] do not impose any implementation constraints on initial values when encoding or decoding starts. To confirm this it is assumed that hardware power-up (or initial data presentation) may cause encoding to commence with either channel. It is further assumed that no provisions for specific initial values in encoder and decoder state memories have been made. If coding starts with I (see equation [B-3]a), the first code symbol will be computed:

$$\|I_0\| = e_0 \oplus \langle \overline{Q_{-1}} \rangle$$

where $\langle . \rangle$ denotes an unknown initial value and double vertical bars denote computed values influenced by initial values. Encoding equations [B-3]a and [B-3]b will progress as follows:

$$\|Q_1\| = o_1 \oplus \|I_0\|$$

$$\|I_2\| = e_2 \oplus \|\overline{Q_1}\|$$

The initial values do establish the absolute sense of code symbols for the duration of transmission; but, on both ends of the process, two of three terms in every equation are affected consistently by the initial value, which by symmetry has no effect on the outcome of exclusive-or operations. Obviously, identical results occur if the encoder starts with Q. Independent of starting channel and initial value then, the first and all subsequent adjacent code symbol pairs contain valid state change information.

Initial decoder values can produce errors. Again starting with I, and using equations [B-4]a and [B-4]b, decoding will progress as follows:

$$\|e'_0\| = I'_0 \oplus \langle \overline{Q'_{-1}} \rangle$$

$$o'_1 = Q'_1 \oplus I'_0$$

It is seen that on the second cycle the initial value of the decoder has been flushed out. At most, one bit will be decoded in error. Similarly, if decoding starts with Q, output will progress:

$$\|o'_1\| = Q'_1 \oplus \langle I'_0 \rangle$$

$$e'_2 = I'_2 \oplus \overline{Q}'_1$$

Again, only the first decoded bit may be incorrect. The conclusion, then, is that initial values can produce at most one decoded bit error; however, there is another source of startup errors that is seen as an initial value problem. Section [B.4] showed that odd phase rotations ($\pi/2$

---

[41] If for some reason the system application requires that one can determine whether a specific symbol was originally transmitted via I or Q, then this code is not appropriate.

and $3\pi/2$) cause a single bit delay in the decoder. Examining this further, the first symbol index value will be $k = 0$. If the decoder starts with equation B-4a, the first decoded bit will be:

$$e'_0 = I'_0 \oplus \langle \overline{Q'_{-1}} \rangle = I_0 \oplus \langle Q_{-1} \rangle = \langle o_{-1} \rangle$$

If the decoder starts with equation B-4b the first result will be:

$$o'_1 = Q'_1 \oplus I'_0 = I_0 \oplus \langle \overline{Q_{-1}} \rangle = \|e_0\|$$

The first case produces the aforementioned delay. The decoder emits an extra bit. The second bit emitted is actually the first bit of the sequence reconstruction and is still subject to the single initial value error probability of startup processing. The latter case does not produce a delay; it only presents the possibility of a first bit decoding error.

B.6.   Error Propagation

Differential encoding incurs a bit error penalty because received code symbols influence more than one decoded bit. First consider a single-symbol detection error in current symbol E' that is labeled ε_k. The following sequence of decoding steps shows how the error propagates. Since the E channel was chosen as current, decoding starts with equation B-4a. The single detection error creates two sequential decoding errors. By symmetry we can state that the same result occurs if a single error occurs in O'.

$$b'_k = \varepsilon_k \oplus \overline{Q}_{k-1} = \overline{b}_k \Rightarrow \text{error}$$
$$b'_{k+1} = Q_{k+1} \oplus \varepsilon_k = \overline{b}_{k+1} \Rightarrow \text{error}$$
$$b'_{k+2} = E'_{k+2} \oplus Q'_{k+1} = b_{k+2} \Rightarrow \text{correct}$$

Next is the case of two symbol detection errors occurring consecutively on E' and O', i.e., detectors emit error symbols $E'_k = \varepsilon_k$ and $O'_{k+1} = \varepsilon_{k+1}$. Starting again with equation B-4a yields:

$$b'_k = \varepsilon_k \oplus \overline{Q}_{(k-1)} = \overline{b}_k \Rightarrow \text{error}$$
$$b'_{(k+1)} = \varepsilon_{(k+1)} \oplus \varepsilon_k = O'_{(k+1)} \oplus E_k = b_{(k+1)} \Rightarrow \text{correct}$$
$$b'_{(k+2)} = E'_{(k+2)} \oplus \varepsilon_{(k+1)} = b_{(k+2)} \Rightarrow \text{error}$$
$$b'_{(k+3)} = O'_{(k+3)} \oplus E'_{(k+2)} = b_{(k+3)} \Rightarrow \text{correct}$$

Two consecutive symbol errors produce two decoding errors but the errors are not adjacent. The conclusion from this is that symbol detection errors influence no more than two decoding cycles, i.e., the maximum error multiplication factor is 2.

B.7.   Recursive Processing and Code Memory

Most systems reconstruct the original bit rate clock and $\{b\}$ by merging $\{e'\}$ and $\{o'\}$. For a variety of reasons, designers might be tempted to multiplex $\{I'\}$ and $\{Q'\}$ into a bit rate code symbol sequence $\{B_n\}$ prior to decoding; however, the same considerations that foster desire for post-multiplex decoding are likely to be accompanied by loss of transmitted code

symbol order, i.e., loss of knowledge whether a given code symbol came from *I* or *Q*. The question arises as to whether {B_n} alone contains enough information for unique decoding. The answer is no, and the proof is shown below.

Proof:

A decoding function can be derived by inspection of equations B-5 and B-6. Equation B-5 can be rearranged as follows:

$$I_k = e_k \oplus o_{k-1} \oplus \bar{I}_{k-2} \qquad \text{B-7}$$

Similarly, from equation B-6 we can write

$$Q_{k+1} = o_{k+1} \oplus e_k \oplus \bar{Q}_{k-1} \qquad \text{B-8}$$

Here are two instances of a seemingly identical recursive relationship, i.e., the current code symbol is the difference between the current bit, the previous bit, and the inverse of the most recent code symbol from the current channel. We can consolidate these equations by converting to post-multiplex bit rate indexing, i.e.,

$$B_n = b_n \oplus b_{(n-1)} \oplus \bar{B}_{n-2} \qquad \text{B-9}$$

from which we can immediately write the decoding function

$$b'_n = b'_{(n-1)} \oplus B'_n \oplus \bar{B}'_{(n-2)} \qquad \text{B-10}$$

On the surface it seems that Equation B-10 will work;[42] however, these relations involve two differences, rather than one, and therefore introduce superfluous initial condition dependence. For brevity, only the pitfalls of B-10 are examined herein, assuming that a non-recursive encoder is used. From startup, decoding will progress as follows.

$$\left\| b'_0 \right\| = \left\langle b'_{-1} \right\rangle \oplus B'_0 \oplus \left\langle \bar{B}'_{-2} \right\rangle$$
$$\left\| b'_1 \right\| = \left\| b'_0 \right\| \oplus B'_1 \oplus \left\langle \bar{B}'_{-1} \right\rangle$$
$$\left\| b'_2 \right\| = \left\| b'_1 \right\| \oplus B'_2 \oplus \bar{B}'_0$$
$$\left\| b'_3 \right\| = \left\| b'_2 \right\| \oplus B'_3 \oplus \bar{B}'_1$$

.

.

.

As seen, absolute polarity of the first and all subsequent decoded bits is determined by three initial values. Absent appropriate side information for selecting initial values, the post-multiplex decoder offers a 50-50 chance of decoding with correct polarity. The code sequence defined by equations at B-3 has a two-symbol memory. Additional symbols do not provide new information regarding the trajectory history. Another way to view this problem is to note that this

---

[42] The interested reader is left to confirm that equation C-10 is indeed rotation invariant.

recursive decoder does not guarantee preservation of symbol order, which is a prerequisite to reliable decoding.

B.8.   Frequency Impulse Sequence Mapping for SOQPSK

The SOQPSKs first described by Hill[43] and Geoghegan[44] are defined as special cases of CPM. Since 1998, at least two manufacturers have exploited the fact that modern digital waveform synthesis techniques enable direct implementation of the CPM equations with virtually ideal frequency modulators and filter impulse responses. A generic model of these implementations is in Figure B-6. The I and Q channels, per se, do not exist in this transmitter. At the beginning of each bit interval, impulses from the bit-to-impulse alphabet mapper direct the impulse filter/frequency modulator to advance the carrier phase by 90°, retard it by or 90°, or leave the phase unchanged. This is accomplished with a ternary alphabet of frequency impulses having normalized amplitudes of $\{-1,0,1\}$.[45] This structure cannot be mapped directly into the constellation convention of a quadriphase implementation because there is no way to control absolute phase. The equations at B-3 can be applied to this non-quadrature architecture via pre-coding. A general treatment SOQPSK pre-coding is contained in Simon.[46] The pre-coding truth table given in Table B-3 applied to the model in Figure B-7 will yield a phase trajectory history identical to one generated by the quadriphase counterpart of Figure B-2 using the equations at B-3; however, one more constraint is necessary to establish compatibility with the IRIG-106 quadriphase convention. Table B-3 assumes the stipulation that positive sign impulse values will cause the modulator to increase carrier frequency.
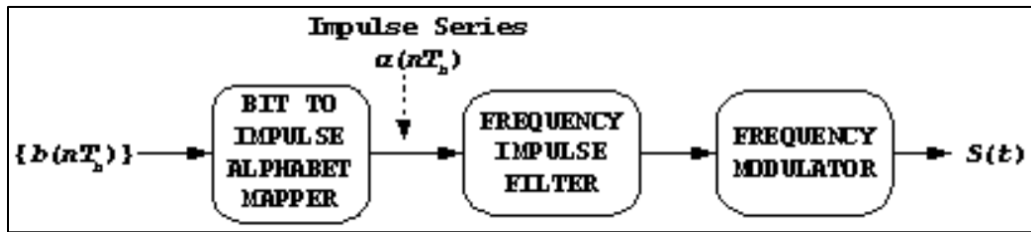
Figure B-6.   SOQPSK Transmitter

Table B-3. SOQPSK Pre-Coding Table for IRIG-106 Compatibility									
MAP α_K FROM I_K					MAP α_{K+1} FROM Q_{K+1}				
I_k	Q_{k-1}	I_{k-2}	$\Delta\Phi$	α_k	Q_{k+1}	I_k	Q_{k-1}	$\Delta\Phi$	α_{k+1}
-1	X*	-1	0	0	-1	X*	-1	0	0
$+1$	X*	$+1$	0	0	$+1$	X*	$+1$	0	0
-1	-1	$+1$	$-\pi/2$	-1	-1	-1	$+1$	$+\pi/2$	$+1$
-1	$+1$	$+1$	$+\pi/2$	$+1$	-1	$+1$	$+1$	$-\pi/2$	-1
$+1$	-1	-1	$+\pi/2$	$+1$	$+1$	-1	-1	$-\pi/2$	-1

[43] Hill, "An Enhanced, Constant Envelope, Interoperable Shaped Offset QPSK."
[44] Geoghegan, "Implementation and Performance Results."
[45] The so-called ternary alphabet is actually 2 binary alphabets {-1,0} and {0,1}, the appropriate one chosen on a bit-by-bit basis according to certain state transition rules.
[46] Marvin Simon. "Multiple-Bit Differential Detection of Offset Quadriphase Modulations." IPN Progress Report 42-151. 15 November 2002. Jet Propulsion Laboratory, Pasadena, CA. Retrieved 17 May 2021. Available at http://ipnpr.jpl.nasa.gov/progress_report/42-151/151A.pdf.

+1	+1	−1	−π/2	−1	+1	+1	−1	+π/2	+1
* Note: Does not matter if "X" is a +1 or a −1									
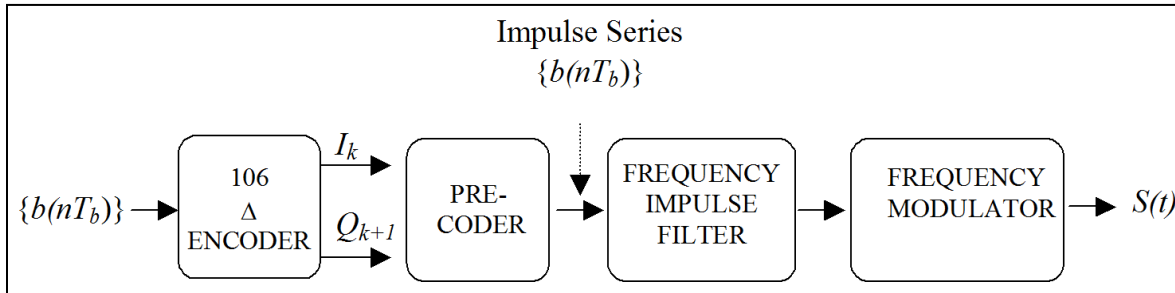
Figure B-7.   OQPSK Transmitter (With Precorder)

B.9.   Summary

This investigation confirmed that the differential encoder defined in the equations at B-3 is entirely satisfactory for SOQPSK, FQPSK-JR, and FQPSK-B systems where conventional coherent demodulation and single-symbol detection is used. In addition, a method of extending this code to SOQPSK is presented without proof.

Specifically, the following has been shown.

a.   When accompanied by consistent sign conventions, a consistent symbol-to-phase mapping rule, and preservation of symbol order, the OQPSK differential code defined in B-3 and the decoding rule defined in B-4 is rotation invariant and unambiguously reconstructs the original data bit sequence.

b.   Decoding is instantaneous.

c.   Equations B-3 and B-4 do not require attention to initial values.

d.   At most, two consecutive output bits will be in error after carrier and symbol synchronization is acquired.

e.   The recursive relations in equations B-9 and B-10 are ambiguous and therefore unreliable.

f.   The code exhibits a detection error multiplication factor of at most two.

B.10.   System-Level Software Reference Implementation of Differential Encoder Defined in IRIG Standard 106 for FQPSK and SOQPSK Modulations

B.10.a. Introduction

The Matlab®™ program listings below provide a Matlab function "Desysdemo" and an execution control script "runDEdemo". In the context of differential encoding, the function provides a complete system simulation including a differential encoder, an ideal vector modulator, channel phase rotation, demodulation, the functional equivalent of an ideal single-symbol sample and hold detector, and a decoder. The user can create sample data vectors or use the example data provided. In addition, the user can manipulate the initial value vectors to explore all possible initial value and demodulator phase rotation combinations of the quadriphase implementation model.

By setting the variable "style" to zero, the function will also emulate the pre-coded frequency modulator architecture required for SOQPSKs; however, the initial value of transmitter carrier phase is hard-coded at 45°. This was done to avoid proliferation of initial value options and is thought to be an insignificant omission because it does not affect generality of the phase rotation options.

This material assumes that the user is familiar with Matlab workspace operation. The program relies only on basic Matlab license libraries. No special toolboxes or blocksets are required.

B.10.b. Matlab Workspace Operation

The user should place the script (shown below in Section B.10.c) in the directory of choice and make that directory current in the workspace. In order to execute the canned example, the user needs to create the variable "example" in the workspace and set its value to 1.

Executing the script "runDEdemo" should produce the output displayed in Table B-4.

Table B-4. Script "runDEdemo" Output				
results =				
Model: Quadriphase Vector Modulator				
Demodulator Phase Rotation = 0°				
Initial States:	Encoder Memory	Encoder Channel	Decoder Memory	Decoder Channel
	(0,0)	0	(0,0)	0
Input Bit	TX Phase	RX Phase	Output Bit	Decoding Error
1	225	225	1	0
1	135	135	1	0
1	45	45	1	0
0	45	45	0	0
0	135	135	0	0
1	135	135	1	0
0	135	135	0	0
1	135	135	1	0
1	45	45	1	0
1	315	315	1	0
0	315	315	0	0
0	45	45	0	0
1	45	45	1	0
0	45	45	0	0

The first column of the results shown above is a replica of the input data vector. The second column shows the initial value-dependent evolution of transmitted phase. The third column shows the effect of any non-zero phase rotation chosen. The fourth column shows the decoded output bit stream. The fifth column flags decoding errors with values of 1. Certain combinations of phase rotation and initial values will produce values of 9 in the fourth and fifth

columns; results of this nature are associated with cases that delay the output decoding process by one bit.

Variable definitions and implied instructions for manipulating the runtime options can be obtained by using the normal Matlab help command for these specific programs.

B.10.c. Script for Modules

Electronic copies of these programs have been provided to the RCC Telemetry Group. The script for the modules discussed above is shown on the following pages.

```
% Control Script 'runDEdemo', for running system demonstration
% of differential encoder and phase mapping convention
% defined in RCC standard IRIG-106 for FQPSK-B modulation.
% This version extends demonstration options to the pre-coder
% required for implementing SOQPSK with frequency modulators.
%
% Each example run requires input variables in the Matlab workspace:
%
% "example" - a flag to run with user supplied data vector or run
%    the example data set that consists of two repetitions of a
%    a 7-bit pseudo random sequence(0=user, 1=example)
% "data" - optional user supplied binary bit sequence (arbitrary
length)
% "rotation_choice" - pointer to demodulator phase rotation options:
%  1=0, 2=pi/2, 3= pi, 4=3*pi/2
% "initTX" - vector of binary encoder startup values:
%  initTX(1)= 1st of two encoder code symbol memory values(binary,
arbitrary)
%  initTX(2)= 2nd encoder code symbol memory value(binary, arbitrary)
%  initTX(3)= starting channel for encoder(binary, 0=I, 1=Q)
% "initRX" - vector of binary decoding startup values
%  initRX(1)= 1st of two decoder state memory values(binary, arbitrary)
%  initRX(2)= 2nd decoder state memory value(binary, arbitrary)
%  initRX(3)= starting channel for decoder(binary, 0=I, 1=Q)
% "style" - 1=quadriphase transmitter architecture (FQPSK)
%      0=frequency modulator transmitter architecture (SOQPSK)
% The example values are:
%  data=[1 1 1 0 0 1 0 1 1 1 0 0 1 0]
%  rotation_choice=1
%  initTX=[0 0 0]
%  initRX=[0 0 0]
%  style=1

% R.P.Jefferis, TYBRIN Corp., JULY, 2002
% SOQPSK model added 14JUL03
% This version has been tested with Matlab versions:5.2,6.1

% *** Sample Input Setup ***
if example
   data=[1 1 1 0 0 1 0 1 1 1 0 0 1 0];
   rotation_choice=1;
   initTX=[0 0 0];
   initRX=[0 0 0];
   style=1;
end

% *** Run the Reference Implementation ***

[test,delay]=DEsysdemo(data,rotation_choice,initTX,initRX,style);

% *** Prepare Screen Output ***
```

```
ROTATION=[0 90 180 270];
if style
   results=sprintf('Model: Quadriphase Vector Modulator\n')
else
   results=sprintf('Model: Frequency modulator (SOQPSK) model\n')
end
results=[results sprintf('Demodulator Phase Rotation = %3.0f
degrees\n',ROTATION(rotation_choice))];
results=[results sprintf('Initial States: Encoder Encoder Decoder
Decoder\n')];
results=[results sprintf('                     Memory  Channel Memory
Channel\n')];
results=[results sprintf('---------------------------------------------
----\n')];
results=[results sprintf('                     (%d,%d)     %d    (%d,%d)
%d\n\n',...
      initTX(1:2),initTX(3),initRX(1:2),initRX(3))];
results=[results sprintf(' Input  TX      RX    Output Decoding\n')];
results=[results sprintf(' Bit   Phase   Phase   Bit    Error\n')];
results=[results sprintf('-----------------------------------\n')];
for n=1:length(data)
   results=[results sprintf(' %d     %3.0f    %3.0f      %d
%d\n',...
         test(n,:))];
end
results


% _____END OF CONTROL SCRIPT_____

function [result,delay]=
DEsysdemo(inbits,rotation_choice,initTX,initRX,style)
% Reference simulation for Range Commanders Council standard IRIG 106-
2000
%  FQPSK-B differential encoding and phase mapping convention.
%
% Input arguments: see "help" for "runDEdemo" script
% Output arguments:
% "result" - Mx5 matrix,M=number of input bits,columns contain:
%  (:,1)input bit,(:,2)TX phase,(:,3)RX phase,(:,4)output
bit,(:,5)status
% "delay" - overall encode/decode process delay in bits

% "TX" prefixes refer to transmitter/encoder variables, "RX" prefixes
% refer to receiver/decoder variables
% Robert P. Jefferis, TYBRIN Corp., July,2002.
% SOQPSK model added 14JUL03
% This version has been tested with Matlab versions: 5.2,6.1
numbits=length(inbits)

% ********************
% *   Transmitter    *
% ********************
```

```
% *** differential encoder (also SOQPSK pre-coder)****

% encoder memory initial values:
%[(last I ch. code symbol) (last Q ch. code symbol)]
TXlastSYM=initTX(1:2);
% point encoder to either I or Q starting channel(0=I)
TXpoint=initTX(3);
for n=1:numbits
   switch TXpoint
   case 0
      %TXlastSYM
      % compute "current" I channel code symbol
      TXnewISYM=xor(inbits(n),~TXlastSYM(2));
      TXcodeSYM(n,:)=[TXnewISYM TXlastSYM(2)]; % new phase
coordinates(I,Q)
      TXlastSYM(1)=TXnewISYM; % update encoder memory state
      TXpoint = ~TXpoint; % point to Q channel eq. for next bit
   case 1
      % compute "current" Q channel code symbol
      TXnewQSYM=xor(inbits(n),TXlastSYM(1));
      TXcodeSYM(n,:)=[TXlastSYM(1) TXnewQSYM]; % new phase
coordinates(I,Q)
      TXlastSYM(2)=TXnewQSYM;% update encoder memory state
      TXpoint= ~TXpoint;   % point to I channel eq. for next bit
   otherwise
      disp('Invalid Specification of Encoder starting channel');
   end
end

% *** modulate ***

switch style
case 1 % ** Quadriphase vector modulator **

   % RCC IRIG 106 FQPSK-B phase mapping convention: (I,Q)
   for n=1:numbits
      index=floor(2*TXcodeSYM(n,1)+TXcodeSYM(n,2));
      switch  index
      case  3    % [1 1]
         TXphase(n)=45; % TX phase angle, degrees
      case  1    % [0 1]
         TXphase(n)=135;
      case  0 % [0 0]
         TXphase(n)=225;
      case  2    % [1 0]
         TXphase(n)=315;
      otherwise, disp('map error')
      end
   end
case 0 % ** Frequency modulator w/pre-coder **
```

```matlab
    % * pre-coder *
    % map code symbol sequence to frequency impulse series, alpha(n)
    alpha=zeros(1,numbits);
    TXpoint=initTX(3); % in this mode, points to start index
    for n=3:numbits
        if TXpoint % Q(k+1) map
            if TXcodeSYM(n,2)==TXcodeSYM(n-2,2)
            elseif xor(TXcodeSYM(n,2),TXcodeSYM(n-1,1))
                alpha(n)=-1;
            else
                alpha(n)=1;
            end
        else % I(k) map
            if TXcodeSYM(n,1)==TXcodeSYM(n-2,1)
            elseif xor(TXcodeSYM(n,1),TXcodeSYM(n-1,2))
                alpha(n)=1;
            else
                alpha(n)=-1;
            end
        end
        TXpoint=~TXpoint; % switch to complement function for next bit
    end

    % convert alpha to phase trajectory
    lastTXphase=45; % initial phase of S(t)
    for n=1:numbits
        TXphase(n)=mod(lastTXphase+alpha(n)*90,360);
        lastTXphase=TXphase(n);
    end
otherwise
end

% ************
%  * Receiver *
% ************

% *** Demodulator Phase Rotation ***
ROTATE=[0 pi/2 pi 3*pi/2];
rotate=ROTATE(rotation_choice);
for n=1:numbits
    switch rotate
    case 0
        RXphase(n)=TXphase(n);
    case pi/2
        RXphase(n)=mod(TXphase(n)+90,360);
    case pi
        RXphase(n)=mod(TXphase(n)+180,360);
    case 3*pi/2
        RXphase(n)=mod(TXphase(n)+270,360);
    otherwise
    end
end
```

```
% *** detector ***
for n=1:numbits
   switch RXphase(n)
   case 45
      RXcodeSYM(n,:)=[1 1];
   case 135
      RXcodeSYM(n,:)=[0 1];
   case 225
      RXcodeSYM(n,:)=[0 0];
   case 315
      RXcodeSYM(n,:)=[1 0];
   otherwise
   end
end

% *** decode and reconstruct data bit sequence ***

% decoder memory initial values:
% [(last decoded I channel bit) (last decoded Q channel bit)]
RXlastSYM=initRX(1:2);
% point decoder channel to either I or Q starting channel (0=I)
RXpoint=initRX(3);
for n=1:numbits
   switch RXpoint
   case 0
      % compute "current" decoded I channel bit
      RXbits(n)=xor(RXcodeSYM(n,1),~RXlastSYM(2));
      RXlastSYM=RXcodeSYM(n,:);  % update decoder state
      RXpoint = ~RXpoint; % point to Q channel eq. for next bit
   case 1
      % compute "current" decoded Q channel bit
      RXbits(n)=xor(RXcodeSYM(n,2),RXlastSYM(1));
      RXlastSYM=RXcodeSYM(n,:);  % update decoder state
      RXpoint= ~RXpoint; % point to I channel eq. for next bit

   otherwise
   end
end

% _____ END OF TX and RX Processing _____

% *****************
% * Assemble Output *
% *****************

% identify delay incurred in overall process
offset=xcorr(inbits,RXbits);
offset(1:numbits-1)=[];
[offset,delay]=max(offset(1:min(length(offset),10)));
delay=delay-1;
```

```
% adjust RX output bit vector to compensate for delay,
% inserting values of 9 at beginning of vector to represent
% artifact bits associated with asymmetric rotation cases
checkbits=inbits;
if delay
   newfront=ones(1,delay)*9;
   checkbits=[newfront inbits];
   checkbits(end-delay+1:end)=[];
   RXbits(1:delay)=9;
end
% identify decoding errors in reconstructed bit stream
xmsn_error=checkbits~=RXbits;
xmsn_error(1:delay)=9;
% assemble output matrix
result(:,1)=inbits';
result(:,2)=TXphase';
result(:,3)=RXphase';
result(:,4)=RXbits';
result(:,5)=xmsn_error';

% _____END OF FUNCTION DEsysdemo_____
```

APPENDIX 2-C
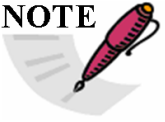
Telemetry Transmitter Command and Control Protocol

C.1. Introduction

This appendix provides standards for commands, queries, and status information when communicating with telemetry transmitters configured with communication ports. The commands are divided into two categories of command sets as follows.

a. Basic. The basic command set contains the minimum (required) commands for transmitter control, query, and status.

b. Extended. The extended command set contains optional commands that may or may not be implemented and may be shown as references.

C.2. Command Line Interface

C.2.a. User Command Line Interface

This interface is the default upon power up of the transmitter. Each command or query is ended by a carriage return <CR>. Information returned from the transmitter will be followed by a carriage return <CR> and the ">" will be displayed to indicate the transmitter is ready to receive commands or queries.

NOTE	With regard to this standard, it is assumed that a carriage return <CR> is followed by a line feed. The transmitter will return the "OK" mnemonic for each command that is accepted. The transmitter will return "ERR" for a command or query that was interpreted as an error. Verification that a query was either accepted or found to be in error will be the response to the query. All commands are case-insensitive. The transmitter will operate in half-duplex mode and will echo typed characters to the command terminal.

In addition to the required user command line interface items, the following list contains options that may or may not be implemented.

a. Backspacing to correct typed errors.

b. A character input to recall the last command line. The "^" character followed by a <CR> is recommended.

C.2.b. Optional Programming Interface

If the transmitter is not commanded or queried though a terminal program (human interface), there may be an option to operate in half-duplex mode so that concatenated commands can be sent directly to the transmitter (bulk transmitter set-up). If this option is used, the transmitter will only return a single accepted "OK" response if the entire string was interpreted and accepted. When concatenating commands, the semicolon is used as the delimiter for each command. If this optional programming interface is implemented, the transmitter will identify the semicolon delimiter, recognize the character string as a bulk command, and recognize the start of a new command after each delimiter.

C.3.   Initialization

Upon successful communication initialization, the transmitter will provide the controlling terminal with (as a minimum) the manufacturer's name, model number, serial number, and supported IRIG-106 release number. Other information (such as information on firmware and temperature) deemed appropriate by the manufacturer is allowed. This information will be displayed only upon a successful power up and communication initialization of the transmitter. Should an unsuccessful power up occur, based upon criteria of the transmitter manufacturer, the transmitter shall return "ERR" and allow only the RE(RES) command to reset the transmitter (see Subsection C.4.b(9)).

Upon successful communication, after a power up, a communication connection, a command, or a query, the transmitter will send a carriage return followed by a ">" to signify the transmitter is ready to accept commands and queries.

C.4.   Basic Command Set

C.4.a. Basic Command Set Summary

The basic command fields use a minimum two characters with the optional capability of using a maximum of four characters. If possible, the longer four-character field should be used to add intuitiveness to the basic command set. The commands in the basic command set are shown in Table C-1.

Table C-1. Basic Command Set	
Command	**Function**
FR(FREQ)	Sets or queries the carrier frequency.
MO(MOD)	Sets or queries the modulation mode.
RA(RAND)	Sets or queries the setting of data randomization (ON or OFF).
RF	Sets or queries the RF output (ON or OFF).
QA(QALL)	Queries the status of all basic commands.
VE(VERS)	Queries, at a minimum, the manufacturer's name, model number, and serial number of the transmitter.
SV(SAVE)	Saves the current set-up of the transmitter to on-board nonvolatile random access memory (RAM).
RL(RCLL)	Retrieves a transmitter set-up from on-board nonvolatile RAM.
RE(RES)	Resets the transmitter to a known configuration or restarts the internal power-up sequence.
DS(DSRC)	Sets or queries the data source (INT or EXT).
CS(CLKS)	Sets or queries the clock source (INT or EXT).
ID(IDP)	Sets or queries the internal data pattern (one of five possible settings).
IC(ICR)	Sets or queries the internal clock rate.
TE(TEMP)	Queries the internal temperature (in Celsius).
FC(FEC)	Sets or queries FEC.
ST(STC)	Sets or queries Space Time Coding.

C.4.b. Commands: Basic Command Set

C.4.b(1)   Carrier Frequency
Carrier frequency is set or queried with the FR(FREQ) mnemonic as described below.

a. Set Frequency. Use "FR(FREQ) XXXX.X <CR>" where XXXX.X is the commanded frequency in MHz in 0.5-MHz steps. If the command is accepted, an "OK <CR>" is issued as a response.

In the event of an incorrect commanded carrier frequency (for example the commanded frequency is out of the tuning range of the transmitter), the transmitter will default to the currently set carrier frequency before the command was issued. The transmitter will then return "ERR FR(FREQ) XXXX.X <CR>" where XXXX.X is the prior frequency set in the transmitter.

b. Query Frequency. "FR(FREQ) <CR>" queries the currently set carrier frequency and returns "FR(FREQ) XXXX.X <CR>" where XXXX.X is the current set frequency in MHz.

C.4.b(2)   Modulation Mode
Modulation mode is set or queried with the MO(MOD) mnemonic.

a. Set Modulation Mode. Use "MO(MOD) X <CR>" where X corresponds to the modulation mode. If the command is accepted, an "OK <CR>" is issued as a response.

Command	Modulation Type
MO(MOD) 0	PCM/FM
MO(MOD) 1	SOQPSK-TG
MO(MOD) 2	ARTM-CPM
MO(MOD) 6	Modulation off (carrier only)

In the event of an incorrect commanded modulation mode, the transmitter will default to the previous modulation mode and return "ERR MO(MOD) X <CR>" to indicate the error and the current modulation mode. The "MO(MOD) 6" command turns off the modulation for carrier-only mode. Modulation will return upon a new commanded modulation mode. If the transmitter is in single mode, only single mode commands are valid and the above error response will be sent should an invalid modulation mode command be sent. The same logic applies when the transmitter is in dual mode.

b. Query Modulation Mode. "MO(MOD) <CR>" queries the currently set modulation mode and returns "MO(MOD) X <CR>" where the integer X is represented in the above table.

C.4.b(3)   Data Randomization
Data randomization is set or queried with the RA(RAND) mnemonic. For additional information on randomization, see Subsection 2.3.3.5. This command only enables/disables the randomizer specified in Annex A.2, Figure A.2-2.

a. Set Data Randomization. Use "RA(RAND) X <CR>" where X corresponds to a 1 or 0. If the command is accepted, an "OK <CR>" is issued as a response.

Command	Randomization
RA(RAND) 1	On
RA(RAND) 0	Off

NOTE	When FEC is enabled, randomization per Section D.6 should be implemented. If RA(RAND) was enabled prior to enabling FEC, it will be disabled when FEC is enabled. The default state for RA(RAND) will be off when FEC is enabled.

In the event of an incorrect data randomization command, the transmitter will default to its current setting and return "ERR RA(RAND) X <CR>" to indicate the error and the currently set state. If FC(FEC) is enabled, a "RA(RAND) 1" command will return an ERR RA(RAND) 1<CR>.

b. Query Randomization Mode. "RA(RAND) <CR>" queries the currently set randomization and returns "RA(RAND) X <CR>" where integer X is represented in the above table.

C.4.b(4)   RF Output
The RF output is set or queried with the RF mnemonic.

a. Set RF Output. Use "RF X <CR>" where X corresponds to a 1 or 0. If the command is accepted, an "OK <CR>" is issued as a response.

Command	RF Output
RF 1	On
RF 0	Off

In the event of an incorrect RF output command, the transmitter will maintain its current state and return "ERR RF X <CR>" to indicate the error and return the current RF output setting for the transmitter.

b. Query RF Output. "RF <CR>" queries the currently set RF output and returns "RF X <CR>" where X corresponds to the numbers in the above table.

C.4.b(5)   Query All
The "query all" command is executed with the QA(QALL) mnemonic.

a. Query Transmitter Configuration. The command "QA(QALL) <CR>" requests the current setting of all basic commands. The transmitter response will contain, as a minimum, the following, in this order:

(1)   Carrier Frequency.   [FR(FREQ) XXXX.X]<CR>

(2)   Modulation Mode.   [MO(MOD) X] <CR>

(3)   Randomization setting.   [RA(RAND) X] <CR>

(4)   RF Output setting.   [RF X] <CR> OK<CR>

(5)   Data Source.   [DS(DSRC) X] <CR>

(6)   Internal Data Pattern   [ID(IDP) X] <CR>

(7)   Clock Source   [CS(CLKS) X] <CR>

(8)   Internal Clock Rate   [IC(ICR) XX.XXX] <CR>

(9) Internal Temperature   [TE(TEMP) XXX] <CR>

(10) Forward Error Correction   [FC(FEC) X] <CR>

(11) Space Time Coding   [ST(STC) X] <CR>

b. <u>Status of Other Commands</u>. If other commands are implemented in the transmitter beyond the basic set, a complete status should be given for each implemented command.

C.4.b(6) Version

The "version" command is executed with the VE(VERS) <CR> mnemonic.

a. <u>Query Transmitter Version</u>. "VE(VERS) <CR>" requests the current version of the transmitter. The response will contain (at a minimum) the following information about the transmitter and in this order:

(1) Manufacturer Name

(2) Model Number

(3) Serial Number

b. <u>Formatting and Delimiting the Fields</u>. It is left up to the transmitter manufacturer to format and delimit the above fields and, if chosen, add additional information to the response.

C.4.b(7) Save

The "save" command is executed with the SV(SAVE) mnemonic.

For "Save Transmitter Set-Up", "SV(SAVE) X<CR>" saves the current settings of the transmitter to register "X" in nonvolatile memory within the transmitter. If only one location is available, the value of "X" is zero. This document puts no limit to the number of storage registers as this is limited by available nonvolatile memory.

The command "SV(SAVE) <CR>" will save to the default location 0.

In the event of an unsuccessful save command, the transmitter will return ERR SV(SAVE) X<CR> to indicate the error and no save function will be performed.

In order to avoid the situation of fielding a flight test item that has been inadvertently programmed to use internal clock and data sources, the transmitter power up configuration will always have the clock and data source as <u>external</u>. In addition, when saving to register "0" clock and data sources will always be set to <u>external</u>.

C.4.b(8) Recall

The recall command is executed with the RL(RCLL) mnemonic.

For "Recall Transmitter Set-up", "RL(RCLL) X<CR>" retrieves and restores the transmitter set-up from register "X" in nonvolatile memory within the transmitter. Values of X start at zero. The "0" register location should be used exclusively for the default set-up, which is the memory location that is loaded during power-up.

The command "RL(RCLL) <CR> will recall from the default regitster location "0".

In the event of an unsuccessful recall command, the transmitter will return ERR RL(RCLL) X<CR> to indicate the error and no recall function will be performed.

During a recall operation the transmitter will always set the clock and data sources to external (see Subsection C.4.b(7)).

C.4.b(9)   Reset

The transmitter can be reset with the RE(RES) mnemonic.

a. Reset Transmitter. "RE(RES) <CR>" resets the transmitter by reinitializing the transmitter. The transmitter will use the following basic settings as a base configuration.

Transmitter Setting	Command	Result
Carrier frequency	[FR(FREQ)]	Lowest valid frequency within the tuning range
Modulation mode	[MO(MOD)]	MO(MOD) 0, PCM/FM
Differential encoding	[DE X]	DE 0, Differential encoding off
Randomization	[RA(RAND) X]	RA(RAND) 0, Randomization off
RF output	[RF X]	RF 0, RF output off
Data source	[DS(DSRC)]	DS(DSRC) 0 External
Clock source	[CS(CSRC)	CS(CSRC) 0 External
Internal Data Pattern	[ID(IDP)] 11	[ID(IDP)] 11 PN11 (2^{11}-1)
Internal Clock Rate	[IC(ICR)]	IC(ICR) 05.000 5 MHz
Forward Error Correction	[FC(FEC)]	FC(FEC) 0, Forward Error Correction is off
Space Time Coding	[ST(STC)]	ST(STC) 1, Space Time Coding is on

b. Example Command Use. The Reset command would be used if resetting to a known configuration is required, communication to the transmitter could not be established, if commands were not being recognized, or if some other unknown transmitter state was experienced.

C.4.b(10)   Data Source

Data source is set or queried with the DS(DSRC) mnemonic.

a. Set Data Source. Use "DS(DSRC) X <CR>" where X corresponds to a 1 or 0. If the command is accepted, an "OK <CR>" is issued as a response.

Command	Source
DS(DSRC) 0	External
DS(DSRC) 1	Internal

In the event of an incorrect data source command, the transmitter will return "ERR DS(DSRC) X <CR>" to indicate the error and return the currently set data source state.

b. Query Data Source. "DS(DSRC) <CR>" queries the currently set data source and returns "DS(DSRC) X <CR>" where integer X is represented in the above table.

c. Saving Data Source. See Subsection C.4.b(7) regarding saving the data source setting.

C.4.b(11)   Clock Source

The clock source is set or queried with the CS(CLKS) mnemonic.

a. <u>Set Clock Source</u>. Use "CS(CLKS) X <CR>" where X corresponds to a 1 or 0. If the command is accepted, an "OK <CR>" is issued as a response.

Command	Source
CS(CLKS) 0	External
CS(CLKS) 1	Internal

In the event of an incorrect command, the transmitter will return "ERR CS(CLKS) X <CR>" to indicate the error and the current clock source setting for the transmitter.

b. <u>Query Clock Source</u>. "CS(CLKS) <CR>" queries the currently set clock source and returns "CS(CLKS) X <CR>" where integer X is represented in the above table.

c. <u>Example Command Use</u>. Internal data can be clocked either with an external or internal clock. This command allows the user to clock the known data with an existing external clock or select the internal clock for more flexibility.

d. <u>Saving Clock Source</u>. See Subsection <u>C.4.b(7)</u> regarding saving the clock source setting.

C.4.b(12) Internal Data Pattern
The internal data pattern is set or queried with the ID(IDP) mnemonic.

a. <u>Set Internal Data Pattern</u>. Use "ID(IDP) X" where X corresponds to the internal data pattern. If the command is accepted, an "OK <CR>" is issued as a response.

b. <u>Example Internal Data Patterns</u>. Example patterns are shown below.

Command	Pattern	
ID(IDP) 9	2^9-1	(511 bits)
ID(IDP) 11	$2^{11}-1$	(2047 bits)
ID(IDP) 15	$2^{15}-1$	(32767 bits)
ID(IDP) 20	$2^{20}-1$	(1048575 bits)
ID(IDP) 23	$2^{23}-1$	(8388607 bits)
ID(IDP) 0000	0x0000	Fixed repeating
ID(IDP) FFFF	0xFFFF	Fixed repeating
ID(IDP) AAAA	0101010	Fixed repeating
ID(IDP) XXXX	0xXXXX	Fixed repeating

The minimum supported patterns shall be PN11, PN15, and AAAA. Selection of which additional patterns to implement is left up to the manufacturer. If an error occurs, the transmitter will return "ERR ID(IDP) X <CR>" to indicate the error and return the current data source setting for the transmitter.

c. <u>Query Internal Data Pattern</u>. "ID(IDP) <CR>" queries the currently set internal data pattern and returns "ID(IDP) X <CR>" where integer X is represented in the above table.

d. <u>Example Command Use</u>. This feature can be used for system characterization and troubleshooting. A known bit pattern can be used to test and characterize telemetry systems end-to-end or isolate baseband signal problems to the transmitter.

C.4.b(13)   Internal Clock Rate
The internal clock rate is set or queried with the IC(ICR) mnemonic.

a. Set Internal Clock Rate. Use "IC(ICR) XX.XXX <CR>" where XX.XXX corresponds to the clock frequency in MHz and is used to clock the selected internal data pattern. See Subsection C.4.b(12). Actual range for the clock frequency is left to the manufacturer but should correspond to the specified useable input clock frequency range. Resolution should be ±1 kHz. Accuracy for the internal clock is left to the manufacturer but should correspond to internal values for the transmitter. If the command is accepted, an "OK <CR>" is issued as a response.

In the event of an incorrect command, the transmitter will identify the error, default to its current state, and return "ERR IC(ICR) XX.XXX <CR>" where "XX.XXX" indicates the current clock source for the transmitter.

b. Query Internal Clock Rate. "IC(ICR) <CR>" queries the currently set internal clock rate and returns "IC(ICR) XX.XXX" where XX.XXX is the current set internal clock rate in MHz.

C.4.b(14)   Internal Temperature
Internal temperature is only a query with the TE(TEMP) mnemonic.

Using TE(TEMP) will query the current internal temperature of the transmitter and returns "TE(TEMP) XXX" where XXX is the temperature in Celsius.

C.4.b(15)   Forward Error Correction
When used, FEC is set or queried with the FC(FEC) mnemonic. If FEC per Appendix 2-D is implemented in the transmitter, this command will enable, disable, or query the current setting.

a. Set Forward Error Correction. Use "FC(FEC) X <CR>" where X corresponds to the table below. If X=1, then the command structure is "FC(FEC) 1 xxxx yy <CR>" where xxxx corresponds to the block size and yy corresponds to the code rate. If the command is accepted, an "OK <CR>" is issued as a response. When FC(FEC) is enabled, randomization in the transmitter [RA(RAND)] shall be disabled.

Command	Source	Block Size	Code Rate
FC(FEC) 0	Disable		
FC(FEC) 1 xxxx yy	Enable/Block Size/Code Rate	1024 or 4096	12 selects 1/2 23 selects 2/3 45 selects 4/5
FC(FEC) X	Future Error Correction Code Capability		

In the event of an incorrect FEC command, the transmitter will return "ERR FC(FEC) X <CR>" to indicate the error and return the current FEC setting for the transmitter.

b. Query Forward Error Correction Setting. "FC(FEC) <CR>" queries the currently set FEC condition and returns "FC(FEC) 0<CR>", when FEC is disabled and returns "FC(FEC) 1 xxxx yy" when FEC is enabled.

c. Refer to Appendix 2-D for additional details on FEC and the associated randomization used.

C.4.b(16) Space Time Coding

An STC-enabled transmitter is two independent transmitters when STC is disabled. The command prompt indicates which transmitter is communicating over the serial port. When STC is enabled modulation will be SOQPSK-TG per Appendix 2-E.

a. Set Space Time Coding. Use "ST(STC) X <CR>" where X corresponds to a 1 or 0. If the command is accepted, an "OK <CR>" is issued as a response.

Command	Space Time Coding	Prompt
ST(STC) 0	Disable	RF1> or RF2>
ST(STC) 1	Enable	>

b. Query Space Time Coding. "ST(STC) <CR>" returns "ST(STC) X<CR>" where integer X is represented in the table above. "STC 0" is associated with a command prompt of RF1> or RF2>.

c. Independent Commanding. The following command structure allows independent commanding when STC is disabled.

- Upon issuing an "ST(STC) 0 <CR>" command, the command prompt changes from ">" to "RF1>", indicating communication with the transmitter associated with RF port 1 (Xmtr1). The default command prompt is "RF1>".

- To change to the other transmitter, issue the command "RF2" and the command prompt changes to "RF2>", indicating communication with the transmitter associated with RF port 2 (Xmtr2).

- Commands apply to both transmitters independently.

- Issuing "ST(STC) 1 <CR>" returns the ">" prompt indicating STC mode is enabled and commands apply as they would to a single transmitter. At the ">" prompt independent control of each transmitter is not available.

d. Example Command Use. The examples in Figure C-1 illustrate the use of several commands to cinfugre transmitter parameters.

>	transmitter is ready to receive commands or queries
>ST	Queries STC mode
>ST 1	Responds STC is enabled
>	transmitter is ready to receive commands or queries
>ST 0	Disables STC
RF1>	Responds RF1 is ready to receive commands or queries
RF1>MO 0	Sets RF1 modulation mode to PCM/FM
RF1>ST 1	Enables STC
>	transmitter is ready to receive commands or queries
>MO	Queries modulation mode
>MO 1	Responds modulation mode is SOQPSK
>	transmitter is ready to receive commands or queries
>ST 0	Disables STC
RF1>	RF1 is ready to receive commands or queries
RF1>FR 4450.5	Sets RF1 frequency to 4450.5 MHz
RF1>DS 0	Sets RF1 data source to External
RF1>CS 0	Sets RF1 clock source to External
RF1>RF2	Selects RF2 to receive commands or queries
RF2>	RF1 is ready to receive commands or queries
RF2>MO 0	Sets RF2 to PCM/FM modulation mode
RF2>FR 4460.5	Sets RF2 frequency to 4460.5 MHz
RF2>DS 0	Sets RF2 data source to External
RF2>CS 0	Sets RF2 clock source to External
RF2>MO 2	Sets RF2 modulation mode to ARTM-CPM
RF2>ST 1	Enables STC
>	transmitter is ready to receive commands or queries

Figure C-1.   Terminal Window for STC-Enabled Transmitter

C.5.   Extended Command Set

C.5.a. Extended Command Set Summary

Although the extended command set does not include all possible commands, its use provides a standard way of implementing known features of transmitters. This standard will be updated at appropriate intervals should new capabilities arise. Commands in the extended command set are shown in Table C-2.

Table C-2. Extended Command Set	
Command	**Function**
DP(DPOL)	Sets or queries data polarity (NORM or INV)
RP(RPWR)	Sets or queries the output RF power (HI or LO)
SP(SLP)	Low-power consumption mode, sleep mode
VP()	Variable RF power command
CP()	Sets or queries the input clock phase
DE()	Sets or queries differential encoding (ON or OFF)
RZ()	Sets or queries RF power on/off pin polarity

C.5.b.   Commands: Extended Command Set

C.5.b(1)   Data Polarity
   Data polarity is set or queried with the DP(DPOL) mnemonic.

a.   Set Data Polarity. Use "DP(DPOL) X <CR>" where X corresponds to a 1 or 0. Actual data polarity, when referenced to the input clock, does not need to be known; this command either inverts the incoming data or does not. If the command is accepted, an "OK <CR>" is issued as a response.

Command	Polarity
DP(DPOL) 0	Normal
DP(DPOL) 1	Inverted

In the event of an incorrect data polarity command, the transmitter will maintain its current setting and return "ERR DP(DPOL) X <CR>" to indicate the error and return the current data polarity setting for the transmitter.

b.   Query Data Polarity. "DP(DPOL) <CR>" queries the current data polarity and returns "DP(DPOL) X <CR>" where integer X is represented in the above table.

C.5.b(2)   RF Power (High/Low)
   High output power or low output power is set or queried with the RP(RPWR) mnemonic.

a.   Set RF Output Power. Use "RP(RPWR) X <CR>" where X corresponds to a 1 or a 0. If the command is accepted, an "OK <CR>" is issued as a response.

Command	Output RF Power Level
RP(RPWR) 0	Low
RP(RPWR) 1	High

b.   Query RF Output Power Level. "RP(RPWR) <CR>" queries the currently set output RF power level and returns "RP(RPWR) X <CR>" where integer X is represented in the above table.

In the event of an incorrect RF power command, the transmitter will return "ERR RP(RPWR) X <CR>" to indicate the error and return the current RF power setting for the transmitter.

c.   Example use. The low setting could be used for lab testing or ground checks when transmitter and receiver antennas are co-located. The high power setting is for normal, over-the-air telemetry transmission.

C.5.b(3)   Low Power Consumption, Sleep Mode
   The transmitter can be placed into a mode of low input power consumption with the SP(SLP) mnemonic.

a.   Set Low Power Mode. Use "SP(SLP) X" where X corresponds to a 1 or 0 as shown in the following table. If the command is accepted, an "OK <CR>" is issued as a response.

Command	Source
SP(SLP) 0	Full Operation Mode
SP(SLP) 1	Sleep Mode

Sleep mode powers down all nonessential circuitry within the transmitter to reduce input power consumption. Note, in order to return from sleep mode, the transmitter must monitor and recognize the SP(SLP) 0 command. In the event of an incorrect command, the transmitter will return "ERR SP(SLP) X <CR>" to indicate the error and the current power mode setting for the transmitter.

b. Query Power Mode. "SP(SLP) <CR>" queries the power mode setting and returns "SP(SLP) X <CR>" where integer X is represented in the above table.

C.5.b(4)   Variable Power Mode
The transmitter can support user-selectable output power levels using the VP XX<CR> mnemonic.

a. Set Variable Power Level. Use "VP XX<CR>" or "VP X<CR>" to set a range of RF output power levels available in discrete predefined steps. If the command is accepted, an "OK<CR>" is issued as a response. In the event of an incorrect command, the transmitter will return "ERR VP XX<CR>" to indicate the error and the current variable power level for the transmitter.

b. Query Variable Power Level. "VP<CR>" queries the power mode setting and returns "VP XX<CR>" where integer XX is represented in the table below.

c. Look Up Table. The actual value of output power that corresponds to "XX" is undefined. Each manufacturer will provide an equation or lookup table that defines the output power as a function of "XX".

Command	RF Power Level
VP XX	Full Power (equivalent to RP 1)
VP (XX – 1)	Less than full power
VP 1 (or VPP 01)	More than low power
VP 0 (or VPP 00)	Low Power (equivalent to RP 0)

d. Variable Power in STC Transmitters. For transmitters with STC capability, the VP command applies to both transmitters. When STC is disabled, output power for each transmitter can be independently controlled with the VP command.

C.5.b(5)   Input Clock Phase
The transmitter can support user-selectable input clock phasing using the CP X<CR> mnemonic.

a. Set Input Clock Phase. Use "CP X<CR>" where X corresponds to a 1, 0, or A. If the command is accepted, an "OK<CR>" is issued as a response. In the event of an incorrect input clock phase command, the transmitter will return "ERR CP X<CR>" to indicate the error and return the current input clock phase setting for the transmitter.

b. <u>Query Input Clock Phase</u>. "CP<CR>" queries the input clock phase setting and returns "CP X<CR>" where the value of X is represented in the table below.

Command	Input Clock Phase	Data Transitions
CP 0	0°	Rising Edge of Clock
CP 1	180°	Falling Edge of Clock
CP A	0° or 180°	Edge with greatest margin with respect to data transitions

C.5.b(6)   Differential Encoding

Differential encoding is set or queried with the DE mnemonic. For additional information, refer to <u>Appendix 2-B</u>. This command is only applicable when modulation mode is set to SOQPSK-TG (MO 1).

a. <u>Set Differential Encoding</u>. Use "DE X <CR>" where X corresponds to a 1 or 0. If the command is accepted, an "OK <CR>" is issued as a response.

Command	Differential Encoding
DE 1	On
DE 0	Off

In the event of an incorrect differential encoding command, the transmitter will return "ERR DE X<CR>" to indicate the error and return the current differential encoding setting.

b. <u>Query Differential Encoding</u>. "DE <CR>" queries the currently set differential encoding status and returns "DE X <CR>" where integer X is represented in the above table.

c. <u>Default</u>. When switching modulation modes the differential encoding shall be switched appropriately. For example, when switching from SOQPSK-TG to PCM/FM, the differential encoding will be set to off.

d. <u>Manual Control</u>. For the PCM/FM and ARTM-CPM modulation modes, differential encoding will always be disabled (off). For SOQPSK-TG modulation mode, differential encoding will be enabled upon selection of that mode; however, the user can exercise manual control of differential encoding when using SOQPSK-TG modulation. Additionally if either FEC or STC are enabled, differential encoding will be disabled.

C.5.b(7)   RF Power On/Off Pin Polarity

The RF power on/off pin polarity is set or queried with the RZ mnemonic. This command sets the polarity of the pin, either a low or high level, to enable RF power output.

a. <u>Set RF Power On/Off Pin Polarity</u>.

Command	RF Power
RZ(RFZ) 1	On when pin is high
RZ(RFZ) 0	On when pin is low

In the event of an incorrect RF power command, the transmitter will return "ERR RF X<CR> X<CR>" to indicate the error and return the current RF power setting.

b. <u>Query RF Power On/Off Pin Polarity</u>. "RZ(RFZ) <CR>" queries the currently set RF power status and returns "RZ(RFZ) X <CR>".

c. <u>Default</u>. The transmitter will initialize in the RF power pin polarity on/off "On when pin is high" setting.

C.6.   Transmitter Communication Example

A typical terminal window is shown in Figure C-2 for clarity. Transmitter communication initialization is assumed.

```
>FR 1435.5
>OK
>FR
>FR 1435.5
>MO 0
>OK
>DE 1
>ERR DE 0
>MO 7
>ERR MOD 0
>RGDW
>ERR
>TE
>TE 085
>QA
>FR 1435.5
>MO 0
>DE 0
>RA 1
>RF 1
>
```

Figure C-2.   Typical Terminal Window

C.7.   Non-Standard Commands

NOTE	This paragraph is reserved for transmitter commands that fall outside of the commands and command structure discussed above. Additions to this section will be made as non-standard commands are derived and found applicable to this standard.

C.8.   Physical Layer(s)

The above command sets are independent of the physical layer over which the commands are transferred. The command set should be implemented in such a way that it can be translated over any physical layer interfacing with the transmitter.

Should a three-wire serial interface be chosen, it should be compatible with TIA-232.[47] The intent of this standard is not to force complete EIA-232 compliance; rather, the intent is to establish a serial communication interface with the transmitter so that any terminal program,

---

[47] Telecommunications Industry Association. *Interface between Data Terminal Equipment and Data Circuit-Terminating Equipment Employing Serial Binary Data Interchange*. TIA/EIA-232-F. 1 October 1997. May be superseded by update. Retrieved 17 May 2021. Available at https://standards.globalspec.com/std/872822/tia-232.

such as Windows® HyperTerminal or Linux Minicom, can be used to communicate with the transmitter. A transmit-and-receive line will be supplied with an associated ground return; the choice of connector pin-out is left up to the manufacturer. The serial interface will operate at one of the common transfer rates. Typical baud rates are 300, 600, 1200, 2400, 4800, 9600, 19200, 38400, 57600, and 115200 baud. The default shall be 9600 baud. Should operation at another baud rate be desired, a command must be implemented to accommodate this capability. The command shall have the form BD(BAUD) as described below.

    a. <u>Baud Rate</u>. Serial communication baud rate shall be set or queried with the BD(BAUD) mnemonic.

    b. <u>Set Baud Rate</u>. Use "BD(BAUD) X <CR>" where X corresponds to a number (0-9) in the following table. If the command is accepted, an "OK" <CR>" is issued as a response.

Command	Rate
BD(BAUD) 0	300
BD(BAUD) 1	600
BD(BAUD) 2	1200
BD(BAUD) 3	2400
BD(BAUD) 4	4800
BD(BAUD) 5	9600
BD(BAUD) 6	19200
BD(BAUD) 7	38400
BD(BAUD) 8	57600
BD(BAUD) 9	115200

    c. <u>Query Baud Rate</u>. "BD(BAUD) <CR>" queries the set baud rate of the transmitter and returns "BD(BAUD) X <CR>" where integer X is represented in the above table.

In the event of an incorrect baud rate command, the transmitter will return "ERR BD(BAUD) X<CR>" to indicate the error and return the current baud rate setting for the transmitter.

Communication should be compatible with a terminal set-up consisting of one of the above baud rates with 8 data bits, 1 stop bit, 1 start bit, and no parity. ASCII characters will be transmitted and received. No hardware or software handshaking should be implemented and connector pin-out is left to the manufacturer.

This page intentionally left blank.

APPENDIX 2-D

Low-Density Parity-Check Codes for Telemetry Systems

D.1. Background

The LDPC codes presented are intended to decrease error probabilities in a primarily noisy transmission channel for use in the AMT test environment.

The LDPC code is a linear block code. This type of code maps a block of k information bits together with a codeword (or codeblock) of n bits. Think of a linear block code as a chunk of input bits mapped through a coder to a longer chunk of output bits. This is sometimes called an n-k code. When k bits are mapped to a length n codeblock there are 2^k codewords; however, there are 2^n possible codewords composed of n bits. The idea with error correction codes is to pick the 2^k codewords of the 2^n total possible codewords that are far enough apart (in terms of Hamming distance) to guarantee you are able to correct a certain number of errors.

This particular version of LDPC code is systematic, meaning the transmitted codeblock contains duplications of the bits of the original information. It is also a quasi-cyclic linear block code, meaning the construction of these codes involves juxtaposing smaller cyclic submatrices (circulants) to form a larger parity matrix, all through linear operations.

This code, like all other FEC schemes, requires an encoder on the transmission side and a decoder on the receiving side of the telemetry link. The codes offer much higher decoding speeds via highly parallelized decoder structures. The LDPC code itself does not guarantee sufficient bit transitions to keep receiver symbol synchronizers in lock so a randomizer, defined in this appendix, is required when implementing this FEC code.

Since LDPC is a block code, the start of a codeblock(s) must be identified in order for the decoder to function properly. This identifier, known as the attached synchronization marker (ASM), provides this marker and also aids in detection at very low values of E_b/N_0. Differential encoding/decoding normally associated with SOQPSK-TG modulation is NOT required and should be disabled. Phase ambiguities will have to be resolved using the ASM.

D.2. Code Description

The LDPC code is a linear block code with options for $\{n,k\}$, where n is the length of the codeblock and k is the length of the information block. An LDPC code can be entirely defined by its parity check matrix, **H**. The k X n generator matrix that is used to encode a linear block code can be derived from the parity check matrix through linear operations.

Code rates, r, chosen for this AMT application are 1/2, 2/3, and 4/5. Information block sizes (k) are 1024 and 4096 bits. Given the code rate and information block sizes, codeword block sizes are calculated using $n = k/r$. See Table D-1.

Table D-1. Codeblock Length per Information Block Size			
Information Block Length, k	Codeblock Length, n		
	Rate 1/2	Rate 2/3	Rate 4/5
1024	2048	1536	1280
4096	8192	6144	5120

The *k* X *n* generator matrix **G** shall be used to encode a linear block code. The matrix **G** can be derived from the parity check matrix **H**.

For each {*n,k*} in Table D-1 a parity check matrix **H** is constructed from size *M* x *M* submatrices per Table D-2.

Table D-2. Submatrix Size per Information Block Size			
Information Block Length, *k*	Submatrix size *M*		
	Rate 1/2	Rate 2/3	Rate 4/5
1024	512	256	128
4096	2048	1024	512

D.3. Parity Check Matrices

Given the {*n,k*} in Table D-1, there are six parity check matrices that need to be constructed. Section 3.3 in CCSDS standard 131.1-0-2 (CCSDS September 2007) describes how each parity check matrix is constructed and is repeated here for clarity.

The **H** matrices for each code rate are specified below. $\mathbf{I}_M$ is the *M* x *M* identity matrix (main diagonal is 1's, all other entries are 0) and $\mathbf{0}_M$ is the zero matrix.

Parity Check Matrices

$$H_{1/2} = \begin{bmatrix} 0_M & 0_M & I_M & 0_M & I_M \oplus \Pi_1 \\ I_M & I_M & 0_M & I_M & \Pi_2 \oplus \Pi_3 \oplus \Pi_4 \\ I_M & \Pi_5 \oplus \Pi_6 & 0_M & \Pi_7 \oplus \Pi_8 & I_M \end{bmatrix}$$

$$H_{2/3} = \begin{bmatrix} 0_M & 0_M & 0_M & 0_M & I_M & 0_M & I_M \oplus \Pi_1 \\ \Pi_9 \oplus \Pi_{10} \oplus \Pi_{11} & I_M & I_M & I_M & 0_M & I_M & \Pi_2 \oplus \Pi_3 \oplus \Pi_4 \\ I_M & \Pi_{12} \oplus \Pi_{13} \oplus \Pi_{14} & I_M & \Pi_5 \oplus \Pi_6 & 0_M & \Pi_7 \oplus \Pi_8 & I_M \end{bmatrix}$$

$$H_{4/5} = \begin{bmatrix} 0_M & 0_M & 0_M & 0_M & 0_M & 0_M \\ \Pi_{21} \oplus \Pi_{22} \oplus \Pi_{23} & I_M & \Pi_{15} \oplus \Pi_{16} \oplus \Pi_{17} & I_M & \Pi_9 \oplus \Pi_{10} \oplus \Pi_{11} & I_M \\ I_M & \Pi_{24} \oplus \Pi_{25} \oplus \Pi_{26} & I_M & \Pi_{18} \oplus \Pi_{19} \oplus \Pi_{20} & I_M & \Pi_{12} \oplus \Pi_{13} \oplus \Pi_{14} \end{bmatrix} \left| H_{1/2} \right.$$

Permutation matrix Π_k has non-zero entries in row i and column entries are defined by $\pi_k(i)$ for $i \in \{0, \Kappa, M-1\}$

$$\pi_k(i) = \frac{M}{4}\left(\left(\theta_k + \lfloor 4i/M \rfloor\right) \bmod 4\right) + \left(\phi_k\left(\lfloor 4i/M \rfloor\right) + i\right) \bmod \frac{M}{4}$$

where θ_k and $\phi_k(j)$ are defined in the following tables for the submatrix sizes defined in Table D-2 for each code rate and information block size.

Code Rate =1/2, Information Block Size = 1024, $M = 512$

k	Θ_k	$\phi_k(0,M)$	$\phi_k(1,M)$	$\phi_k(2,M)$	$\phi_k(3,M)$
1	3	16	0	0	0
2	0	103	53	8	35
3	1	105	74	119	97
4	2	0	45	89	112
5	2	50	47	31	64
6	3	29	0	122	93
7	0	115	59	1	99
8	1	30	102	69	94

Figure D-1.   Parity Check Matrix H for (n=2048, k=1024) Rate 1/2

k	Θ_k	$\phi_k(0,M)$	$\phi_k(1,M)$	$\phi_k(2,M)$	$\phi_k(3,M)$
1	3	108	0	0	0
2	0	126	375	219	312
3	1	238	436	16	503
4	2	481	350	263	388
5	2	96	260	415	48
6	3	28	84	403	7
7	0	59	318	184	185
8	1	225	382	279	328
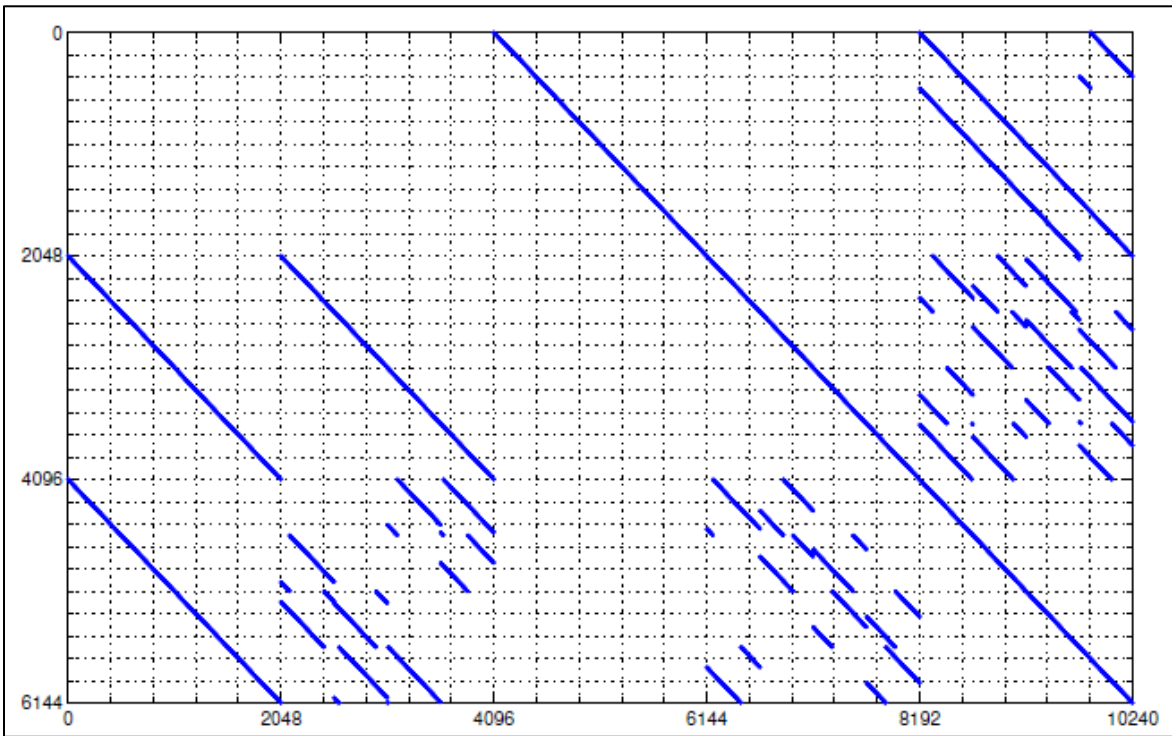
Figure D-2.   Parity Check Matrix H for (n=8192, k=4096) Rate 1/2

k	Θ_k	$\phi_k(0,M)$	$\phi_k(1,M)$	$\phi_k(2,M)$	$\phi_k(3,M)$
1	3	59	0	0	0
2	0	18	32	46	44
3	1	52	21	45	51
4	2	23	36	27	12
5	2	11	30	48	15
6	3	7	29	37	12
7	0	22	44	41	4
8	1	25	29	13	7
9	0	27	39	9	2
10	1	30	14	49	30
11	2	43	22	36	53
12	0	14	15	10	23
13	2	46	48	11	29
14	3	62	55	18	37
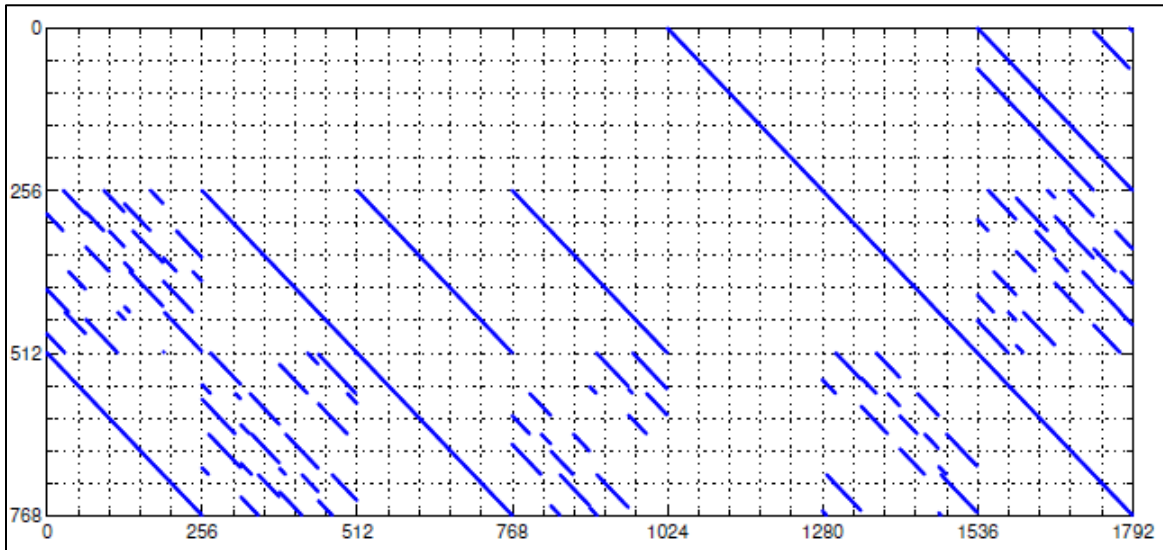
Figure D-3.   Parity Check Matrix H for (n=1536, k=1024) Rate 2/3

Code Rate =2/3, Information Block Size = 4096, $M = 1024$

k	Θ_k	$\phi_k(0,M)$	$\phi_k(1,M)$	$\phi_k(2,M)$	$\phi_k(3,M)$
1	3	160	0	0	0
2	0	241	182	35	162
3	1	185	249	167	7
4	2	251	65	214	31
5	2	209	70	84	164
6	3	103	141	206	11
7	0	90	237	122	237
8	1	184	77	67	125
9	0	248	55	147	133
10	1	12	12	54	99
11	2	111	227	23	105
12	0	66	42	93	17
13	2	173	52	20	97
14	3	42	243	197	91
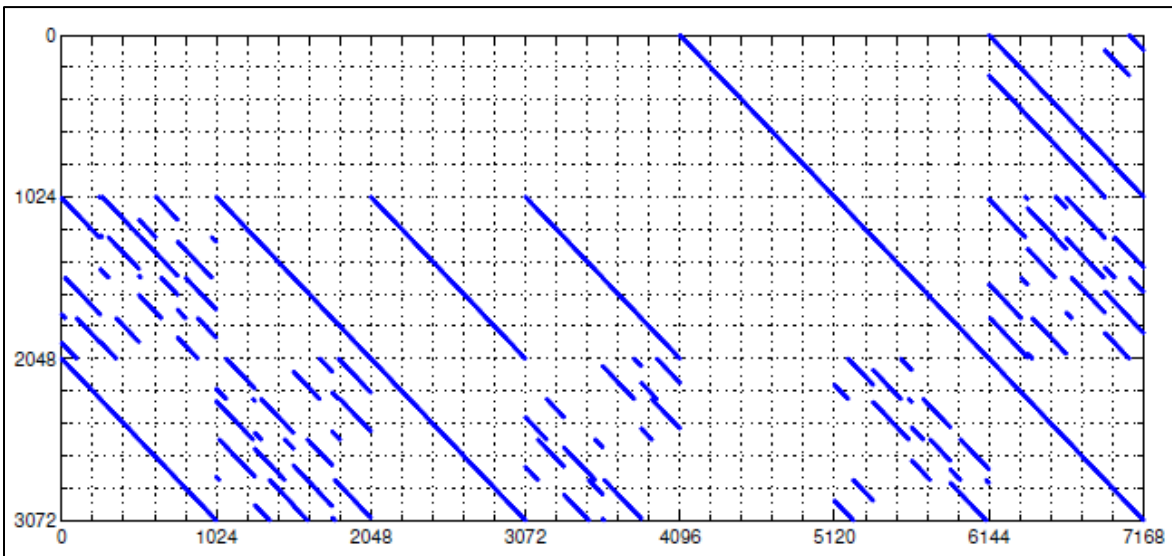
Figure D-4.   Parity Check Matrix H for (n=6144, k=4096) Rate 2/3

Code Rate =4/5, Information Block Size = 1024, M = 128

k	Θ_k	$\phi_k(0,M)$	$\phi_k(1,M)$	$\phi_k(2,M)$	$\phi_k(3,M)$
1	3	1	0	0	0
2	0	22	27	12	13
3	1	0	30	30	19
4	2	26	28	18	14
5	2	0	7	10	15
6	3	10	1	16	20
7	0	5	8	13	17
8	1	18	20	9	4
9	0	3	26	7	4
10	1	22	24	15	11
11	2	3	4	16	17
12	0	8	12	18	20
13	2	25	23	4	8
14	3	25	15	23	22
15	0	2	15	5	19
16	1	27	22	3	15
17	2	7	31	29	5
18	0	7	3	11	21
19	1	15	29	4	17
20	2	10	21	8	9
21	0	4	2	2	20
22	1	19	5	11	18
23	2	7	11	11	31
24	1	9	26	3	13
25	2	26	9	15	2
26	3	17	17	13	18
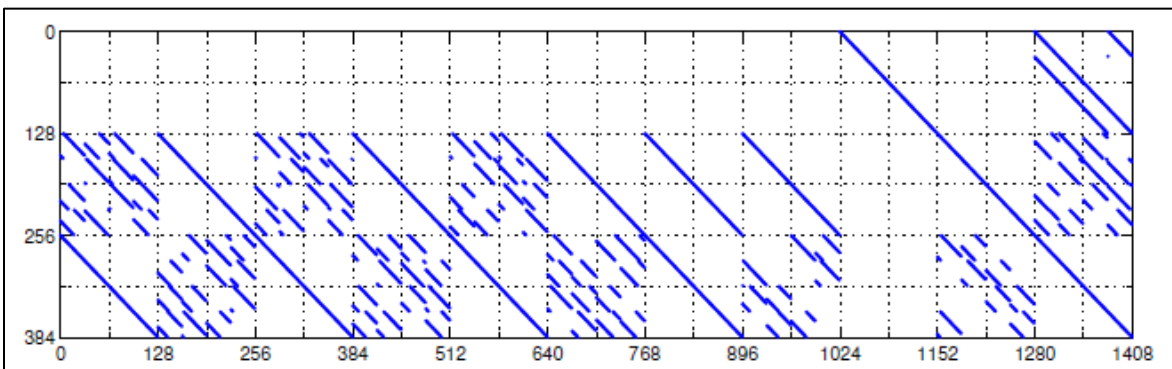
Figure D-5.   Parity Check Matrix H for (n=1280, k=1024) Rate 4/5

Code Rate =4/5, Information Block Size = 4096, $M = 512$

k	Θ_k	$\phi_k(0,M)$	$\phi_k(1,M)$	$\phi_k(2,M)$	$\phi_k(3,M)$
1	3	16	0	0	0
2	0	103	53	8	35
3	1	105	74	119	97
4	2	0	45	89	112
5	2	50	47	31	64
6	3	29	0	122	93
7	0	115	59	1	99
8	1	30	102	69	94
9	0	92	25	92	103
10	1	78	3	47	91
11	2	70	88	11	3
12	0	66	65	31	6
13	2	39	62	19	39
14	3	84	68	66	113
15	0	79	91	49	92
16	1	70	70	81	119
17	2	29	115	96	74
18	0	32	31	38	73
19	1	45	121	83	116
20	2	113	45	42	31
21	0	86	56	58	127
22	1	1	54	24	98
23	2	42	108	25	23
24	1	118	14	92	38
25	2	33	30	38	18
26	3	126	116	120	62
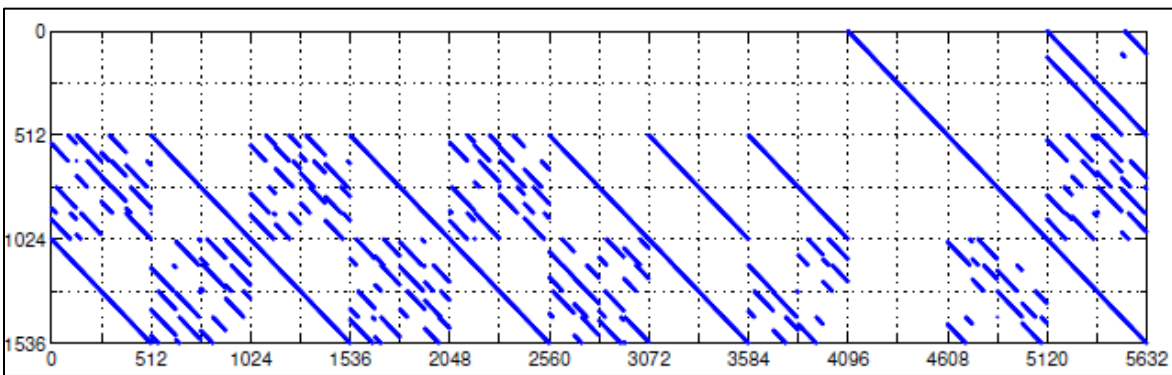
Figure D-6.   Parity Check Matrix H for (n=5120, k=4096) Rate 4/5

D.4.   Encoding

The recommended method for producing codeblocks consistent with the parity check matrices is to perform matrix multiplication (modulo-2) by block-circulant generator matrices. This family of codes supports rates $K/(K+2)$, where $K=2$ for a rate 1/2 code, $K=4$ for rate 2/3, and

K=8 for rate 4/5. Generator matrices, **G**, have size $MK \times M(K + 3)$ if punctured columns are described in the encoding. (Note: If punctured columns are omitted, as in this case, **G** will have a size equal to $MK \times M(K + 2)$). Table D-3 lists the size of **G** for each information block size and code rate.

<table>
<tr><th colspan="4">Table D-3.   Generator Matrix Sizes</th></tr>
<tr><th>Information Block
Length, k</th><th colspan="3">Generator Matrix (**G**) Size</th></tr>
<tr><th></th><th>Rate 1/2</th><th>Rate 2/3</th><th>Rate 4/5</th></tr>
<tr><td>1024</td><td>1024×2048</td><td>1024×1536</td><td>1024×1280</td></tr>
<tr><td>4096</td><td>4096×8192</td><td>4096×6144</td><td>4096×5120</td></tr>
</table>

These generator matrices may be constructed as follows.

1. Let P be the $3M \times 3M$ submatrix of H consisting of the last 3M columns. Let Q be the $3M \times MK$ submatrix of H consisting of the first MK columns.
2. Compute W=(P−1Q)T, where the arithmetic is performed modulo-2.
3. Construct the generator matrix G=[IMK W] where IMK is the MK $\times$ MK identity matrix, and W is a dense matrix of circulants of size MK $\times$ M(N−K). The dimension of W is MK $\times$ 2M.

Because the LDPC code is systematic and the generator matrix **G** is block-circulant, an efficient bit-serial encoder can be implemented as shown in Figure D-7. Initially, the binary pattern for the first row of circulants is placed in the shift registers, and the accumulator is set to the length 2M zero vector. The contents of the shift registers are added (modulo-2) to the accumulator if the first message bit is a 1, and the shift registers are cyclicly shifted right one place. This is repeated for each subsequent message bit until m=M/4 cyclic shifts have been performed. The shift registers are then loaded with binary patterns for the next row of circulants, and the process continues in this manner until all message bits have been encoded.
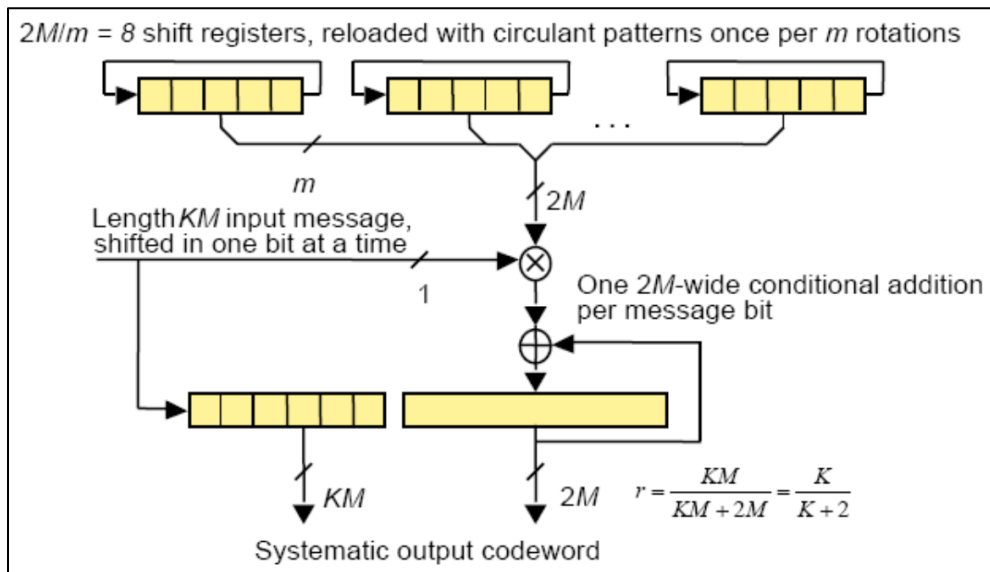
Figure D-7.   Quasi-Cyclic Encoder Using Feedback Shift Register

Computing the generator matrix **G** involves inverting a large binary matrix, a computationally demanding task. For convenience, **G** for each information bock size and code rate is tabulated here in a compact form.

D.4.a. Code Rate =1/2, Information Block Size = 1024, $M = 512$

The first 1024 columns of **G** form a 1024×1024 identity matrix and the remaining 1024 columns of **G** form a block matrix composed of 16 rows and 8 columns of circulant matrices, each of size 128×128. The first row of each circulant is given in hexadecimal format in Table D-4 according to its location in **G**. Subsequent rows of each circulant can be computed by applying the corresponding number of right circular shifts to the first row.

Table D-4. First Rows of Circulants in Generator Matrix, r=1/2, k=1024	
Row 1	
Columns 1025-1152	CFA794F49FA5A0D88BB31D8FCA7EA8BB
Columns 1153-1280	A7AE7EE8A68580E3E922F9E13359B284
Columns 1281-1408	91F72AE8F2D6BF7830A1F83B3CDBD463
Columns 1409-1536	CE95C0EC1F609370D7E791C870229C1E
Columns 1537-1664	71EF3FDF60E2878478934DB285DEC9DC
Columns 1665-1792	0E95C103008B6BCDD2DAF85CAE732210
Columns 1793-1920	8326EE83C1FBA56FDD15B2DDB31FE7F2
Columns 1921-2048	3BA0BB43F83C67BDA1F6AEE46AEF4E62
Row 129	
Columns 1025-1152	565083780CA89ACAA70CCFB4A888AE35
Columns 1153-1280	1210FAD0EC9602CC8C96B0A86D3996A3
Columns 1281-1408	C0B07FDDA73454C25295F72BD5004E80
Columns 1409-1536	ACCF973FC30261C990525AA0CBA006BD
Columns 1537-1664	9F079F09A405F7F87AD98429096F2A7E
Columns 1665-1792	EB8C9B13B84C06E42843A47689A9C528
Columns 1793-1920	DAAA1A175F598DCFDBAD426CA43AD479
Columns 1921-2048	1BA78326E75F38EB6ED09A45303A6425
Row 257	
Columns 1025-1152	48F42033B7B9A05149DC839C90291E98
Columns 1153-1280	9B2CEBE50A7C2C264FC6E7D674063589
Columns 1281-1408	F5B6DEAEBF72106BA9E6676564C17134
Columns 1409-1536	6D5954558D23519150AAF88D7008E634
Columns 1537-1664	1FA962FBAB864A5F867C9D6CF4E087AA
Columns 1665-1792	5D7AA674BA4B1D8CD7AE9186F1D3B23B
Columns 1793-1920	047F112791EE97B63FB7B58FF3B94E95
Columns 1921-2048	93BE39A6365C66B877AD316965A72F5B
Row 385	
Columns 1025-1152	1B58F88E49C00DC6B35855BFF228A088
Columns 1153-1280	5C8ED47B61EEC66B5004FB6E65CBECF3
Columns 1281-1408	77789998FE80925E0237F570E04C5F5B
Columns 1409-1536	ED677661EB7FC3825AB5D5D968C0808C

Columns 1537-1664	2BDB828B19593F41671B8D0D41DF136C
Columns 1665-1792	CB47553C9B3F0EA016CC1554C35E6A7D
Columns 1793-1920	97587FEA91D2098E126EA73CC78658A6
Columns 1921-2048	ADE19711208186CA95C7417A15690C45
Row 513	
Columns 1025-1152	BE9C169D889339D9654C976A85CFD9F7
Columns 1153-1280	47C4148E3B4712DAA3BAD1AD71873D3A
Columns 1281-1408	1CD630C342C5EBB9183ADE9BEF294E8E
Columns 1409-1536	7014C077A5F96F75BE566C866964D01C
Columns 1537-1664	E72AC43A35AD216672EBB3259B77F9BB
Columns 1665-1792	18DA8B09194FA1F0E876A080C9D6A39F
Columns 1793-1920	809B168A3D88E8E93D995CE5232C2DC2
Columns 1921-2048	C7CFA44A363F628A668D46C398CAF96F
Row 641	
Columns 1025-1152	D57DBB24AE27ACA1716F8EA1B8AA1086
Columns 1153-1280	7B7796F4A86F1FD54C7576AD01C68953
Columns 1281-1408	E75BE799024482368F069658F7AAAFB0
Columns 1409-1536	975F3AF795E78D255871C71B4F4B77F6
Columns 1537-1664	65CD9C359BB2A82D5353E007166BDD41
Columns 1665-1792	2C5447314DB027B10B130071AD0398D1
Columns 1793-1920	DE19BC7A6BBCF6A0FF021AABF12920A5
Columns 1921-2048	58BAED484AF89E29D4DBC170CEF1D369
Row 769	
Columns 1025-1152	4C330B2D11E15B5CB3815E09605338A6
Columns 1153-1280	75E3D1A3541E0E284F6556D68D3C8A9E
Columns 1281-1408	E5BB3B297DB62CD2907F09996967A0F4
Columns 1409-1536	FF33AEEE2C8A4A52FCCF5C39D355C39C
Columns 1537-1664	5FE5F09ABA6BCCE02A73401E5F87EAC2
Columns 1665-1792	D75702F4F57670DFA70B1C002F523EEA
Columns 1793-1920	6CE1CE2E05D420CB867EC0166B8E53A9
Columns 1921-2048	9DF9801A1C33058DD116A0AE7278BBB9
Row 897	
Columns 1025-1152	4CF0B0C792DD8FDB3ECEAE6F2B7F663D
Columns 1153-1280	106A1C296E47C14C1498B045D57DEFB5
Columns 1281-1408	968F6D8C790263C353CF307EF90C1F21
Columns 1409-1536	66E6B632F6614E58267EF096C37718A3
Columns 1537-1664	3D46E5D10E993EB6DF81518F885EDA1B
Columns 1665-1792	6FF518FD48BB8E9DDBED4AC0F4F5EB89
Columns 1793-1920	BCC64D21A65DB379ABE2E4DC21F109FF
Columns 1921-2048	2EC0CE7B5D40973D13ECF713B01C6F10

D.4.b. <u>Code Rate =1/2, Information Block Size = 4096, *M* = 2048</u>

The first 4096 columns of **G** form a 4096 × 4096 identity matrix and the remaining 8192 columns of **G** form a block matrix composed of 16 rows and 8 columns of circulant matrices,

each of size 512×512. The first row of each circulant is given in hexadecimal format in Table D-5 according to its location in **G**. Subsequent rows of each circulant can be computed by applying the corresponding number of right circular shifts to the first row.

Table D-5.	First Rows of Circulants in Generator Matrix, r=1/2, k=4096
Row 1	
Columns 4097-4608	616DB583006DB99954780CD6DFC9908772D8260D390B1D462A8F62DE8809216194BE0531EE408AEAF27F50F3AD71865AC7910EEF8824A858CA7B13FC843DAFB1
Columns 4609-5120	BA3E0B010860D09066A8632E2B273DABDF90C26FCDD989C2831874EA7FBA23D940A294111C1B0C1CF62F56A376B94CF64FA594B987B19226E525704D7F2BC66E
Columns 5121-5632	226C671C22A59AC062490596EB1536C9F66AE799C2489FAD2C131E29ED64A25CB0ADC88D04C5EC8FECD7F78B3825E626858CFAA0DE77772CE8822C7AA39628A0
Columns 5633-6144	123B1C426E2A93366D067D26DE51362EA0BA916EBD1229521B1B044459B325785F3F3E24199B2460151E4CAA9FD26A5DC46BE0D6DA907EFAF38F413642F702F5
Columns 6145-6656	324AFD5D62F4CC251FF5C0FD95DE0FAB061F0C92CA5BC97F976118AD84E0663A3BF1B4F07D1CCCC2DF9E09D506B073DED87CC0653C944FC7D438223C0DF3EB67
Columns 6657-7168	E62AE13F8D4000D616E814045495F6E969C473B059386F5DDBCC25F4002EB132D73A98414D85346F55DEBFF875F7CB9D2466A412D180E0A1ADA18D281376A671
Columns 7169-7680	8EB0FB6BB7B9AD2A2132010511077F6BD424B6F5B578C11D0076B781930F755EBB72C41ED17519476C257C31C3159BF31FADA2755F1B8A23B22D6A428AA290E2
Columns 7681-8192	54CC73C7599AB67C6807C4286BECF8423F3216EF04E1B6DE61349DDB23E3A0EB0EF70C5BE1AD91D31B0BB532C1098DC619BF80F3853EEA357091C05D95170A7E
Row 513	
Columns 4097-4608	5E6381A718C0A817F8101ECDCDBF825E732E4356CEC42C222DBC476BD704837C382B7FBF282B739EDC22B5EEA2909F0EB3ACB9E41FE2AC791130A36A9CBFC1D9
Columns 4609-5120	D4F8DE28FA77F37E4A6B5A82A58CE917CA74C8397E9DB8EDCB2BF65DB91954457707FE876DFF812D4B99466DF479A00114F27E702249DB3E9311301E9CE98703
Columns 5121-5632	74FEAD0013FD861D67D7CE69D3635ECC6266E862D08B63077B45D3098306EA74159DAEA2263E58705EA5ABE58B7FD41862B9EC1D0F1BD47CD6CB42739C24F7FE
Columns 5633-6144	7ACFF6D64C8E8F94BEABE280CFDCFCFB26AC7330073C25E0313DCB75E6C5261F15D82AFA665F73A4B4DA4E5D1648EAB051EDEB9857C13C2F019FCBBA4F9DF2E1
Columns 6145-6656	9CEFF1147D792C14AA2E211C3B9B94B2C9F24F49B0B1ED6E200C88D743F5AC1EE283C3A0AC79B9F1F496BDE74A2AA591ACF2F526FB24413A58B495F91905F596

Columns 6657-7168	D8F1469BCA9CC5041C50F1FB479CF2680503AD85BA2C0C6D01D2D739F3129315E49A9F57236D9585CC0B8A9B4BFE9ADCD97BED9006C33976ACC00468693D56FA
Columns 7169-7680	1EE66371B0EA6C4E1E172C2C5D76806CB7376B8CDEAD96B14A1EC2B656298B9425EA2F0671082D70AA23C267D1F215C59239AEB40186DF0AB284625DC6BAF45E
Columns 7681-8192	FBFBE26BED98BB3B697764A6F82C94039CBF14CB538A7D87801ACBD3A444A858BB74F0A4707592EE6B7DC6D21B8F6B4A184B567C8AA4CD825EBF7F1EDCE015A5
Row 1025	
Columns 4097-4608	25453670647D23C5E445A705953F3BF4A5AF02E7BC46C969C8141D8782F171C9CFF7EBB20945DE5D363AD36D3BD5A0BA081C079CDD04B6E5968187C8A665344A
Columns 4609-5120	23E9B1897A6FDF427B5E910AA8D71F9CC6351474BC4563C20FD38953295D3BA15E7D1010503B7BA1C148251DB8A88AC64E6AF8C1CC056E4EEF1C927FEC40C35D
Columns 5121-5632	57140969483D9E33429FAFD177D031A43B727CF832C8DFFE8D8960CB55BE4BE27B69CC26F2FB731B53250D6F8EE7DFDA98812B9AAE9C02AE2FEDEA598D6B6E2F
Columns 5633-6144	22B6CCA50541BD9F5D48565E551B310E10A0DFCB8035A5EC86EB9CD8C811CDCBCCCEC3732EF93EE8C9418E25CA5744E07C45F9B161E277BCECE388B9B84AAEC4
Columns 6145-6656	DA37FE277C72CB5CB1BE92AD373867403E46B3535159687ADC79C39DEF7005C1F11F1CBD5F8877DA66AAC156EF27BB893F5F1132336D52E8AEB60EACF9BEB3CF
Columns 6657-7168	D204D92DFA496DAF564272E3FEC51CE53C8F2DF6ACB191E60E14CDEA28FD5ED0EBE09672ED11A3F6466FE3A967A4EC8390303059AE00DD83102A9F33B2943E4E
Columns 7169-7680	6E56928E7FEE3333A36FF3EE7598744CF7C298FEF3EACC7CCC0F36DCBA6D87BDD441081163A65E27C958AF79C33A98B81814015E77F82EF5120FBDAB540893B4
Columns 7681-8192	7BEB68CC37F23835C91F5D36D6BA6F0A5E68FEBB6E6A2F247EB5CF57684D0770249460788DFDC4A1218652BF881B4BB06308EF86484E7070AACC72D3977CF5D0
Row 1537	
Columns 4097-4608	6230DEF1ACD4425F7B155A2A285CB2A32CB9D46DA09B28167826E77AEBD85F0C416595E136184841451F5B3E1F17D02C3DB32C2AF50091D6376406D8CB78A9E3
Columns 4609-5120	D3B19911ACC450679EAE25B0F290FF372300F1A4BC91A43CB79DB270133D41DC4970F1420E71C0F816EF938C3C17F0FCBB6E920ED853EAF6D2DC6792BF87098A
Columns 5121-5632	B94C2E5DDE78C974AD6F423CD5ACA01EC9420AAF3FE83BEC31D47AACD3D62FA2476C38595BD66639368181E75B44BAA7ADBC2B42E1D82D7A59312BB9A16F7D35

Columns 5633-6144	0B13B44D828071E69DD90DCD9B713A05FD8C21AA5E6E6D8DA49A5C3B3 4F98A4E5E822513F0DA200235C65BFCA1DC2CE4AB21D146B778F6806680 B8AC75285760
Columns 6145-6656	FEF66B861AA67C768A76D585DFADC8EB6556AD841DEA9F44ACB42B601 6142B6B69F1833474FADEB0400CE4D9F3BD62AD96E57F3E93DD229180F2 D4B5E77D098F
Columns 6657-7168	EEBE2DFA4D4D86ECB07EEE9565FB589855E1F53BA1B9784A8D195A0E37 21551270089C535216636FBEB4D9E50A9EAC3DCB27891A7005A2AD87427 E6B8326F6B3
Columns 7169-7680	CA225C7B2A9EABFFDDDBC130B5342917848B029917BA98FFD6EF238900 6A6B417F678C61458EF625C96C0D3D07945ABB9836CF80823EB6244D86D1 14CC5DC2B1
Columns 7681-8192	94F5D55C398B16A71497C4CF102C2F1035C19D5DFC8A301B8DE33D41D90 9C15A3093B09E7489CE6AA14B331B70E76637FE6DDFFFA6DC4C510371C B0D2A6EA3DA
Row 2049	
Columns 4097-4608	AC5F866DD75CD4C2D5959AC37DE4E1E870313A5B2902F234CD939FE39F3 1FEBF8B46DAC906E3EBA9C3A74DE46E7A9140D3716667BB1EC22A87D5F 8D048BDC5BA
Columns 4609-5120	57B6024327CDDFF3296BE6508C48045B71FA519156F8C125F4E3B7356576F 32C63BC588908C4E8B3F9F2D12A9E8F35B6FCF296C17FD8E8D076406FA11 D16175F
Columns 5121-5632	CC45AE82D672979E8A0A359B2328C79AE61F87EBE04DAC93430305486597 32000CE627417B3F8CFD4A992E7F2B680216AF773385B9337E1743D43FD96 5282CF5
Columns 5633-6144	AE71B0CAFEB4DA3E0B95F1341667C519FB9F89D7CEC711E57485F04A965 CDC832CBEC0BE1B2A3E23B5EAF4C5DAD8767E054B2225A60B88BE1DB6 A35E0BAEB237
Columns 6145-6656	A206BC721B252D52EA1F8E311203DFF0AE8D65BD1986055701A3C7FEB2D DEDD2D57C3BBA6A2BC56A9157677D7B48AD2907927176F6B22E8A92F6E 9863C9E16D9
Columns 6657-7168	11B6209E06EFE6ACBBBA2214EF5AEAB9D76645476B2C16B8D14E1AE3F3 A85188835922B914D3F32FE05B7987A2516B3D3C8983AE176DFD04349A45 359B422E1E
Columns 7169-7680	01CC2266F2B68A4323F8931D7AA37B1CBD70DC2FEE91592327207AA6121 795150A0DC918704A1A293778FE75A99FDCE77E820D0905EF7AC72A682F2 487A6E0FE
Columns 7681-8192	03F42D94FDE1C13F958DF61112DB4A27A8A8EF35087FD089729F0864C270 6CCB2B6CBD91A9A7B7B31E08EA3570A6E1BED495FC84FACD829F3234B 1D1DC574B67
Row 2561	
Columns 4097-4608	900AA496432959141795C615CBAEA98002440A0D447EF990435E452CC6902 03BDEBCBA3EEFC7A7CE71EB54B1728AEA9EDE70A7E6A1A8AE8616870 9A899738CCB

Columns 4609-5120	C5B7A094AEBEA8EC95A414A8DE5D3DBE6745CB0D330B78435AC2BB666 6BB2D43A19EAD3B3D9536D0BB92DB949570981C22805E7DEA452FA649C 84EDC4324A7FB
Columns 5121-5632	E6A9CAF4EE48400720B8F84CAC3A42483B7E571846E2A5F77A983EE31117 9CEC2D99878FF5AA06ACA0CBBA63B36985E0970761E7F837650BC46C9A 2EB1AEFA95
Columns 5633-6144	AC4D8AA5C970BB55FDF3408356C9EB2683B6FEE593736B66B49C055BD65 03EEF3C7CADD15C9B86DCA626E1ABF4B971D04C0A9A5AEF8305C3D0E4 CC02C32FA91E
Columns 6145-6656	D8949EF8FEADF7DA39D395B52D2779A0B305C4FD10C33A434878967D932 1B4835C035CA5802C37F6DC1E39AC30337253114176BBB26576317C72E954 8F179A5A
Columns 6657-7168	A200FC35B6A0934D57543A60F6114B7B0D78D8DD8932538E545D806A1D9 E47390F092501F4A470CF7B1F9144D0A8F1B0C3D607930A75E5A150233DC EEDB4C10B
Columns 7169-7680	217C8EB38D4D2A0EF12557321D504ECA670B41E496441FDE341F0232101D 4E3F4158FF6F4EAECC073AA811DD450F528BC6095868B7BF953926056BD4 09E5FE36
Columns 7681-8192	B82831B150B80A736D6CF7B16660ADCD5E1F4DB96E36E33DCC2F1506C7 B8B0F2A4EC362FB0CF7B8B3B08D6CD1AF7440729D4C3C02627AD8733A0 C94B2EBAF526
Row 3073	
Columns 4097-4608	FDB4463E6F8FBAF565B1C3320F5704A87309E529842378ECB733784F1CBD 85F4F87FB0525C7C4D307061F74DE2FB3BDFBC77E04EAB75A64FFE51203 AB925E807
Columns 4609-5120	1D1101A16A2C41DBDCA94C128560BEFDA4ECA6F22B44C6E5085A23F841 06E4FD870FAA789E03FC37086E67B69FC8EB6421AA57FBA27866DFF712D 5FEDA21FC51
Columns 5121-5632	76EE3CB2C4A8629C20FC646A7ADF2A4BE73DCEF53FC926067EB9964996 BCEE403C5642CD2F8084E0C14D3627FAD9F0180DADF07331246C007F3AF 95CC9B451CC
Columns 5633-6144	3638887EB493F5EE3361F07E00F115BC04AF404BE6BA3467322B37A8E6AB F47710D56C3BC751892CFD12F29CC4319D0562005562D05261D39FDF528A 11E65BBE
Columns 6145-6656	A0BF07C52E9A9ED7AC3F0FB9196A450E162009509F20BEE74FCC6316BC4 824D93CBAC25E470A7468A629EB520E980DE31F8C8873F4ED21B57AAEB F43A5754359
Columns 6657-7168	CD089ABE548975678C2123223CF3F345AE0CECF0A3726BFBB130E34169A 874B6C4CDEFC0A05D7DA1EE475E5407F1535399086700874C13000E2EE21 DF3EEFB65
Columns 7169-7680	4BEF6F2B4137DC6EF197D514E904B8F31BAD6C846D6BD7D7480F4818C3C 57B4C7F53F168E48020273702071EE48EC53422C71C90AA0262982B82BB6F F3100D8A

Columns 7681-8192	EB3E8F033DA73FA82B3B93E50C60E5936A07D3218946588D0EFB39E1A55C0FB9DBA87DA50C4697EE2ED72B004301019E595B92A2F55F7F1B37C2030B79057F52
Row 3585	
Columns 4097-4608	59CA13359E16B10A7F8778BBAF5D45E32C643B524022FE777A8F557C14141D638E84BC4DBB1CE5866CD0B89C1CC5C6F7BF7E25D2B4FC28A16E67CF8BFAC4F4BD
Columns 4609-5120	A612F30067700487B6584B1AD578659FC2B7443228B2B7B443882DABBF55739CB9660F530631A2CFDCBE94D21692CAC01DA9EB5048FFF17BC4FB5957E8C9DF1F
Columns 5121-5632	29E0573D85359FB7924AABBDDDCD26F5740FFA6824FCFCBD53BF1DFB587E0667641DD3F82962F5E6EA26461279B0F69479645462983DBBBCC544DA90255121EA
Columns 5633-6144	A97C7B71923F0382DF60C9E34D84CAC289B578899EBCF924F4304B80581C9887B1198F074143DCC4324D7DF301466AC97903E688DD2E9186EDD2D90C34202AA3
Columns 6145-6656	90815D489B715FF604788F335322DF5C8856FD85F753785A96F4B2561990F458C69D3F99A8ED1BE99C3F5A14B19B37AC729B3F35ABF52006E814B597145FA3FD
Columns 6657-7168	86A5A2038BB67CF8225BCCF7A587E0D09B47D26BC4DB017F6A77B6DEC5AF5B117E399D8A336358D4AABE9C8E7EAAF6447638F2DC66EF65C100D06EE202013042
Columns 7169-7680	AD845A43D23E66FBA72D9D56457D66C7E44D98ED1E5F1D063A5D01043930E9C2EDED8BA9DEE5F9DFF91CD887F097B9A2DF0099E278C253E0A549C7A2D81078C6
Columns 7681-8192	680566EA7A1E724A99B5D7099AED278A3065BBC64BED441154DCD346D38C9771648D55656B16CF012D0C6EC8F616D3B758089A8147D731AE077D557204256F93

D.4.c.   Code Rate =2/3, Information Block Size = 1024, *M* = 256

The first 1024 columns of **G** form a 1024 × 1024 identity matrix and the remaining 512 columns of **G** form a block matrix composed of 16 rows and 8 columns of circulant matrices, each of size 64 × 64. The first row of each circulant is given in hexadecimal format in Table D-6 according to its location in **G**. Subsequent rows of each circulant can be computed by applying the corresponding number of right circular shifts to the first row.

Table D-6. First Rows of Circulants in Generator Matrix, r=2/3, k=1024	
Row 1	
Columns 1025-1088	51236781781D416A
Columns 1089-1152	B0C8419FA21559A8
Columns 1153-1216	5F14E1E4D88726F1
Columns 1217-1280	762F6ED6CF32F06D
Columns 1281-1344	8ABFD971E17A0BE9
Columns 1345-1408	A5D147741B698D14

Columns 1409-1472	2A58AB30E2BC32D3
Columns 1473-1536	9F251FBC5DB8C768
Row 65	
Columns 1025-1088	D73C205BBEB231CB
Columns 1089-1152	CAB5EFF5B2C76C71
Columns 1153-1216	FA70FAD48828355F
Columns 1217-1280	68C6138FA5524A61
Columns 1281-1344	BB20031D7AA8FE69
Columns 1345-1408	432ADE446F49CE27
Columns 1409-1472	5E5DB9CCCEBD1326
Columns 1473-1536	E8782B1B01F2ABA2
Row 129	
Columns 1025-1088	4748E9513B41147A
Columns 1089-1152	17B1FBB78B4F914C
Columns 1153-1216	281F5680BA56DE50
Columns 1217-1280	74B0FB0817E33E2B
Columns 1281-1344	DD166CFB774B5959
Columns 1345-1408	AC7FDCEA4FECB5BE
Columns 1409-1472	ED747C81B540D66A
Columns 1473-1536	B2A6A2039A87967F
Row 193	
Columns 1025-1088	4780DCB2DC5CBFAE
Columns 1089-1152	55BC8FF84EC89440
Columns 1153-1216	E5D411223F09979F
Columns 1217-1280	DDDE9D940A15A801
Columns 1281-1344	194064639D254969
Columns 1345-1408	1BE32DDC829B0032
Columns 1409-1472	1326515A22EE88A2
Columns 1473-1536	0EC664DD2D701891
Row 257	
Columns 1025-1088	69748DFE6372F2EF
Columns 1089-1152	15F3B0D400ACD68A
Columns 1153-1216	CF4144CE1FE2581C
Columns 1217-1280	79B1A55BA59E54AE
Columns 1281-1344	65A2B47EEBAB0CF3
Columns 1345-1408	24DD87572CB0F71D
Columns 1409-1472	F24ABF15590F4DA6
Columns 1473-1536	9C3BAE51969C6502
Row 321	
Columns 1025-1088	D3A714B60B22789B
Columns 1089-1152	3DF5504D80F54C5A
Columns 1153-1216	9D75CF1465031211
Columns 1217-1280	09834A0C9F659C99
Columns 1281-1344	B9241BDF76EB3788

Columns 1345-1408	6F927251C86DECF1
Columns 1409-1472	390BE9F5BBB93D05
Columns 1473-1536	C6F435BFA1FF96B6
Row 385	
Columns 1025-1088	222461B658DC3E91
Columns 1089-1152	B01DF2A2EAD2DAA6
Columns 1153-1216	5572EE6278F6F63A
Columns 1217-1280	17B63CB2FDA3B97F
Columns 1281-1344	B233BB259F3D83F7
Columns 1345-1408	F64760C774989384
Columns 1409-1472	46F57E03F55B1C0B
Columns 1473-1536	5AC8A6CEA05466C1
Row 449	
Columns 1025-1088	AE8825521F85CA31
Columns 1089-1152	37BEED74B5303407
Columns 1153-1216	751FC9A15FCEE486
Columns 1217-1280	93F0F69BD04E72A4
Columns 1281-1344	C0EBFA3F49DF4DBB
Columns 1345-1408	03E52D815DC99A1D
Columns 1409-1472	98FE8BF01BB2CD6D
Columns 1473-1536	009C5290D81A18F6
Row 513	
Columns 1025-1088	4FFBAD88545CAA95
Columns 1089-1152	0C74659FA4828CA3
Columns 1153-1216	60CE56E32DA28B2E
Columns 1217-1280	299D4BF82FE54B81
Columns 1281-1344	51047BE3B3AE4F4B
Columns 1345-1408	F3AC9578B9477A4C
Columns 1409-1472	3730F81F92767E11
Columns 1473-1536	04E84EC3A3AD1F19
Row 577	
Columns 1025-1088	2D0E0CAB8EDD2185
Columns 1089-1152	CEFBE8F2F538522A
Columns 1153-1216	92DAEDC22C441893
Columns 1217-1280	BCB999157B35619D
Columns 1281-1344	069951BFB90A08E1
Columns 1345-1408	54C7E270CBA1656E
Columns 1409-1472	7FBBB806B6A06FB3
Columns 1473-1536	7224943B1C3A5723
Row 641	
Columns 1025-1088	1BAA14752EFCEBC0
Columns 1089-1152	CFF0894975557623
Columns 1153-1216	FA95908DC3F34D48
Columns 1217-1280	FECA650999A26E91

Columns 1281-1344	245433EBBE9CDA13
Columns 1345-1408	5771EAFF9B02D8FC
Columns 1409-1472	BCEBCA573D3775C8
Columns 1473-1536	1E46F2B951D0EAAB
Row 705	
Columns 1025-1088	32942F7F4743DDF4
Columns 1089-1152	8FA2F60AD62095EF
Columns 1153-1216	80E4A736B5E1A3A3
Columns 1217-1280	0119062872DAEDF4
Columns 1281-1344	E78006958CD99F95
Columns 1345-1408	D20625057C99C7A3
Columns 1409-1472	B569736DE2167610
Columns 1473-1536	0E1C6183ADF09FD0
Row 769	
Columns 1025-1088	E5C492DBB48B319A
Columns 1089-1152	E2D83ADEFEBBDEFE
Columns 1153-1216	AA944EEA53C77DB3
Columns 1217-1280	0FAA85D9C13B1F73
Columns 1281-1344	8ACED57F3BE4E807
Columns 1345-1408	33CB72627624F426
Columns 1409-1472	A0C6E669B5C74980
Columns 1473-1536	ABBAEFEA2D3B69AA
Row 833	
Columns 1025-1088	F8366DDAE56A6DDC
Columns 1089-1152	FDED5582F4EA6525
Columns 1153-1216	4C9628278ED17036
Columns 1217-1280	6E711B6D20A67966
Columns 1281-1344	3B28BDF004C21B93
Columns 1345-1408	1BC37B730FFC1786
Columns 1409-1472	5D20C81D345FE4B9
Columns 1473-1536	1D14A5663D369A93
Row 897	
Columns 1025-1088	5EBD4BD39B2217D0
Columns 1089-1152	56833BE1CDDBA6BC
Columns 1153-1216	B288169B4E3BB726
Columns 1217-1280	C2ED28FBFC395D1F
Columns 1281-1344	035B30C68F9A6B6F
Columns 1345-1408	539836A6E56A7B16
Columns 1409-1472	CEB1525C6ADB65A5
Columns 1473-1536	5F71754AA458B11A
Row 961	
Columns 1025-1088	0DB9D180B21C0B13
Columns 1089-1152	417D86C59DF33E49
Columns 1153-1216	183A8F6C44DAFA24

Columns 1217-1280	4E224C180C1F0B45
Columns 1281-1344	C93CD9CA23658555
Columns 1345-1408	7DDEC5E9451AD519
Columns 1409-1472	B122C72A6177EE99
Columns 1473-1536	1290B4C6B007D973

D.4.d. Code Rate =2/3, Information Block Size = 4096, *M* = 1024

The first 4096 columns of **G** form a 4096 × 4096 identity matrix and the remaining 2048 columns of **G** form a block matrix composed of 16 rows and 8 columns of circulant matrices, each of size 256 × 256. The first row of each circulant is given in hexadecimal format in Table D-7 according to its location in **G**. Subsequent rows of each circulant can be computed by applying the corresponding number of right circular shifts to the first row.

Table D-7.   First Rows of Circulants in Generator Matrix, r=2/3, k=4096

Row 1	
Columns 4097-4352	80924F648C014F2C73889C8B87D0491FA9FA060D2902D7ACC8B679CF61EEB5D9
Columns 4353-4608	6BB9E90F5C157AA1BF03EF756245D9179063F2CD999EF1E7F7925B3FB7AC7B2D
Columns 4609-4864	6CD39516B201F491E2BDCA4E34542B5AF3703B3C8EE753FBE998E87323F0B228
Columns 4865-5120	D1F551B2D7E7822F201E24066584D63CAA00E8DB909EB41C4157EBA0F5C76A50
Columns 5121-5376	F7C5731746C6DAC260A345189009C0B23372F1E9E0C5A079D00B09158E164B22
Columns 5377-5632	33D5F8A268041CAB66317898CD0024E3106EED5C2171B3F6276B8EA59AA981E0
Columns 5633-5888	010BFF3F52A49ED9A6FA7F151FCC72B2AF3BD932065043F7447B4D0FC4A2B93B
Columns 5889-6144	F8D345E6D2B0008D1B363BFE296B55AF38E3E16EC5856A122E4931CB3F2424B1
Row 257	
Columns 4097-4352	A099B776C642FF1D84B0DB797098E17E75FE9BB5CF7FA8739711A89660DAF24D
Columns 4353-4608	3CA8DE5500F68DB449BFF74251B24E4691EAF386C81014C91AC700298E095F0B
Columns 4609-4864	12CEE8B5F6B93C11AD628CB6CB81F76BE095C2C994A8BDDB4E2C48C942B4D481
Columns 4865-5120:	1F7E191B30E8FFD6D4A7E9BEF81BBB0AE6608F647B1AED9CCA7FEC5498C03F0F
Columns 5121-5376:	1132E816BDFA0C3450C3993911E10EB1097CD7A1F32C54C8B009654E56B25A2D
Columns 5377-5632:	5FD58EEAED460CEFC18E2FBAD2954467E32118F01D05456DEA2926A1E761DF76

Columns 5633-5888:	4C6C7BF3A2245C1B4630775DC59EA74A14EBCD8B5D72E343BC6F7FEA452F2CC2
Columns 5889-6144:	C09CE802B35EBF46D1F3069957DF1D152377F45ADF614CC0F5DAB8FCF394CCD0
Row 513	
Columns 4097-4352	FEFBA8CE169FD3775B2280EF3BD870FDDF7CB95F2943D0EEA84529FF0D1B1C19
Columns 4353-4608	0CA5DB06A87541C81BEF913D5145F20EFAD861F673B32028B4713377C056CE97
Columns 4609-4864	CA3F213365EE380F7E90466945BDE9F44087C8C73A7CC5F9DE71B7683D018D86
Columns 4865-5120	A6CDFD8D8117748A4B41C3F5A66765495711EDC02F9581F3E7C2E0FD9004B03B
Columns 5121-5376	77D0EF5DE2ACACA2A4371A5B111B877D0EDDF83C3341A5AA51261FA4B5A0D7EA
Columns 5377-5632	7C563512A6B73B3B43F8D1D113D751D6B2CABBC350FF0F8C29361DCE5EB87C8F
Columns 5633-5888	F6DFA5C672C2517931371ACB6462A596D41419CD4F0F84EFF98DCBBE610AE03E
Columns 5889-6144	05FF840FB320DD5C3FB4FE4A5858510914A5161B2AD3C3E7FD02358505190F0F
Row 769	
Columns 4097-4352	5B6D534EDE13068A2459CB07007121B0F07B08B8227047C1A629DCA5A4E30D28
Columns 4353-4608	5D00E72E5B6AD57A9F0F9E0608702BDE8BDBFA371C06D96BFE0E603775A875CB
Columns 4609-4864	692EB7DA76BD0D4AFE92FCB5B5184BAA3EEE37900144CA03B7A22EADE2F061FF
Columns 4865-5120	B3CDE2464AF1212979A99380340974A9F85478E5A2E8B907E74EEFA4CB7625E5
Columns 5121-5376	41AF736E0AA1416EA676E43CF5DFF372CFFC30D6C0A58A333268136A3020033F
Columns 5377-5632	F50111382FEBA594C255896AB59C06638406956F19B67F80A3A7276060D4E7F6
Columns 5633-5888	DCB75287BE9A2620A1F594570B269097A51A32548BAA6DD9B429B8AAF992C8C0
Columns 5889-6144	6210A36B63DE9C732339DC1AFA94CAB475574A6D1C4D0C17F148B8AD12816B47
Row 1025	
Columns 4097-4352	E24D7C17BCC46297EDC41AA9B5C9D93689843027C6A78449F8D151E1F42BE98F
Columns 4353-4608	4544BD9E6975DDD4BC9B3EFAD50AFC582CAE269677B130FED2C39D5EBDEE56B8
Columns 4609-4864	6A13BB53C03B0C8A4E0D1697322A1A3055054229A69B6CCB7E1FB0B885B90CD2

Columns 4865-5120	BE5C66B252E5C51D7D9E9E25922566C18F0234F2A330041AEC6A4F2729A2A30B
Columns 5121-5376	1E04A65CF0BA05C62B15FEF9967ECD975EC43C035DE4EE6422237F56834AC746
Columns 5377-5632	4FD0C1AF8A61F56686326F93EF63E2C114D55726A5F74BFD99AE7713DF2DE6CF
Columns 5633-5888	A9CC4B50995A682C6F6F12C80929FF208C72007D6A253FD36DE363E8EBF2B614
Columns 5889-6144	95F6F59DA4CE4BA4D6D4D371A2484F16EFA33CD34F71B81702F0E99C031B089D
Row 1281	
Columns 4097-4352	E16A7B75AB838252D1840EF2935AA1CCA5C8470F98202BABA93EEACE43EE56E1
Columns 4353-4608	B2D767F35B0F34FCE855B53B6B8DB8DD08BCF47684E904FA47965D72107897D1
Columns 4609-4864	3D38403A0D2696A767679C6F9CC37537A93A125CE7041EC4F39AD7452597ED13
Columns 4865-5120	A0CCD841B7CA93DB6F7039B929A820F55A95AA3786C96E0434DA46A084653B1A
Columns 5121-5376	08A907831A27892D0DD5B6C9FCB5229C0C03663794A4E94E3FB22E4068ED0EE8
Columns 5377-5632	53BCBD15AA8DEC3451CEF53541B04056E4DCA0393836E9B6DFCF9B01E901D933
Columns 5633-5888	BD160166307B70BE5618C6E0B4ADEBA46F65C69080D4C3FAADF1AA22911C2C69
Columns 5889-6144	42FB1575074655ABD1EFF5784CBE7FA0B110981C8A0BDF01C650189C2DC9FC74
Row 1537	
Columns 4097-4352	B403563011DDE16F92630CF312B3F7F495E74B3B582DFB9401F509A35BD2528C
Columns 4353-4608	A81600F6437FBD00FCF0E4AD41DE3598434EE3903CD1A17CF618E8E2A47EBC4C
Columns 4609-4864	A1D7816AE33BA46E3A9D5B3CBDACF93D538802ED0FCCEFF193DB9D6B79C7E508
Columns 4865-5120	54B42DDFAA7DE9B5299F4C1B5DA05487562D20349282F7061E3159E4EAB09D03
Columns 5121-5376	E15D45F2D1694FF3FF1AA1FC1E58E3FBD6875B71B982AD57AC96CD3B7BE8ACC6
Columns 5377-5632	90CADDAD41374E4BCA29AAB22CAD61989158C474E0725B4C4C5442D6A12D94D8
Columns 5633-5888	2827752CE49CB9C385AD35C1291109892EF85A7A6C043BD8E3BA4AC3D5146FB7
Columns 5889-6144	87002794AC4020B7D229EAE70E01E72F1772B0DA401ABE2C2D487EF60724DC83

Row 1793	
Columns 4097-4352	413A0F58974C76AB4C17AB24F37CB1055FC1827A1DDB0456CCAA7F9477CA64FC
Columns 4353-4608	904E1D9338D0795C6844F79ED8B26A9D306F66975CE704A925E72EC95509188B
Columns 4609-4864	2B5EC3212ADF35954F1CDA9CB6CCC28E422F23AF81659F6E4AFDD03EFB8AD730
Columns 4865-5120	84D1CCA3B5036F031EEDE0F1121E6F62D232DFB74A0582EB3303D1E98810A6C9
Columns 5121-5376	221F0EFCA2C81259B57F8E6943D0CD36088A64DA7FE2E6E7E0F63EAF873B8A79
Columns 5377-5632	57E9B39245C6173088B024F34ED7B64F8784413FF95E476474FECDAE7BD62E5A
Columns 5633-5888	807A807832F6AC83BC7CA7F754BBC7DE72CCC85425068F50ED52419643561832
Columns 5889-6144	1B9CF54C055FB01B40740A0D469855292AE8A0C58756BDD3C6DABE268551FD5F
Row 2049	
Columns 4097-4352	DD8CE660B7403DC8672EA620E65301B0865A23FE568C173669EE1D7F7A1BD748
Columns 4353-4608	3CCFAC84AB188D906D70525D092C3E2B46C6675C1CF4B30AB346022E43DA20B8
Columns 4609-4864	A01DC1159652EA260B411971B0E3D0393C1E75AB0EA462E1D07D0847EFA9CFBA
Columns 4865-5120	4153E6B4F4687D434414BAA200FA38CE46B28D3B4055C633AAD0ED2FACD6B415
Columns 5121-5376	5234FA7B72F478A193EC14698C611F3CB70BF72C15E0DCE9CC048A526AC1F46A
Columns 5377-5632	969C10820390DF8D90AD0138202A32182398B70405520538D08C1F799FBC0755
Columns 5633-5888	53D8304A8B5213FF88DD1620B1A5125AF1CC9A07F95C61C5C6C625F64FFCDBE6
Columns 5889-6144	ED1E06EC959FF323FD3E8AF3553D90BD529D699B08B873F164F59B1CD522AC0F
Row 2305	
Columns 4097-4352	A5C8A02849509DECECFADD4C89C03A78E1564A548D89DECD90DDBCAC7964E9F0
Columns 4353-4608	545B207877BBAFB5DED6AEAD3967CA72272E128C97B06868FD3BB85996640432
Columns 4609-4864	2995ED49B525D47CE868EFD6FDBB0BB6975DC82C8580D00ABCB9FFC6F532A0CB
Columns 4865-5120	9F0B1EC3BC16C2E7C94F5149D03677AD039452180B24DA434F5BBAA0BCEE64ED
Columns 5121-5376	910009CE6C11178F5BC794754EBA72003E9A53CDA988B33CE2D0A0965DAACA23

Columns 5377-5632	BF8A7AE5330F4813AE7F8E4F25666EAB3F0351BD34ABBFA8874D88D5FC4E9385
Columns 5633-5888	45A0C20F7DFD392872ABDCB19E4F6F097044266B9EA6F0B318A5011D0E51E735
Columns 5889-6144	EE58F5FC44AE859564B64F3D173C58FAE938AFB934CBB97245F7B1A1DDD4C559

Row 2561

Columns 4097-4352	C7DF1E821B249BE35E6CAB842F3DFCD0141E428141C28BDCF54B0985329F6E2A
Columns 4353-4608	D8C083075232BDEADEA797B6C9E15606A72B8B48502B1C044BA89A8DBC54EB6E
Columns 4609-4864	718EF66E726EA72E631B9B22E193F012F3FB2D112468B0DB89F0C3C8A143E9B1
Columns 4865-5120	7D6BE8EA6A522A10F46EC5A56E3F572586884547536AFFAD0C82A42D88AAA64B
Columns 5121-5376	0B740E17EEF10A800DE1916C291C1535845114313E908D313B58018EB77DED61
Columns 5377-5632	9A5F7429731308EFAB68D1725D8F9501234F9035869415A62262095D77A9613A
Columns 5633-5888	9BDCBC26ABDE4672BE5F130E1089BE8BF5CA0ED3FCD9F28B75CC07E9822AA2EF
Columns 5889-6144	6AC735D6621C86CEA203E9E1FC993207EDC164396C7C8FF227F92979A313914D

Row 2817

Columns 4097-4352	8E1D4E308C03F66D73D76A715F859BEDBC8D709D4BEFC1558D74B49860A90ABA
Columns 4353-4608	B67C75041BFB3A61BBBB73DE2B3D7BB5CB254F10257495E3185C71C3559D9CD0
Columns 4609-4864	ACB7A163EB1E088624F946909B29B2C7373C5CF4F6B1F3A75DC49B1574B3AAB8
Columns 4865-5120	327C55142CE3D1382EA917A7C6730E01BA6BA43767D53E84FFB7D61D6EAD24AD
Columns 5121-5376	CFAAC26024A1D642C795400B8646533A435A4FE899704FAFAE2BF452BD9AF093
Columns 5377-5632	53759538B5F4A8614F1AB4840CFC1EFD8CAFCB067C991FDF2658ABA23F8B0B93
Columns 5633-5888	6B3A35CDECD26C58B9F1318AF46F13767758FC0F74B7DD050A9B1A1C7F98B930
Columns 5889-6144	4B4C20D040F3A8C746453ECE10C0A1F4F74BDDB1A8FCFE1DE2C19148A5E88F1C

Row 3073

Columns 4097-4352	A98B4DE68DDB2434893BEF8F2CF8DB584CEE8F0E39D30CD4C87017E7EE6886F8
Columns 4353-4608	23024E83F777D7DF0D7E46A8B5F9B1331D0BC2F79BF5559C3241D5BDC7E7A665

Columns 4609-4864	9E1DD50373C16CC97A5E390921B471EF5B39731CCC2CBDD08876080680F9D974
Columns 4865-5120	9DF22EE3AB758F85FD490012FCFF20B3329A5648D25859036C0586C65F46236C
Columns 5121-5376	B009BA2650ABAFC45653D61D2BFA255DE767D0B25AC7736E8E5200D21EE3E28F
Columns 5377-5632	FD96F63D0A22CD574ED61899ECDEB4BEB333F994AC7791FF89EC600B857D4DDD
Columns 5633-5888	C2773C7DCE36709F70180CFFAE22AD44A4A20211224F8ECFB336A54A681A1F59
Columns 5889-6144	5C00C419C78A79ADA49562EFB784ECE44BAF45C1E75BD84DE7C1C69100F8B93A
Row 3329	
Columns 4097-4352	DAB0C7C65F0D096351BF8A0EE9CEF5F7756A9A47B4EE80420DEFA16B0E74CF18
Columns 4353-4608	0FAB86E762595261852E38F9D797D4F796DA18169AFAC99E8235D4DD6C2BB887
Columns 4609-4864	15D0F65E9ADB2C67A887E5D8EF4E1080AC968F4C0D673CA7A74759A7F1B4E383
Columns 4865-5120	1B5641CE5FADE005EB947BE5E20E7DDAF6372655825B3516F2EC5B36D687895F
Columns 5121-5376	2C0BB35E3C3EDA32C19BFF6F3A2397A8E25C646059359D90A1372FCAEE250A43
Columns 5377-5632	8AABBF162C4499F2FECFA27F8D7582FB607B88D04F4A6100A3D2F8A88A2E5E80
Columns 5633-5888	D9C26C2A023943BC62F3C18658A0F5C64130BFF0D74BBB85EBFFFE197C94C6EC
Columns 5889-6144	0AED385393F69FA9F7E69DDC061B85E4E77D0BE2013061E94A0DB8AC2995096F
Row 3585	
Columns 4097-4352	775369B59AA940DA96B47429C339536B51ECC59C60BAD762FA275A6A8F90885A
Columns 4353-4608	922A84AE2B06B4003C0A7BE22FB211365376C3FBFC03EB0DEA264F6769B57EE2
Columns 4609-4864	E518ED3DD8553DC8815E57F23DADC1A3E99030AA02A3529604EE4BD66D770F8E
Columns 4865-5120	8AB3C94077F85772647897A76CFE4EC56FCAA7A28968065CC73BDD88ADA4D60C
Columns 5121-5376	9430F05CFEF8ACBBA73038463A9AD3BDE5BA4E94FDA81C6C51AB3C69201906E1
Columns 5377-5632	2613EFCF235670383ED865C6161C8A8958DC09289EA03658376277BE6E4E62AA
Columns 5633-5888	3C90B273B9870A069FE0F5164AA8F837B9905EEE7D3AEB794BA2F4CAA4F1EB01

Columns 5889-6144	01C2973BD37D564B7D21243A206BD8A7B435428BA8DD3DB7045541BCCE000F5F
Row 3841	
Columns 4097-4352	CEA89305914BEB1BE84B59A4A18CC1AEB5CC96326ADC69F3B4957198C60BB6E7
Columns 4353-4608	DB38C42E2947EFC39D2BBFA07C18C320A22C7B9C6CBFB72E6909BDC131B2E15E
Columns 4609-4864	ABECA69DD1395554C852ED7EE6817A6152B39B42F6D7D56B781D1803B8307C79
Columns 4865-5120	386FFC16B79E309255E7D5933870D116DE3828C68348493D8E288C8A3FBF741F
Columns 5121-5376	0936252D32CDEC49ACFE91F2BA885044E0A9ADFEA526F53641F97B86668C5972
Columns 5377-5632	F9D8560A97AFA4282DBCC4250B75A871276434FFA80959F04D3400D81937617D
Columns 5633-5888	799C3EDF3F1345908B306D8372A740E96707761FCCA9B861402134AE9488387F
Columns 5889-6144	F2DA86FE2BAA7E675DFDED45499AF1B40AE292B1DE6B7A7D4799C3B88177704D

D.4.e. Code Rate =4/5, Information Block Size = 1024, M = 128

The first 1024 columns of **G** form a 1024×1024 identity matrix and the remaining 256 columns of **G** form a block matrix composed of 32 rows and 8 columns of circulant matrices, each of size 32×32. The first row of each circulant is given in hexadecimal format in Table D-8 according to its location in **G**. Subsequent rows of each circulant can be computed by applying the corresponding number of right circular shifts to the first row.

Table D-8. First Rows of Circulants in Generator Matrix, r=4/5, k=1024	
Row 1	
Columns 1025-1056	678ECB51
Columns 1057-1088	FE821D5C
Columns 1089-1120	FA5F424B
Columns 1121-1152	F55927AA
Columns 1153-1184	3E826913
Columns 1185-1216	32E04B0C
Columns 1217-1248	4F88862B
Columns 1249-1280	803432EF
Row 33	
Columns 1025-1056	42B27625
Columns 1057-1088	9F8DA1E1
Columns 1089-1120	F8472D1B
Columns 1121-1152	D943D394
Columns 1153-1184	29261575

Columns 1185-1216	BA434C68
Columns 1217-1248	18EF349A
Columns 1249-1280	27CA1CC4
Row 65	
Columns 1025-1056	EC900397
Columns 1057-1088	64A4A063
Columns 1089-1120	9BCEC4A6
Columns 1121-1152	D05BA70F
Columns 1153-1184	E7155BE1
Columns 1185-1216	7FF09CC1
Columns 1217-1248	6E2E2059
Columns 1249-1280	7F1567E5
Row 97	
Columns 1025-1056	5616101C
Columns 1057-1088	EA060E2B
Columns 1089-1120	B673068B
Columns 1121-1152	923BDF8B
Columns 1153-1184	B9B9343D
Columns 1185-1216	049C63A8
Columns 1217-1248	333E9CFE
Columns 1249-1280	809B362D
Row 129	
Columns 1025-1056	9D41634C
Columns 1057-1088	404E17DA
Columns 1089-1120	3B4161F2
Columns 1121-1152	5235992E
Columns 1153-1184	EA4B4B8B
Columns 1185-1216	4690BCE1
Columns 1217-1248	F9DA36A1
Columns 1249-1280	16439BB1
Row 161	
Columns 1025-1056	5D7254B5
Columns 1057-1088	15B4978B
Columns 1089-1120	00D05224
Columns 1121-1152	107BD904
Columns 1153-1184	C85D7E58
Columns 1185-1216	0451F1A5
Columns 1217-1248	EE9D1897
Columns 1249-1280	913DA6F9
Row 193	
Columns 1025-1056	42819F61
Columns 1057-1088	343773CA
Columns 1089-1120	11A6492A
Columns 1121-1152	4832F43F

Columns 1153-1184	849C11ED
Columns 1185-1216	F0FE864F
Columns 1217-1248	CC270400
Columns 1249-1280	9726D66E
Row 225	
Columns 1025-1056	89EE2A44
Columns 1057-1088	685C1F67
Columns 1089-1120	1DF6E416
Columns 1121-1152	507BF2EF
Columns 1153-1184	8759C2FB
Columns 1185-1216	52162ABF
Columns 1217-1248	2B61D3FB
Columns 1249-1280	988708C4
Row 257	
Columns 1025-1056	4A8FEA09
Columns 1057-1088	53452354
Columns 1089-1120	A33E2E73
Columns 1121-1152	271E8211
Columns 1153-1184	16DF62E5
Columns 1185-1216	03DF81F4
Columns 1217-1248	8848BD0F
Columns 1249-1280	F95DF357
Row 289	
Columns 1025-1056	9BE0A7B3
Columns 1057-1088	617256EB
Columns 1089-1120	9A4D0BB4
Columns 1121-1152	FE3A3A19
Columns 1153-1184	FAA63D9E
Columns 1185-1216	65328918
Columns 1217-1248	D699BA35
Columns 1249-1280	4CDE6FE0
Row 321	
Columns 1025-1056	848B1FE5
Columns 1057-1088	0AB58A6F
Columns 1089-1120	341707F1
Columns 1121-1152	EF36474B
Columns 1153-1184	F623A7A5
Columns 1185-1216	A35EC9BA
Columns 1217-1248	24909B6E
Columns 1249-1280	64A7A898
Row 353	
Columns 1025-1056	BDDF3BAE
Columns 1057-1088	7202FA26
Columns 1089-1120	86F90C57

Columns 1121-1152	A0399F20
Columns 1153-1184	972B9A31
Columns 1185-1216	87B245AE
Columns 1217-1248	E0C5A338
Columns 1249-1280	4959AAD9
Row 385	
Columns 1025-1056	CF726C27
Columns 1057-1088	7B38429A
Columns 1089-1120	BA37C244
Columns 1121-1152	EE7717DB
Columns 1153-1184	E45C99CA
Columns 1185-1216	7E3E013B
Columns 1217-1248	7B800CA4
Columns 1249-1280	6527F2E7
Row 417	
Columns 1025-1056	75C63782
Columns 1057-1088	1CC40137
Columns 1089-1120	51E69F16
Columns 1121-1152	414B155F
Columns 1153-1184	DF1964DE
Columns 1185-1216	F13C71F7
Columns 1217-1248	6E9E8044
Columns 1249-1280	6C5CEC86
Row 449	
Columns 1025-1056	6F2A6DF8
Columns 1057-1088	9FF2BF82
Columns 1089-1120	D3625355
Columns 1121-1152	24466981
Columns 1153-1184	D5F14AC1
Columns 1185-1216	E1C24AEA
Columns 1217-1248	A8850D83
Columns 1249-1280	7A3C5120
Row 481	
Columns 1025-1056	BAABADC3
Columns 1057-1088	1ECF066D
Columns 1089-1120	76538348
Columns 1121-1152	FC5D4D54
Columns 1153-1184	43AD46CF
Columns 1185-1216	3342012C
Columns 1217-1248	63EBE2DC
Columns 1249-1280	D832EF8E
Row 513	
Columns 1025-1056	E6EC82F1
Columns 1057-1088	4AAFE782

Columns 1089-1120	14D89E38
Columns 1121-1152	23C83402
Columns 1153-1184	8B48D6BF
Columns 1185-1216	C823B89A
Columns 1217-1248	68A35626
Columns 1249-1280	E89FE121
Row 545	
Columns 1025-1056	4BBAA331
Columns 1057-1088	20EC16C9
Columns 1089-1120	6ADABE06
Columns 1121-1152	D803DA6D
Columns 1153-1184	FCC89D41
Columns 1185-1216	E57B10E8
Columns 1217-1248	CC3FF014
Columns 1249-1280	4DB74206
Row 577	
Columns 1025-1056	503FD586
Columns 1057-1088	52F68B91
Columns 1089-1120	97D69DF3
Columns 1121-1152	129C764E
Columns 1153-1184	8B2143F7
Columns 1185-1216	A36EF3BA
Columns 1217-1248	7C27896C
Columns 1249-1280	560F67B5
Row 609	
Columns 1025-1056	D70390E6
Columns 1057-1088	98B337EA
Columns 1089-1120	89568363
Columns 1121-1152	2A1681DF
Columns 1153-1184	4B4E928C
Columns 1185-1216	41EC3D9C
Columns 1217-1248	DFD92EB2
Columns 1249-1280	A5D5C85C
Row 641	
Columns 1025-1056	2A5088BD
Columns 1057-1088	76CB6810
Columns 1089-1120	CB693D21
Columns 1121-1152	C0E9EFD5
Columns 1153-1184	F992506E
Columns 1185-1216	299CE082
Columns 1217-1248	901155A6
Columns 1249-1280	0B93AA16
Row 673	
Columns 1025-1056	18FEFECE

Columns 1057-1088	B0063536
Columns 1089-1120	95487089
Columns 1121-1152	4BB31BB9
Columns 1153-1184	66F3FD97
Columns 1185-1216	E32B58A0
Columns 1217-1248	2A39427A
Columns 1249-1280	5CD8DE9F
Row 705	
Columns 1025-1056	1A8F8616
Columns 1057-1088	C5F7D2B2
Columns 1089-1120	5AD2BC4E
Columns 1121-1152	BF1E86DB
Columns 1153-1184	ACF7BFFA
Columns 1185-1216	F3589597
Columns 1217-1248	A777654C
Columns 1249-1280	12DD1364
Row 737	
Columns 1025-1056	FFC03A59
Columns 1057-1088	DC450527
Columns 1089-1120	33B4C871
Columns 1121-1152	BAA2EA33
Columns 1153-1184	93A751A6
Columns 1185-1216	F9D72E4D
Columns 1217-1248	69B50C7F
Columns 1249-1280	F74151F9
Row 769	
Columns 1025-1056	7BE8519D
Columns 1057-1088	AF6FFAFA
Columns 1089-1120	268DBA73
Columns 1121-1152	A356128C
Columns 1153-1184	0418BE2C
Columns 1185-1216	1A43465A
Columns 1217-1248	60C6DF65
Columns 1249-1280	0E2438A0
Row 801	
Columns 1025-1056	EC25DC05
Columns 1057-1088	66AEE4A8
Columns 1089-1120	A72A030A
Columns 1121-1152	B11FB610
Columns 1153-1184	DD74DAF7
Columns 1185-1216	62F6D565
Columns 1217-1248	554EAEB7
Columns 1249-1280	15F7AE6C

Row 833	
Columns 1025-1056	5147F90A
Columns 1057-1088	FF0EEC01
Columns 1089-1120	12A9966C
Columns 1121-1152	871705B1
Columns 1153-1184	E935FF30
Columns 1185-1216	46E32957
Columns 1217-1248	546D69FC
Columns 1249-1280	B8A1BD06
Row 865	
Columns 1025-1056	6A80EA6F
Columns 1057-1088	71A29506
Columns 1089-1120	EF78AACF
Columns 1121-1152	8D52B5ED
Columns 1153-1184	9F0A4966
Columns 1185-1216	61B3B68E
Columns 1217-1248	4B17AF96
Columns 1249-1280	5B282C2E
Row 897	
Columns 1025-1056	75582272
Columns 1057-1088	16E54299
Columns 1089-1120	7D070B9C
Columns 1121-1152	AB130157
Columns 1153-1184	76C619D2
Columns 1185-1216	5500E2D5
Columns 1217-1248	1F980459
Columns 1249-1280	5D9C7F83
Row 929	
Columns 1025-1056	6A0DDA1D
Columns 1057-1088	F6E8B610
Columns 1089-1120	25D0E0A1
Columns 1121-1152	242749E0
Columns 1153-1184	FEDA4A06
Columns 1185-1216	072D69D6
Columns 1217-1248	03C7DA79
Columns 1249-1280	51AA3355
Row 961	
Columns 1025-1056	6E9FEFF0
Columns 1057-1088	0797CBF1
Columns 1089-1120	E936C824
Columns 1121-1152	C9C1EAF5
Columns 1153-1184	D4607E46
Columns 1185-1216	88ED7B0E
Columns 1217-1248	92E160AD

Columns 1249-1280	731140AD
Row 993	
Columns 1025-1056	32FEFCAF
Columns 1057-1088	70863B75
Columns 1089-1120	3846F110
Columns 1121-1152	C4E23DFF
Columns 1153-1184	79D3F753
Columns 1185-1216	064648FA
Columns 1217-1248	830452F5
Columns 1249-1280	B9ED8445

D.4.f.   Code Rate =4/5, Information Block Size = 4096, M = 512

The first 4096 columns of **G** form a 4096 × 4096 identity matrix and the remaining 1024 columns of **G** form a block matrix composed of 32 rows and 8 columns of circulant matrices, each of size 128 × 128. The first row of each circulant is given in hexadecimal format in Table D-9 according to its location in **G**. Subsequent rows of each circulant can be computed by applying the corresponding number of right circular shifts to the first row.

Table D-9. First Rows of Circulants in Generator Matrix, r=4/5, k=4096	
Row 1	
Columns 4097-4224	473BC533A12C3596F642673D0DBF1142
Columns 4225-4352	079A3868E1A6F556F0DF3DCA4493AE54
Columns 4353-4480	AE4C50F12AEF6EEDEA9BB30605F4A24C
Columns 4481-4608	B0B2B4B9035331ABF53DE4752E7EDABF
Columns 4609-4736	E7E08EF3E22EE7EFE645E9E59507A206
Columns 4737-4864	52E4A2C06270B2D1A418134BC0D58678
Columns 4865-4992	0A84E53303F4092DB47056AD3C0847AD
Columns 4993-5120	2DEF73813B17101E79A3A58A7E91C4E2
Row 129	
Columns 4097-4224	667AA815610234DBA0FFA951CABB8BA7
Columns 4225-4352	A3271642E4BCDD24F8D89BD783317ABB
Columns 4353-4480	CC64FA95F06AE45C7E38935D78BF5F80
Columns 4481-4608	510CE9ABC6156F008B317C79E0122B09
Columns 4609-4736	3CB09E20016A5F93E207C144E889F3B9
Columns 4737-4864	AE6185E4345C5971E03AD499EF850D33
Columns 4865-4992	FA8B392CE78B5712290CB2F518F3E0CC
Columns 4993-5120	429C39F0915EB60CA0545B6AB2967149
Row 257	
Columns 4097-4224	FE9FF6C26898CB926F9BCD129AA52083
Columns 4225-4352	3FC159DB58B64D39CB27847434F177E2
Columns 4353-4480	E040D71365D96A1D54FD20051D3A50E7
Columns 4481-4608	E8AC736B6D2BB5468FBF68DDF5789C2F
Columns 4609-4736	4954E4153CFF0F52F8F8F5B243A03E2B

Columns 4737-4864	99A1DDD23204D103E323158E0FEE7673
Columns 4865-4992	43C2A07046BA1B4307BA6CEC7D740CFE
Columns 4993-5120	CB4E113F94C6CAA4652EFD867B43D199
Row 385	
Columns 4097-4224	081E779BF01F34C97337A3ABC8698644
Columns 4225-4352	9C9E794155E27547283C1AB2706A388D
Columns 4353-4480	FB9DFD194731EC2AE99EA6B641B309A2
Columns 4481-4608	258D45A1BBEAFFC787E61289A54A2473
Columns 4609-4736	FDF3E96C7679E979911C4BE65A333250
Columns 4737-4864	178259F846AA95577C2EC448EE709423
Columns 4865-4992	A61BE7CCED0342965CA234AF02914916
Columns 4993-5120	E045B3C585714F272D40C8085AE5E8F4
Row 513	
Columns 4097-4224	7FB352B26E544BDC18D76B323C3CE1BB
Columns 4225-4352	8421967EE08A6F719B675F06F13FF05B
Columns 4353-4480	672C29DC5B80E18E2F4C42D0F6D5D6D4
Columns 4481-4608	7DE072F73A8015862A275B2CEA2FFC1C
Columns 4609-4736	284B87ABA22362D98952442BBDFBF4A3
Columns 4737-4864	2B798BCD5D8C0B02BBE5DE4A96569F99
Columns 4865-4992	409E72F4138595F8B3C14074BD8E33E0
Columns 4993-5120	3B07838358BBAE631C8258D6B07D2E1C
Row 641	
Columns 4097-4224	403149A1C88E4D4893FE719B2638B7FF
Columns 4225-4352	9886F3E90FC018699F3B39183F2219DC
Columns 4353-4480	F5B0D3AA451225867913FF8FF979BBE0
Columns 4481-4608	795DFCBCC98210C028FD21380EBDDABF
Columns 4609-4736	0BBE0D91FA504DC4DC8848AEA001577F
Columns 4737-4864	51653E755F6CB4F75ACE347EC899304D
Columns 4865-4992	1D0EE239D8A6C2E2EA13D4CFB3394FCA
Columns 4993-5120	BF707E3ACD882B91FDDD44A7EA0D1F3D
Row 769	
Columns 4097-4224	14EB386A5A4524983682993353F8D76E
Columns 4225-4352	F9850534D2FB4F19F787897435C5EB0F
Columns 4353-4480	B680840F8D34A0995BA0A94E309A9194
Columns 4481-4608	6C66CAA0567BFFD609B6484BCD477702
Columns 4609-4736	B62A4053A6916719693D50608EC1D717
Columns 4737-4864	23C38E6F64963EE836ADC6BBF39F4CD1
Columns 4865-4992	A40947C16AEAD43F621457BDB766A157
Columns 4993-5120	DD6118ACF503356D0B3479828C296016
Row 897	
Columns 4097-4224	AAB1061EC9FA6BA21E81D7E22D3A7ED2
Columns 4225-4352	F902B6C336258F5B6B54628AC96116DE
Columns 4353-4480	5968E3167BB1E221714B0F4B3B9D7E0A
Columns 4481-4608	F12374361559D0F0E0C7FCC959B1A9D8

Columns 4609-4736	C103B779B3A769AA8D955160E4B9F9B7
Columns 4737-4864	231B28E0B7490C8EB883F29AF6CC4F12
Columns 4865-4992	A7D1FA32F82AAF128FBC6AC53532AB89
Columns 4993-5120	17AC06392CDAC681817D2F5475016296
Row 1025	
Columns 4097-4224	434D8612F27169A49ED244393B87DB5E
Columns 4225-4352	B66D806A5A9ADF46D83C7DCFDB4B72CA
Columns 4353-4480	A78E0C64307885C6E67C870BD21EC431
Columns 4481-4608	11B79B0BB0B977D9792535C16AA7D982
Columns 4609-4736	B597FD60982B8C42D019390EFA14B3D5
Columns 4737-4864	C57FF5CFA1C438AC576782A5B48B78AA
Columns 4865-4992	AE278E95DA048F720B7DB5FB6488287B
Columns 4993-5120	893C7E7E8DCB6E5ED5DB819D8901B32C
Row 1153	
Columns 4097-4224	B7BA8906FC3AEADE22254872ECA99117
Columns 4225-4352	74F39404FA2779F4C55D649E5A6AA628
Columns 4353-4480	4A1F8910EBF76F2F4E3EF686266CEBB8
Columns 4481-4608	8363A57CF1377C68419BEFE6C848FEDA
Columns 4609-4736	8F141154BFA88D31446EF367ED965F98
Columns 4737-4864	1242B3F840426E98010B84A957090390
Columns 4865-4992	9CE9E0B619E61C4A481F1DD44360BCAC
Columns 4993-5120	0938AE511B2B47A42F5F59FBF547D991
Row 1281	
Columns 4097-4224	85B68FFC07A32A495D9A708FAECD2C41
Columns 4225-4352	69CFDFFD21D6B2CF3F91CF5820823B83
Columns 4353-4480	7D62406050908C82C21CF32B862166F2
Columns 4481-4608	82AF2DF8E6CADB5D043FBF863ACE6599
Columns 4609-4736	700097EE5FDDD825468C544985C983CE
Columns 4737-4864	69EE0178288A8E1A12009EBF2E4382DE
Columns 4865-4992	2B8D59DE631991AE1B67C70786B43BE2
Columns 4993-5120	860FC3354C9FE4253EBF307D1C643E22
Row 1409	
Columns 4097-4224	905330D76B16340120BB399A08061CBE
Columns 4225-4352	9D5765CE993D7092A8150DE46D6CA810
Columns 4353-4480	E03534D4DA2B66A0BF2AEF3B833E18DF
Columns 4481-4608	6C1C0D9EAB1E26FD2481F6BB6AB674C6
Columns 4609-4736	D98BD8D3FC0E0557352CF52EEA654A92
Columns 4737-4864	0DF8D4B0FD41AD3EE547119C2446F840
Columns 4865-4992	4C1F458D1E2F4B70D9023F0DFC06EFE9
Columns 4993-5120	24349C5D9DE2B048DC74D3E888043526
Row 1537	
Columns 4097-4224	E864E5EE002EB3B4C31A8D3B3E22D2C6
Columns 4225-4352	B3C4136542237F8E3C75AA228AB1B2F5
Columns 4353-4480	43DF20DF407EAC80CAF22FDDADD586C9

Columns 4481-4608	9414219FF80742652531AC5CC0E52866
Columns 4609-4736	1A68E6BC5CA7FCA386396D0F56A2E7A3
Columns 4737-4864	D9EC25B8DEA08EDB6A9E6CFFEC7B15C1
Columns 4865-4992	CD48176480B2E0FED349142BE9888043
Columns 4993-5120	9A70BAD89B53A4461301DF6C1763EB67
Row 1665	
Columns 4097-4224	5C9B0F852875D4B06EFA7FF418710592
Columns 4225-4352	6F7C0712083341F6A97F398A275243DC
Columns 4353-4480	3D046D9B0B0B6AB3FEB99F72A70BAF35
Columns 4481-4608	50F7B484C2530BEF63537B68EBDCF01C
Columns 4609-4736	672E8B1DD956431036302F8557CBB4E0
Columns 4737-4864	C9CAD206AB0AD88C655E0F52C70AEEA1
Columns 4865-4992	FF7EC97F9439C9D4CD71487F10065DE0
Columns 4993-5120	532339617D706AEFA50A23B90B57978C
Row 1793	
Columns 4097-4224	B7E0C9A5F3EF66B9ABA49150144FCBEF
Columns 4225-4352	2C9E63DC18BE8ADDA0FD7E7E8F7FC5FE
Columns 4353-4480	5C55C60E14C3D7AC4D00D9F6C827E1EC
Columns 4481-4608	4E40D57E1740089DB1248707D195C038
Columns 4609-4736	4500AD976DD321E6133113D244711330
Columns 4737-4864	0260379D0A20D10A899019157631007D
Columns 4865-4992	4DF741A808694A9956E493B4668B67FD
Columns 4993-5120	F89442CABAA2262C398171D62E938504
Row 1921	
Columns 4097-4224	CCF8A4E13D655D5591DC40D2C6607CEF
Columns 4225-4352	353E539A020B0C608F843A855BA9B7AE
Columns 4353-4480	CD31CCCB9388FECDEBEE1CCF42943E77
Columns 4481-4608	9CA39E64D8AC9E23F15A0CB4C73ACB80
Columns 4609-4736	3BF0F0DA9576923D95089979081ACA77
Columns 4737-4864	359B090725B62278F00D0222CAD4C0FF
Columns 4865-4992	4ABA29056D55C5AAD990AA10A9A1A9B2
Columns 4993-5120	27A09750826682C157BD7CD2178FDC96
Row 2049	
Columns 4097-4224	AFC3076AF8AFB82B45FE8F2628F489F1
Columns 4225-4352	2CFA95663A96A30FB3831F756D9E666A
Columns 4353-4480	011EE24F6C5EE283C3EE09A1D5FAF1B9
Columns 4481-4608	7B49CB7B94EDEB207221A9436E1FFDF5
Columns 4609-4736	5D36302EEBDD74AD27158F4D9DF0FA6E
Columns 4737-4864	497015959B333E79885FBE22B9B72707
Columns 4865-4992	E330EEAD520B31BAD1A5DC55EF54193A
Columns 4993-5120	D6C112F89677E27A26F1DC62E08DF49C
Row 2177	
Columns 4097-4224	2DF5B0291E619A18D802502086037C46
Columns 4225-4352	730D20AE9364A6AD090B789D8AA6C6CC

Columns 4353-4480	EA476A585503E90BCAAD943DD30E1BCC
Columns 4481-4608	1D5C236ED01E9E5C8E94E96FA7252ABF
Columns 4609-4736	3EB2DB84FB4837EA5153CA825D11F86B
Columns 4737-4864	574E63C92DD0E75AD8DDFF2B37CC97C9
Columns 4865-4992	5E83299E60C44293BF0824C62EB7980C
Columns 4993-5120	5678B852002834EB2D630EAC536FFB78
Row 2305	
Columns 4097-4224	9A41F048C1C68187734BFB916EC3BFAF
Columns 4225-4352	4B23BDA1162B30CB7AEA9F03BEBCF597
Columns 4353-4480	C65460BFAF9C8913608F9888E738F4A1
Columns 4481-4608	017AEE470FCA60F9711E9BE5EB98E7C9
Columns 4609-4736	4EE8869A59EDF8BDD52C5B5388B35249
Columns 4737-4864	8EB0D25B439273CA6545E82E69D8677C
Columns 4865-4992	5B23991A53041EA4B276405C156A9DE5
Columns 4993-5120	A90889BC74530A5F87CCF024E591E18F
Row 2433	
Columns 4097-4224	22735E1E720A8B3C29A80F3696D6F157
Columns 4225-4352	F68ED2F2389D5D2CDC59D706495D815F
Columns 4353-4480	D0EE25B73218D5717572387BFA03A7C2
Columns 4481-4608	A0717B27763FE223BDA3EB0DAFBEF276
Columns 4609-4736	9DBB8235D11298BEE28B39772ED91A35
Columns 4737-4864	92DE6FED2F6766E01DBA188153DEA205
Columns 4865-4992	48930E9A21873E62863CA15D6DB058D9
Columns 4993-5120	61A29088FE3983D0E1699EF0AAFA5FD1
Row 2561	
Columns 4097-4224	A7300569009888938225287 3E627D6FB
Columns 4225-4352	7862DE8A3D0F1A9387963F38A82E4703
Columns 4353-4480	78BAB9252EE72FB0C798C7C684B6E789
Columns 4481-4608	B7480D9712BFA72D122F243674AD887F
Columns 4609-4736	EC1851EB80A37133B68F0F709DB32E05
Columns 4737-4864	A809CB3638414FD6E156821BDAC256E0
Columns 4865-4992	B75342B6CFF7ED428521AB48A4C55D66
Columns 4993-5120	C9AB047D79A484289C820E8FADD87251
Row 2689	
Columns 4097-4224	A69C02525644F41D03197EF26112D606
Columns 4225-4352	3DF71AD0410035AE1AE7B0AB310B6967
Columns 4353-4480	C4F82E31B4D9B491EF8E4992FDBA61B0
Columns 4481-4608	B6B367CDE8DE0CAE22875F641288E733
Columns 4609-4736	5C142A9C7C2E259BD38D66117E9E861C
Columns 4737-4864	D27BF85E8EEE1920B57D0C62B512E2D6
Columns 4865-4992	68B4500340B7B92EDD05A44D36AC1651
Columns 4993-5120	4E77C4ABE92FE174B5D9F79070685288
Row 2817	
Columns 4097-4224	A22B2A6C9A75D7A6EEA5A0DF8A4950E2

Columns 4225-4352	24C4830123FAE1EB6EB0AC9C2D8C508E
Columns 4353-4480	1BB99D6785EBCCDD9CD6A50CF53CCA00
Columns 4481-4608	0624E36FD0817F2E198340098E60DFBF
Columns 4609-4736	A4EB92DD48085594C6F755C563F35020
Columns 4737-4864	04BDFF9A2309C6E673CE08D94A45BBC4
Columns 4865-4992	8B8EC43906C28869AD4E41FB147A7696
Columns 4993-5120	8AB66E9B68FA00BEF90D3E078D0C6FFC
Row 2945	
Columns 4097-4224	89A79E9CF0BE90A3D86305B6491A49B9
Columns 4225-4352	222A27A68236765AB32D41B1E0616C83
Columns 4353-4480	99931668E57EB6378C8F4ED1C27BEDD3
Columns 4481-4608	35166846D0C673B9A8D2184C1901433A
Columns 4609-4736	4D768A5E0109B5CBC198869334D81C43
Columns 4737-4864	2C6A48CC47FD21F9608107FF80FE37AA
Columns 4865-4992	4DD3A7395630BE4B64F776C5FC6B2C31
Columns 4993-5120	4DC16B1E2B2A7F6E0E9FDAE3B60F8FAA
Row 3073	
Columns 4097-4224	CFA794F49FA5A0D88BB31D8FCA7EA8BB
Columns 4225-4352	A7AE7EE8A68580E3E922F9E13359B284
Columns 4353-4480	91F72AE8F2D6BF7830A1F83B3CDBD463
Columns 4481-4608	CE95C0EC1F609370D7E791C870229C1E
Columns 4609-4736	71EF3FDF60E2878478934DB285DEC9DC
Columns 4737-4864	0E95C103008B6BCDD2DAF85CAE732210
Columns 4865-4992	8326EE83C1FBA56FDD15B2DDB31FE7F2
Columns 4993-5120	3BA0BB43F83C67BDA1F6AEE46AEF4E62
Row 3201	
Columns 4097-4224	565083780CA89ACAA70CCFB4A888AE35
Columns 4225-4352	1210FAD0EC9602CC8C96B0A86D3996A3
Columns 4353-4480	C0B07FDDA73454C25295F72BD5004E80
Columns 4481-4608	ACCF973FC30261C990525AA0CBA006BD
Columns 4609-4736	9F079F09A405F7F87AD98429096F2A7E
Columns 4737-4864	EB8C9B13B84C06E42843A47689A9C528
Columns 4865-4992	DAAA1A175F598DCFDBAD426CA43AD479
Columns 4993-5120	1BA78326E75F38EB6ED09A45303A6425
Row 3329	
Columns 4097-4224	48F42033B7B9A05149DC839C90291E98
Columns 4225-4352	9B2CEBE50A7C2C264FC6E7D674063589
Columns 4353-4480	F5B6DEAEBF72106BA9E6676564C17134
Columns 4481-4608	6D5954558D23519150AAF88D7008E634
Columns 4609-4736	1FA962FBAB864A5F867C9D6CF4E087AA
Columns 4737-4864	5D7AA674BA4B1D8CD7AE9186F1D3B23B
Columns 4865-4992	047F112791EE97B63FB7B58FF3B94E95
Columns 4993-5120	93BE39A6365C66B877AD316965A72F5B

Row 3457	
Columns 4097-4224	1B58F88E49C00DC6B35855BFF228A088
Columns 4225-4352	5C8ED47B61EEC66B5004FB6E65CBECF3
Columns 4353-4480	77789998FE80925E0237F570E04C5F5B
Columns 4481-4608	ED677661EB7FC3825AB5D5D968C0808C
Columns 4609-4736	2BDB828B19593F41671B8D0D41DF136C
Columns 4737-4864	CB47553C9B3F0EA016CC1554C35E6A7D
Columns 4865-4992	97587FEA91D2098E126EA73CC78658A6
Columns 4993-5120	ADE19711208186CA95C7417A15690C45
Row 3585	
Columns 4097-4224	BE9C169D889339D9654C976A85CFD9F7
Columns 4225-4352	47C4148E3B4712DAA3BAD1AD71873D3A
Columns 4353-4480	1CD630C342C5EBB9183ADE9BEF294E8E
Columns 4481-4608	7014C077A5F96F75BE566C866964D01C
Columns 4609-4736	E72AC43A35AD216672EBB3259B77F9BB
Columns 4737-4864	18DA8B09194FA1F0E876A080C9D6A39F
Columns 4865-4992	809B168A3D88E8E93D995CE5232C2DC2
Columns 4993-5120	C7CFA44A363F628A668D46C398CAF96F
Row 3713	
Columns 4097-4224	D57DBB24AE27ACA1716F8EA1B8AA1086
Columns 4225-4352	7B7796F4A86F1FD54C7576AD01C68953
Columns 4353-4480	E75BE799024482368F069658F7AAAFB0
Columns 4481-4608	975F3AF795E78D255871C71B4F4B77F6
Columns 4609-4736	65CD9C359BB2A82D5353E007166BDD41
Columns 4737-4864	2C5447314DB027B10B130071AD0398D1
Columns 4865-4992	DE19BC7A6BBCF6A0FF021AABF12920A5
Columns 4993-5120	58BAED484AF89E29D4DBC170CEF1D369
Row 3841	
Columns 4097-4224	4C330B2D11E15B5CB3815E09605338A6
Columns 4225-4352	75E3D1A3541E0E284F6556D68D3C8A9E
Columns 4353-4480	E5BB3B297DB62CD2907F09996967A0F4
Columns 4481-4608	FF33AEEE2C8A4A52FCCF5C39D355C39C
Columns 4609-4736	5FE5F09ABA6BCCE02A73401E5F87EAC2
Columns 4737-4864	D75702F4F57670DFA70B1C002F523EEA
Columns 4865-4992	6CE1CE2E05D420CB867EC0166B8E53A9
Columns 4993-5120	9DF9801A1C33058DD116A0AE7278BBB9
Row 3969	
Columns 4097-4224	4CF0B0C792DD8FDB3ECEAE6F2B7F663D
Columns 4225-4352	106A1C296E47C14C1498B045D57DEFB5
Columns 4353-4480	968F6D8C790263C353CF307EF90C1F21
Columns 4481-4608	66E6B632F6614E58267EF096C37718A3
Columns 4609-4736	3D46E5D10E993EB6DF81518F885EDA1B
Columns 4737-4864	6FF518FD48BB8E9DDBED4AC0F4F5EB89
Columns 4865-4992	BCC64D21A65DB379ABE2E4DC21F109FF

Columns 4993-5120	2EC0CE7B5D40973D13ECF713B01C6F10

D.4.g. Example Data Test Patterns and Resulting Parity Values

The following examples are intended to provide a means to verify parity generation correctness for each of the six LDPC variants. These examples are provided for the purpose of LDPC encoder design verification; were generated using fixed test pattern data blocks; and provide the corresponding parity values for each of the standard rates. The examples include one fixed test pattern data block for a block size of 1024 bits as well as one for a block size of 4096 bits along with the resulting parity bit results for the three different rates.

D.4.g(1) Data Block (k = 1024 bits) Test Pattern Information

The example test pattern for this block size consists of 16-bit values that count up from zero with a trailing 32-bit frame sync occupying the last two words for a total of 64 16-bit values. This example data block was used to generate the resulting parity values for the three standard code rates.

Example 1024-bit test pattern values in hexadecimal are as follows.

0000000100020003000400050006000700080009000A000B000C000D000E000F001000110012
00130014001500160017001800190001A001B001C001D001E001F0020002100220023002400250
0026002700280029002A002B002C002D002E002F003000310032003300340035003600370038
0039003A003B003C003DFE6B2840

The following are the resulting parity values using the above 1024-bit test pattern and applying the proper code rate encoding computation.

Parity (Code Rate = 1/2, Information Block Size = 1024, M = 512):
88C25789C85FFC52B331FFD279EB689EAF7007024078EDE8248057851F3E877693663BEA
FFE58810265686F4C51B698F366584549FA83C52FA23AC7AE1AF2D0D10268182D4E3B82
98990A514A6854A3D6FEFF59B69296BD601B16A7C1E827A2DC13045F1EA883A7F7ADF
621666D0865DCD14B094C280CC9E0948F460E5113622

Parity (Code Rate = 2/3, Information Block Size = 1024, M = 256):
D4E830063C6EA310B7DC85CC05E7E7721078503ED0061FCA7B796F1612C79A6B89171D
8AF5D773868EA94F2DD722F0F7952AE2034E6CCF0E1DD9FC5224B2AF3F

Parity (Code Rate = 4/5, Information Block Size = 1024, M = 128):
799EE0CE3994059D9FA69D26C6A0DF9BAF29C7B008F16B88A020056356BF8915

D.4.g(2) Data Block (k = 4096 bits) Test Pattern Information

The example test pattern for this block size consists of 16-bit values that count up from zero with a trailing 32-bit frame sync occupying the last two words for a total of 256 16-bit values. This example data block was used to generate the resulting parity values for the three standard code rates.

Example 4096-bit test pattern values in hexadecimal are as follows:

0000000100020003000400050006000700080009000A000B000C000D000E000F001000110012
00130014001500160017001800190001A001B001C001D001E001F0020002100220023002400250
0026002700280029002A002B002C002D002E002F003000310032003300340035003600370038
0039003A003B003C003D003E003F004000410042004300440045004600470048004900440A004
B004C004D004E004F005000510052005300540055005600570058005900 5A005B005C005D0

05E005F0060006100620063006400650066006700680069006A006B006C006D006E006F0070
0071007200730074007500760077007800790007A007B007C007D007E007F0080008100820083
0084008500860087008800890008A008B008C008D008E008F009000910092009300940095096
009700980099009A009B009C009D009E009F00A000A100A200A300A400A500A600A700A8
00A900AA00AB00AC00AD00AE00AF00B000B100B200B300B400B500B600B700B800B90
0BA00BB00BC00BD00BE00BF00C000C100C200C300C400C500C600C700C800C900CA00
CB00CC00CD00CE00CF00D000D100D200D300D400D500D600D700D800D900DA00DB00
DC00DD00DE00DF00E000E100E200E300E400E500E600E700E800E900EA00EB00EC00ED
00EE00EF00F000F100F200F300F400F500F600F700F800F900FA00FB00FC00FDFE6B2840

The following are the resulting parity values using the above 4096-bit test pattern and applying the proper code rate encoding computation.

Parity (Code Rate = 1/2, Information Block Size = 4096, M = 2048):

AE1BA1553F901C1966B2115918D55011CF585B2397867854FBEA39176232555211A92640
C1105814503C7F2096343AD836CCE6733793E2D45EBEC36E42993424690A1B95341E0B8
ED20D1DAC0400817DBC8BDF995402928C67602BA3448805F80DA2D4632ED279F0C5C2
A6BA4B9386FBC5E4121AD98B0C2FD18F4A977C3D9B9012D278E0F46F2822EDD0B57B
B165C45407A53E42BB05FC4A97005E1E677DBEA8EBEE1CA4F9CCC7C31EDA7065A57
A49BBA775914EAFBA330239F955DDEB32061DD6D40D995B6C47BF1B08C38023837617
E53C82715EA4D11AE422E11CEAA97A35DBC62A475359826B7A9EABB6E8A3B7B4ABC
BF32C2D9CC090D20F320CAAA85759BCE91A5E32068A60B2EAEC0B321D6F22F31F91A
6C73FD94EA4F26D91F88F353293177938276EEC3AF050BC3FB8F9258B88423BE8A0F8A
EC609971D0B22752161A81FE5BC88F396C73430FF0B79B555440D17A1F0E9D5375B6D9
AD6337AFFAF743E7E198D8B45BCC80E27D3441D57F9C362A0385F0C2774E038E1DBAC
256BCD61AA2DB82681CABA315E759B1F24D6B729294B4C2DAB81A6CB701C564CAE8
DDC3D281449DBCEDF2D1B6625781CC9CDAB32354F05548645AB2D720BC6CE69360D5
1D876B987FFF35C020D9FB6255B452A215B77810B7283CC3EE98C288B2B8B3C2AFF023
3AB9AA77E39466677AD8AB97363CE8F0BF4120333191CDF0E36E91ABF64

Parity (Code Rate = 2/3, Information Block Size = 4096, M = 1024):

5406F5FAD70A1D1012D88BFEBF612626CAE419504EED672004CFAA84FE66E1B8B74F4
1B820AB5C9740171B8314FA8CED9E54812F5CB84C5ED3DDEAD5B8993CEA6852F144E
DFE9F39BA1BDC299699965BEC1B5FAAA373668952AC4B53717A4285D40B6118672BA
D9A6D2BCA70F00CD4E99CCB726B7D15D893407E54CE7083D9A6B9B1A6224B7D8FCD
EBCB6EA0AD5F049870AA8BB22DC6DB74C2B71E7D37CF7164E3E057953646BEB15C4A
06206D3A54668DD769457F25821DDB7C45F5720E2CCE95F06287844A0E24CA1B7170F67
DD71AD528B85A6D28BE08F692F54FEA2D255913FB917264304B890F6348DAAFE421C3
B312A69E30F5B99D4DC008DC2722620B

Parity (Code Rate = 4/5, Information Block Size = 4096, M = 512):

29B2733B0F079239C6DF5D72D10F3BC5AC7DEAF808B3FF7F1AC0ABF1991B77CC5086
D31E93D4C900840EE689B9C4D1400E99C64C71C9BAA48FA5EA007B63964EB965EC624
5F9084729C4C19BB42679924F88FFF268CF2BD1E23EDED11C2C444E2A29903778C846B4
EFBE05B280AA42B661FE33B650F4F431E6EE7CAF9BB0AAF9

D.5. Synchronization

Current receiver/demodulator designs can perform either coherent or non-coherent detection and demodulation. To accomplish symbol/bit synchronization, the transmitted synchronization sequence must contain sufficient transitions to ensure symbol/bit acquisition and tracking. At the same time, the symbol/bit synchronizer loop bandwidth should be designed for optimal phase-noise filtering and symbol tracking performance. Since the use of LDPC code does not guarantee sufficient bit/symbol transitions to acquire or maintain synchronization, it is highly recommended that a pseudo-randomizer be used after LDPC encoding in accordance with Section D.6.

The ASM, depicted in Figure D-8 and Table D-10, is not randomized. Randomization ensures that coded symbols are spectrally near-white, thus allowing each ASM to provide synchronization for a set of randomized codeblocks in a codeblock frame.
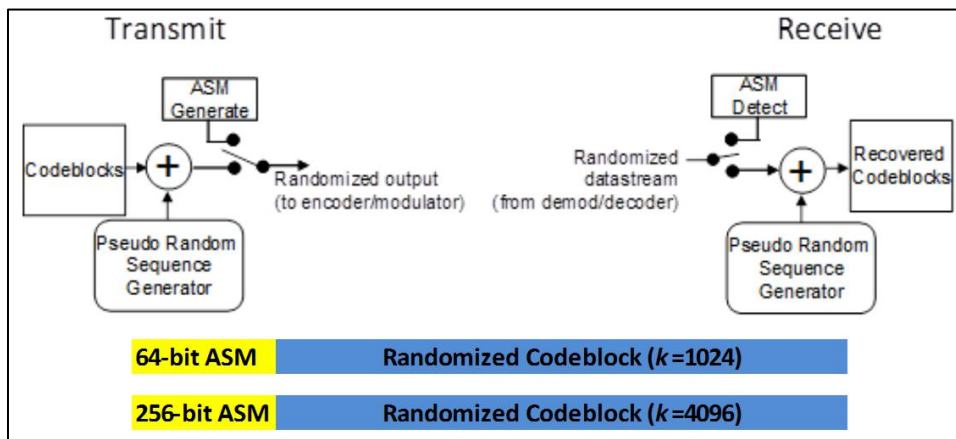
Figure D-8.   ASM/Codeblock Structure

Table D-10. ASM Definition	
64-bit Sequence	Definition (hex)
A	FCB88938D8D76A4F
$\bar{A}$	034776C7272895B0

At the transmitter side, the ASM is prepended to each set of randomized codeblocks as the synchronization header. At the receiver side, the ASM is detected and located in the received data stream. Refer to Figure D-8.

Length of the ASM is determined by the information block length (k). For $k=1024$ the ASM length will be 64 bits. For $k=4096$ the ASM will be 256 bits. The ASM is constructed with 64-bit sequences. The 64-bit ASM requires one 64-bit sequence; the 256-bit ASM sequence requires four 64-bit sequences. Let A be one 64-bit sequence and $\bar{A}$ is the inverse of A. The structure of the 64-bit sequence is A; the structure of the 256-bit ASM is $AA\bar{A}A$. Table D-10 defines the two 64-bit sequences.

The resulting randomized codeblock plus ASM is transmitted leftmost bits first, making the first series of bits to be transmitted as FCB8……… or 1111110010111000……… This is true for both 64-bit and 256-bit ASMs.

With the addition of the ASM prepended to the codeblock, over-the-air channel rate is no longer the inverse of the code rate r. Table D-11 shows the exact bandwidth expansion factor for each choice of code rate and information block length.

Information Block	Bandwidth Expansion Factor		
Length, k	Rate 1/2	Rate 2/3	Rate 4/5
1024	33/16	25/16	21/16
4096	33/16	25/16	21/16

Table D-11. Bandwidth Expansion Factor

As an example, assume an incoming baseband data rate of 5 Mbps. If an information block length of 1024 bits and rate 1/2 are chosen, the new over-the-air channel rate will be:

$$(5 \text{ Mbps})*(33/16) = 10.3125 \text{ Mbps}$$

D.6.   Randomization

At the transmitter/encoder, a set of codeblocks in a codeblock frame shall be randomized by exclusive-ORing the first bit of the first codeblock with the first bit of the pseudo-random sequence until the end of the codeblock. The pseudo-randomizer resets to the initial state of all 1s at the start of each codeblock frame for each ASM period.

The pseudo-random sequence is generated using the following polynomial: $h(x) = x8 + x7 + x5 + x3 + 1$. It has a maximal length of 255 bits with the first 40 bits of the pseudo-random sequence from the generator as 1111 1111 0100 1000 0000 1110 1100 0000 1001 1010….. The sequence begins at the first bit of a first codeblock in a codeblock frame and repeats after 255 bits, continuing repeatedly until the end of the last codeblock in a codeblock frame. The leftmost bit of the pseudo-random sequence is the first bit to be exclusive-ORed with the first bit of the codeblock. Figure D-9 illustrates the pseudo-randomizer block diagram.
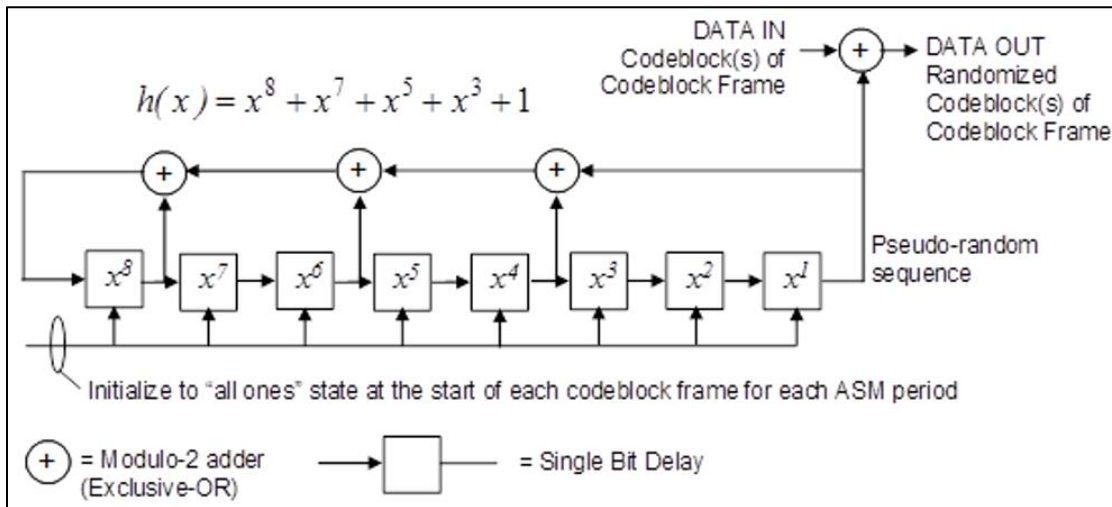
Figure D-9.   Codeblock Randomizer

At the receiver, each original codeblock of a codeblock frame is reconstructed using the same pseudo-random sequence. After locating the ASM, the pseudo-random sequence is

exclusive-ORed with the received data bits immediately following the ASM. The pseudo-randomizer resets to the initial state of all 1s at the start of each received codeblock frame for each ASM period.

D.7.   Performance

The trade that must be made when choosing the information block size and coding rate is one between required coding gain, bandwidth expansion, and fading channel characteristics. Detection performance of the code is tightly coupled to the type of SOQPSK-TG demodulator used. Plots of simulated performance for all six combinations of information block size and code rates with two different types of SOQPSK-TG demodulators on are shown in Figure D-10 and Figure D-11. Other demodulator configurations are considered in Perrins.[48]
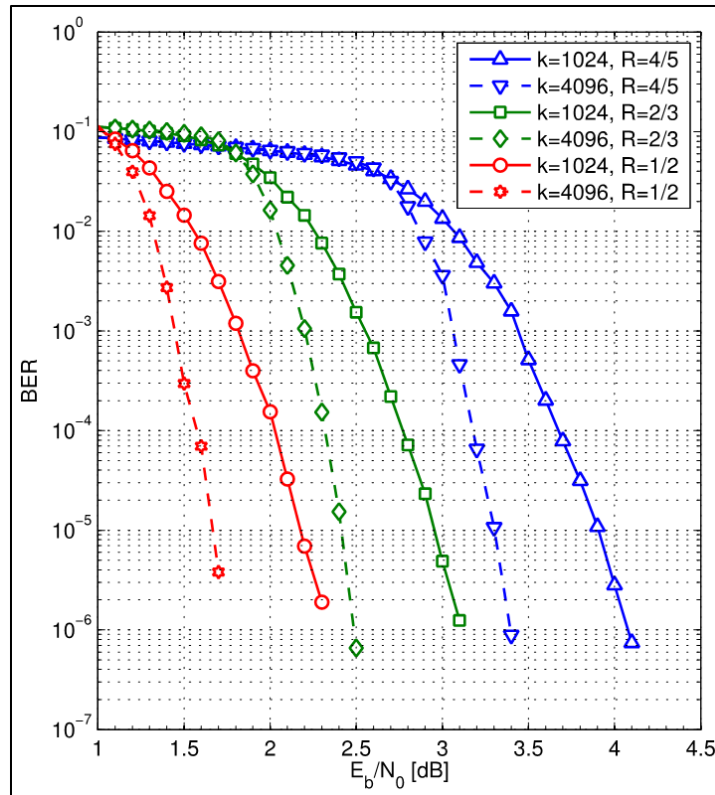
Figure D-10.   LDPC Detection Performance with 4-state Trellis Demodulator

---

[48] Perrins, "FEC Systems for Aeronautical Telemetry."
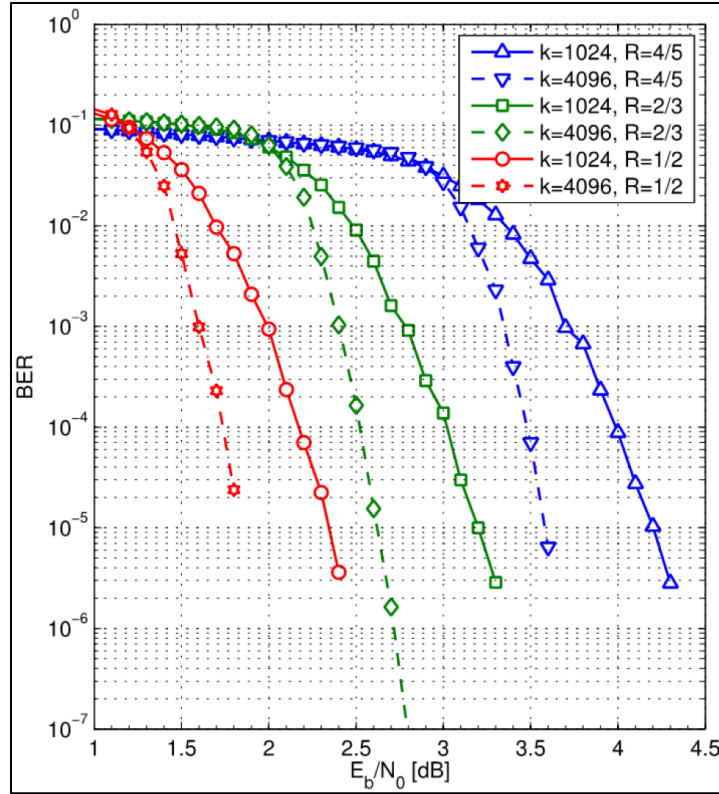
Figure D-11.   LDPC Detection Performance with Symbol-by-Symbol Demodulator

APPENDIX 2-E

Space-Time Coding for Telemetry Systems

E.1.   Code Description

The STC used in this standard is based on the Alamouti STC[49] and applied only to SOQPSK-TG or any of its fully interoperable variants. The Alamouti STC may be described in terms of the OQPSK IRIG-106 symbol-to-phase mapping convention illustrated in Figure E-1.
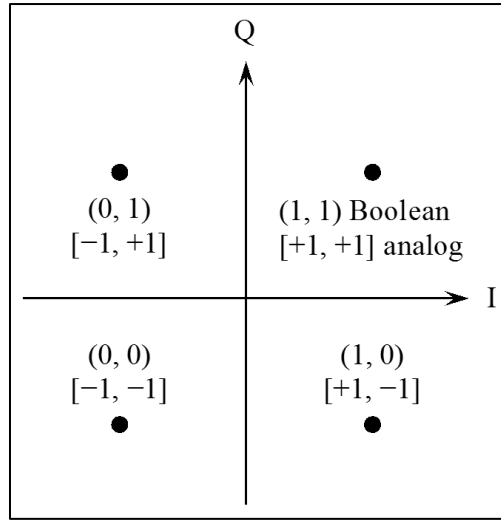
Figure E-1.   Symbol-to-Phase Mapping for IRIG-106 Offset QPSK Modulation

The starting point is the normalized analog values corresponding to each of the OQPSK symbols. Let $[a_n, b_n]$ with $a_n = \pm1$, $b_n = \pm1$ be the analog value of the n-th symbol. Suppose the bit sequence defines the sequence of symbols

$$[a_0, b_0], [a_1, b_1], [a_2, b_2], [a_3, b_3], \ldots, [a_{2k}, b_{2k}], [a_{2k+1}, b_{2k+1}], \ldots$$

The Alamouti STC organizes the symbols into blocks of two symbols, starting with the even-indexed blocks as shown. The Alamouti STC assigns the k-th block of symbols

$$[a_{2k}, b_{2k}], [a_{2k+1}, b_{2k+1}]$$

to antenna 0 and antenna 1 over two consecutive symbol times as shown below.

antenna	symbol time $2k$	symbol time $2k+1$
0	$[a_{2k}, b_{2k}]$	$[-a_{2k+1}, b_{2k+1}]$
1	$[a_{2k+1}, b_{2k+1}]$	$[a_{2k}, -b_{2k}]$

[49] S. Alamouti. "A Simple Transmit Diversity Technique for Wireless Communications." *IEEE Journal on Selected Areas in Communications*, vol. 16, no. 8, pp. 1451-1458, October 1998.

Using the bit (Boolean) assignments shown in [Figure E-1](), the Alamouti encoder can be restated in terms of the input bits as follows. Let the sequence of input bits be

$$b_0 \; b_1 \; b_2 \; b_3 \mid b_4 \; b_5 \; b_6 \; b_7 \mid \ldots \mid b_{4k} \; b_{4k+1} \; b_{4k+2} \; b_{4k+3} \mid \ldots$$

The STC encoder groups the bits into non-overlapping blocks of four bits each as indicated by the vertical lines. The STC encoder produces two bit streams in parallel: $\mathbf{b}_0$, which is applied to antenna 0, and $\mathbf{b}_1$, which is applied to antenna 1. The relationship between the input bit sequence and these two bit sequences is

$$\mathbf{b}_0 = b_0 b_1 \overline{b}_2 b_3 \mid b_4 b_5 \overline{b}_6 b_7 \mid \ldots \mid b_{4k} b_{4k+1} \overline{b}_{4k+2} b_{4k+3} \mid \ldots$$
$$\mathbf{b}_1 = b_2 b_3 b_0 \overline{b}_1 \mid b_6 b_7 b_4 \overline{b}_5 \mid \ldots \mid b_{4k+2} b_{4k+3} b_{4k} \overline{b}_{4k+1} \mid \ldots$$

where $\overline{b}_n$ is the logical complement of bit b_n.

An important point here is the notion of even- and odd-indexed bits. The SOQPSK-TG modulator treats even-indexed and odd-indexed bits slightly differently. Each codeblock must begin with an even-indexed bit.

An example of encoding is as follows. Suppose the input bit sequence is

$$1 \; 0 \; 1 \; 1 \; 0 \; 1 \; 0 \; 0$$

The two STC encoded bit sequences are

$$\mathbf{b}_0 \;\; = \;\; 1 \quad 0 \quad 0 \quad 1 \quad 0 \quad 1 \quad 1 \quad 0$$
$$\mathbf{b}_1 \;\; = \;\; 1 \quad 1 \quad 1 \quad 1 \quad 0 \quad 0 \quad 0 \quad 0$$

To make provision for the estimation of frequency offset, differential timing, and the channels, a block of known bits, called pilot bits, is periodically inserted into each of the two bit streams. A 128-bit pilot block is inserted every 3200 Alamouti-encoded bits. The pilot bits inserted into the $\mathbf{b}_0$ bit stream are denoted $\mathbf{p}_0$ and the pilot bits inserted into the $\mathbf{b}_1$ bit stream are denoted $\mathbf{p}_1$. These pilot bit sequences are

$\mathbf{p}_0 = 1\,0\,1\,0\,1\,0\,0\,0\,1\,0\,0\,0\,1\,1\,0\,1\,1\,0\,0\,1\,1\,0\,1\,0\,1\,1\,0\,1\,0\,1\,0\,0$
$\phantom{\mathbf{p}_0 = } 1\,1\,0\,1\,1\,1\,0\,0\,0\,1\,0\,0\,0\,0\,0\,0\,0\,1\,0\,0\,1\,0\,0\,1\,0\,1\,0\,0\,0\,1\,1\,1$
$\phantom{\mathbf{p}_0 = } 1\,1\,1\,0\,0\,0\,1\,0\,1\,0\,0\,1\,0\,0\,1\,0\,0\,0\,0\,0\,0\,0\,1\,0\,0\,0\,1\,1\,1\,0\,1\,1$
$\phantom{\mathbf{p}_0 = } 0\,0\,1\,0\,1\,0\,1\,1\,0\,1\,0\,1\,1\,0\,0\,1\,1\,0\,1\,1\,0\,0\,0\,1\,0\,0\,0\,1\,0\,1\,0\,1$

$\mathbf{p}_1 = 1\,1\,1\,0\,0\,0\,1\,1\,1\,1\,0\,0\,0\,1\,1\,1\,0\,1\,1\,1\,0\,1\,1\,1\,0\,1\,1\,0\,0\,0\,0\,1$
$\phantom{\mathbf{p}_1 = } 1\,1\,1\,1\,0\,0\,0\,0\,0\,1\,1\,1\,0\,0\,0\,0\,0\,0\,1\,1\,0\,1\,1\,0\,1\,0\,1\,1\,1\,1\,1\,0$
$\phantom{\mathbf{p}_1 = } 0\,1\,1\,1\,1\,1\,0\,1\,0\,1\,1\,0\,1\,1\,0\,0\,0\,0\,0\,0\,1\,1\,1\,0\,0\,0\,0\,0\,1\,1\,1\,1$
$\phantom{\mathbf{p}_1 = } 1\,0\,0\,0\,0\,1\,1\,0\,1\,1\,1\,0\,1\,1\,1\,0\,1\,1\,1\,0\,0\,0\,1\,1\,1\,1\,0\,0\,0\,1\,1\,1$

A notional diagram illustrating how $\mathbf{p}_0$ and $\mathbf{p}_1$ are periodically inserted into $\mathbf{b}_0$ and $\mathbf{b}_1$, respectively, is illustrated in [Figure E-2](). Note that the bits comprising $\mathbf{b}_0$ and $\mathbf{b}_1$ may change with every occurrence as defined by the input data, but the pilot bits $\mathbf{p}_0$ and $\mathbf{p}_1$ do not change with each occurrence.
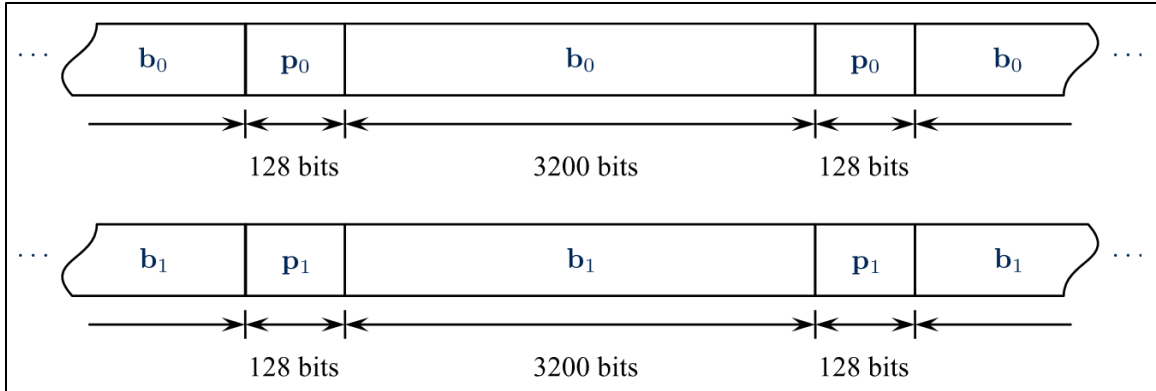
Figure E-2.   Notional Diagram Illustrating the Periodic Insertion of 128 Pilot Bits Every 3200 Alamouti-Encoded Bits

E.2.   Modulation

The bit sequences described in the previous section are modulated by a pair of SOQPSK-TG modulators (or modulator/transmitters). The modulators should be constructed and used as follows.

- The modulators share a common clock. This common clock is 26/25 times the input clock to accommodate the periodic insertion of 128 pilot bits every 3200 Alamouti-encoded bits.

- The modulators should share a common carrier reference. If this is not possible, the two carrier references should be phase-locked ideally, or frequency-locked at a minimum.

- Randomization, if required, should be applied before the STC encoder.

- Differential encoding should be disabled. The periodically inserted pilot bits are to be used by the demodulator to estimate the magnitudes and phases of the antenna 0-to-receiver channel and the antenna 1-to-receiver channel. There is no need to use differential encoding because data-aided phase estimates do not possess a phase ambiguity.[50]

Figure E-3 is a notional block diagram that shows the relationship between the input data and clock, the bit-level space-time encoder, the periodic pilot bit insertion, and the SOQPSK-TG modulation.

---

[50] M. Rice. *Digital Communications: A Discrete-Time Approach*. Pearson/Prentice-Hall. Upper Saddle River, NJ, 2009.

Figure E-3. Notional Block Diagram of the Space-Time Code Transmitter
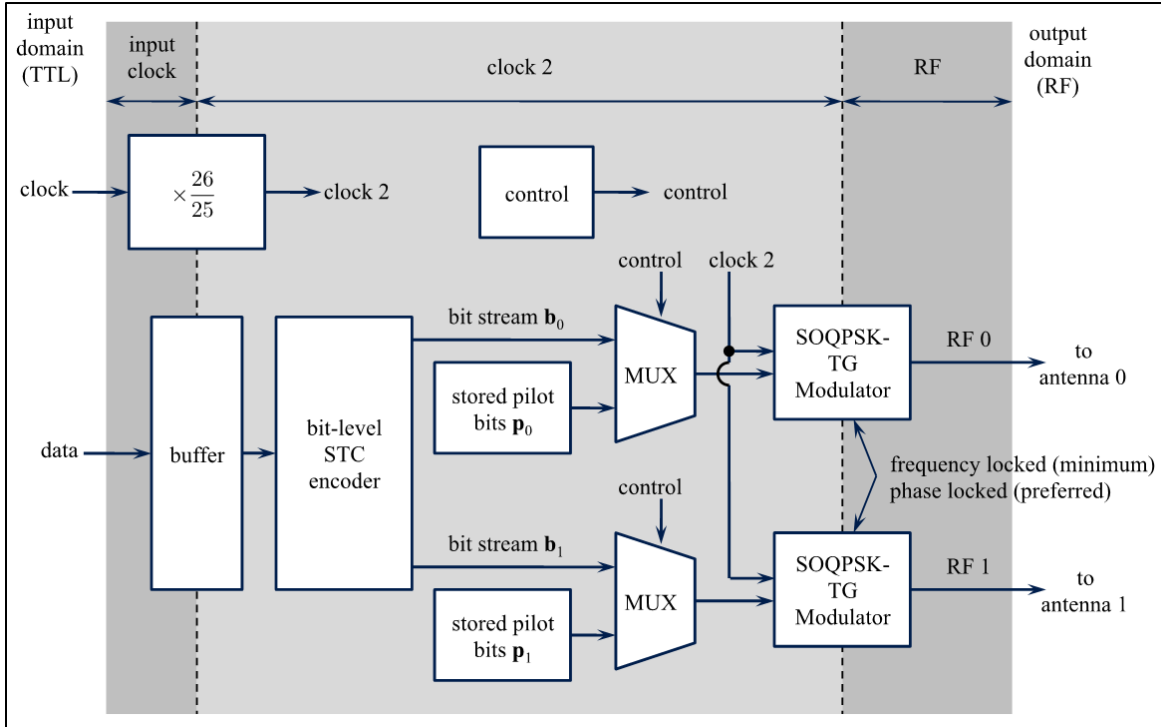
E.3. Performance

The STC process involves the transmission of two separate, but related, orthogonal signals to compensate for the self-interference that accompanies dual-antenna transmission of the same signal. The transmitted signals must each travel through a transmission channel that will affect each signal prior to being presented to the telemetry receiver. If $S_0(t)$ represents the transmitted signal corresponding to $\mathbf{b}_0$ and $S_1(t)$ represents the transmitted signal corresponding to $\mathbf{b}_1$, then the received signal, assuming no frequency offset, may be expressed as

$$r(t) = h_0 S_0(t - \tau_0) + h_1 S_1(t - \tau_1) + n(t)$$

Where:

h_0 is the attenuation of the path between transmitter output $S_0(t)$ and the receive antenna

h_1 is the attenuation of the path between transmitter output $S_1(t)$ and the receive antenna

τ_0 is the delay between the transmitter output $S_0(t)$ and the receive antenna

τ_1 is the delay between the transmitter output $S_1(t)$ and the receive antenna

$n(t)$ is the thermal noise of the receiver

Each of the channel attenuations are complex valued: $h_0 = |h_0|e^{j\theta_0}$ where $|h_0|$ represents the magnitude of the attenuation and θ_0 represents the phase shift associated with the attenuation. Similarly, $h_1 = |h_1|e^{j\theta_1}$. The channel attenuations model the connector and cabling losses between the transmitter output and the transmit antenna, the antenna radiation pattern in the direction of the receive antenna, blockage by the test article (shadowing), atmospheric propagation, and the gain of the receive antenna. In general, h_0 and h_1 are different because the

antennas transmitting $S_0(t)$ and $S_1(t)$ are in different locations. For the same reasons, τ_0 and τ_1, θ_0 and θ_1 are, in general, different. Figure E-4 plots the detection curves for several examples of $|h_0|/|h_1|$, $\tau_0 - \tau_1$, and $\theta_0 - \theta_1$.
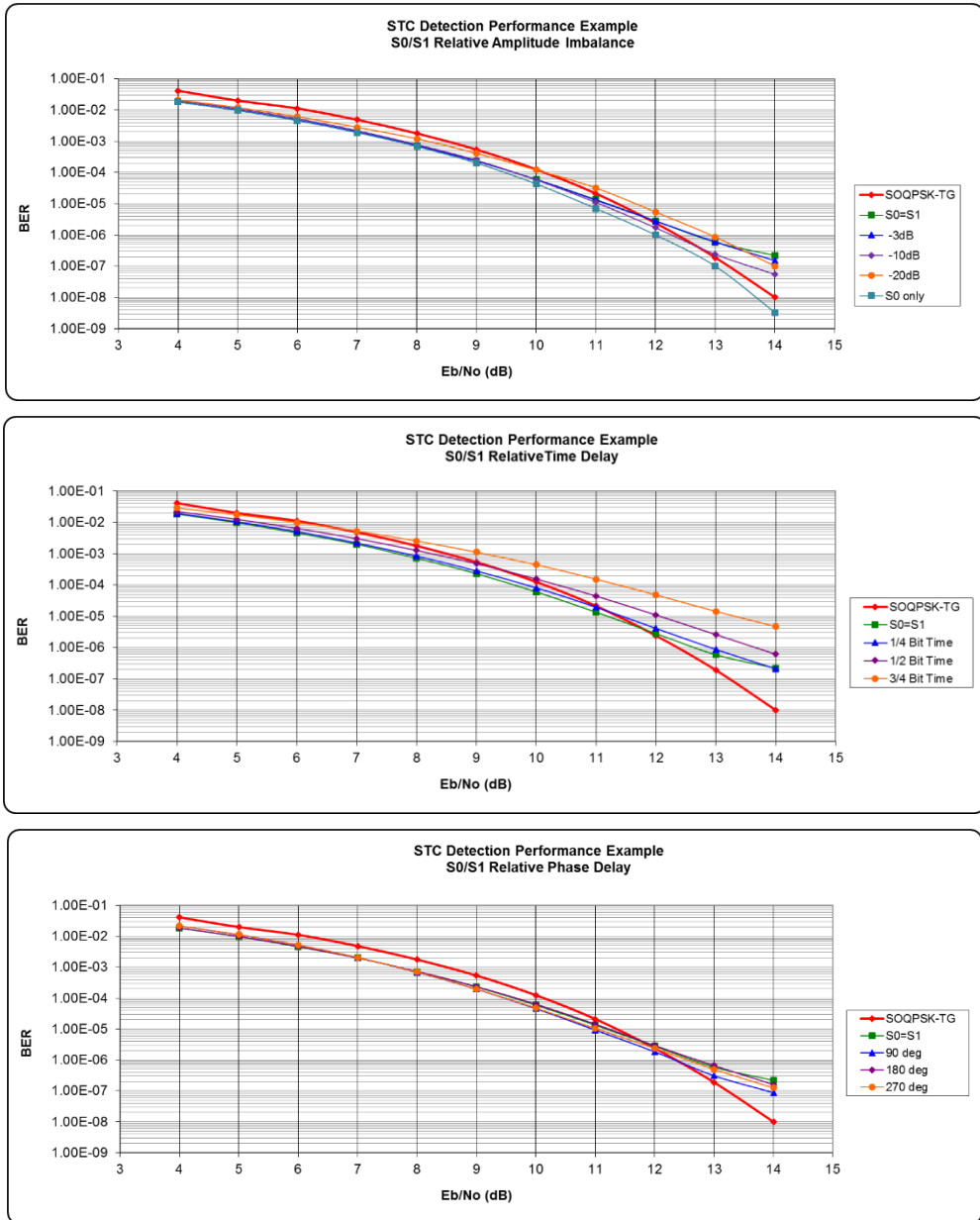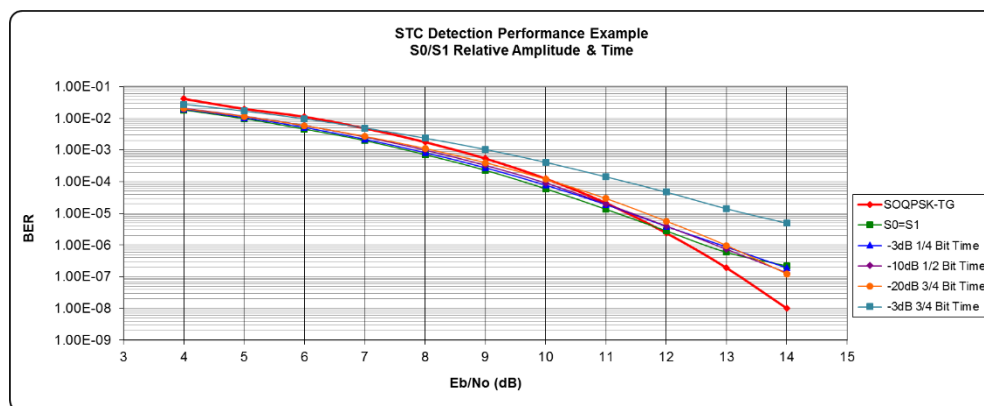
Figure E-4.   Example Detection Curve Performance

E.4.   Resources

Jensen, et al.[51] first described the application of space-time coding to the two-antenna problem. Experimental flights confirmed the effectiveness of the technique.[52,53,54] A detailed mathematical description along with a thorough mathematical analysis were also accomplished for this technique.[55,56]

E.5.   Combining Coding Schemes

The STC and LDPC schemes can be combined if the manufacturer's equipment supports both and the two are applied in the proper order. The transmitter should apply LDPC encoding first, followed by STC encoding. At the receiver, STC decoding is performed first, followed by LDPC decoding.

Note that some manufacturers may limit the LDPC coding rate and/or block size that can be used with STC. Detection performance of this STC-LDPC combination is on par with the curves published in Appendix 2-D.

---

[51] Jensen, M., M. Rice, and A. Anderson. "Aeronautical Telemetry Using Multiple-Antenna Transmitters." *IEEE Transactions on Aerospace and Electronic Systems*, vol. 43, no. 1, pp. 262-272, January 2007.
[52] M. Rice, "Space-Time Coding for Aeronautical Telemetry: Part 1 – System Description," in *Proceedings of the International Telemetering Conference*, Las Vegas, NV, October 2011.
[53] Rice, M. and K. Temple, "Space-Time Coding for Aeronautical Telemetry: part II – Experimental Results," in *Proceedings of the International Telemetering Conference*, Las Vegas, NV, October 2011.
[54] K. Temple. "Performance Evaluation of Space-Time coding on an Airborne Test Platform." Paper presented at the 50th International Telemetering Conference, San Diego, CA, October 2014.
[55] Rice, M., J. Palmer, C. Lavin, and T. Nelson. "Space-Time Coding for Aeronautical Telemetry: Part I – Estimators." *IEEE Transactions on Aerospace and Electronic Systems*, vol. 53, no. 4, pp. 1709-1731, August 2017.
[56] Rice, M., T. Nelson, J. Palmer, C. Lavin, and K. Temple. "Space-Time Coding for Aeronautical Telemetry: Part II – Decoder and System Performance." *IEEE Transactions on Aerospace and Electronic Systems*, vol. 53, no. 4, pp. 1732-1754, August 2017.

APPENDIX 2-F

Use of Recommendation ITU-R M.1459 for Protection of AMT Ground Stations from Terrestrial, Airborne, and Satellite Interference

F.1. Introduction and Summary

Since it was approved for use by the Radiocommunication Sector of the ITU in 2000, Rec M.1459 has been the international and US standard for defining the interference protection criteria and the use of those criteria for AMT ground stations.

Despite its title, Rec M.1459 pertains to interference not only from satellites, but also from terrestrial sources and has been so applied both domestically and internationally. The methodology presented in Annex A of Rec M.1459 for computing band-specific protection levels also makes it applicable to any frequency band. The protection criteria for lower L and upper S bands given in Rec M.1459 have thus been extended to include protection criteria for upper L, lower S, and lower, middle, and upper C bands. The protection criteria are included in Chapter 2.

The protection criteria provided by Rec M.1459 are in the form of PFD levels defined at the aperture of the affected AMT ground station antenna. Thus, when performing interference analysis, it is not necessary to require information about the specific technical parameters of the affected AMT ground station, such as the actual AMT receive antenna gain, pointing direction, noise figure, or system gain over noise temperature. The only details needed are:

- the geographic location of the AMT ground station antenna;
- the height above ground of the AMT ground station antenna;
- the mid-band value of the wavelength for the frequency band under consideration;
- an accurate terrain data base in/around the AMT receive site (1 arc-second, or 30 meter resolution) for use with propagation models when computing interference from terrestrial sources;
- a composite antenna pattern based on the methodology of Rec M.1459, but adjusted for the average wavelength of the band under consideration, to be used when aggregation from a large number of terrestrial sources is being analyzed.

Section F.2 contains several sample computations that illustrate how this information is used in practice. The examples begin with simple cases involving a small number of satellite and terrestrial interference sources. The scenarios presented increase in size and complexity to include networks comprised of thousands of interference sources (e.g., cellular towers). A variety of models, equations, and computational techniques is demonstrated, underscoring the versatility and comprehensive applicability of the Rec M.1459 protection criteria. A final example provides guidance on how to handle special cases, such as when antennas larger than those anticipated in Rec M.1459, are used.

F.2. Practical Application of the Rec M.1459 Protection Criteria

The examples in this section include, but are not limited to, interference from satellites, terrestrial microwave towers, cellular base stations, portable medical telemetry devices, and smartphones. Both adjacent channel and co-channel interference scenarios are included. Each

example is intended to provide and illustrate one or more building blocks that will sometimes, and perhaps often, be used in end-to-end interference analysis.

The discussions and computations here are based on a combination of publicly available data, standard assumptions regarding typical values of common parameters, and emission limits stipulated in FCC regulations. In some of the scenarios, FCC regulations are used as a source of band-specific emission masks that define the worst-case limits, as a function of frequency, that are permitted for OOBE from a particular frequency band or set of bands. Thus, the examples that follow are just that: examples. They are intended to demonstrate computational techniques and analysis. Unless otherwise stated, they should not be interpreted as either assertions or policy statements regarding whether interference does or does not exist in a particular scenario.

Examples 1 - 11 address:

1. Co-channel interference from a planned BSS satellite in geostationary orbit into AMT ground stations operating in the lower L-band between 1435 – 1525 MHz;
2. Co-channel interference from multiple spot-beam communication satellites in geostationary orbit into AMT ground stations operating in a portion of the lower L-band from 1518 – 1525 MHz;
3. Out-of-band interference from a SiriusXM broadcast satellite into an AMT ground station in the upper S-band from 2360 – 2390 MHz;
4. Frequency scaling of interference and interference criteria to different reference bandwidths;
5. Computation of path loss using the two-ray model;
6. Rayleigh fading of the aircraft telemetry signal;
7. Computation of path loss using commercial software that implements the Longley-Rice (L-R)/Irregular Terrain Model (ITM) and P.452 models;
8. Consideration of the antenna patterns of cellular base stations;
9. Aggregation of interference from a network of cellular base stations to one or more AMT ground stations;
10. Considerations for the modeling of interfering systems;
11. Coordination of AMT with 4G Long-Term Evolution (LTE)-A user equipment;
12. Special considerations regarding AMT antennas.

Each of these scenarios was chosen to illustrate a particular point or technique that is independent of Rec M.1459, but which is needed in order for the protection criteria of Rec M.1459 to be properly applied.

At the outset, it should be noted that the curvature of the earth complicates the trigonometry for computing elevation, azimuth, and bearing angles. For example, the elevation angle computed for the path from an AMT ground station to a flight test aircraft 320 km away operating at an altitude of 30,000 feet will be close to zero degrees due to the curvature of the earth.

Using a flat-earth approximation, the angle would be computed to be approximately 4 degrees, thus suggesting incorrectly that interference from terrestrial sources would not be received in the main beam of the AMT ground station.

The equations used in the representative examples below assume a spherical earth, as evidenced by the inclusion of the value for the radius of the earth in km (e.g., 6358 km). The flat-earth approximation is obtained by letting the value of the earth's radius go to infinity.

Use of the correct formulas is particularly important when computing the bearing angle from a cellular tower to an AMT ground station and when coding the table look-up algorithms for choosing appropriate cellular tower sector antenna gain values as functions of pointing angles from the appropriate antenna pattern files.

Example 1.   Co-channel interference from a planned BSS satellite in geostationary orbit into AMT ground stations operating in the lower L-band between 1435 – 1525 MHz

Use of Rec M.1459 begins with a simple equation,

$$pfd_{rec} = P_{xmt}G_{xmt} \times (Path\_Loss) \times \frac{4\pi}{\lambda^2} \qquad \text{F-1}$$

where *PFD* is the received PFD in watts per square meter. The quantity $P_{xmt}G_{xmt}$ is the product of the transmit power of the interfering source and the gain of the transmit antenna. Path loss depends on distance, signal blockage due to terrain blockage and/or clutter (e.g., buildings), and wavelength λ. For free-space propagation, however, path loss is given by:

$$path\ loss = \frac{\lambda^2}{(4\pi)^2 r^2} \qquad \text{F-2}$$

Free-space propagation is appropriate for modeling signals from satellites, such as from a geostationary satellite to an AMT ground station antenna. This yields the simple result that:

$$pfd_{rec} = \frac{P_{xmt}G_{xmt}}{4\pi r^2} \qquad \text{F-3}$$

For the sake of completeness, the received power, as measured at the terminals of the receive antenna, requires inclusion of the effective area of the receive antenna. This will be discussed in detail in example 7. It is sufficient to quote the result here:

$$P_{rec} = pfd_{rec} \times A_{eff} = \frac{P_{xmt}G_{xmt}\lambda^2 G_{rec}}{(4\pi)^2 r^2} \qquad \text{F-4}$$

This is the Friis equation, where A_{eff} is the effective area of the receive antenna. For a parabolic dish, A_{eff} is often approximated by $0.5 \times \pi(D/2)^2$, where D is the diameter of the dish. The value for the wavelength of the signal λ is typically the mid-band value where $\lambda = c/f$.

The distance r and elevation angle α from an AMT ground station antenna to a geostationary satellite are determined using either standard textbook equations (included in Example 2), web-based calculators, or from FCC filings, which can be particularly useful because they also include information about the channel bandwidths, signal power, and transmit antenna gain.

The elevation angle α, which does not appear in equations <u>F-1</u> – <u>F-3</u>, is needed in order to determine the appropriate protection criterion from Rec M.1459. For example, the lower L-band protection criteria from <u>Table 2-7</u> present these criteria as functions of α.

To apply this to a particular case, a comparison of the PFD contours at ground level of a BSS satellite is compared with the angle-of-arrival dependent protection criteria of Rec M.1459. The contours were made available by the developers of the satellite. The comparison shows conclusively that the planned deployment of the satellite would cause harmful interference to AMT ground stations in the United States (e.g., −150 decibels relative to one watt [dBw]/m^2 in 4 kHz, versus the allowed limit of −180 dBW/m^2 in 4 kHz). As a consequence of this analysis, the satellite was not deployed.

Specifically, the co-channel emissions were so large with respect to the Rec M.1459 protection criteria that it wasn't necessary to perform a detailed, angle-of-arrival-dependent computation of the interference from the satellite.

Example 2.   Co-channel interference from multiple spot-beam communication satellites in geostationary orbit into AMT ground stations operating in a portion of the lower L-band from 1518 – 1525 MHz

The 2003 World Radiocommunication Conference coincided with the launch of a new generation of Mobile Satellite Service geostationary communication satellites. These satellites, including Inmarsat IV and Thuraya, introduced the use of complex phased-array beam-forming networks with large parabolic reflectors. The resulting spot beams permit the following: the use of portable handsets with omnidirectional antennas for making telephone calls via satellite; and the simultaneous generation of dozens, and even hundreds, of simultaneous beams. Each beam serves a separate user.

In seeking additional spectrum to support the use of these satellites, the mobile satellite community proposed the allocation of the AMT spectrum from 1518 – 1525 MHz for co-channel sharing with the Mobile Satellite Service. As with the BSS satellite in example 1, application of Rec M.1459 demonstrated that co-channel sharing was not feasible.

In recognition of this, WRC-2003 modified Table 21-4 of Article 21 of the International Radio Regulations[57] to include the following PFD fence that protects AMT operations in the continental United States. In other words, the Conference incorporated the protection criteria of Rec M.1459 in the international radio regulations. Figure F-1 is an excerpt of Article 21.16 of these regulations.

---

[57] International Telecommunications Union. "Radio Regulations: Articles." 2012. May be superseded by update. Retrieved 17 May 2021. Available at http://search.itu.int/history/HistoryDigitalCollectionDocLibrary/1.41.48.en.101.pdf.

21.16 § 6 1) The power flux-density at the Earth's surface produced by emissions from a space station, including emissions from a reflecting satellite, for all conditions and for all methods of modulation, shall not exceed the limit given in Table **21-4**. The limit relates to the power flux-density which would be obtained under assumed free-space propagation conditions and applies to emissions by a space station of the service indicated where the frequency bands are shared with equal rights with the fixed or mobile service, unless otherwise stated.

TABLE **21-4** (Rev.WRC-12)

Frequency band	Service*	Limit in dB(W/m²) for angles of arrival (δ) above the horizontal plane				Reference bandwidth
		0°-5°	**5°-25°**		**25°-90°**	
1 670-1 700 MHz	Earth exploration-satellite Meteorological-satellite	−133 (value based on sharing with meteorological aids service)				1.5 MHz
1 518-1 525 MHz (Applicable to the territory of the United States in Region 2 between the longitudes 71° W and 125° W)	Mobile-satellite (space-to-Earth)	**0° ≤ δ ≤ 4°**	**4° < δ ≤ 20°**	**20° < δ ≤ 60°**	**60° < δ ≤ 90°**	4 kHz
		−181.0	−193.0 + 20 log δ	−213.3 + 35.6 log δ	−150.0	

Figure F-1.   Excerpt from Article 21 of the International Radio Regulations

Example 3.   Out-of-band interference from a SiriusXM broadcast satellite into an AMT ground station in the upper S-band from 2360 – 2390 MHz

This next example provides a computation of OOBE into an AMT ground station from an operational geostationary satellite. This example serves to show an end-to-end computation of the out-of-band signal received at an AMT ground station antenna at Patuxent River (Pax River), Maryland from the SiriusXM satellite denoted as FM-6. This is a Satellite Digital Audio Radio Service (SDARS) broadcast satellite in geostationary orbit above the equator at 115.2 degrees west longitude.[58] FM-6 broadcasts in a 4.1-MHz portion of the 2320.0 – 2332.5 MHz band.

Note that the SDARS band (2320-2345 MHz) is separated from the 2360 – 2390 MHz AMT band by the 2345 – 2360 MHz WCS band (which is the topic of example 6, below).

Given that the SDARS channel is more than 15 MHz away from the edge of the AMT band at 2360 MHz, co-channel sharing is not relevant; however, the OOBE of the FM-6 satellite remain a concern, due to the high gain (30 – 40 decibels isotropic [dBi] and more) of a typical AMT ground station antenna.

The FCC restricts the OOBE of FM-6, relative to its mean transmitter power level P_{xmt} (and not including the effects of the satellite's antenna gain G_{xmt}) in the FCC Rules, part §25.202(f) (1), (2), and (3).[59] These are available online, but are restated here:

---

[58] The satellite is actually in operation at 116.1° W, but the computations here are performed for its originally intended geostationary orbital slot.

[59] Code of Federal Regulations, Frequencies, frequency tolerance, and emission limits, title 47, sec. 25.202.

The mean power of emissions shall be attenuated below the mean output power of the transmitter in accordance with the following schedule:

(1)   In any 4 kHz band, the center frequency of which is removed from the assigned frequency by more than 50 percent up to and including 100 percent of the authorized bandwidth: 25 dB;

(2)   In any 4 kHz band, the center frequency of which is removed from the assigned frequency by more than 100 percent up to and including 250 percent of the authorized bandwidth: 35 dB;

(3)   In any 4 kHz band, the center frequency of which is removed from the assigned frequency by more than 250 percent of the authorized bandwidth: An amount equal to 43 dB plus 10 times the logarithm (to the base 10) of the transmitter power in watts.

Since the authorized bandwidth of FM-6 is 4.1 MHz and the AMT band is removed from this frequency by more than 250%, the *43 + 10 log (P)* rule applies, where P is the out-of-band transmitter PSD in watts per 4 kHz of bandwidth. Specifically, the value *43 + 10 log(P)* is the amount the OOBE must be attenuated with respect to the transmitter power P per 4 kHz of bandwidth. With the rule written in this manner, if the transmitter power P is increased, the amount by which the OOBE must be attenuated increases by the same amount.

(This is a well-recognized OOBE standard, but it is essential to note that the reference bandwidth for the example here is stipulated to be 4 kHz, whereas a reference value of 1 MHz may be more common in FCC rules).

The purpose of the *log(P)* term is to set a hard OOBE power limit that is independent of the mean in-band transmitter power P. For the purpose of computing interference into AMT operations in 2360 – 2390 MHz using equations F-1 – F-3, the interference from FM-6 can be characterized simply by setting the transmitter power P to 0 dBW. Then, the magnitude of the interfering level P_{xmt} is *−43 dBW*, which is equal to −13 dBm, or 50 µW per 4 kHz. This corresponds to an attenuation of the in-band power by 43 dB. Note that if the in-band power is set to 10 dBW, the *43 + 10 log(P)* rule requires 53 dB of out-of-band attenuation, and the value of P_{xmt} is unchanged.

With respect to equations F-1 – F-3, to compute the interference from FM-6 into any AMT ground station, it is also necessary to know the following.

- The satellite's transmit antenna gain G_{xmt} in the direction of the affected AMT site (in order to convert the *43 + 10 log(P)* value into a radiated power level). This satellite-specific information is usually derived from information provided by the satellite operator or from FCC and/or ITU technical filings. For this example, the information is obtained from an FCC filing, as shown later in this section.
- The angle of arrival of the signal at the AMT site (in order to determine the appropriate value of the protection criteria). This can be obtained from a graph in the same FCC filing or can be computed from equations F-5a and F-5b.
- The distance from the satellite to the ground station (in order to compute the free space path loss). This is computed from Equation F-6.

Note that these equations, as written, apply only to geostationary satellites.[60]

$$\alpha_s = arcsin[cos(\theta_e)cos(\phi_{se})] \qquad \text{F-5a}$$

$$\alpha = arctan\left\{\frac{sin(\alpha_s) - \left. R_{earth}\right/ R_{satellite}}{cos(\alpha_s)}\right\} \qquad \text{F-5b} \qquad \text{F-5}$$

$$r = \sqrt{R_{satellite}{}^2 - R_{earth}{}^2 cos^2(\alpha)} - R_{earth}sin(\alpha) \qquad \text{F-5c}$$

where α is the elevation angle to the satellite (which is the same as the angle of arrival α of the interference from the satellite), θ_e is the latitude of the AMT ground station, ϕ_{se} is the difference in the longitude values of the earth station and the satellite, and r is the distance from the AMT ground station to the satellite. Note that for geostationary satellites, the orbital radius $R_{satellite}$ is the radius of the earth, 6358 km, added to the height of the satellite above the surface of the earth, 36,000 km. For an angle of arrival of α = 90°, Equation F-5 yields the value of $r = (R_{satellite} - R_{earth})$.

The geometry described by these equations in shown in Figure F-2, excerpted from the text by Richharia.[61] The angle η in the figure corresponds to the angle α in equations F-5 and F-6. The elevation cut is a two-dimensional surface for which the trigonometry of the earth's curvature can be solved by inspection. For the sake of completeness, the geometry used for computing the azimuth angle is also shown. Although computation of the azimuth angle is not required here, it is needed for, and discussed in, example 8.

---

[60] This is because the declination of the satellite is set to 0°, which causes several of the terms from a more general set of equations to disappear.

[61] M. Richharia. *Satellite Communications Systems, Second Edition*, New York; London: McGraw-Hill, 1999, page 37.
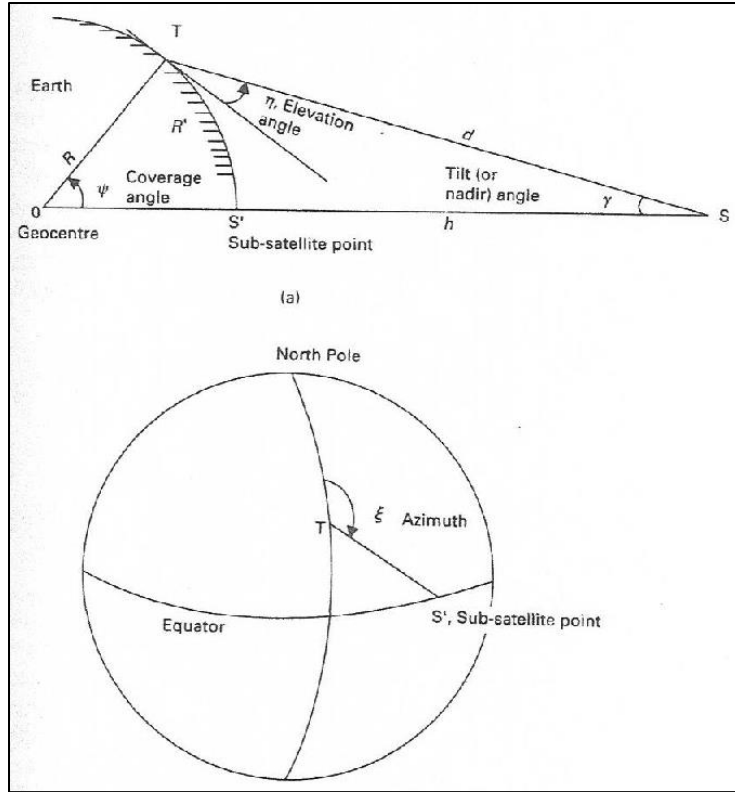
Figure F-2. Geometry of a Geostationary Link Showing (a) Elevation, (b) Azimuth from a Point T on the Earth

For Pax River, the latitude/longitude is approximately 38°N/76°W. Assuming an earth radius of 6358 km, a satellite orbital radius of 6358 km + 36,000 km, a satellite sub-orbital longitude (also known as Right Ascension) of 115.2°W, an OOBE of −43 dBW/4kHz, and the maximum value of the FM-6 antenna gain of 34.7 dBi (from Figure F-3) yields:

$$\alpha_s = arcsin[cos(38°)cos(115.2° − 76°)] = 37.64° \hspace{2em} \text{F-6a}$$

$$\alpha = arctan\left\{ \frac{sin(\alpha_s) − 6358km/42358km}{cos(\alpha_s)} \right\} \hspace{2em} \text{F-6b} \hspace{2em} \text{F-6}$$

$$r = \sqrt{42358^2 km^2 − 6358^2 \ km^2 cos^2(30.18°)} − 6358 \ km \ sin(30.18°) = 38804 \ km \hspace{2em} \text{F-6c}$$

Contours shown in Figure F-3 are −2, −4, −6, −8, −10, −15, and −20 dB relative to the beam peak of 34.7 dBi.

Figure F-3.   Digital Audio Radio Service Downlink Beam Gain Contours

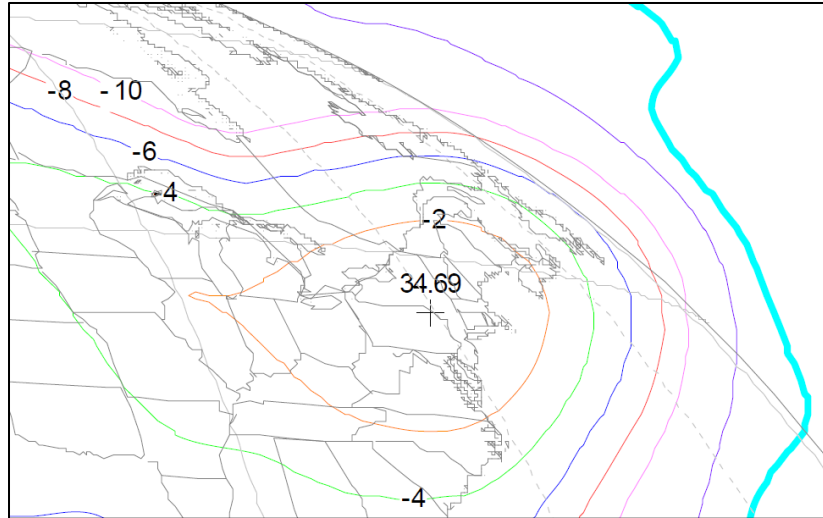Thus, the elevation angle $\alpha = 30.2°$ and the distance r from the ground station to the satellite is 38,804 km. Using the Friis equation, we have a received PFD at the ground station PFD_{rec} of

$$\frac{P_T G_T}{4\pi r^2} = \frac{10^{-4.3} \times 10^{3.47}}{4\pi(38804 \times 10^3)^2} = -171 \ {dBW}/{m^2} \text{ in 4 kHz} \qquad \text{F-7}$$

The upper S-band protection criteria provide three PFD protection values as a function of α, as shown in Table 2-7.

Thus, the relevant Rec M.1459 protection criterion for this example is the value for an interference angle of arrival $>11.5°$, which is -162 dBW/m^2 in 4 kHz.

Since the OOBE fall below the maximum level stipulated by Rec M.1459 for this angle of arrival, there is no out-of-band interference from FM-6 to the AMT site at Pax River. Note that the derivation of this result required no information about the size, tower height, or pointing direction of the AMT antenna.

Repeating the computation for other ground stations is straightforward; however, since no analytic expression for the antenna gain of the satellite is available, the appropriate value of the gain of the satellite's downlink antenna must be obtained from Figure F-3. Figure F-4, which shows the angle of arrival of the signal from the satellite, provides a convenient check of the computation of α from equations F-5a and F-5b.
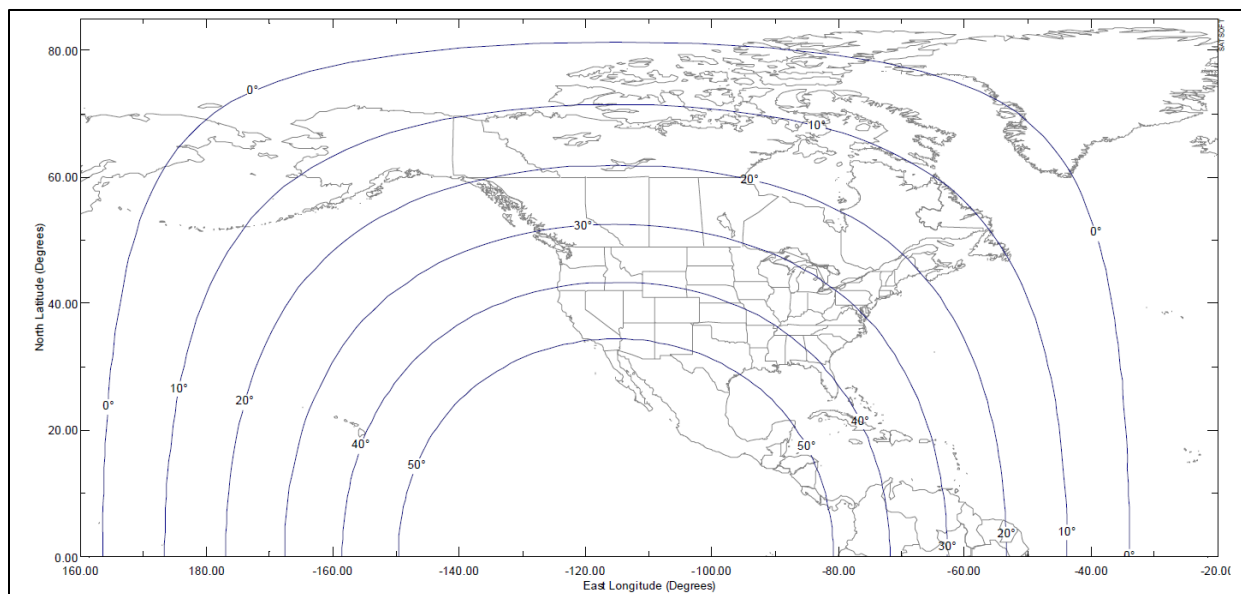
Figure F-4.   Elevation Angles from Surface of the Earth to the 115.2° West Longitude Orbital Location

Example 4.   Frequency scaling of interference and interference criteria to different reference bandwidths

As mentioned above, the reference bandwidth of 4 kHz for the PFD protection levels in Rec M.1459 is easily scaled to other values. This is done assuming that the required protection level is independent, of which 4 kHz of a typically 1 – 5 MHz AMT channel is affected.

This example must also take into account the reference bandwidths. For example, the permitted interference into a 1-MHz AMT channel is $10^6/4000$ times the appropriate dB(W/m^2) in 4 kHz protection level from the list above; however, the spectral density of the interference into, for example, a 5-MHz AMT channel at 1520 – 1525 MHz, may vary across the 5 MHz in question. In addition, the reference bandwidth specified for the protection criterion for a given frequency band may be as large as 27 MHz, which is the case for the EESS band from 1400 – 1427 MHz; however, the interference <u>into</u> the AMT band may be a function of frequency. This is the case for interference from the WCS service in 2345 – 2360 MHz (i.e., the band that separates SiriusXM from the AMT frequencies in the upper S-band from 2360 – 2395 MHz).

In Section 27.53 of its rules (cf. footnote 392 of the FCC's Order on Reconsideration)[62], the FCC stipulates that interference into the AMT band at 2360 – 2390 MHz from the WCS band at 2345 – 2360 MHz is to decrease as a function of frequency according to the following emission mask:

Specifically, WCS base and fixed stations' OOBE must be attenuated by a factor of not less than 43 + 10 log (P) dB in the 2360-2362.5 MHz band, 55 + 10 log (P) dB at 2362.5-2365 MHz band, 70 + 10 log (P) dB at 2365-2367.5 MHz band, 72

---

[62] Federal Communications Commission. "Amendment of Part 27 of the Commission's Rules to Govern the Operations of Wireless Communications Services in the 2.3 GHz Band." WT Docket No. 07-293. In *Order on Reconsideration*. FCC 12-130. 17 October 2012. Retrieved 17 May 2021. Available at https://apps.fcc.gov/edocs_public/attachmatch/FCC-12-130A1.pdf.

+ 10 log (P) dB at 2367.5-2370 MHz band, and 75 + 10 log (P) dB above 2370 MHz. WCS mobile and portable devices' OOBE must be attenuated by a factor of not less than 43 + 10 log (P) dB at 2360-2365 MHz, and 70 + 10 log (P) dB above 2365 MHz. *See 2010 WCS R&O*, 25 FCC Rcd at 11766 para. 135, 11785 para. 182; 47 C.F.R. §§ 27.53(a)(1)(iii) and (4)(iii).

[Figure F-5](#) shows the FCC-specified emissions profile in graphical form. The vertical axis represents *xx + 10 log(P)* in dB.
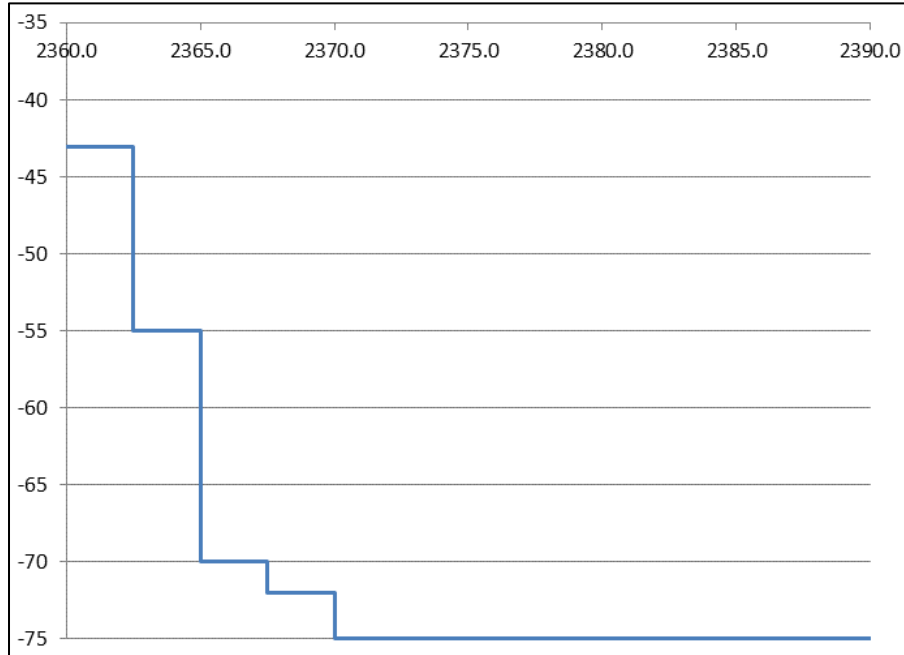
Figure F-5.   FCC Emission Mask for the WCS OOBE Band from 2360 – 2390 MHz

The rule above provides the guidance on how to compute the net interference from a WCS transmitter into a 5-MHz AMT band, for example, operating at 2360 – 2365 MHz. The two OOBE levels, −43 dBW and −55 dBW are averaged according to the following equation:

$$OOBE\ in\ Watts\ per\ 4\ kHz\ averaged\ across\ 5\ MHz\ at\ (2360 - 2365\ MHz)$$

$$= G_{WCS\ xmt} \times \frac{4\times10^3}{5\times10^6} \times \left\{ \left(\frac{2.5}{5} \right) \times 10^{-4.3} + \left(\frac{2.5}{5} \right) \times 10^{-5.5} \right\} \qquad \text{F-8}$$

To convert from watts to dBW, the result of Equation [F-8](#) is converted to a base ten logarithm and multiplied by 10, as usual.

Note that G$_{WCSxmt}$ is the gain of the WCS transmit antenna in the direction of the AMT ground station antenna that is being considered. Equation [F-8](#), the 4E3/5E6 term re-normalizes the average OOBE level across the 5-MHz-wide AMT channel width to the 4-kHz reference bandwidth of Rec M.1459.

Equation [F-8](#) is the EIRP of the interfering WCS transmitter as measured at the aperture of the WCS transmit antenna. To compute the interference received at the aperture of the AMT

ground station antenna, it is necessary to include the path loss by using Equation F-1. It is necessary when using Equation F-1 to convert the path loss to dB or the EIRP from dBW to watts when using Equation F-1. For comparison with the protection levels of Rec M.1459, the result of Equation F-1 should be converted to dBW/m^2 in 4 kHz.

It is important to note that the OOBE levels given above represent a "stair-step pattern", where the OOBE in each segment of spectrum (in this case, each 2.5-MHz segment) is constant. Actual OOBE measurements, which are typically used for computations when available, decrease from one end of the band segment to the other. In order to average the OOBE properly in these conditions, the 2.5-MHz segments are broken up into, for example, 0.1 to 1.0-MHz segments. These are then averaged using the methodology of Equation F-8, but with more terms inside the curly brackets. To determine whether the segments are narrow enough, it is sufficient to keep dividing the segments by a factor of 2 and then re-computing the OOBE using Equation F-8. This is repeated until the end result is constant within the desired resolution of the computation (e.g., 0.1 dB).

Figure F-6 illustrates the difference between the stair-step emissions masks published by the FCC and by an industry group, in this case the Third Generation Partnership Project, or 3GPP consortium. Figure F-6 also shows the simulated in-band and OOBE of a 4G LTE-A handset uplink as a function of the number of resource blocks assigned to a particular signal.
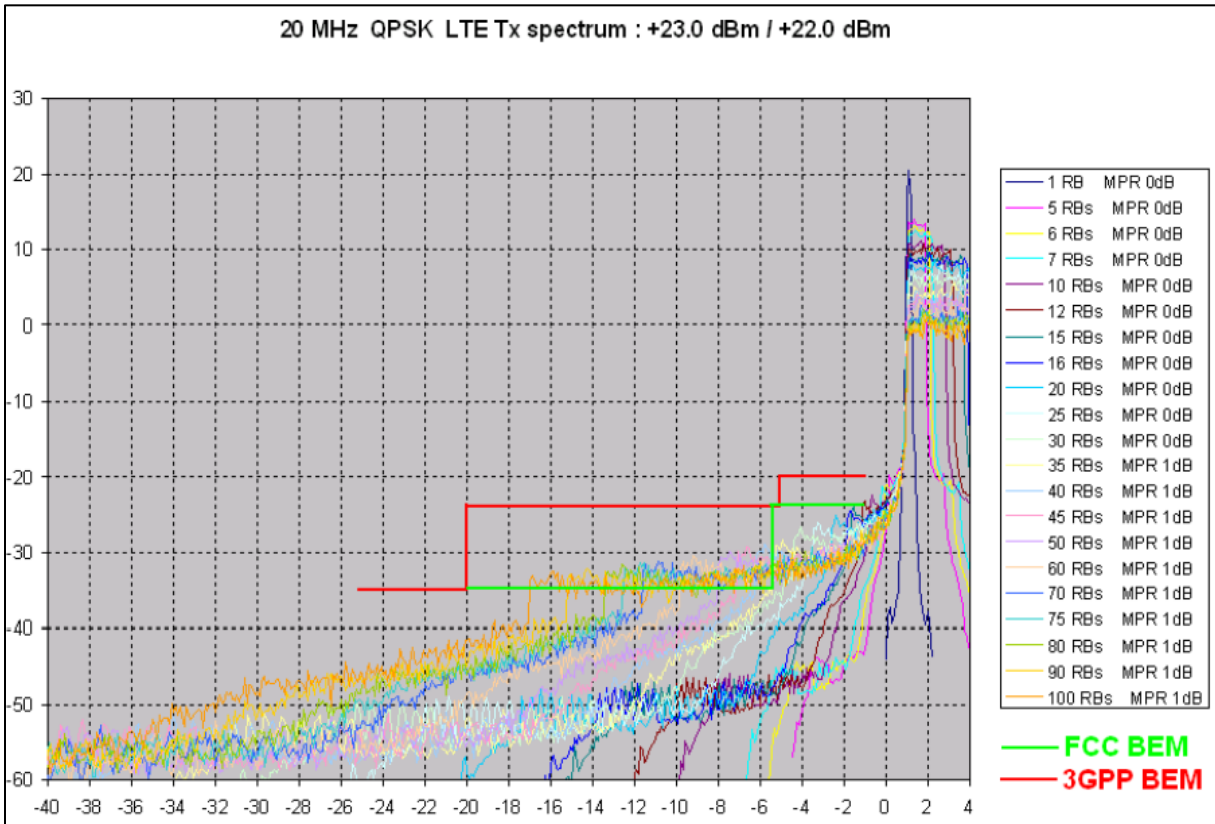

Figure F-6.   Simulated OOBE Emissions from an LTE Handset[63]

---

[63] Wireless Communications Association. "4G Device Out of Band Emissions and Larger Channel Bandwidths," October 2011. Retrieved 17 May 2021. Available at https://ecfsapi.fcc.gov/file/7021715550.pdf.

It is useful to work the problem of OOBE from aircraft AMT transmitters into the EESS spectrum from 1400 – 1427 MHz. Resolution 750[64] stipulates that the net radiated OOBE from an AMT transmitter operating in the band 1429 – 1452 MHz (not including the gain of its antenna), when averaged over the entire 27-MHz EESS band,[65] should not exceed a power level of −28 dBW.

Chapter 2 stipulates that the OOBE in any 1 MHz from an AMT transmitter be attenuated by an amount of at least 55 + 10 log(P) dBW. When scaled to a bandwidth of 27 MHz, an additional 10 log(27 MHz/1 MHz) = 14.3 dB must be added to the −55 dBW OOBE level. This yields an OOBE of −41 dBW per 27 MHz, which is well below the requirement of Resolution 750.

The point here is that when scaling from one reference bandwidth to another, at least some insight into the context of the problem is needed. Simply applying the same rule, by rote, from one scenario to another can lead to errors.

Example 5:   Computation of path loss using the two-ray model

For computing interference to an AMT ground station from terrestrial sources, it is necessary to include the effects of terrain, the curvature of the earth, ground reflections, Fresnel zone impingement, etc. All of these effects can be lumped into the value of path loss that is defined by Equation F-2.

With the exception of what is known as the two-ray model, consideration of these effects in a path loss computation requires, in addition to antenna height information and the distance between the interferer and victim receiver, an accurate terrain database (i.e., a topographical map of the path between the interference source and the AMT site). Other effects, such as additional path loss caused by buildings and other clutter, can be included as long as the details of such loss are justified by measurements and databases whose accuracy and precision go well beyond the 1 arc-second (30 meter) resolution that is typically used for path loss modeling at this time.

The two-ray model treats the ground as a reflector, and takes into account the interference nulls caused by this reflection that occur at various distances and heights from the transmitting aircraft or interference source. Figure F-7 shows this graphically. When a resulting null coincides in position with the aperture of the AMT receive antenna, a significant signal fade (15 – 30 dB) occurs. Depending on the bandwidth of the signal, the fade can cause attenuation across the entire bandwidth of the signal, or can cause just a portion of the signal bandwidth to suffer a reduction in received signal power.

---

[64] International Telecommunications Union. "Compatibility between the Earth exploration-satellite service (passive) and relevant active services." *Final Acts WRC-15 – World Radiocommunication Conference*. Geneva, 2015. pp. 399-403.

[65] The wideband radiometric sensors aboard EESS satellites apparently receive signals across the entire 27 MHz of the band at once, with no effort made to determine where in the band a signal originates.
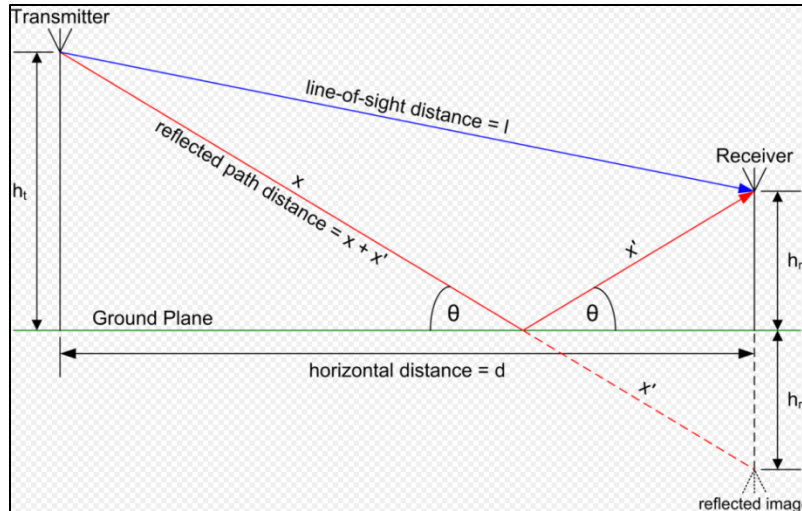
Figure F-7.   Graphical Representation of the Two-Ray Model

Reflection can also cause enhancement of the received signal (or interference); however, for a two-ray, as opposed to three-or-more-ray model, this enhancement cannot exceed 3 dB. As noted, the fades can always be considerably larger than 3 dB in their amplitude. In fact, for aircraft, fades can occur not only from ground reflection of the telemetry signal, but from unwanted reflections of the telemetry signal from aircraft structures or from blockage of the direct signal path from the aircraft antenna to the ground station during aircraft maneuvers.

Since an aircraft in flight is constantly moving, telemetry signal fades are strong functions of time. For modeling purposes, this time dependence is characterized by a change in the availability of the telemetry link. This is a key feature of Rec M.1459, and is the subject of example 6.

For static interferers, such as interference from a cellular tower, fades can be regarded as being constant, and are accounted for in the path loss software.

A graphical representation of path loss versus distance of the two-ray model is shown in Figure F-8.[66] Note that the fades are deep and the signal enhancements are shallow. It is important to understand that the graph is for a particular combination of tower heights and signal wavelength.

---

[66] Thomas Schwengler. "Radio Propagation Modeling." Chapter 3 in *Wireless and Cellular Communications*. Retrieved 17 May 2021. Available at http://morse.colorado.edu/~tlen5510/text/classwebch3.html.
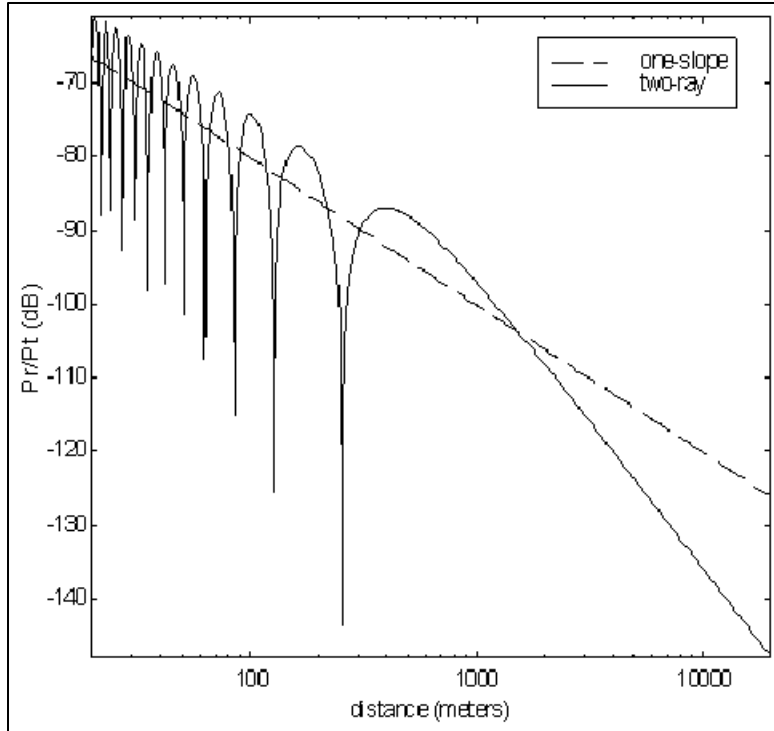
Figure F-8.   Comparison of Free-Space One-Slope and Two-Ray Propagation Models

Fades are most prominent near the transmitter. For example, the two-ray model is evident on airport aprons when a telemetry test cart is used to receive TM signals from an aircraft parked several hundred feet away. More importantly, the long-range reduction in signal strength for the two-ray model falls faster than the $1/r^2$ (i.e., 20 dB per decade of frequency) of the free-space single-ray signal. The $1/r^4$ roll-off of the two-ray model is 40 dB per decade.

The equations for computing the two-ray model can be found online, in text books, or from direct computation. If path loss software is available, it is convenient to compute the two-ray results for a particular situation by setting the terrain height to zero and using the default value of ground electrical conductivity provided by the software.

Although the equations for the two-ray model can be rather daunting, in its simplest form, one uses flat-earth trigonometry to compute the difference in path lengths between the direct and reflected signals. This depends on the horizontal distance d, the altitude of the aircraft h_t, and the height above ground of the AMT receive antenna, h_r. Using trigonometry and assuming that the signal is reflected from the ground and/or sea with a reflection coefficient of magnitude 1, the aircraft altitudes and locations can be computed for which positive and negative signal reinforcement due to multipath occur. When the direct path and the reflected path differ by an even number of signal half-wavelengths $\lambda/2$, signal reinforcement occurs. When they differ by an odd number of half-wavelengths, deep fades occur.

For reflections from a smooth ocean surface, the conductivity of salt water can be used; however, Rec M.1459 anticipates this, and most interference to AMT ground station paths are not over water. Hence, the default value for ground conductivity is typically the correct value to use.

The equation for computing the curve shown in is given by

$$p_0(t) = \sqrt{(G_t G_r)}\frac{\lambda}{4\pi}\left(\frac{\exp(j2\pi l_0/\lambda)}{l_0} + \Gamma\frac{\exp(j2\pi l'_0/\lambda)}{l'_0}\right)$$ F-9

Where l_0 and l'_0 are the line-of-sight (LOS) distances l and $x + x'$ shown in Figure F-7.

With respect to the phrase "direct line of sight", it is convenient to note that this is computed as

$$D_{LOS} = \sqrt{2h_1 R_{earth} \times 4/3} + \sqrt{2h_2 R_{earth} \times 4/3}$$ F-10

where h_1 and h_2 are the heights of the transmit and receive antennas, R_{earth} is the nominal radius of the earth of 6358 km, and the factor of 4/3 accounts for atmospheric refraction.

Example 6.   Rayleigh fading of the aircraft telemetry signal

There is a generalization of the two-ray model that adds the effects of reflections of the telemetry signal from aircraft structures and/or blockage of the telemetry signal by these same structures during aircraft maneuvers. This is Rayleigh scattering that plays an important role in the technical details of Rec M.1459. The resulting Rayleigh distribution can be used to predict the percentage of time that the link margin of any air-to-ground telemetry link will fall below the threshold value needed for the link to be viable. This is illustrated by Figure F-9, Figure F-10, and Figure F-11.
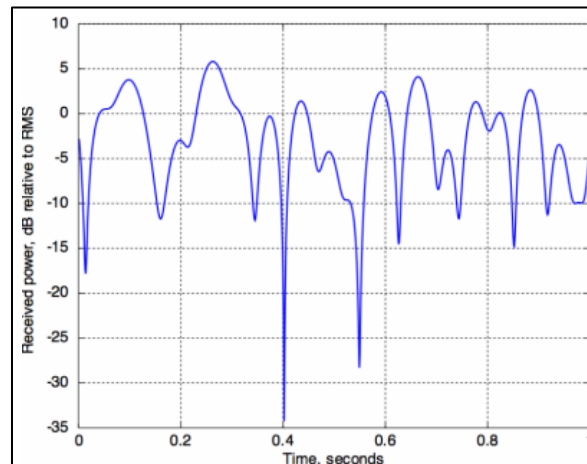
Figure F-9.   Rayleigh Fading of a Signal Transmitted from a Moving Platform[67]

[67] Wikipedia. "Rayleigh fading." Retrieved 17 May 2021. Available at
https://en.wikipedia.org/wiki/Rayleigh_fading

Figure F-10.   S-band Telemetry Signal Received from an Aircraft in Flight[68]

[68] D.G. Jablonski. "Demonstration of Closed Loop Steering of Antenna Patterns for Mitigating Antenna-to-Antenna Interference in Two-Antenna Telemetry Installations on Military Aircraft," Instrumentation Test Technical Symposium, New Orleans, LA, 25 August 2004.
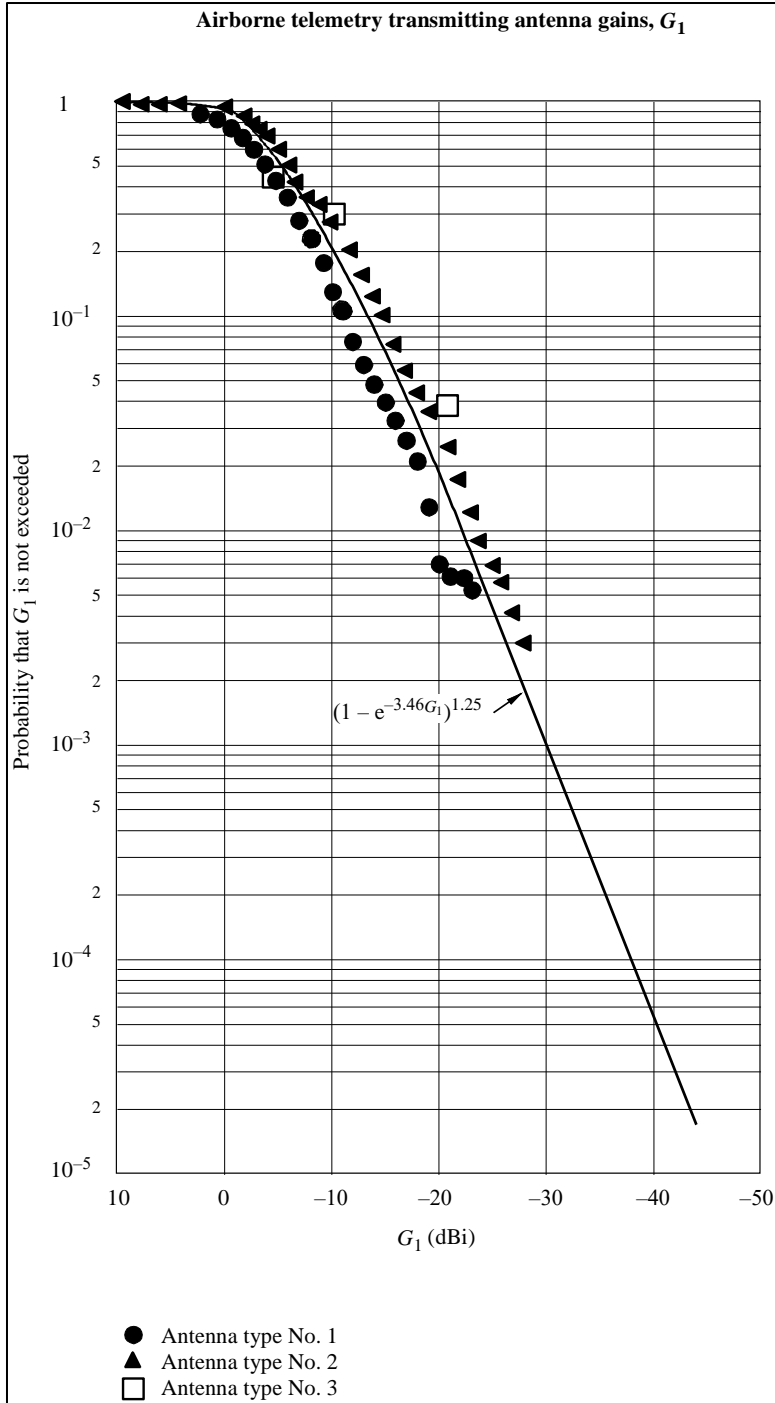
Figure F-11.   Rayleigh Distribution as Presented in Figure 2 of Rec M.1459 (Jablonski 2004)

Figure F-9 is a one-second time slice of the strength of a Rayleigh-faded signal as received from a moving transmitter. Figure F-10 is the measured signal strength of a Rayleigh-faded aircraft telemetry signal as a function of time as received at an AMT ground station.

Figure F-11 relates the depth of a fade to a numerical value of the probability as a percentage of time that such a fade will occur. The mathematical expression given in the figure is

an essential component of the computations of the Rec M.1459 protection criteria. Specifically, the Rayleigh distribution provides the connection between interference and link availability. This is an extension of less-sophisticated link budgets that consider only the effect of interference on BER, without considering whether the interference will cause the link to fail completely.

Note that the Rayleigh distribution presented above is typically used in AMT link budget computations by including the fade in the instantaneous value of the gain G_{xmt} of the aircraft telemetry transmit antenna, as opposed to including it as a component of the path loss. This keeps the consideration of fading due to aircraft geometry and motion independent of the consideration of terrain effects (described below), for which Rayleigh scattering is typically not relevant.

Rec M.1459 requires a threshold signal-to-noise value of $(C/N)_T$ of 15 dB. For the AMT system values specified in Rec M.1459, the AMT channel bandwidth is 3 MHz and the system noise temperature is 250 Kelvin. The required AMT telemetry signal receive power is

$$C = kTB \times 10^{1.5} = 1.38 \times \frac{10^{-23} Joule}{Kelvin} \times 250 \, Kelvin \times (3 \times 10^6 \, Hz) =$$
$$3.27 \times 10^{-13} \, Watts = -124.85 \, dBW. \tag{F-11a}$$

The corresponding expression for the Friis equation for an aircraft antenna transmit gain of -25 dB and including the effective area of $\lambda^2 G_{rec}/4\pi$ of the AMT ground station receive antenna with $P_T = 3W$, $G_{rec} = 41.2$ dB, $r = 320$ km, and $\lambda = 0.2$ meter (per Rec M.1459) is

$$\frac{P_T G_T \lambda^2 G_{rec}}{(4\pi r)^2} = \frac{3 \times 10^{-2.5} \times (.2)^2 \times 10^{4.12}}{(4\pi)^2 \times (320 \times 10^3)^2} = 3.09 \times 10^{-13} \, Watts = -125.10 \, dBW \tag{F-11b}$$

Example 7:   Computation of path loss using commercial software that implements the L-R/ITM and P.452 models

Since the two-ray model is seldom adequate for predicting path loss over terrain, a wide assortment of models that include the effects of terrain has been developed. These are based on different combinations of assumptions regarding reflection, refraction, diffraction, signal blockage, Fresnel zone impingement, etc., and are available with terrain databases already included. These include several, such as Terrain-Integrated Rough-Earth Model, L-R, ITM, and Free-space plus reflection and multiple diffraction.

Another category of models is contained in ITU-R recommendations that are similar in structure to Rec M.1459. Three of the most important models are:

- P.452-16: Prediction procedure for the evaluation of interference between stations on the surface of the Earth at frequencies above about 0.1 GHz;[69]
- P.1546: Method for point-to-area predictions for terrestrial services in the frequency range 30 MHz to 4000 MHz;[70]

---

[69] International Telecommunication Union. "Prediction procedure for the evaluation of interference between stations on the surface of the Earth at frequencies above about 0.1 GHz." ITU-R Recommendation P.452-16. July 2015. May be superseded by update. Retrieved 17 May 2021. Available at https://www.itu.int/rec/R-REC-P.452/en.

[70] International Telecommunication Union. "Method for point-to-area predictions for terrestrial services in the frequency range 30 MHz to 3 000 MHz." ITU-R Recommendation P.1546-6. August 2019. May be superseded by update. Retrieved 17 May 2021. Available at https://www.itu.int/rec/R-REC-P.1546/en.

- • P.528: Propagation curves for aeronautical mobile and radionavigation services using the VHF, UHF, and SHF bands.[71]

As this example only makes use of the L-R/ITM and P.452 models, information regarding the other two models is excluded from this document. The P.452 model can be regarded as the internationally approved version of the ITM, which is an outgrowth of the L-R model. The ITM and L-R models were developed for domestic purposes by the United States at the National Institute of Standards and Technology. Because of the need for technical studies presented to the ITU to utilize ITU-sanctioned models, P.452 has become the de facto standard for domestic studies that require path loss computations based on actual terrain.

In order to use P.452, it is necessary to purchase a commercial software package such as EDX Signal Pro (favored by the AMT community at the present time), ATOLL (used by cellular carriers), or Visualyse (used by those who need to consider platform motion and the time-dependent effects of this on interference). Such commercial packages typically include most, and sometimes all, of the models listed here.

There is also a non-commercial version of P.452, in the form of macro-enabled Excel spreadsheets, that is available free of charge from the ITU at www.itu.int. It models the effects of terrain using data imported from, readily available terrain databases.

For AMT, the fundamental terrain database is usually the government-provided, freely available USGS 1 arc-second (30 meter) resolution topographic map data. The Shuttle Radar Topography Mission database is sometimes used, although it is comprised of overhead measurements, and its validity for computing point-to-point path loss is sometimes questioned.

It is important to consider how accurate these propagation models are. A comparison study[72] suggests that error bars of 15 dB in the path loss computation are typical. Perhaps a better approach is to use existing measurement data from NTIA,[73] which exist in the form of five separate studies that are available from the Defense Technical Information Center. It is straightforward to insert the location, frequency, and antenna height details provided in the studies into any of the commercial models for comparison purposes.

Figure F-12 and Figure F-13 illustrate how data obtained using a commercial package, in this case EDX Signal Pro, are presented for a series of point-to-point links between cellular towers and an AMT receive site at Pax River. The purpose of the simulation is to compute path loss values from each of the cellular sites to the AMT ground station. The assumption that Pax River is the transmitter site is a feature of the software package's point-to-multipoint analysis routine. Since the purpose of the analysis is to compute a value for the path loss for each link, including the effects of terrain, reversing the roles of transmitter and receiver is of no numerical consequence.

---

[71] International Telecommunication Union. "Propagation curves for aeronautical mobile and radionavigation services using the VHF, UHF, and SHF bands." ITU-R Recommendation P.528-4. August 2019. May be superseded by update. Retrieved 17 May 2021. Available at https://www.itu.int/rec/R-REC-P.528/en.

[72] Phillips, C., D. Sicker, and D. Grunwald. "Bounding the Practical Error of Path Loss Models." International Journal of Antennas and Propagation, Volume 2012 (2012). Retrieved 17 May 2021. Available at https://www.hindawi.com/journals/ijap/2012/754158/.

[73] For example, Hufford, G. A. and F. K. Steele. "Tabulations of Propagation Data over Irregular Terrain in the 75-To 8400-Mhz Frequency Range - Part V: Virginia." NTIA Publication 91-282, December 1991. Retrieved 17 May 2021. Available at https://www.its.bldrdoc.gov/publications/download/91-282.pdf.
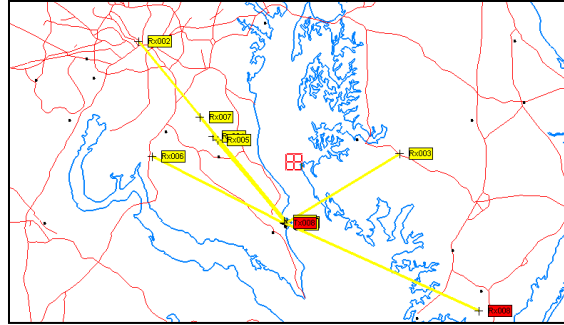
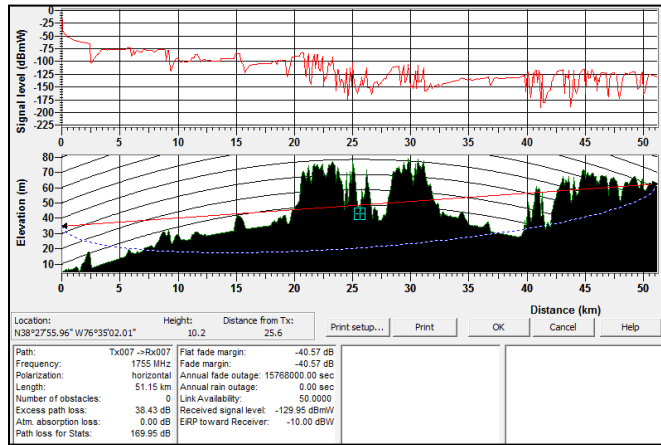Figure F-12.   EDX Signal Pro Map of Hypothetical Transmitters and Receivers in the Pax River Region

Figure F-13.   EDX Signal Pro Path Loss Profile for the TX007 to RX007 Path

The simulation results of Figure F-12 and Figure F-13 are followed in Figure F-14 by experimental data measured by NTIA engineers and reported in Hufford and Steele.
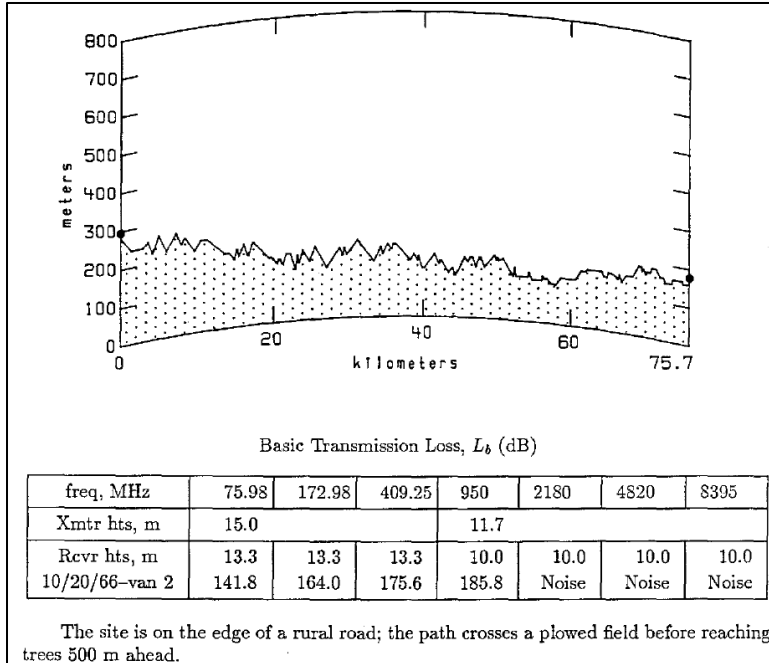
Figure F-14.   Actual Measured Path Loss Data from an NTIA Report (Hufford and Steele)

[Figure F-12](#) is a map showing various point-to-point transmitter-to-receiver links, TX001 to RX001, TX002 to RX002, etc. On the map, the same geographic location is used for all the transmitters, with the active transmitter for the example analysis (TX008) displayed on top of the other transmitters. Map data such as this is essential for computing aggregate interference as a function of bearing angle to an AMT site.

[Figure F-13](#) shows the terrain profile, including the effects of the earth's curvature, for the TX007-to-RX007 data link. The path loss, computed in this example using the L-R model, is 169.95 dB. The dashed blue line represents the extent of the Fresnel zone, showing how the terrain blockage impinges the zone, thus creating excess path loss.

For these simulations, it is typically appropriate to use average value settings for parameters related to variability. Although actual values for terrain blockage are used throughout the simulation, it is necessary to make a similar (e.g., average) assumption about whether diffraction due to terrain is modeled as knife-edge versus smooth-edge model.

In any case, it is important to validate model simulations using actual measurements wherever possible. This is the purpose of including [Figure F-14](#), which is an example path profile from the many measurements made by NTIA.

The terrain data in [Figure F-14](#) was obtained from manual inspection of a topographic map by members of the NTIA team, and was hand-entered into the graphing software used for preparing the measurement report. This is an important point. In interference studies, it is often the case that only a few cellular towers or other interference sources cause the aggregate level of interference to exceed Rec M.1459 limits. It is possible to re-create the data used in a commercial package by reference to a local topographic map and enter the data in the ITU-R

P.452 spreadsheet for analysis. The results are as accurate as those produced by the expensive packages, but can be obtained by using Excel spreadsheets.

Given the major effort required to collect experimental data, it is generally not practical to make measurements at all of the frequencies of interest with respect to interference computation. It might well be the case that the path loss at 1500 MHz, rather than the loss at the measured frequency of 2180 MHz, is the value of interest.

Since the wavelength is a component of the path loss value, and since the wavelength depends on the signal frequency, it is necessary to consider how to convert a measurement made at one frequency to an estimate of path loss at a different, but relatively close, value of frequency, such as the 2180-MHz to 1500-MHz example given here.

To a first approximation, path loss is independent of frequency in the 1 – 6 GHz bands, although effects of building attenuation are significant and signal absorption by foliage becomes important at the higher end of this frequency range. At even higher frequencies, such as the 12.6-MHz carrier frequency used for satellite television downlinks, foliage and rain attenuation are both significant. At even higher frequencies atmospheric absorption due to water vapor is extremely important, and care is often taken to operate in windows in the 35-GHz and 90-GHz ranges.

The explicit inclusion of a value for λ in Equation F-2 for the path loss is a computational artifact. In the Friis equation, it more properly connects the gain G_{rec} of the receive antenna to its effective area $\lambda^2 G_{rec}/4\pi$. Shifting λ^2 from the effective area to the path loss portion of the equation makes the path loss a dimensionless parameter, which is necessary in order for its value to be specified in dB.

Thus, when a path loss value for 2180 MHz is used as an estimate for the path loss at 1500 MHz, it is necessary to correct the path loss value using Equation F-12.

$$path\ loss_{1500} = \left(\lambda_{1500}/\lambda_{2180}\right)^2 \times path\ loss_{2180} \qquad \text{F-12}$$

Example 8. Consideration of the antenna patterns of terrestrial cellular base stations

It is necessary to know specific details of the gain pattern, location, height above ground, and pointing direction of the interfering antenna in order to replicate the computation for the case of a terrestrial interferer. If the terrestrial interferer is a cellular tower that hosts multiple sectored antennas, this requires specific knowledge about the antennas that are used and how their electronic adjustments, specifically electrical down-tilt, are configured.

This example requires the equation for computing the bearing angle from a cellular tower to an AMT site, and vice versa, when the latitude and longitude of each are specified. This is done using the mathematics of spherical trigonometry for the great circle arc that leads from one site to the other.

Then, using the sector antenna pointing angles relative to true north, the gain of each sectoral antenna on the tower in the direction of the AMT site is derived. The gain of tower-mounted cellular antennas may be specified as two pattern files, one for a 360° horizontal sweep at 0° elevation, and one for a 360° vertical sweep at zero degrees of azimuth with respect to the main lobe of the antenna.

To further complicate the problem, the main beam of each sectoral antenna can be pointed downward by varying increments of angle (e.g., 0 – 9 degrees) by remote control using the electrical down-tilt feature of the antenna. For the cellular antennas of interest, each permissible value of down-tilt is accompanied by its own pair of pattern files.

Mechanical down-tilt can also be used. This requires modifying the indexing of entries in the vertical file for the antenna so that, for example, the vertical pattern gain entries are shifted by the amount of the mechanical down-tilt.

The purpose of down-tilt is to permit adjustment of patterns to improve coverage of a typically urban or suburban area as new, additional cellular towers are in-filled, e.g., when a network is expanded to maintain coverage while increasing capacity.

In any case, it is necessary to combine the two-dimensional horizontal and vertical patterns into a single three-dimensional pattern using an interpolation algorithm. Manufacturers of cellular antennas of interest are not the main source of advice on how to do this. Instead, the academic literature summarizes and compares four different algorithms. These are called:

- Arithmetic mean;
- Bi-linear interpolation;
- Weighted bi-linear transformation;
- Horizontal projected interpolation.

With respect to the antenna pattern files, G_{vert} and G_{horiz}, θ represents elevation (with positive θ in the downward direction from $\theta = 0$ at the horizon) and the azimuth ϕ equals 0 in the center of the main lobe (with positive ϕ going counterclockwise as viewed from above).[74]

The formula for the arithmetic mean is the simplest, and is given by:

$$G(\theta, \phi) = \frac{1}{2} \left(G_{vert}(\theta) + G_{horiz}(\phi) \right) \qquad \text{F-13}$$

The equations for the second and third algorithms are rather complicated, and are not repeated here.

The final algorithm, horizontal projected interpolation, is used by one of the major commercial software packages. It has also been incorporated into an AFTRCC-developed production-grade interference analysis software package. The algorithm is given by:

$$G(\phi, \theta) = G_h(\phi) - \left[\frac{\pi - |\phi|}{\pi} \cdot \left(G_h(0) - G_v(\theta) \right) + \frac{|\phi|}{\pi} \cdot \left(G_h(\pi) - G_v(\pi - \theta) \right) \right] \qquad \text{F-14}$$

It is necessary to determine the appropriate values of ϕ and θ to use the interpolation algorithms. These are often generated by the software package that is used to compute the path loss between the AMT site and the individual cellular tower. Typically, the elevation angle θ is close enough to being horizontal that it can be assumed to be zero. Given that the angular resolution of the pattern files is only one degree and that $G_v(0°)$ is approximately equal to $G_V(1°)$, this is a reasonable approximation.

---

[74] Sign conventions for θ and ϕ should be verified for each case by inspection of the antenna files and cross-checking with the manufacturer's data sheets.

Even when the azimuth angle f is produced by the path loss software, it is helpful to use the formula below to confirm that no data entry errors that would change the value of azimuth have occurred. This is done using the following formula from spherical trigonometry:

$$sin(\phi) = \frac{cos(latitude_{AMT})}{sin\left(\frac{(Distance_{cell-AMT})}{R_{earth}}\right)} \cdot sin(longitude_{cell} - longitude_{AMT}) \qquad \text{F-15}$$

Note that ϕ represents the azimuth angle from the cellular tower to the AMT ground station antenna. For computing the gain of the cellular antenna in the direction of the AMT antenna, the direction that each sectoral antenna mounted on the tower is pointed with respect to north must be added (or subtracted, as appropriate) to compute the sectoral antenna's bearing to the AMT ground station.

As shown in the next example, when computing aggregate interference from an ensemble of cellular towers, it is necessary to compute the bearing of the AMT site to each cellular tower and the angular offset of this bearing from the main lobe of the AMT antenna. This is done by reversing the roles of the AMT site and the cellular tower in the above equation.

Alternatively, the reverse bearing can be computed directly from ϕ for the cellular tower, but certain quadrant conventions are needed in order to resolve ambiguities between the bearing angle ϕ_{amt} and its complement $180 - \phi_{amt}$. This issue is typically discussed in basic satellite communication textbooks, and is resolved by depicting a simple drawing of the cellular tower and AMT site locations on a chart. When processing hundreds of tower-to-AMT locations at once, the quadrant correction must be programmed carefully.

As always, care must be taken to not inadvertently default to the equations of flat-earth trigonometry. In this limit, the elevation angles to an aircraft from a cellular tower are always overstated, leading to a misapplication of the Rec M.1459 protection criteria.

Example pattern files can be found online.[75] It is common for the files to give a maximum value of the gain at the center of the main beam of the pattern. The file entries then correspond to the relative attenuation of the pattern relative to this value of G_{max}.

Example 9. Aggregation of interference from a network of cellular base stations to one or more AMT ground stations[76]

The large-scale simulation of interference from thousands of cellular base stations and their associated handsets will be a major activity for both the civil and DoD AMT communities as government spectrum is auctioned for use by commercial broadband carriers. This example presents a stand-alone, step-by-step procedure for accomplishing this. It can be implemented in a variety of ways, including as a collection of Excel spreadsheets in conjunction with the commercial software packages (e.g., EDX Signal Pro) referenced earlier in this appendix.

The steps for completing a coordination of a large collection of emitters with a single AMT ground station are as follows.

---

[75] CommScope. "Calculators and Tools." Retrieved 17 May 2021.
http://www.commscope.com/Resources/Calculators/.

[76] Analysis of the aggregation of handsets requires the inclusion of statistical parameters that are developed in example 10. The analysis of an aggregation of handsets is provided in example 12.

1.   The composite AMT ground station antenna pattern provided by equations 1(a) – 1(f) of Rec M. 1459[77] is used instead of patterns obtained on a site-specific basis for each of the hundreds of AMT ground stations in the United States. This composite pattern is shown in [Figure F-15](). Use of this composite antenna pattern addresses several features unique to AMT operations and eliminates the need for detailed, site-specific technical details that are subject to change from one flight-test program to another, or even during individual test flights. The Rec M. 1459 pattern is to be used in lieu of, for example, the Wolfgain and Statgain patterns given in NTIA Report TM-13-489[78], although the Rec M. 1459 composite patterns are closely related to the Statgain patterns, as shown later in this appendix.
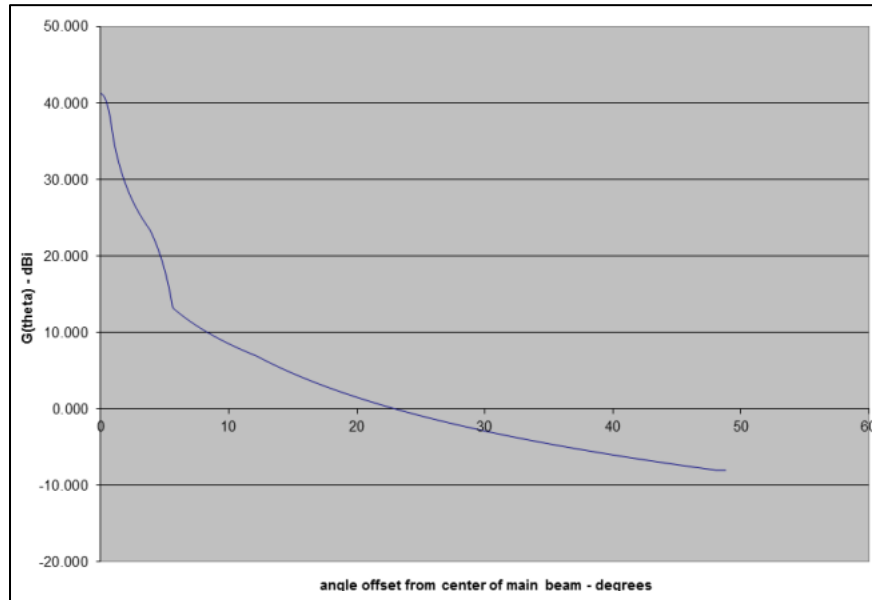
Figure F-15.   Composite AMT Pattern from Rec M.1459

2.   Instead of traditional interference-to-noise ratio (I/N) criteria, interference received at an AMT ground station is to be computed using the appropriate PFD limit from Rec M.1459. For example, this might be the Rec M. 1459 PFD limit for $0 - 2°$ angles of arrival (with respect to the horizon) for L or S bands, namely -180 or -181 dB W/m^2 in 4 kHz. These levels represent the total permitted aggregate interference, as computed using the technique given in steps 3 - 5.

3.   It is necessary to consider the interference from all directions with respect to the ground station antenna, including interference received through the side lobes and back lobes to compute aggregate interference. Furthermore, this aggregate interference must be recomputed for all possible pointing angles (in azimuth) of the AMT ground station antenna, which can rotate to point in any direction. It would be appropriate, for example, to compute aggregate interference for each of 720 pointing angles, measured in 0.5° increments.

4.   To compute aggregate interference from hundreds of base stations, for example, it is necessary to group the eNodeBs into 0.5°-wide azimuth-of-arrival wedges, then to compute the

---

[77] The antenna pattern shown in Figure 1 of Rec M.1459 is not the pattern to be used here.
[78] Wang, C. W. and T. Keech. *Antenna Models For Electromagnetic Compatibility Analyses*, NTIA Report TM-13-489. October 2012. Retrieved 17 May 2021. Available at https://www.ntia.doc.gov/report/2012/antenna-models-electromagnetic-compatibility-analyses.

aggregate PFD per wedge for each of these for each of 720 possible pointing angles of the AMT ground station. The aggregate PFD values for each wedge are converted in a received power value using the composite AMT ground station antenna pattern. This pattern, including values for side lobes and back lobes, provides the necessary weighting factors for converting PFD values in W/m^2 to absolute power in watts (cf. equations F-1 - F-3).

5.   The aggregate power levels for each azimuth-of-arrival wedge are summed for all of the wedges into a single value. This aggregate value is computed for each of the 720 possible pointing angles of the AMT ground station antenna. Each of these 720 values is then converted back into a PFD level and compared with the PFD limit of −180 or −181 dBW/m^2 in 4 kHz. This yields a graph and/or table of interference values versus azimuth for the AMT ground station, as shown in notional form in Figure F-16. Note that the scaling of the full bandwidth of the co-channel or adjacent channel interference to the 4-kHz reference bandwidth of the Rec M.1459 protection criteria uses the same linear transformation that is used for a traditional I/N analysis.
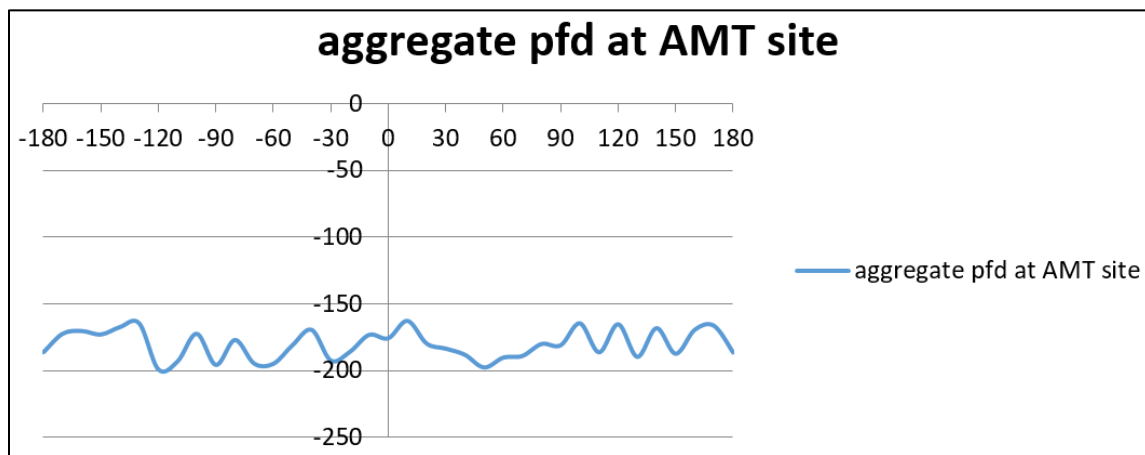
Figure F-16.   Aggregate Interference as a Function of AMT Antenna Pointing Angle

6.   The above approach is summarized quantitatively in the equations below, which elaborate on those presented earlier, and are re-stated here for the convenience of the reader.

- The value of wavelength that is part of the expression for the effective area of the AMT ground station receive antenna is grouped with the $1/4\pi r^2$ spreading term, which is then redefined as path loss. This regrouping then permits the spreading term to be replaced with a single term that includes the effects of spreading, terrain and clutter loss, Fresnel zone impingement, and ground reflection. The numerical computation of values for this composite path loss value is independent of the use of Rec M.1459.

- The conversion of PFD values to received power and vice versa involves the scaling term $4\pi/\lambda^2$. It is important to account for the presence, or absence, of this term in the equations presented below, so as to not inadvertently delete it or count it twice. This is why the equations below err on the side of redundancy; it is easier to ignore an unneeded equation than to re-derive it.

    With this as a reference, the following evolution of equations should prove useful.

1.   Start with the free-space Friis equation. A_{eff} is the effective area of the AMT ground station receive antenna:

$$P_{rec} = EIRP_{xmt} \times \frac{1}{4\pi r^2} \times A_{eff} \qquad \text{F-16}$$

2.   Add antenna gains, the definition of antenna effective area, and the definition of PFD to arrive at:

$$P_{rec} = P_{xmt}G_{xmt} \times \frac{1}{4\pi r^2} \times \frac{\lambda^2 G_{rec}}{4\pi} = pfd_{rec} \times A_{eff} = pfd_{rec} \times \frac{\lambda^2 G_{rec}}{4\pi} \qquad \text{F-17}$$

3.   Move $\lambda^2/4\pi$ from effective area term and group with the $\frac{1}{4\pi r^2}$ term per the traditional mathematical definition of path loss. Terrain, ground reflection, clutter, and Fresnel zone effects can now be included in the numerical value used for path loss in subsequent computations:

$$P_{rec} = P_{xmt}G_{xmt} \times \frac{\lambda^2}{4\pi r^2} \times \frac{G_{rec}}{4\pi} = pfd_{rec} \times A_{eff} = pfd_{rec} \times \frac{\lambda^2 G_{rec}}{4\pi} \qquad \text{F-18}$$

$$pfd_{rec} \times \frac{\lambda^2 G_{rec}}{4\pi} = P_{xmt}G_{xmt} \times \frac{\lambda^2}{(4\pi)^2 r^2} \times \frac{G_{rec}}{1} = P_{xmt}G_{xmt} \times (Path\_Loss) \times \frac{G_{rec}}{1} \qquad \text{F-19}$$

4.   The gain of the AMT ground station receive antenna, G_{rec}, disappears from the equations when computation of the PFD level at the AMT ground station receiver is the desired result:

$$P_{rec} = pfd_{rec} \times \frac{\lambda^2 G_{rec}}{4\pi} = P_{xmt}G_{xmt} \times (Path\_Loss) \times \frac{G_{rec}}{1} \qquad \text{F-20}$$

$$P_{rec} = pfd_{rec} \times \frac{\lambda^2 G_{rec}}{4\pi} = P_{xmt}G_{xmt} \times (Path\_Loss) \times \frac{G_{rec}}{1} \qquad \text{F-21}$$

5.   Use the appropriate eNodeB antenna gains described in step 4 to compute $P_{xmt}G_{xmt}$. Use the speed of light to compute, for this example, the wavelength λ corresponding to a frequency of 1500 MHz. Scale the EIRP values to the 4-kHz reference bandwidth of the Rec M.1459 PFD protection level. This yields the interference from a single handset as a PFD level measured at the location of the AMT ground station antenna. This value can be compared directly with the protection level from Rec M.1459.

$$pfd_{rec_{in\ 4\ kHz}} = (Interference\ in\ Watts\ per\ MHz) \times G_{xmt} \times (Path\_Loss) \times \frac{4\pi}{\lambda^2}$$
$$\times \frac{4000\ Hz}{1\ MHz} \qquad \text{F-22}$$

$$\lambda = \frac{3 \times 10^8}{1500 \times 10^6} = 0.20\ meter \qquad \text{F-23}$$

$$= Interference \times G_{xmt} \times (Path\_Loss) \times \frac{4\pi}{(.20)^2} \times \frac{4000\ Hz}{1\ MHz}$$

6.   Now that the relationships between interference power, path loss, PFD, and P_{rec} are defined, the aggregation process described earlier can be implemented. The important point is that the PFD values due to each sector of each eNodeB, as measured at an AMT ground station location, are grouped within an angle of arrival wedge, then multiplied by the appropriate value of AMT composite antenna pattern for each angle of arrival value. The total interference from all directions for each possible AMT pointing angle is computed, then changed back into an aggregate value of PFD by the conversion factor $4\pi/\lambda^2$ to arrive at a single value of aggregate

PFD for each of the 720 possible AMT antenna pointing angles. Each entry in this table of values is then compared with the protection limit from Rec M. 1459.

7.   Finally, note that interference to an AMT signal is typically averaged over the bandwidth of the affected AMT channel(s), as described previously. This averaging is accomplished in the same manner that would apply to a traditional I/N analysis. The 4-kHz reference bandwidth in Rec M.1459 must be scaled to correspond to AMT channel bandwidths of 1 – 20 MHz, with 5 MHz being a common value for use in analysis.

Example 10.   Additional considerations for the modeling of interfering systems

It is important to include effects such as network load factors, transmitters that emit intermittently, and the use of dynamic power control. Note that there are no similar effects related to the performance of AMT operations that need be considered, as these are already captured in Rec M.1459. Annex 2 of Rec M.1459 accounts for signal fades, for the requirement of a minimum value of telemetry link availability, and for the constantly changing location of test aircraft in the sky with respect to both satellite and terrestrial interference sources.

Consider Example 9, coordination of an AMT ground station with emissions from a large network of cellular towers. The cellular industry has noted repeatedly that its networks seldom operate at full load factor. This means that, averaged over several weeks, an individual cellular tower is transmitting only about 60% of the time. Cellular proponents thus advocate a decrease in the computed value of aggregate interference used in analysis by 40%.

The decrease in cellular tower activity at off-peak times corresponds with time slots where flight test activities are also at a minimum (e.g., at night). Furthermore, the time scales over which base station load factors are averaged (weeks) have no correlation with the time duration of interference causing an AMT link to fail (fractions of a second). Short-term interference can cause loss of antenna tracking, which can be difficult to re-establish without the need to re-fly test points.

The point is that when the probability of interference depends on time, it is necessary to use the same time scales for analyzing both the interfering and the victim systems. In the case of AMT operations, this means that all computations need to be performed for the time scale that corresponds to the interval of time that it takes an interfering signal to cause loss of AMT telemetry link bit synchronization. As stated in the previous paragraph, this is not weeks or days, but fractions of a second. In any case, loss of even small amounts of data can make it necessary to re-fly part, or even all, of the maneuvers included in a particular test flight.

Coordination of AMT ground stations with emissions from cellular handsets introduces similar issues. These handsets use dynamic power control, in which a cellular tower measures the received signal from a handset in real time and sends instructions to the handset to adjust its transmit power.

In addition, LTE and WiMAX (i.e., 802.16) systems operate by using orthogonal frequency division multiplexing, in which data are coded among several adjacent frequency subcarriers spread across the 10 – 20 MHz LTE bands.[79] The power amplitudes of each subcarrier vary with time, yielding variations characterized by what is called the peak-to-average-power-ratio (PAPR*)*. For LTE, the PAPR is about 6 dB, with variations occurring on the

---

[79] WiMAX will be used for the AeroMACS system at 5091- 5150 MHz, co-channel with AMT.

order of milliseconds. For WiMAX, the PAPR is as high as 13 dB. The statistical distribution as a function of time for each system is characterized by a complementary cumulative distribution function.

It remains an open question whether PAPR fluctuations, which include reductions as well as surges in transmit power, are a concern.

Example 11. Special considerations regarding AMT antennas

The use of a composite antenna in Rec M. 1459 is referenced multiple times in this appendix. In the recommendation, however, the development of the composite antenna pattern is described in the body of Annex A only for the case of lower L-band, which has a pattern that is based on the NTIA Statgain antenna model of parabolic dish antennas (Wang and Keech, 2012), and is derived numerically for antennas having diameters of 10 meters and 2.44 meters. The composite pattern is derived by comparing the 10-meter and 2.44-meter patterns side-by-side and choosing the value of gain that is higher for a given off-axis pointing angle.

Although not described explicitly in the recommendation, the antenna pattern was modified for the purpose of computing the protection criteria for upper S-band that are also published in the recommendation. The L- and S-band frequencies are sufficiently close in value that the same composite pattern can be used for both bands for purposes of computing aggregate interference. This is a result of certain complex convolution computations described in the methodology provided by the recommendation; however, this simplification does not apply as telemetry systems are deployed at C-band and higher frequencies.

To address the computation of the protection criteria for upper L, lower S, and lower, middle, and upper C-bands, new composite antenna patterns were computed using the NTIA Statgain antenna pattern formulas given below.

Although the antenna patterns are not needed again for purposes of determining the protection criteria, they are needed when computing aggregation from large numbers of terrestrial interferers. For this purpose, the process of computing composite antenna patterns is straightforward, and is described below.

With respect to the computation of composite antenna patterns, the gain of both a 10-meter and 2.44-meter diameter dish were computed for each band using the Statgain formulas with the gain parameter G_{max} for each dish computed using the formula

$$G_{max} = 0.55 \times \left(\pi D / \lambda \right)^2 \tag{F-24}$$

where 0.55 represents the nominal efficiency of the dish antennas.

Then, using the equations below, patterns were computed for both the 10-meter and 2.44-meter antennas for each value of signal wavelength λ. Using a simple spreadsheet, the gains of the two antennas as a function of off-axis angle for each value of λ were compared. The higher gain value of the two antennas was chosen as the value for that angle for the corresponding composite antenna. Although this is a slight simplification of the side-lobe averaging technique used in the recommendation, the impact on the numerical values of the protection criteria was found to be negligible. This means that for computational purposes, the Statgain antenna patterns can be used for C and higher bands without modification.

In addition to the Statgain formulas, which provide an envelope function for the maximum values of the gain pattern, the more general pattern equations are also provided. These are difficult to find in textbooks, but are often useful.

The Statgain radiation patterns, $G(\phi)$, as a function of the angle from the main-beam axis, ϕ, are shown in Table F-1 (Wang and Keech 2012) and the Statgain envelope pattern is presented in Figure F-17 (Wang and Keech 2012). The more general pattern equations, published as part of the Satellite Toolkit software, are provided afterwards.

Table F-1.	Statgain Formulas	
Category	**Gain(ϕ) (dBi)**	**Angular Range (deg.)**
$G_{max} \geq 48$ dBi	$G_{max} - 4 \times 10^{-4}(10^{G_{max}/10})\phi^2$	$0 \leq \phi \leq \phi_m$
	$0.75 \times G_{max} - 7$	$\phi_m < \phi \leq \phi_{r1}$
	$29 - 25 \times \log(\phi)$	$\phi_{r1} < \phi \leq \phi_{b1}$
	-13	$\phi_{b1} < \phi \leq 180°$
$22 \leq G_{max}(dBi) < 48$	$G_{max} - 4 \times 10^{-4}(10^{G_{max}/10})\phi^2$	$0 \leq \phi \leq \phi_m$
	$0.75 \times G_{max} - 7$	$\phi_m < \phi \leq \phi_{r2}$
	$53 - (G_{max}/2) - 25 \times \log(\phi)$	$\phi_{r2} < \phi \leq \phi_{b2}$
	$11 - G_{max}/2$	$\phi b1 < \phi \leq 180°$
$10 \leq G_{max}(dBi) < 22$	$G_{max} - 4 \times 10^{-4}(10^{G_{max}/10})\phi^2$	$0 \leq \phi \leq \phi_m$
	$0.75 \times G_{max} - 7$	$\phi_m < \phi \leq \phi_{r3}$
	$53 - (G_{max}/2) - 25 \times \log(\phi)$	$\phi_{r3} < \phi \leq \phi_{b3}$
	0	$\phi_{b3} < \phi \leq 180°$

All angles are in degrees.
$\phi_m = 50(0.25 G_{max} + 7)^{0.5}/(10^{G_{max}/20})$
$\phi_{r1} = 27.466 \times 10^{-.03 G_{max}/10}$
$\phi_{r1} = \phi_{r1} = 250/(10^{G_{max}/20})$
$\phi_{b1} = \phi_{b2} = 48$
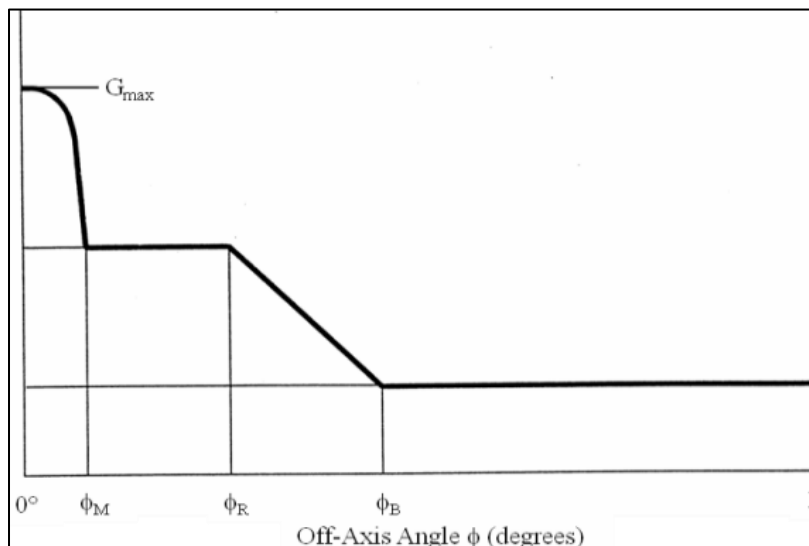$\phi_{b3} = 131.8257 \times 10^{-G_{max}/50})$

Figure F-17.   Statgain Pattern

Note that the Statgain patterns provide an upper envelope of the antenna pattern. The more-generalized parabolic dish equations are available as part of the Analytical Graphics (AGI) Satellite Toolkit software tool.[80] These equations provide details about the peaks and nulls of the antenna side-lobes as opposed to providing an envelope of the pattern, and are given below.

The parabolic antenna parameters are:

d = diameter of the parabolic dish

λ = wavelength

The gain of a parabolic antenna is modeled by the equations F-25a, F-25b, and F-25c:

$$x = \frac{\pi d}{\lambda}\sin\phi \qquad \text{F-25a}$$

$$G_{Max} = \rho_e \left(\pi\frac{d}{\lambda}\right) \qquad \text{F-25b} \qquad \text{F-25}$$

$$G(\phi) = G_{Max}\left(\frac{2J_1(x)}{x}\right) \qquad \text{F-25c}$$

where ρ_e = the antenna efficiency, ϕ = angle off boresight, and J_1 = first-order Bessel function. This model is for a uniformly illuminated circular aperture dish.

On a final note, the question has been posed of how to compute protection criteria for antennas whose diameter falls outside the range of 2.44 – 10 meters. The simple and reasonable approach is to recognize that both the gain and beamwidth of a parabolic-dish antenna are related to the parameter D/λ. For the case of an antenna that is 13 meters in diameter but operating at upper L-band (for example), D/λ is about 75. This is comparable to a 10-meter antenna operating at a wavelength of 0.133 meters. Since the protection criteria for upper S-band correspond to a wavelength of 0.128 meters, it seems appropriate to use the protection criteria for upper S-band as the values for a 13-meter diameter antenna operating at upper L-band.

---

[80] Maral, G., and M. Bousquet. *Satellite Communications Systems: Systems, Techniques and Technology*. 2nd ed. Chichester: Wiley (1993), sec. 2.1.3; Gagliardi, Robert M. *Satellite Communications*. 2nd ed., New York: Van Nostrand Reinhold (1991), sec. 3.2.

APPENDIX 2-G

Standards for Data Quality Metrics and Data Quality Encapsulation

G.1. Purpose

This appendix provides a standard for a DQM, determined in the telemetry receiver demodulator, and a standard for DQE allowing for transport of the received telemetry data and associated DQM to a distant best source selector or similar device. The DQE standard enables telemetry receivers to generate a serial data stream that includes a standardized measurement of the real-time probability of error for a grouping of bits.

G.2. Scope

The DQM standard describes how to map the estimated BEP of the received telemetry data to a 16-bit word. The DQM standard does not define how the telemetry receiver performs BEP estimates. The DQE standard describes how to format received telemetry data with the associated DQM for transport.

G.3. Data Quality Metric

The general case of DQM is calculated using:

$$DQM = -log_{10}(LR)$$

where:

$$LR = \frac{BEP}{(1 - BEP)}$$

is the likelihood ratio. For mapping this value into an n-bit word with a lowest BEP exponent equal to k, the equation becomes:

$$DQM = \begin{cases} X, & X \leq 2^n - 1 \\ 2^n - 1, & \text{otherwise} \end{cases} \qquad X = \left[\frac{-\log_{10}(LR)}{k} \times 2^n \right]$$

Where the notation $[z]$ denotes the greatest integer less than or equal to z.

NOTE	For this standard, $k=12$ and $n=16$.

a. The measurement value corresponds to the average quality of the data bits in the payload.

b. The DQM value is associated with the payload bits in the current block frame. Table G-1 defines LR and DQM for various values of BEP.

Table G-1. BEP Versus DQM

BEP	LR	DQM
0.5	1.00	0
1e−01	1.11111e−01	5211
1e−02	1.01010e−02	10898

1e−03	1.00100e−03	16381
1e−04	1.00010e−04	21845
1e−05	1.00001e−05	27306
1e−06	1.00000e−06	32767
1e−07	1.00000e−07	38229
1e−08	1.00000e−08	43690
1e−09	1.00000e−09	49151
1e−10	1.00000e−10	54613
1e−11	1.00000e−11	60074
1e−12	1.00000e−12	65535

NOTE	It is not required that BEP be estimated to the 1.0e−12 level. Estimates to a lesser level are acceptable; however, the format above shall be followed in all cases. For example, if estimating BEP to the 1.0e−8 level, the applicable range of DQM values shall be 0 to 43690.

G.4. Data Quality Encapsulation Protocol

The block format is equivalent to a fixed-length PCM frame. Transmission of payload data shall be first in - first out. Transmission of other fields shall be most significant bit first.

16 Bits	12 Bits	4 Bits	16 Bits	1024 – 16384 Bits
SW	RSV	VER	DQM	PAYLOAD

a. SW = Sync Word. The sync word is a fixed value of 0xFAC4.

b. RSV = Reserved. Reserved for future use. These bits shall be set to zero (0) until used.

c. VER = IRIG 106 Version number. Version number shall start with Version 0 (0000) for IRIG 106-17 and be incremented when revisions to this appendix are made.

Version	Release
0 (0000)	106-17
1 (0001)	106-22
2 (0010)	

d. DQM = Data Quality Metric. This field will contain the DQM value as defined in Section G.3

e. PAYLOAD = Telemetry data payload to which the DQM value applies. The DQM and the data payload are contained in the same block. The minimum payload size shall be 1024 bits and the maximum size shall be 16,384 bits. Payload size can be any multiple of 32 bits between the minimum size and maximum size. In the absence of any other determining factor the default payload size is 4096 bits.

When block coding is applied to the telemetry link the default payload size is set by the information block size. If multiple block codes are applied the default payload size is set by the information block size of the outer code. The default payload sizes for each are as follows.

STC (see Appendix 2-E): 3200 bits

LDPC (see Appendix 2-D) or STC-LDPC (k=1024): 1024 bits

LDPC or STC-LDPC (k=4096): 4096 bits

Any bit manipulation should be done prior to placing the data into the PAYLOAD field without affecting the 48 bits of header encapsulation. Examples of bit manipulation are inversion and de-randomization.

This page intentionally left blank.

APPENDIX 2-H

Dynamic Multipath Channel Model for Aeronautical Mobile Telemetry

H.1. Preliminaries

Theoretical considerations for aeronautical multipath channels were published by Bello.[81] The aeronautical channel comprised three terms, an LOS term, a specular reflection term, and a diffuse reflection term. The application of this three-ray model to aeronautical mobile telemetry was confirmed by channel sounding experiments performed by Rice et al.[82]

The impulse response for a static three-ray multipath channel is

$$h(t) = \delta(t) + \Gamma_1 e^{-j2\pi f_c \tau_1} \delta(t - \tau_1) + \Gamma_2 e^{-j2\pi f_c \tau_2} \delta(t - \tau_2) \qquad \text{H-1}$$

Notes:

- Just as signals have an in-phase/quadrature-component (I/Q) representation, a channel also has an I/Q representation. The I/Q representations of signals and channels are usually represented by complex-valued waveforms where the real part of the waveform defines the I component and the imaginary part defines the Q component. The impulse response (Equation H-1) is the I/Q representation of the multipath channel.

- The first term on the right-hand side of Equation H-1 represents the LOS propagation. No propagation losses (such as "$1/R^2$" spreading losses and atmospheric attenuation) or gains (such as transmit and receive antenna gains) are included. The LOS component has unity gain and zero delay. In this sense, the impulse response (Equation H-1) is normalized to the LOS component. The losses and gains show up as a bulk attenuation factor applied to all three terms on the right-hand side of Equation H-1. The bulk attenuation impacts the received signal-to-noise ratio, not the properties of the multipath propagation.

- The second term on the right-hand side of Equation H-1 is the specular reflection. The parameters that define the specular reflection are as follows.

    Γ_1 the complex-valued reflection coefficient at the reflection point. The value of the reflection coefficient is defined by the carrier frequency, the electrical properties of the reflection medium, and the incidence angle (Rice et al).

    f_c the carrier frequency in Hz.

    τ_1 the relative delay between the LOS component and the specularly reflected component. The delay is determined by the geometry defined by the position of the airborne transmitter, the position of the ground-based receiver, and location of the reflection point. In almost all scenarios, the reflection is a ground- or sea-based reflection.

Using $\Gamma_1 = |\Gamma_1| e^{j\gamma 1}$ to represent the reflection coefficient, the specular reflection experiences an attenuation equal to $/\Gamma_1/ < 1$ and a phase shift γ_1 relative to the LOS component. The term $2\pi f_c \tau_1$ is an additional phase shift due to the longer propagation

---

[81] Phillip Bello. "Aeronautical channel characterization." *IEEE Transactions on Communications*, vol. 21, no. 5, pp. 548–563, May 1973.

[82] Rice, M., A. Davis, and C. Bettweiser. "Wideband channel model for aeronautical telemetry." *IEEE Transactions on Aerospace and Electronic Systems*, vol. 40, no. 1, pp. 57–69, January 2004.

path from transmitter to receiver via the specular reflection point. The specular reflection is determined completely by the geometry.

- The third term on the right-hand side of Equation H-1 is called the diffuse reflection. The parameters that define the diffuse reflection are as follows.

Γ_2 the complex-valued reflection coefficient at the reflection points. The value of the reflection coefficient is defined by the carrier frequency, the electrical properties of the reflection medium, and the incidence angles (Rice et al).

f_c the carrier frequency in Hz.

τ_2 the relative delay between the LOS component and the diffusely reflected component. The delay is determined by the geometry defined by the position of the airborne transmitter, the position of the ground-based receiver, and location of the reflection points.

This term is called diffuse because it is the result of many weak reflections with statistically independent amplitudes, phases, and delays. Consequently, the reflection coefficient Γ_2 and delay τ_2 are less well-defined. This term is the result of the interaction with non-smooth reflectors some distance away from the specular reflection point, such as mountains and hills (in the case of a land-based range) or large sea swells (in the case of a sea-based range). Theoretically the diffuse reflection is determined completely from the geometry defined by the position of the airborne transmitter, the position of the ground-based receiver, and the positions of all non-specular reflectors. Because detailed terrain or sea-state information is rarely known at sub-wavelength resolution, a deterministic evaluation of this parameter is not practical. For this reason, statistical characterizations of Γ_2 and τ_2 are used.

- If $s(t)$ represents the I/Q representation of the transmitted signal, then the I/Q representation of the received signal is given by the convolution of $s(t)$ with Equation H-1:

$$r(t) = s(t) + \Gamma_1 e^{-j2\pi f_c \tau_1} s(t - \tau_1) + \Gamma_2 e^{-j2\pi f_c \tau_2} s(t - \tau_2) \qquad \text{H-2}$$

Note here that the received signal comprises three copies of the transmitted signal. The first copy of the signal is the signal itself and represents LOS propagation. The second and third copies are delayed, phase-shifted, and attenuated versions of the transmitted signal.

H.2. The Dynamic Multipath Channel

Multipath propagation is a spatial phenomenon in the sense that the parameters that define multipath propagation are a function of the geometry defined by the positions of the airborne transmitter, the ground-based receiver, and the reflectors. As the airborne transmitter moves, the relative positions of receiver and reflectors change. Because the airborne position changes with respect to time, the geometry defining multipath propagation changes with respect to time. Consequently, the four constants Γ_1, Γ_2, τ_1, and τ_2 are replaced by functions of time: $\Gamma_1(t)$, $\Gamma_2(t)$, $\tau_1(t)$, and $\tau_2(t)$. The impulse response (Equation H-1) is modified to produce the time-varying impulse response

$$h(t) = \delta(t) + \Gamma_1(t)e^{-j2\pi f_c\tau_1(t)}\delta\big(t - \tau_1(t)\big) + \Gamma_2(t)e^{-j2\pi f_2\tau_2(t)}\delta\big(t - \tau_2(t)\big) \qquad \text{H-3}$$

Notes:

- The first term on the right-hand side of Equation H-3 represents the LOS propagation component. Its properties are same as the LOS component in Equation H-1.

- The second term on the right-hand side of Equation H-3 is the specular reflection. The parameters that define the specular reflection are described in the previous section. The theoretical analysis in Rice and Ebert [83] shows that $\Gamma_1(t)$ changes so slowly that it may be considered constant for a multipath event. Consequently, changes in the specular reflection are due entirely to changes in $\tau_1(t)$. It is shown in Rice and Ebert that the specular reflection term may be expressed as

$$\Gamma_1(t)e^{-j2\pi f_c\tau_1(t)}\delta(t - \tau_1(t)) \approx |\Gamma_1|e^{-j(2\pi f_d t+\theta_1)}\delta((t - \tau_1(t)) \qquad \text{H-4}$$

  where f_d is the Doppler frequency and θ_1 is a constant. Computation of the Doppler frequency f_d is discussed in Rice and Ebert. The Doppler frequency produces a time variation in the frequency of the spectral null caused by the specular reflection. The time variation is linear in the time variable giving rise to the often-observed "sweeping" of the spectral null across the signal spectrum during a test flight.

- The third term on the right-hand side of Equation H-3 is called the diffuse reflection. The parameters that define the diffuse reflection are described in the previous section. Statistical characterizations of $\Gamma_2(t)$ and $\tau_2(t)$ were investigated in Bello where it was shown that $/\Gamma_2(t)/$ is a Rayleigh random process with a Gaussian power spectral density given by

$$S_2(f) = \frac{\sqrt{2}}{B_{\text{rms}}\sqrt{\pi}}\exp\left\{-2\left(\frac{f}{B_{\text{rms}}}\right)^2\right\} \qquad \text{H-5}$$

  where B_{rms} is the rms Doppler spread. For the purposes of this channel model, the delay $\tau_2(t)$ is set equal to the average delay $\overline{\tau_2(t)}$ of the diffuse component.

H.3. Channel Emulator Settings

The impulse response described in the previous section was instantiated on a Spirent SR5500 Wireless Channel Emulator. This example is broadly applicable to a variety of channel emulators because most channel emulators have similar user interfaces. A channel emulator defines a number of propagation paths through which the input signal passes. The outputs of the propagation paths are combined to create channel emulator output. Here, three paths are used to represent propagation through a channel defined by the impulse response (Equation H-3) with parameters for the reflection coefficients, delays, and Doppler frequencies obtained from Rice et al and corresponding to a flight path along Cords Road at Edwards AFB at an altitude of 5,000 feet above mean sea level and velocity of Mach 1:

---

[83] Rice, M. and J. Ebert. "Derivation and analysis of the IRIG-106 dynamic multipath channel model," in *Proceedings of the International Telemetering Conference*, Las Vegas, NV, 25-28 October 2021 (forthcoming).

$|\Gamma_1| = 0.944, |\Gamma_2| = 0.1, \tau_1(t) = 10$ ns, $\overline{\tau_2(t)} = 155$ ns, and $f_d = 3 \times 10^{-11} f_c$ Hz

In the Spirent 5500, "Path 1" is the LOS component, "Path 2" is the specular reflection, and "Path 3" is the diffuse reflection. The parameters for the three paths in the channel emulator are shown in Table H-1, Table H-2, and Table H-3.

Notes:

- The power spectral density for the diffuse component should be the Gaussian power spectral density given by Equation H-5 and plotted in Figure H-1. Unfortunately, the Spirent SR5500 does not have the option for producing a Gaussian power spectral density. The available options for the Spirent SR5500 are shown in Figure H-2. Of the available options, the "Rounded 12 dB" is closest to the Gaussian power spectral density. Consequently, the fading spectrum shape for the Path 3 is set to "Rounded 12 dB" in Table H-1, Table H-2, and Table H-3.

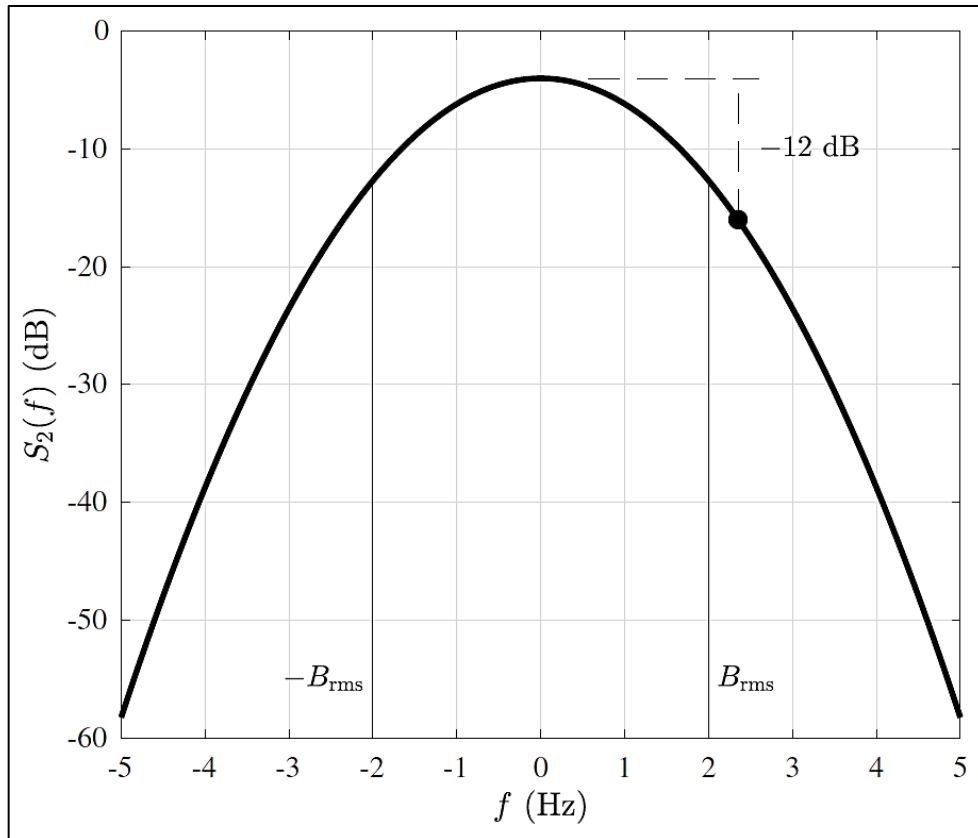

Figure H-1.   The Gaussian Power Spectral Density $S_2(f)$ given by Eq. H-5 for B_{rms}=2 Hz
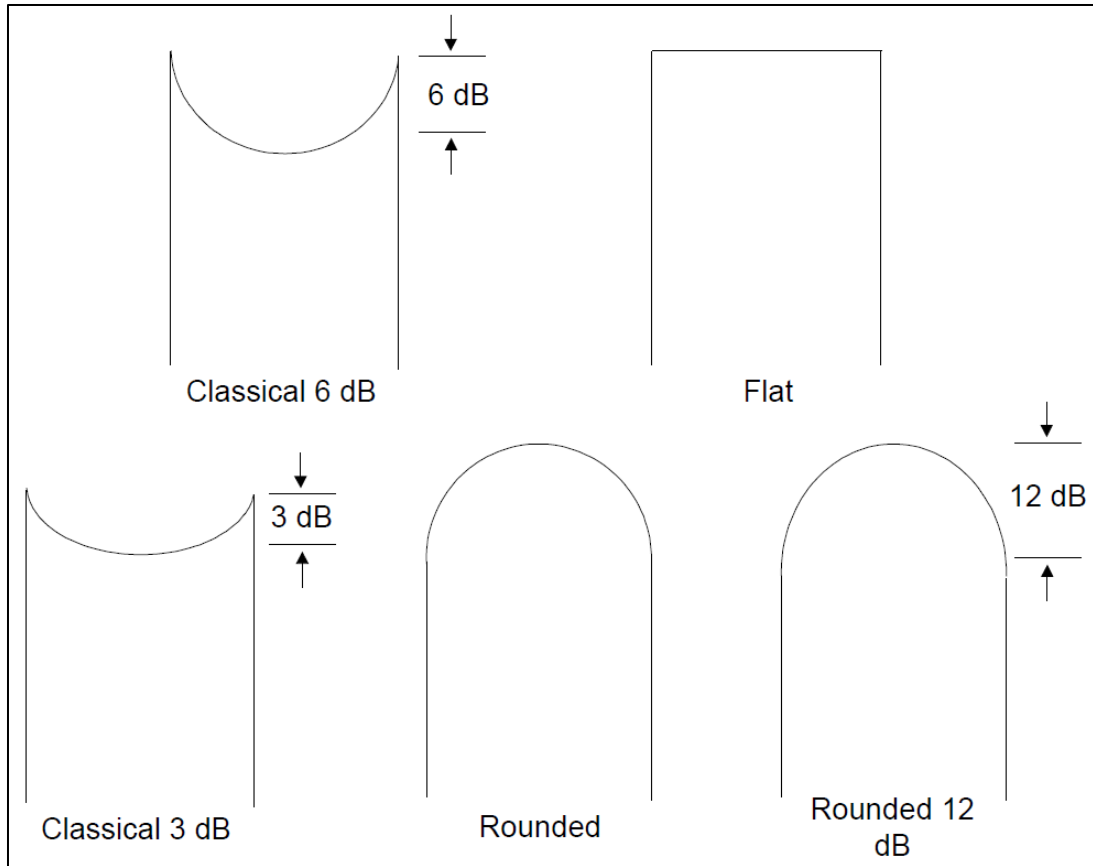
Figure H-2.   The Options for the Power Spectral Density of the Diffuse Component in the Spirent SR5500 Wireless Channel Emulator (Spirent, p. 153)

- The Spirent SR5500 does not operate at C band because the operational range is 400 to 2700 MHz .[84] C-band testing can be accomplished using a transmitter operating a C-band connected to a C-band downconverter (see Subsection 2.4.7) whose output is connected to the channel emulator. The transmitter carrier frequency should be chosen to ensure the output of the C-band downconverter is greater than 400 MHz. The carrier frequency setting on the channel emulator should be the output frequency of the C-band downconverter.

- These channel settings best model the Cords Road scenario described in Rice et al and Rice and Ebert where the velocity of the airborne transmitter is Mach 1. For other scenarios, the reflection coefficients and channel delays may be different. The differences will depend largely on the geometry defined by the position of the airborne transmitter, the position ground-based receiving station, and the positions of the reflecting media (Rice and Ebert).

---

[84] Spirent. *SR5500 Wireless Channel Emulator User Manual*. Copyright 2011. 71-003547, Version A7. May be superseded by update. Retrieved 17 May 2021. Available at https://support-kb.spirent.com/resources/sites/SPIRENT/content/live/DOCUMENTATION/10000/DOC10397/en_US/UM_SR5500_v3_50_A7.pdf.

- For different velocities, the Path 2 frequency shift and Path 3 fading Doppler scale proportionally.

- On most test ranges, multipath propagation is an intermittent phenomenon. The settings here do not capture the "birth" and "death" of multipath events, but instead the dynamics of multipath propagation during a multipath event.

Table H-1. Spirent SR5500 Wireless Channel Emulator Settings for Three Paths that Define the Dynamic Multipath Channel for Aeroautical Mobile Telemetry in L-Band					
Path 1		**Path 2**		**Path 3**	
Modulation	Static	Modulation	Static	Modulation	Rayleigh
Fading Doppler	N/A	Fading Doppler	N/A	Fading Doppler	1.32 Hz
Phase shift	0°	Phase shift	0°	Phase shift	0°
Frequency shift mode	Fixed	Frequency shift mode	Fixed	Frequency shift mode	Fixed
Frequency shift	0 Hz	Frequency shift	0.05 Hz	Frequency shift	0 Hz
Fading spectrum shape	N/A	Fading spectrum shape	N/A	Fading spectrum shape	Rounded 12 dB
Delay mode	Fixed	Delay mode	Fixed	Delay mode	Fixed
Delay value	0 µs	Delay value	0.01 µs	Delay value	0.155 µs
Relative path loss	0 dB	Relative path loss	0.5 dB	Relative path loss	20 dB
Log-normal enable	No	Log-normal enable	No	Log-normal enable	No

Table H-2. Spirent SR5500 Wireless Channel Emulator Settings for Three Paths that Define the Dynamic Multipath Channel for Aeroautical Mobile Telemetry in S-Band					
Path 1		**Path 2**		**Path 3**	
Modulation	Static	Modulation	Static	Modulation	Rayleigh
Fading Doppler	N/A	Fading Doppler	N/A	Fading Doppler	2.0 Hz
Phase shift	0°	Phase shift	0°	Phase shift	0°
Frequency shift mode	Fixed	Frequency shift mode	Fixed	Frequency shift mode	Fixed
Frequency shift	0 Hz	Frequency shift	0.07 Hz	Frequency shift	0 Hz
Fading spectrum shape	N/A	Fading spectrum shape	N/A	Fading spectrum shape	Rounded 12 dB
Delay mode	Fixed	Delay mode	Fixed	Delay mode	Fixed
Delay value	0 µs	Delay value	0.01 µs	Delay value	0.155 µs
Relative path loss	0 dB	Relative path loss	0.5 dB	Relative path loss	20 dB
Log-normal enable	No	Log-normal enable	No	Log-normal enable	No

Table H-3. Spirent SR5500 Wireless Channel Emulator Settings for Three Paths that Define the Dynamic Multipath Channel for Aeroautical Mobile Telemetry in C-Band					
Path 1		Path 2		Path 3	
Modulation	Static	Modulation	Static	Modulation	Rayleigh
Fading Doppler	N/A	Fading Doppler	N/A	Fading Doppler	4.52 Hz
Phase shift	0°	Phase shift	0°	Phase shift	0°
Frequency shift mode	Fixed	Frequency shift mode	Fixed	Frequency shift mode	Fixed
Frequency shift	0 Hz	Frequency shift	0.15 Hz	Frequency shift	0 Hz
Fading spectrum shape	N/A	Fading spectrum shape	N/A	Fading spectrum shape	Rounded 12 dB
Delay mode	Fixed	Delay mode	Fixed	Delay mode	Fixed
Delay value	0 µs	Delay value	0.01 µs	Delay value	0.155 µs
Relative path loss	0 dB	Relative path loss	0.5 dB	Relative path loss	20 dB
Log-normal enable	No	Log-normal enable	No	Log-normal enable	No

APPENDIX 2-I

Citations

Code of Federal Regulations, Table of Frequency Allocations, title 47, sec. 2.106.

Code of Federal Regulations, Frequencies, frequency tolerance, and emission limits, title 47, sec. 25.202.

CommScope. "Calculators and Tools." Retrieved 17 May 2021. http://www.commscope.com/Resources/Calculators/.

Consultative Committee for Space Data Systems. *Low Density Parity Check Codes for Use in Near-Earth and Deep Space Applications*. Standard CCSDS 131.1-O-2-S. September 2007. Rescinded. Retrieved 17 May 2021. Available at https://public.ccsds.org/Pubs/131x1o2e2s.pdf.

D.G. Jablonski. "Demonstration of Closed Loop Steering of Antenna Patterns for Mitigating Antenna-to-Antenna Interference in Two-Antenna Telemetry Installations on Military Aircraft," Instrumentation Test Technical Symposium, New Orleans, LA, 25 August 2004.

Department of Defense. "Requirements for the Control of Electromagnetic Interference Characteristics of Subsystems and Equipment." MIL-STD-461-G. 11 December 2015. May be superseded by update. Retrieved 17 May 2021. Available at https://quicksearch.dla.mil/qsDocDetails.aspx?ident_number=35789.

E. L. Law. "RF Spectral Characteristics of Random PCM/FM and PSK Signals." International Telemetering Conference Proceedings, pp. 71 80, 1991.

E. Perrins. "FEC Systems for Aeronautical Telemetry". *IEEE Transactions on Aerospace and Electronic Systems*, vol. 49, no. 4, pp. 2340-2352, October 2013.

Federal Communications Commission. "Amendment of Part 27 of the Commission's Rules to Govern the Operations of Wireless Communications Services in the 2.3 GHz Band." WT Docket No. 07-293. In *Order on Reconsideration*. FCC 12-130. 17 October 2012. Retrieved 17 May 2021. Available at https://apps.fcc.gov/edocs_public/attachmatch/FCC-12-130A1.pdf.

Hufford, G. A. and F. K. Steele. "Tabulations of Propagation Data over Irregular Terrain in the 75- To 8400-Mhz Frequency Range - Part V: Virginia." NTIA Publication 91-282, December 1991. Retrieved 17 May 2021. Available at https://www.its.bldrdoc.gov/publications/download/91-282.pdf.

I. Korn. *Digital Communications*. New York; Van Nostrand, 1985.

International Telecommunications Union. "Compatibility between the Earth exploration-satellite service (passive) and relevant active services" *Final Acts WRC-15 – World Radiocommunication Conference*. Geneva, 2015. pp. 399-403.

———. "Method for point-to-area predictions for terrestrial services in the frequency range 30 MHz to 3 000 MHz." ITU-R Recommendation P.1546-6. August 2019. May be superseded by update. Retrieved 17 May 2021. Available at https://www.itu.int/rec/R-REC-P.1546/en.

———. "Prediction procedure for the evaluation of interference between stations on the surface of the Earth at frequencies above about 0.1 GHz." ITU-R Recommendation P.452-16. July 2015. May bae superseded by update. Retrieved 17 May 2021. Available at https://www.itu.int/rec/R-REC-P.452/en.

———. "Propagation curves for aeronautical mobile and radionavigation services using the VHF, UHF, and SHF bands." ITU-R Recommendation P.528-4. August 2019. May be superseded by update. Retrieved 17 May 2021. Available at https://www.itu.int/rec/R-REC-P.528/en.

———. "Protection criteria for telemetry systems in the aeronautical mobile service…" ITU-R Recommendation M.1459. May 2000. May be superseded by update. Retrieved 17 May 2021. Available at https://www.itu.int/rec/R-REC-M.1459-0-200005-I/en.

———. "Radio Regulations: Articles." 2012. May be superseded by update. Retrieved 17 May 2021. Available at http://search.itu.int/history/HistoryDigitalCollectionDocLibrary/1.41.48.en.101.pdf.

Jensen, M., M. Rice, and A. Anderson. "Aeronautical Telemetry Using Multiple-Antenna Transmitters." *IEEE Transactions on Aerospace and Electronic Systems*, vol. 43, no. 1, pp. 262-272, January 2007.

K. Temple. "Performance Evaluation of Space-Time coding on an Airborne Test Platform." Paper presented at the 50th International Telemetering Conference, San Diego, CA, October 2014.

Kamilo Feher. *Digital Communications: Satellite/Earth Station Engineering*. Englewood Cliffs: Prentice-Hall, 1983, pp. 168-170.

M. G. Pelchat. "The Autocorrelation Function and Power Spectrum of PCM/FM with Random Binary Modulating Waveforms." *IEEE Transactions*, Vol. SET 10, No. 1, pp. 39 44, March 1964.

M. Richharia. *Satellite Communications Systems, Second Edition.* New York; London: McGraw-Hill, 1999, page 37.

Maral, G., and M. Bousquet. *Satellite Communications Systems: Systems, Techniques and Technology*. 2nd ed. Chichester: Wiley (1993), sec. 2.1.3; Gagliardi, Robert M. *Satellite Communications*. 2nd ed., New York: Van Nostrand Reinhold (1991), sec. 3.2.

Mark Geoghegan. "Implementation and Performance Results for Trellis Detection of SOQPSK." Paper presented at the 37th Annual International Telemetering Conference, Las Vegas, NV, October 2001.

———. "Improving the Detection Efficiency of Conventional PCM/FM Telemetry by using a Multi-Symbol Demodulator." *Proceedings of the 2000 International Telemetry Conference*, Volume XXXVI, 675-682, San Diego CA, October 2000.

———. "Optimal Linear Detection of SOQPSK." In *Proceedings of the International Telemetering Conference*, San Diego, CA, October 2002.

Marvin Simon. "Multiple-Bit Differential Detection of Offset Quadriphase Modulations." IPN Progress Report 42-151. 15 November, 2002. Jet Propulsion Laboratory, Pasadena, CA. Retrieved 17 May 2021. Available at http://ipnpr.jpl.nasa.gov/progress_report/42-151/151A.pdf.

Michael Rice. *Digital Communications: A Discrete-Time Approach*. Pearson/Prentice-Hall. Upper Saddle River, NJ, 2009.

———. "Space-Time Coding for Aeronautical Telemetry: Part 1 – System Description," in *Proceedings of the International Telemetering Conference*, Las Vegas, NV, October 2011.

National Telecommunications and Information Administration. "Manual of Regulations and Procedures for Federal Radio Frequency Management." September 2015. May be superseded by update. Retrieved 17 May 2021. Available at https://www.ntia.doc.gov/files/ntia/publications/manual_sep_2015.pdf.

Osborne, W. P. and M. B. Luntz. "Coherent and Noncoherent Detection of CPFSK," *IEEE Transactions on Communications*, August 1974.

P. Laurent. "Exact and Approximate Construction of Digital Phase Modulations by Superposition of Amplitude Modulated Pulses (AMP)." *IEEE Transactions on Communications*, vol. 34, no. 2, pp. 150-160, February 1986.

Perrins, E. and M. Rice. "Reduced-Complexity Approach to Iterative Detection of Coded SOQPSK." *IEEE Transactions on Communications*, vol 55, no. 7, pp 1354-1362, July 2007.

———. "Reduced-complexity Detectors for Multi-h CPM in Aeronautical Telemetry." In *IEEE Transactions on Aerospace and Electronic Systems*, vol. 40, no. 1, pp. 286-300, January 2007.

———. "Unification of Signal Models for SOQPSK." In *Proceedings of the International Telemetering Conference*, Glendale, AZ, 5-8 November 2018.

Phillip Bello. "Aeronautical channel characterization." *IEEE Transactions on Communications*, vol. 21, no. 5, pp. 548–563, May 1973.

Phillips, C., D. Sicker, and D. Grunwald. "Bounding the Practical Error of Path Loss Models." *International Journal of Antennas and Propagation*, Volume 2012 (2012). Retrieved 17 May 2021. Available at https://www.hindawi.com/journals/ijap/2012/754158/.

Proakis, J. G. and M. Salehi. *Digital Communications*. 5th Edition. Boston: McGraw-Hill, 2008.

R. Clewer. "Report on the Status of Development of the High Speed Digital Satellite modem", RML-009-79-24, Spar Aerospace Limited, St. Anne de Bellevue, P.Q., Canada, November 1979. Quoted in Kamilo Feher. *Digital Communications: Satellite/Earth Station Engineering*. Englewood Cliffs: Prentice-Hall, 1983.

Range Commanders Council. "Application for Equipment Frequency Allocation for Aeronautical Mobile Telemetry Systems." In *Telemetry Systems Radio Frequency Handbook*, Appendix A. RCC 120-21. July 2021. May be superseded by update. Retrieved July 10 2021. Available at https://www.trmc.osd.mil/wiki/x/iYu8Bg.

———. *Test Methods for Telemetry Systems and Subsystems Volume 2*. RCC 118-20. June 2020. May be superseded by update. Retrieved 17 May 2021. Available at https://www.trmc.osd.mil/wiki/x/fIu8Bg.

Rice, M., A. Davis, and C. Bettweiser. "Wideband channel model for aeronautical telemetry." *IEEE Transactions on Aerospace and Electronic Systems*, vol. 40, no. 1, pp. 57–69, January 2004.

Rice, M. and J. Ebert. "Derivation and analysis of the IRIG-106 dynamic multipath channel model," in *Proceedings of the International Telemetering Conference*, Las Vegas, NV, 25-28 October 2021 (forthcoming).

Rice, M. and K. Temple, "Space-Time Coding for Aeronautical Telemetry: part II – Experimental Results." *Proceedings of the International Telemetering Conference*, Las Vegas, NV, October 2011.

Rice, M., J. Palmer, C. Lavin, and T. Nelson. "Space-Time Coding for Aeronautical Telemetry: Part I – Estimators." *IEEE Transactions on Aerospace and Electronic Systems*, vol. 53, no. 4, pp. 1709-1731, August 2017.

Rice, M., T. Nelson, J. Palmer, C. Lavin, and K. Temple. "Space-Time Coding for Aeronautical Telemetry: Part II – Decoder and System Performance." *IEEE Transactions on Aerospace and Electronic Systems*, vol. 53, no. 4, pp. 1732-1754, August 2017.

S. Alamouti. "A Simple Transmit Diversity Technique for Wireless Communications." *IEEE Journal on Selected Areas in Communications*, vol. 16, no. 8, pp. 1451-1458, October 1998.

Spirent. SR5500 Wireless Channel Emulator User Manual. Copyright 2011. 71-003547, Version A7. May be superseded by update. Retrieved 17 May 2021. Available at https://support-kb.spirent.com/resources/sites/SPIRENT/content/live/DOCUMENTATION/10000/DOC10397/en_US/UM_SR5500_v3_50_A7.pdf.

T. J. Hill. "An Enhanced, Constant Envelope, Interoperable Shaped Offset QPSK (SOQPSK) Waveform for Improved Spectral Efficiency." Paper presented during 36th Annual International Telemetering Conference, San Diego, CA. October 23-26, 2000.

Telecommunications Industry Association. *Interface between Data Terminal Equipment and Data Circuit-Terminating Equipment Employing Serial Binary Data Interchange*. TIA/EIA-232-F. 1 October 1997. May be superseded by update. Retrieved 17 May 2021. Available at https://standards.globalspec.com/std/872822/tia-232.

Tey, W. M. and T. Tjhung. "Characteristics of Manchester Coded FSK." *IEEE Transactions on Communications*, Vol. COM 27, pp. 209 216, January 1979.

Thomas Schwengler. "Radio Propagation Modeling." Chapter 3 in *Wireless and Cellular Communications*. Retrieved 17 May 2021. Available at http://morse.colorado.edu/~tlen5510/text/classwebch3.html.

W. J. Weber III. "Differential Encoding for Multiple Amplitude and Phase Shift Keying Systems." *IEEE Transactions on Communications*, Vol. COM-26, No. 3, March 1978.

Wang, C. W. and T. Keech. *Antenna Models For Electromagnetic Compatibility Analyses*, NTIA Report TM-13-489. October 2012. Retrieved 17 May 2021. Available at https://www.ntia.doc.gov/report/2012/antenna-models-electromagnetic-compatibility-analyses.

Watt, A. D., V. J. Zurick, and R. M. Coon. "Reduction of Adjacent Channel Interference Components from Frequency Shift Keyed Carriers." *IRE Transactions on Communication Systems*, Vol. CS 6, pp. 39 47, December 1958.

Wikipedia. "Rayleigh fading." Retrieved 17 May 2021. Available at https://en.wikipedia.org/wiki/Rayleigh_fading

Wireless Communications Association, "4G Device Out of Band Emissions and Larger Channel Bandwidths." October 2011. Retrieved 17 May 2021. Available at https://ecfsapi.fcc.gov/file/7021715550.pdf.

**** END OF CHAPTER 2 ****